## *The optical properties of automatically darkening welding filters based on liquid crystal technology*

Stephen John Palmer

# *The Optical Properties of Automatically Darkening Welding Filters based on Liquid Crystal Technology*

**M.Sc Thesis Submitted to the University of Durham, August 1995.**



*Stephen John Palmer,*
*Hörnell Innovation A.B,*
*Tunavägen 281,*
*781 73 Borlänge,*
*Sweden.*

# *The Optical Properties of Automatically Darkening Welding Filters based on Liquid Crystal Technology*

***Stephen John Palmer***

## ABSTRACT

This thesis addresses the problem of the poor optical angular properties displayed by the majority of automatically darkening welding filters currently on the market that are based on liquid crystal technology. It is shown that by reducing the twist-angle present in the liquid crystal cell to below that of $90^{o}$ together with employment of a novel polariser arrangement, an optical shutter design based on a double-cell construction is obtained that boasts a reduced angular transmittance variation when in the activated phase. This gives an optical filter possessing a wide central viewing cone whilst maintaining the remaining optical parameters at a high level.

The only point of compromise comes from the voltage increase requirement upon reduction of the twist-angle in order to maintain cell contrast. Although this inflates the power consumption of the system, beneficial effects upon the total light scattering provoked by the device are also observed.

The final sections deal with a new mode of operation for a twisted-nematic liquid crystal cell when placed between crossed polarisers together with an *interference filter* possessing a high optical transmittance over the central part of the visible spectrum. This mode of operation means that the cell is in a dark state when inactivated. Application of a small stimulating voltage transmutes the unit into the light state, where upon further increment of the driving electronics beyond this point reverts the system back into a low transmittance phase.

Such a mode of operation for a twisted-nematic cell offers several advantages over that of the normally *white* mode when considering the optical lens of an automatically darkening welding filter. In particular, a dark, fail-safe state is provided should the controlling electronics malfunction preventing the unit from holding in a potentially hazardous light phase, a property usually associated with the normally *black* mode of operation, whilst the fast switching speed from the light to the dark state associated with the normally *white* mode of operation is maintained. It is shown that there are only two cell types that display this phenomenon and the optical properties of these two systems are analysed in some detail with the view of developing an automatically darkening welding filter based on this technology.

This thesis is submitted to the University of Durham for the degree of *Master of Science*. All work contained within this thesis was carried out by the author at *Hörnell Innovation AB* in Sweden. No material contained within has been submitted for a previous degree and the copyright of this thesis rests with the author. No quotation from it should be published without his prior written consent and information derived from it should be acknowledged.

## *CONTENTS PAGE*

## *INTRODUCTION*

Welding processes have become routine procedures universally employed in the various manufacturing and construction industries around the World. However, most systems generate the emission of harmful heat and light radiation requiring the operator to utilise some sort of protection equipment. In particular, the eyes are highly susceptible to damage and various types of welding filters have been developed over the years specifically for this purpose.

The general necessity that an operator is able to view his work clearly prior to the commencement of welding in order to ensure that the relevant materials are positioned correctly requires that a fixed-shade protection device either has to possess two viewing lenses, one being light and the other dark, or a technique be employed where a filter can be swung into and out of the line of sight. Neither option is particularly satisfactory and is not capable of offering complete safety at all times, especially in environments where several workers are simultaneously based. In addition to this, the latter alternative also demands that a welder manually adjusts the helmet immediately prior to operation, hence releasing his grip of the working metals leading to both a lower standard of workmanship and a loss of productivity.

In contrast to this, *automatically darkening* welding filters alleviate these problems providing complete protection against harmful radiation at all times. The majority of devices currently on the market are based on liquid crystal technology that offers both a rapid switching time from the light to the dark state together with the possibility of manufacturing filters possessing variable levels of transmittance depending upon the type of welding procedure to be carried out.

However, the poor optical angular properties associated with liquid crystal cells leads to the development of filters that appear lighter when viewed at glazing angles. This gives rise to both a potential source of hazard as well as generating annoyance for the operator. The majority of automatically darkening welding filters that are currently available are afflicted by this problem and it is in this area that this thesis will concentrate with the view of developing new techniques in order to enhance the optical performance of such devices.

Chapter one introduces the various types of welding systems presently in existence and demonstrates the necessity of utilising some sort of radiation block when exploiting such techniques. The concept of an automatically darkening welding filter is developed and a general description of their design is offered. This includes the liquid crystal cells, interference filters and the linear polarisers.

The origin of the poor optical angular properties exhibited by liquid crystal cells is illustrated in chapter two and the prevailing methods employed in order to alleviate these problems are analysed in some detail. The idea of retardation or birefringent layers is introduced and it is shown that the symmetry of the optical properties displayed by such films currently on the market do not match those of the liquid crystal cell when in the activated phase. It is therefore concluded that they are not capable of offering any significant degree of improvement. The final section of chapter two deals with the inactivated phase and indicates the necessity of controlling the intrinsic parameters in order to optimise the overall transmittance of the unit.

The various manufacturing standards regulating the production of automatically darkening welding filters are covered in chapter three. These standards set the framework around which the filter must be

designed. Chapters four and five investigate the effect of changing the various *cell-polariser* assembly parameters upon the optical angular properties, the light state transmittance and the available cell contrast. A novel construction is introduced employing low-twisting liquid crystal cells that boast enhanced optical angular properties when incorporated into a complete welding filter design possessing two or more liquid crystal cells whilst maintaining the remaining pertinent optical properties at a high level.

Chapter six introduces a new mode of operation for a twisted-nematic liquid crystal cell placed between crossed polarisers together with an *interference filter* whereby the unit displays a dark state in the absence of a stimulating voltage. A small electric field of between ± 2.0 and ± 3.0 volts is required in order to attain the light state and further increment of the voltage beyond this point reverts the unit back to a low transmittance condition. Such cells offer advantages over that of the normally *white* mode of operation in that a fail safe, dark phase is provided should the driving electronics malfunction, a property usually characteristic of the normally *black* mode, whilst the fast response time from the light to the dark state associated with the normally *white* mode of operation is maintained. The optical properties of such systems are analysed in some detail with the view of developing a fast automatically darkening welding filter based on this technology. It is shown that although a general working unit can be produced, the properties afforded by such devices fall somewhat short of those for the optimised design based on low-twist cells introduced in chapters four and five. The use of low-twist cells in automatically darkening, welding filters based on liquid crystal technology is patent protected by *Hörnell Innovation AB* of Sweden.

# *CHAPTER ONE*

*This section introduces the concept of welding and briefly discusses the different techniques that currently exist. The necessity of using some type of eye protector whilst working is presented and the advantages of utilising an automatically darkening welding filter over that of a conventional, fixed shade device are shown. The general construction of such filters based on liquid crystal technology is analysed together with the fundamental properties displayed by the individual elements of the unit.*

## *1.1 Welding Techniques.*

Welding is the process of uniting two or more pieces of metal at joint faces melted by heat. Additional filler material of a similar composition to that of the parent metal may or may not be added upon formation of the joint and other related processes include *braze welding*, *brazing*, *soldering* and *thermal cutting*. A quality joint will be at least as strong and robust as the parent metal itself. Because of this, such processes are invaluable and most operators working with metallic based materials will be familiar with these techniques.

To carry out welding, heat must be available at a sufficiently high temperature and concentrated in order to cause melting at the required point. There are three main types of welding processes classified according to the type of heat source employed. These are *flame*, *electric arc* and *electrical resistance heating*. In practice, the actual type of welding process used depends upon the nature of the work and the chemical composition of the parent material. These three basic techniques are briefly discussed in the proceeding sections.

### *1.1.1 Flame Processes.*

In flame processes, a fuel gas such as *ethyne* ( $C_2H_2$ ) and *oxygen* are mixed *(oxyacetylene)*, fed through a blow pipe and ignited producing an extremely hot flame consisting of two cones. The tip of the inner cone gives the maximum temperature rise which is capable of melting most working metals whilst the outer cone, which consists of the combustion products, acts to shield the weld area from the atmosphere and hence prevents oxidation from occurring. This type of process is often referred to as *gas welding*.

### *1.1.2 Electric arc Processes.*

This welding technique uses an electric arc struck between the welding electrode and the work piece in order to melt the parent material and form the joint. If the electrode is of a similar material to that of the

work piece, it also melts and adds filler material to the joint. This type of electrode is referred to as a *consumable* electrode. If however, a tungsten electrode is used for example, a *non-consumable* electrode is formed and only the parent material melts. Note that the electric arc formed during these types of processes is extremely bright.

The non-consumable process is often referred to as *tungsten inert gas (T.I.G)* welding where a shield of inert gas such as argon or helium is used to protect the work area from the surrounding atmosphere. The arc is usually started and maintained by superimposing a large voltage onto the main welding supply at either a high frequency or as a train of pulses.

Consumable electrode processes use an electric arc in order to melt both the welding electrode and the parent metal and are further categorised depending upon the means adopted in order to shield the working region from reacting with the atmosphere. *Manual metal arc (M.M.A)* welding or *stick* welding employs an electrode consisting of a core covered with a flux. The flux reacts during welding to form a shielding gas which protects the arc zone and a slag develops that covers and protects the coolant metal. Meanwhile, *metal inert gas (M.I.G)* or $CO_2$ welding uses an inert gas such as carbon dioxide supplied from a cylinder via a nozzle to shield the solid wire electrode that is supplied on a reel and fed by a motor in order to maintain a constant arc length. Other variants of the same technique include *plasma arc (P.A.W)* or *microplasma* welding where the arc is constricted by passing it through a small orifice in which a stream of gas is also flowing. The gas is ejected at high temperature and velocity which can be used for either welding or cutting whereby the jet blasts away the molten material.

### *1.1.3 Electrical Resistance Heating Processes.*

Electrical resistance techniques employ large electric currents at low voltages applied by highly conducting copper alloy electrodes in order to melt the parent metal at the interface between the touching areas, hence forming the joint at one "spot". A force is applied by the electrodes whilst the current is flowing to forge the weld and is often referred to as *spot* or *flash* welding.

## *1.2 Safety in Welding.*

There are many safety hazards associated with welding processes giving rise to the requirement for both mechanical and electromagnetic radiation protection. In particular, the arc used in welding and to a lesser extent the molten metal in the weld pool emit light and heat, hence necessitating the use of filters to prevent this radiation from damaging the eyes. Ultra-violet (U.V) radiation and in particular the U.V.B and U.V.C components, are absorbed in the outer cell layers of the cornea killing the cells in this membrane. These cells are then rejected leaving bare nerve ends that are extremely sensitive causing a severe irritation on the outer surface of the eyeball occurring several hours after exposure. Such a condition is referred to as *arc-eye*, but fortunately it completely heals itself after several days rest. There is

also some scientific speculation that exposure to the U.V.A component may influence the long term formation of cataracts.

On the other hand, infra-red (I.R) radiation is focused by the lens into a tightly concentrated beam onto the back of the retina. This focusing action can increase the irradiance by as much as $10^7$ times that which initially impinges on the front of the cornea, resulting in the formation of permanent retinal burns. Other effects of over exposure to I.R light include an uncomfortable heating of the welder's face.

Research into the medical effects of harmful radiation upon the human eye have led to the development of various safety standards both in Europe and the U.S.A. Some of this information is reproduced in table 1.1 which shows the distance from a welding arc at which the U.V radiation is reduced to the U.S.A daily threshold limits for various exposure times and welding processes[1].

**Table 1.1: Distance from a welding arc at which the U.V radiation is reduced to the U.S.A daily threshold limits for various exposure times and welding processes.**

| Welding process | Parent metal | Shielding gas | Current in Amps | Distance in metres | | |
|---|---|---|---|---|---|---|
| | | | | 1 min | 10 mins | 8 hours |
| M.M.A | Mild steel | - | 100-200 | 3 | 10 | 70 |
| M.I.G | Mild steel | $CO_2$ | 90 | 0.9 | 3 | 20 |
| T.I.G | Mild steel | Argon | 50 | 0.3 | 1 | 7 |
| | | | 150 | 0.9 | 3 | 20 |
| | | | 300 | 1.6 | 5 | 40 |
| | | Helium | 250 | 3 | 10 | 70 |
| | Aluminium | Argon | 50 A.C | 0.3 | 1 | 7 |
| | | | 150 A.C | 0.8 | 2.7 | 18 |
| | | | 250 A.C | 1.3 | 4 | 30 |
| | | Helium | 150 A.C | 0.7 | 3 | 20 |
| P.A.W | Mild Steel | Argon | 200-260 | 1.6 | 5 | 33 |
| | | Helium | 100 | 2.9 | 9 | 65 |

To alleviate the problems of harmful radiation being emitted by welding processes and other related techniques, special filters have been developed that restrict the passage of both U.V and I.R radiation whilst still possessing sufficiently high transmittances over the visible wavelengths in order to enable the welder to observe his work clearly. When designing and manufacturing such filters, it is necessary to understand and control the optical properties of the individual materials in use.

### *1.3 The Shade number Scale.*

In general, the optical properties of devices such as transmission, reflection and birefringence are wavelength dependent. When dealing with systems being used in conjunction with the human eye, the total integrated luminous properties are usually determined using a white light halogen emitter together with a photopic light detector calibrated to match the sensitivity curve of the eye during day time viewing[2]. The standard sensitivity curve is reproduced in figure 1.1.

**Figure 1.1: Standard relative sensitivity values of the human eye[2] for daytime viewing.**

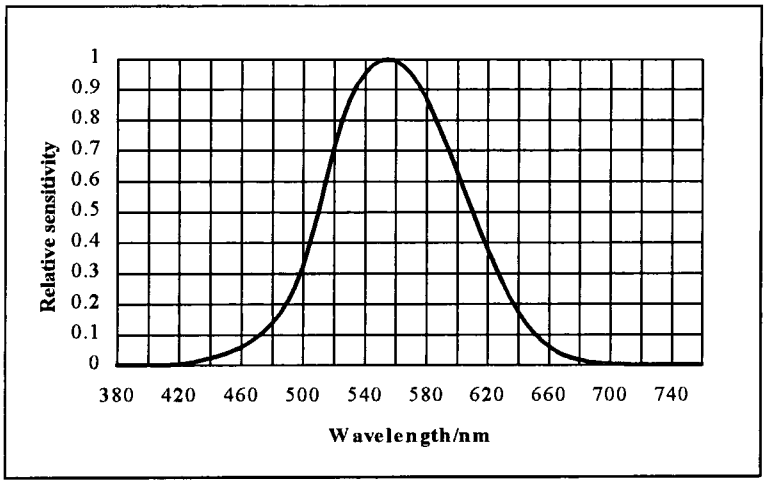


The logarithmic relationship between perceived brightness and radiation intensity is reflected by the so-called *shade number* scale, which is related to the overall integrated luminous transmittance, T expressed as a percentage according to equation 1.1. A luminous transmission of 100% gives a shade number of 1.00 and as the transmittance is reduced, the shade number of the filter increases. This scale ensures that perceived equal brightness steps are represented by even steps in shade number. The relationship between the total integrated luminous transmission and the shade number of an optical device is summarised in table 1.2.

$$\text{Shade number} = \left[\left(\frac{7}{3}\right)\log_{10}\left(\frac{100}{T}\right)\right] + 1 \qquad (1.1)$$

**Table 1.2: Relationship between shade number and the total integrated luminous transmission.**

| Shade number | Integrated luminous transmission / % | Shade number | Integrated luminous transmission / % |
|---|---|---|---|
| 1 | 100 | 9 | 0.03728 |
| 2 | 37.28 | 10 | 0.01389 |
| 3 | 13.89 | 11 | 0.00518 |
| 4 | 5.179 | 12 | 0.00193 |
| 5 | 1.931 | 13 | 0.00072 |
| 6 | 0.720 | 14 | 0.00027 |
| 7 | 0.268 | 15 | 0.00010 |
| 8 | 0.100 | 16 | 0.00004 |

### *1.4 The Experimental Measurement of the Optical Properties.*

There is a lot of optical data contained within this thesis and unless otherwise stated, all measurements are made with equipment built at *Hörnell Innovation AB*. The main problem in designing equipment capable of determining the transmittances of samples comes from the requirement of being able to ascertain the shade number over a wide range of values. This specifies a large region over which the unit is required to operate.

In principle, the shade number of a filter is measured by monitoring the current output from a *photodetector* and normalising this value with the reference current, $I_{ref}$ corresponding to 100% transmittance. If for example, the unit is designed to measure up to a shade number 14, from the definition of shade number, equations 1.2 and 1.3 are obtained.

$$S = \left(\frac{7}{3}\right) \log_{10}\left(\frac{I_{ref}}{I}\right) + 1 \qquad (1.2)$$

$$\log_{10}\left(\frac{I_{ref}}{I}\right) = (S\text{-}1) * \left(\frac{3}{7}\right) = 5.57 \text{ for } S = 14 \qquad (1.3)$$

A *logarithmic amplifier* is therefore required that is capable of dealing with input currents encapsulating at least 5.57 decades of magnitude from 1nA up to 1mA. This places a high demand on the performance of the apparatus, especially when measuring low transmittance levels.

The general equipment used in order to determine the shade number of filters consists of three parts; a *photopic light detector*, *light source* and a *logarithmic amplifier*. The standard light detector used throughout this thesis is an *LMT P10 FC* Photodetector[3] equipped with a *cosine* type diffuser in order to collect radiation impinging on the photosensitive element over a wide range of incident angles. The head consists of a 9mm diameter silicon based photoelement with a surface absorption spectrum adapted to match that of the luminous efficiency curve for the human eye during day time viewing. The output current from the device is linearly proportional to the encroaching radiation intensity. The accuracy of such a device together with the temperature dependence is generally good and is considered to be insignificant for our purposes.

The photodetector is connected directly to a logarithmic amplifier module (*Analogue Devices 755N*). In order to reduce the interference noise particularly apparent when detecting low input currents lying in the nanoampére region, the components are screened from external magnetic and electric fields by a metallic box. The output voltage lies in the -5 to +5 voltage region and rises 1 volt for every decade increase in the input current.

The exiting signal is passed through a precision rectifier and sampled via use of a microprocessor card based on an *Intel 80535* chip. The sampling size is made at 10 bits, corresponding to a 5mV resolution of the amplifier voltage.

The radiation source employed is a 150 watts halogen projector lamp running at 24 volts and focused by a series of lenses and apertures in order to form an intense parallel beam of diameter 5mm. This is focused onto the surface of the photodetector and the amplifier adjusted so as to give a reading of 1.00 corresponding to 100% transmittance. Positioning of the sample between the projector lamp and the detector enables the shade number of the filter to be directly determined.

The experimental precision of both the logarithmic amplifier and the sampling module can be determined using a reference current source as the input signal and measuring the output voltage with a *Fluke 8060A* instrument. Results for this are shown in table 1.3. Since the sampling unit has a resolution of only 5mV, the output voltage is quoted to two decimal places. This table indicates that the signal from both the logarithmic amplifier and the rectifying module as a whole generates a maximum tolerance error given by $0.01*(7/3) = \pm 0.023$ shade numbers.

Such errors influence the numerical accuracy of test equipment designed to measure the optical properties of sample filters. In order to determine the precision of the apparatus, several calibrating reference lenses of known shade numbers were obtained from the *Deutsches Institut für Normung (DIN)*[7] and measured using the experimental set-up.

**Table 1.3: Determining the accuracy of the logarithmic amplifier and the rectifying unit.**

| Input current | Theoretical output voltage | Voltage before rectifier | Voltage after rectifier | Output voltage after sampling | Measured error |
|---|---|---|---|---|---|
| 100μA | - 2.00 | - 2.019 | + 2.019 | - 2.01 | + 0.50 % |
| 10μA | - 1.00 | - 1.009 | + 1.009 | - 1.00 | + 0.00 % |
| 1μA | + 0.00 | - 0.004 | + 0.004 | + 0.00 | + 0.00 % |
| 100nA | + 1.00 | + 0.999 | + 0.999 | + 0.99 | - 1.01 % |
| 10nA | + 2.00 | + 1.997 | + 1.997 | + 1.99 | - 0.50 % |
| 1nA | + 3.00 | + 3.005 | + 3.005 | + 3.00 | + 0.00 % |

Direct comparisons between the two sets of numbers enables the accuracy of the unit to be established. The results are reproduced in table 1.4. It is seen that once again the experimental error lies below that of 0.50% over a wide range of transmittances up to and including a shade number 14. The measured value hence has a precision to within ± 0.04 shade numbers. Experiments also indicate that repetitive measurement of the same filter yields consistent results to within ± 0.01 shade numbers. It is therefore concluded that valid comparisons between the shade numbers of test samples possessing transmittances lying in similar regions can be made up to the second decimal figure.

**Table 1.4: Determining the experimental precision of the in-built equipment used in order to measure the shade numbers of test samples throughout this thesis.**

| Test glass | DIN value | Measured value | Error |
|---|---|---|---|
| 1 | 7.98 | 7.94 | - 0.50 % |
| 2 | 8.89 | 8.89 | + 0.00 % |
| 3 | 10.18 | 10.16 | - 0.20 % |
| 4 | 11.05 | 11.00 | - 0.45 % |
| 5 | 12.01 | 11.97 | - 0.33 % |
| 6 | 12.84 | 12.88 | + 0.31 % |
| 7 | 14.07 | 14.04 | - 0.14 % |

### *1.5 Filters for Specific Welding Processes.*

The *European Standard* [4] recommends the shade numbers of filters suitable for use when carrying out specific welding processes and other related techniques. Some of this information is reproduced in table 1.5 for ease of reference. Other national and international specifications also exist[5,6,7] which differ somewhat in detail from these values but agreement to that of the quoted data is generally good. Note that these recommendations are for guidance only and that a filter possessing an adjacent shade number may be more appropriate for the specific ambient lighting conditions during a given process.

**Table 1.5: Recommended filter shade numbers required for various welding processes.**

| Welding process | Filter shade numbers | | | | | | | | | |
|---|---|---|---|---|---|---|---|---|---|---|
| | **5** | **6** | **7** | **8** | **9** | **10** | **11** | **12** | **13** | **14** |
| Gas welding Acetylene gas flow in ltrs/hr | 70 - 200 | 200 - 800 | >800 | - | - | - | - | - | - | - |
| M.M.A Current limit / A | - | - | - | - | 30 | 60 | 130 | 240 | 400 | - |
| M.I.G Current limit / A | - | - | - | - | - | 100 | 175 | 300 | 500 | 550 |
| T.I.G Current limit / A | - | - | - | - | 20 | 40 | 100 | 175 | 250 | 400 |
| Plasma arc Current limit / A | - | - | - | - | - | - | 150 | 250 | 400 | - |
| Microplasma Current limit / A | 1 | 2.5 | 5 | 10 | 15 | 30 | 60 | 125 | 225 | 450 |

The level of radiation protection required depends upon both the type of welding technique in use and the intensity of the welding process, i.e. the welding current or the rate of gas flow. Although most filters possess similar U.V and I.R transmittance values giving adequate protection against harmful radiation at all times, use of a filter with a shade number below that of the recommended value can give rise to *welding glare* inducing head-aches, whilst a filter which is too dark gives poor sight and hence often leads to a low standard of workmanship. This means that it is necessary for a welder to possess a whole series of filters covering a wide range of shade numbers in order to enable all types of work to be carried out.

### *1.6 Automatically Darkening Welding Filters.*

The conventional, fixed shade welding filter consists of a robust piece of coloured glass hand-held or fastened in a helmet design in front of the eyes. Prior to the commencement of welding, the operator is required to position the working materials correctly. This necessitates good vision and hence the filter must be moved away from the line of sight. For hand-held filters this presents no problem. However, filters attached to a helmet must achieve this either by having a dual lens with one part possessing a high optical transmission and the other part being very dark, or by having a lens that can be pivoted away when not in use. Neither solution is particularly satisfactory and suffer from the fact that upon the commencement of welding, the operator is required to either change his view point of the working area in order to bring the dark part of the lens into the line of sight, or to use one hand to either hold or adjust the equipment already in place, hence releasing the working material.

These types of filters are also unable to provide complete protection against accidental weld-flash or the radiation emitted from neighbouring workers since they do not sit permanently in place but are only used when the individual operator is welding himself. This is a problem in larger working areas where several operators are simultaneously based.

In contrast to these types of conventional welding filter designs, a new type of *automatically darkening* welding filter was first introduced onto the European market[8] in 1981. This type of filter is based upon liquid crystal technology possessing several optical elements laminated together forming a so-called *glass pack* surrounded by controlling electronics. The unit sits in a helmet design and displays a high transmittance prior to welding, enabling the operator to position his work correctly. Upon striking of the welding arc, the electronics detect the presence of harmful radiation and switch the unit into a dark, protective state in less than 50ms, therefore preventing eye damage. Once the work is complete, the electronics again detect the lack of harmful radiation and the unit reverts back to the light phase.

This type of filter offers several advantages over that of the conventional fixed shade device and currently controls about 15% of the World's market by volume, although this is expected to rise dramatically over the next few years as prices fall. The first is that the hands remain free at all times removing the necessity for the operator to relinquish his grip upon the working materials once in position in order to adjust the safety equipment prior to welding. Studies have indicated[9] that this alone can produce a welding productivity rise of up to 15%. Other advantages come from the fact that the unit sits permanently in place offering complete protection at all times from neighbouring workers as well as from the accidental ignition of the arc.

These types of filters utilise liquid crystal cells in combination with polarising sheets in order to produce an optical shutter which can be rapidly switched between a light and a dark state upon application of a stimulating voltage. The device employs light-detectors positioned around the unit in order to sense the level of incoming radiation and hence automatically switch the device into the relevant state depending upon the welding conditions. This ensures that the welder constantly has both hands free and that eye protection is provided the whole time during operation.

Other advantages come from the fact that there are many different types of welding techniques that emit different levels of radiation. This gives rise to the requirement of producing welding filters that can offer varying degrees of protection in the dark state depending upon the type of work to be carried out. The use of liquid crystal technology offers this possibility.

### *1.7 The Basic Construction of Automatically Darkening Welding Filters.*

The complete automatically darkening welding filter can be split into two parts; the optical elements and the controlling electronics. The optical elements typically consist of several layers of liquid crystal cells, polarising sheets and heat shields laminated together with a strong epoxy forming a glass pack. It is this layer that regulates the transmission of radiation through the device. The controlling electronics consist of light detectors, power supply and logic circuits in order to apply the appropriate voltages to the glass pack upon the commencement and cessation of welding. These parts are discussed further in the following sections.

#### *1.7.1 The Glass Pack Design.*

The glass pack typically contains two or more liquid crystal cells placed between several polarising sheets all protected by an initial heat shield or *interference filter*. The cells consist of thin layers of liquid crystal materials sandwiched between glass plates. Due to the spontaneous helical stacking structure present in the liquid crystal layer when in the absence of a stimulating voltage, the cells are capable of rotating the plane of polarised light passing through the device. Application of an external voltage induces molecular alignment parallel with the field due to the dielectric anisotropy present in the molecules, hence destroying the helical structure and removing the optical activity of the unit. Careful control of the driving electronics together with the use of polarising sheets can therefore produce an optical shutter that can be switched between several different transmittance states.

The design of the glass pack in terms of both the number and type of liquid crystal cells and the nature and orientation of the polarising sheets determines the overall optical performance of the welding filter as a whole. It is therefore crucial to have complete manufacturing control and understanding of how the individual elements operate in order to optimise the system and develop the most competitive product possible.

#### *1.7.2 Twisted-nematic (TN) Liquid crystal cells.*

The general construction of a liquid crystal cell is shown in figure 1.2. The thin layer of liquid crystal material sits between two glass plates that are joined together around the edges with a strong epoxy. The inner surfaces of the plates are coated with a thin *transparent conducting oxide (T.C.O)* film in order to

enable an electric field to be applied across the active crystal layer. By overlapping the two glass slides such that a small part of the inner surfaces are exposed along opposite edges, electrical contacts can be made to the system. The individual manufacturing processes required to produce such a cell are discussed in section 1.7.4 of this chapter and only a brief description of the design will be offered here.

**Figure 1.2: General construction of a liquid crystal cell.**

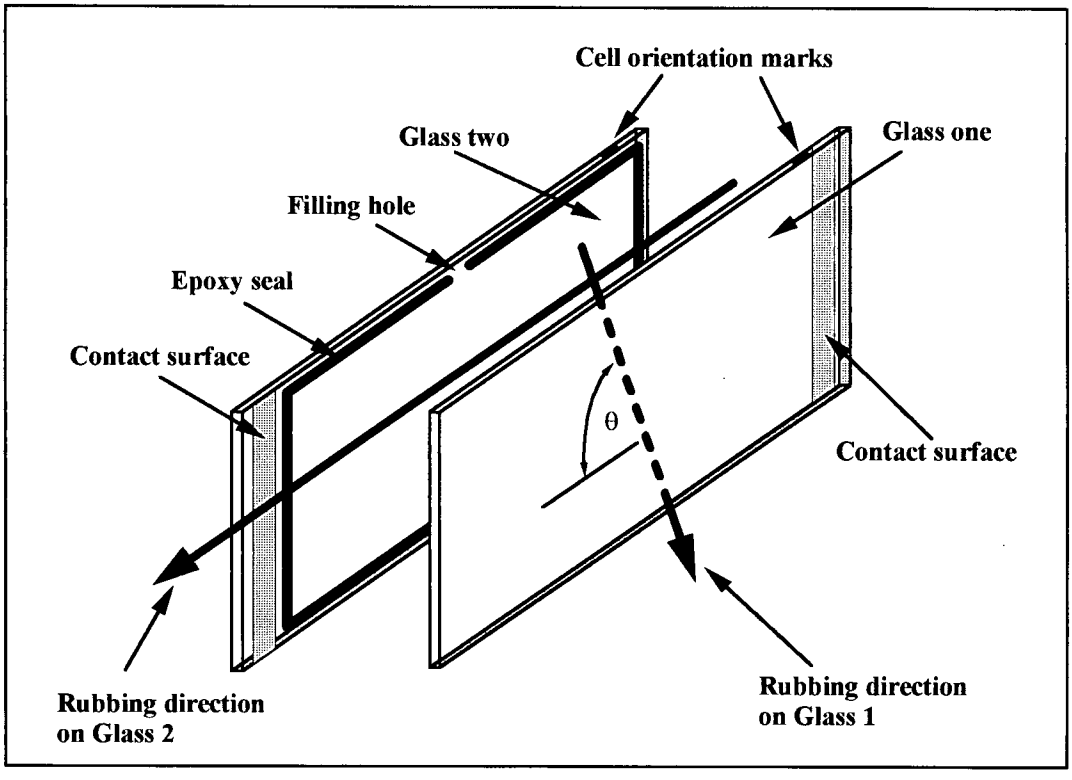


Typical liquid crystal materials consist of elongated, rod-shaped molecules that mimic a liquid in that they are free to flow, but differ from it in that within a certain temperature range, the molecular shape gives rise to a long range stacking order. Other molecular shapes that display this phenomenon include discs and rectangular formed molecules. The long range stacking sequence displays several different phases depending upon the temperature and geometry of the liquid crystal molecules. The most commonly used phase as far as liquid crystal displays are concerned is the *nematic*[10] structure in which the molecules possess a natural tendency for the molecular director axes to align parallel with each other whilst their centre of masses remain randomly distributed throughout the material.

A lowering of the temperature may produce a further ordering of the structure by causing the molecular centre of masses to align in layers, although the molecules still remain randomly distributed within each individual sheet of crystal. This produces both the *Smectic A* and *Smectic C* phases in which the average

molecular axes are aligned respectively perpendicular to and with a small tilt angle to the planes of these layers. Further temperature reduction beyond this point finally produces the *crystalline*, solid phase in which the material also possesses stacking order within the individual layers themselves and are hence held rigidly in an ordered lattice.

The liquid crystal materials used throughout this thesis are all off the shelf products that are widely available on the market[11] and operate in the nematic phase at room temperature. The chemical characteristics of the materials will not be covered in this thesis and only the physical and optical properties of the mixtures as a whole are directly relevant to this work. Appendix one reproduces the data sheets supplied by the relevant manufacturer for the liquid crystal materials appropriate to this research.

A thin *polyimide* layer about one micron thick is deposited on top of the T.C.O layers covering the surfaces of the two glass plates during cell manufacture and simplistically it can be considered that a series of microscopic scratches lying in a uniform direction are formed on the surface by gentle rubbing of a velvet cloth across the top. The liquid crystal molecules at the polyimide face show a tendency to align parallel along the microscopic groves with a small tilt angle of between $1.5^{o}$ and $2.0^{o}$ with the glass surface, shown in figure 1.3. Other alignment techniques also exist such as oblique vacuum deposition procedures[12]. These orientation methods generate different molecular tilt angles but the cell still functions in essentially the same physical manner.

**Figure 1.3: Liquid crystal molecular alignment at the surface of a polyimide alignment layer.**

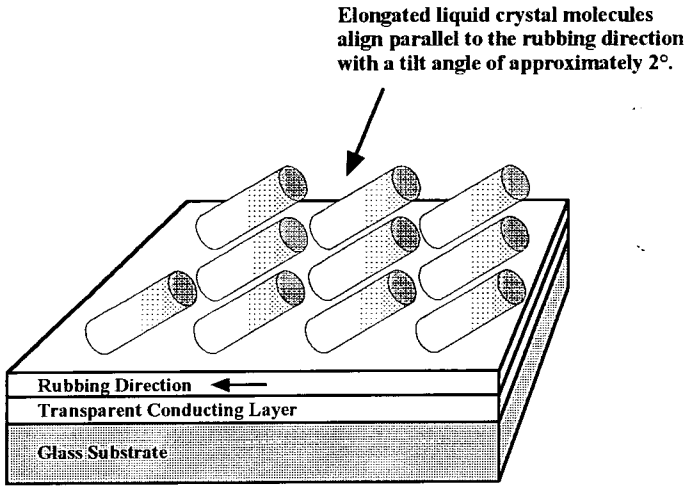


The liquid crystal alignment at both sides of the cell are hence defined during cell manufacture. By careful control, any twist-angle can therefore be induced in the helical structure across the liquid crystal layer. With a twist-angle of exactly $90^{o}$, the standard $90^{o}$ *twisted nematic (TN)* cell is formed. Such a structure is shown in figure 1.4. Twist-angles of less than $90^{o}$ form the *low-twist (LT)* cell whilst by definition, *super-twist*[13] cells are ones possessing twist-angles exceeding $180^{o}$.

**Figure 1.4: Helical stacking structure of a negative twisting 90° TN cell in the inactivated phase.**

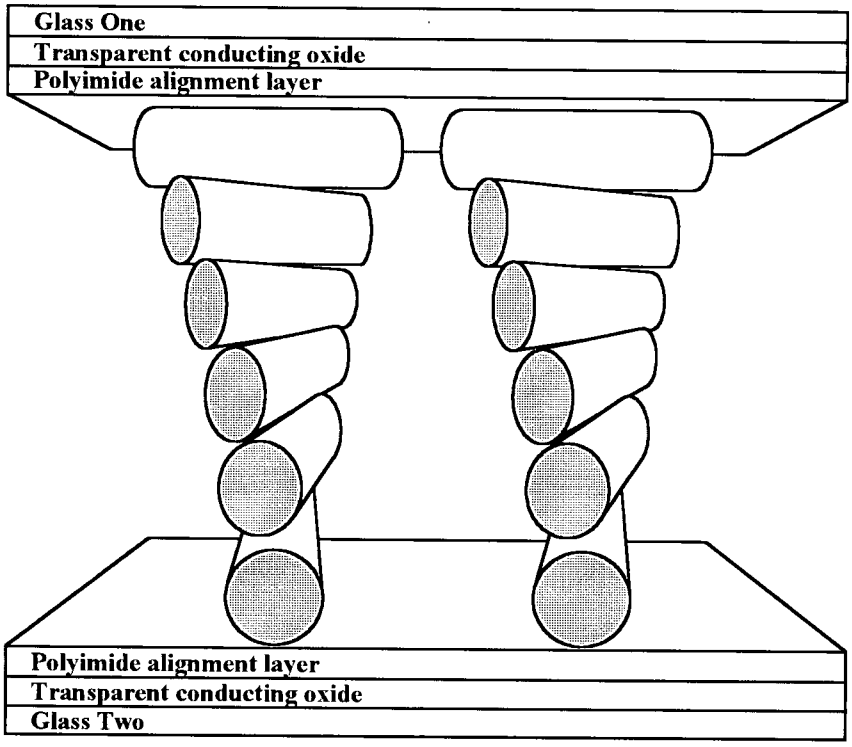


Pure nematic materials can display induced twisting helixes with both the positive and negative senses of rotation depending upon the structure of the cell. However, liquid crystal eutectic mixtures are often doped with small quantities of *cholesteric*[14] components that possess a natural helical stacking structure with a specific direction of orientation. This defines the spontaneous spiralling direction for the overall cell and hence prevents the formation of domains or regions of crystal where a reverse twist of 270° occurs instead of the required 90° structure. Note that unless otherwise stated, all liquid crystal materials used throughout this report are doped with the *Merck*[11] *ZLI-811* cholesteric substance at the 0.1% level by volume. This defines a negative sense of rotation. However, the optical properties of both negative and positive twisting liquid crystal cells are examined in the final sections of chapter five.

In the limit of large cell thickness, such a macroscopic structure is capable of rotating the plane of linearly polarised light with nearly 100% efficiency. Light rotation occurs due to the inherent anisotropic index of refraction present in the molecules of the liquid crystal material. Incident radiation experiences two refractive indexes depending upon the oscillation direction, $n_o$ corresponding to the *ordinary ray* with the electric field vector oscillating perpendicular to the molecular director and $n_e$ for the *extra-ordinary* ray oscillating parallel to this axis. A phase factor or retardation is therefore introduced between the two light components upon passage through the material, corresponding to a rotation of the polarisation.

The *birefringence* or anisotropic index of refraction, $\Delta n$, is defined in equation 1.4. The vast majority of liquid crystal materials currently on the market possess positive anisotropic indexes of refraction, typically

lying between + 0.05 and + 0.30 respectively. In general, Δn is both wavelength and temperature dependent and unless otherwise stated, all quoted values apply to a wavelength of 589nm at 20°C. In practice the variations are relatively modest, Δn becoming somewhat smaller both with increasing wavelength and temperature until the clearing point is reached where upon rapid molecular rotations average out the refractive indexes for both light components and the anisotropic index of refraction for the material approaches zero. As an approximation, these variations are generally ignored in this report and the given values assumed to be valid over the entire visible spectrum.

$$\Delta n = n_e - n_o \tag{1.4}$$

The molecules of liquid crystal materials also have an internal dielectric anisotropy, hence can be predominantly aligned upon application of an external electric field across the cell. This destroys the natural helical stacking structure of the device. A liquid crystal cell in the activated phase is schematised in figure 1.5. The presence of the T.C.O film thus allow the cell to be switched between an optically active and a non-optically active state. When placed between crossed polarisers, the cell is said to be operating in the *normally white mode* and possesses a high transmittance when in the inactivated condition. Positioning between parallel polarisers gives rise to the *normally black mode* where a low transmission is observed in the absence of a stimulating voltage.

**Figure 1.5: TN cell in the activated, hemeotropic state.**

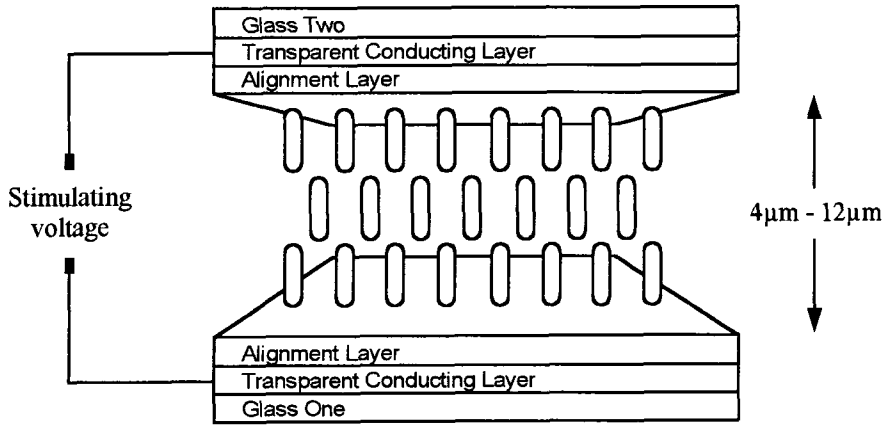


In order to be able to control the orientation of liquid crystal cells during the manufacturing of welding filter glass packs, it is usual to place a small indication mark on one edge of the cell. As a standard, a tiny paint spot was placed on the right-hand, top-edge of the cell when viewed with the nearest glass substrate rubbed in a vertical direction from top to bottom. This ensures that the glass pack is constructed in a consistent manner during the manufacturing processes of automatically darkening welding filters.

### *1.7.3 Guest-Host (GH) Liquid Crystal Cells.*

The type of TN cell introduced in section 1.7.2 operates via the non-rotation or rotation of linearly polarised light upon application or removal of a stimulating voltage, hence requires the presence of polarising sheets in order to obtain cell contrast. However, a variant to this type of liquid crystal cell is the so-called *guest-host (GH)* cell. The GH device does not obtain contrast by being optically active but by doping of the host liquid crystal material with a *dichroic*[15] light absorbing dye. The dye molecules are incorporated into the host crystal structure and only generate light absorption when aligned parallel to the incident radiation oscillations. When in the inactivated phase, the host matrix forms the helical structure and hence the dye molecules are able to absorb the incident light. Activation of the cell causes the host crystal to align parallel with the applied field and hence light absorption no longer occurs. The device then displays a high transmittance and is said to be in the light state.

This type of cell is often included in welding filter designs since it provides a shade number contrast step whilst not being required to be placed between polarising sheets. This reduces the overall number of elements in the welding filter glass pack and simplifies the manufacturing procedure. Unlike the standard TN cell operating in the normally *white* mode, the GH cell also attains a dark state in the absence of a driving voltage, hence provides a degree of safety should the driving electronics of the unit malfunction. This point will be discussed further in chapter six.

Since the GH cell does not operate by rotating the plane of linearly polarised light, the sides of the cell are often rubbed in the same direction producing a *splay* structure rather than that of the conventional helical stacking configuration and hence simplifies the manufacturing procedure. However, as a standard throughout this thesis the GH cell extensively used is an 8μm $90^{o}$ twisting cell filled with the *Merck ZLI-5035/4* liquid crystal material. Incidentally, this crystal is also doped with 0.1% by volume of the negative twisting *Merck ZLI-811* cholesteric component.

### *1.7.4 The Manufacturing Processes of Liquid Crystal Cells.*

This section offers a brief description of the manufacturing techniques required in order to produce liquid crystal cells and gives the specific experimental procedures carried out during the research contained within this thesis. However, the reader may wish to hop over this section for now and use it as a source of reference later on. This can be done without losing too much insight into the results and conclusions expressed in the thesis.

When manufacturing liquid crystal cells, the starting point is with the glass substrates. It is important to obtain a high quality material that possesses a good, planar surface. There are several manufacturers currently offering off the shelf products specifically to this end[16,17]. These substrates must be coated with a transparent conducting layer in order to enable the cell to be activated upon application of an external voltage and the most widely utilised technique for doing this is via the sputter deposition of tin doped, indium oxide (I.T.O) layers onto the glass surfaces. Sheet resistances less than 50 ohms per square can be

obtained for films with thicknesses of 30nm. Such deposition processes are well documented in the literature[18] and in general most commercial glass manufacturers stock glass plates that come ready coated with suitable I.T.O layers.

Due to the absolute necessity of cleanliness, the substrates are cut to size and sent through a cleaning line involving several immersions in alternate baths of acid and alkaline together with the application of ultrasonic vibrations in order to help remove surface particles. Following this, centrifuging at elevated temperatures ensures that the substrates are dry prior to the commencement of cell manufacturing.

The actual assembly of the cell is usually carried out in an automated production line operating in a *clean room* environment, reducing unwanted contaminants. By computer control of the working equipment, small changes in the individual processes can readily be carried out enabling fine tuning and optimisation at every stage.

The first procedure involves application of the alignment layer on to the I.T.O covered glass plates. There are several different alignment techniques that have been developed over the years and the specific deposition procedure utilised depends upon the nature of the materials in use. The method employed here involves application of a thin polyimide coating via spay deposition. The substrates pass under a nozzle emitting a fine mist of a commercially available polyimide called *Rhodeftal 200*[19] dissolved in a solvent of *N-methyl-2-2-pyrrolidone, cyclopentanone* and *dimethylformamide*. There then follows a short period of baking in which the plates are heated at up to 300$^{o}$C to ensure complete curing of the polyimide film and evaporation of the solvents. The thickness of the layer depends upon both the concentration of the solution and the quantity of liquid deposited onto the substrate surfaces and in practice layer thicknesses of around 80nm are used. It must be noted however that such processes give rise to a large manufacturing variance and hence result in it being difficult to maintain tight control of production. Other deposition techniques that offer better process management include off-set *flexographic* printing where the film is rolled onto the substrate from a rotating rubber drum.

Having deposited the alignment layers on top of the I.T.O electrodes, they are then treated in order to induce liquid crystal molecular alignment. This is carried out via gentle rubbing of the surface with a velvet cloth in order to develop a series of parallel microscopic groves along which the crystal molecules tend to align. In practice, this is carried out by positioning of the glass plates underneath a rotating drum covered with the relevant cloth. The plates are held in the required orientation via vacuum suction and the drum passed over the surface so that the velvet makes the desired contact with the polyimide layer. Suitable cloth materials are readily available on the market[20] and it is essential to adjust the contact pressure in order to obtain an optimum alignment of the crystal. This is more of an art than a science and in practice the drum pressure has to be regularly re-adjusted and the performance continually monitored from day to day.

In order to ensure that the correct cell gap is established, *spacers* are applied to the surfaces of the glass plates. These take the form of hard silica spheres with accurately controlled diameters to within $\pm$ 0.05$\mu$m. These are available[21] at regular step intervals ranging from 1.0$\mu$m through to over 20$\mu$m. By formation of a spacer suspension in a *propan-2-ol* solvent, the spacer dust can be spray deposited as a fine mist onto the surface of the substrates. In practice, typical solution concentrations of 0.5mg.cm$^{-3}$ are used producing a

spacer surface density in the cell of the order of 50 spacers per $mm^2$. It is found that a lack of spacers leads to an uneven cell thickness with areas where the two glass plates come into close proximity of each other, whereas an abundance can give rise to a higher light scattering value generated by the device.

The pairs of glass plates are bonded together in order to form the complete cell arrangement. This is usually carried out via application of a thin photopolymer epoxy[22] strip around the edges of one of the substrates whilst that of the second is sprayed with the spacer suspension. In order to further secure the uniformity of the cell thickness, spacers are also added to the epoxy glue. Note that a small gap or *filling hole* typically 10mm long must be left along one edge of the cell in order to enable the unit to be vacuum filled with liquid crystal material at a later stage. Blasting of the plates with compressed air prior to cell assembly ensures that both the spacer solvent has completely evaporated and that any loose foreign particles are removed, reducing contaminants to an absolute minimum. Note that this does not remove the actual spacers.

Pairs of glass plates are bonded together such that the opposite edges marginally overlap in order to expose a small part of the I.T.O layer on each side of the cell. These act as contact points enabling an external voltage to be applied across the liquid crystal material. The substrate pair is then vacuum pressed in order to ensure that the sides are correctly mounted before U.V hardening of the epoxy forming the complete assembly. This gives rise to the construction schematised in figure 1.6.

**Figure 1.6: General construction of a liquid crystal cell arrangement.**

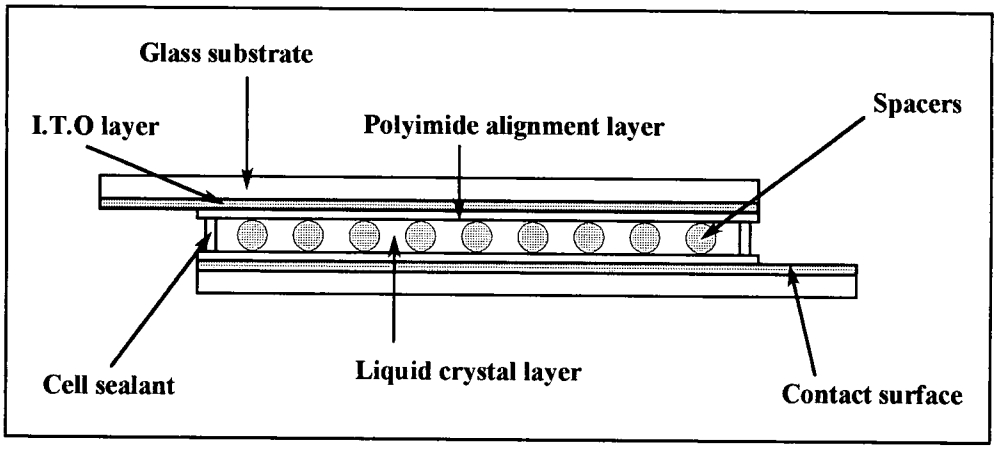


It is at this point that the first quality control check occurs and the cells are visually inspected in order to remove those that are either flawed or contaminated. In particular, small pieces of glass from the edges of the substrate find their way into the cell system. Since these inevitably are of a different thickness to that of the spacers, they usually produce a slight thickening of the cell in the immediate vicinity, hence are

conveniently identified via the associated *Moiré* fringes when illuminated with green light. Other flaws include the leaking out of the epoxy along the edges and various types of marks in the polyimide layer. Typical yields at this point can be as low as 80% when manufacturing 4μm cells in a modern assembly line. Note that the yield is highly sensitive to the cell thickness and in general rises sharply as this parameter is increased.

The next stage is to fill the cells with the relevant liquid crystal material. This is carried out in a vacuum chamber where the crystal material is placed in long baths with the empty cells mounted in rows above in a fixture that can submerse the filling holes below the level of the crystal surface. Such an arrangement allows many hundreds of cells to be processed simultaneously. The system is first pumped down to pressures of $10^{-5}$ mm Hg and stabilised for a period of time to ensure that both the majority of dissolved gasses present in the liquid crystal material itself are removed and that the air contained between the glass plates is drawn out. Note that it is important that the liquid crystal material does not contain any volatile components. For a newly purchased crystal, this process may take several hours to ensure that complete filling of the cells occur and to prevent the formation of small air bubbles inside the unit.

The filling holes are submersed underneath the surface of the liquid crystal material and the pressure in the chamber slowly increased up to atmospheric pressure. During this period, liquid crystal material is drawn into the cells, a process that is aided by capillary action. This may take several hours depending upon the size of the filling hole, the thickness of the cell and the viscosity of the liquid crystal material in use.

The cells are next baked at 125$^{o}$C for several hours in order to ensure that the liquid crystal is correctly aligned at the surfaces of the polyimide layer. It is often found that *filling stripes* exist immediately after processing of the cell which take the form of a series of long *streaks* of crystal incorrectly oriented and extending from the filling hole. By heating the liquid crystal so that it transforms into the isotropic phase followed by a slow cooling process, such regions are removed.

After squeezing of the cells in a press in order to remove excess crystal and ensure that the correct thickness is achieved, the filling hole is sealed. Here, epoxy is applied over the top of the hole and allowed to be drawn into the gap for several minutes upon removal of the pressure. The epoxy is then hardened via U.V irradiation for a short period of time. Note that in practice it is found that excessive U.V exposure has the effect of increasing the conducting properties of the liquid crystal material, attributable to both the evolution of contaminants encapsulated in the various cell layers as well as a possible degradation of the various liquid crystal molecules liberating free charge carriers. In particular, the ubiquitous nature of alkali metal ions makes it difficult to eliminate such contaminants resulting in the necessity to operate the cell with some type of A.C voltage in order to prevent the occurrence of impurity ion migration.

The filled cells are checked both visually and electronically in order to test for possible short circuits across the glass plates and to ensure that the current consumption of the unit does not exceed that of the product specifications. Cell contacting can be carried out via a variety of different techniques. The method employed here uses small cables that are mounted directly onto the surface of the exposed I.T.O layers with a silver paste and hardened in an oven for up to an hour at temperatures exceeding 80$^{o}$C.

Finally, in order to ensure that complete control of the orientation of the liquid crystal cell is achieved during the production of the glass pack, the right hand edge of the cell is marked with a small indicator spot when viewed with the nearest glass substrate being rubbed in a vertical direction from top to bottom. The liquid crystal cell is then at a completed stage and can be used as one of the elements in the optical lens of an automatically darkening welding filter design.

The existence of a whole variety of liquid crystal mixtures available as off the shelf products gives rise to the possibility of fine tuning the desired properties of the cell for the purpose to which it is required. Parameters which can readily be controlled include the twist-angle of the helical structure, the cell thickness and the anisotropic index of refraction present in the liquid crystal material itself. We will be returning to the optimisation of such parameters later on in chapters four and five.

### *1.7.5 Interference filters (I.F).*

Interference filters (I.F) are devices with static optical properties that reflect both I.R and U.V radiation. They typically consist of five or more alternate layers of a dielectric and a reflective material deposited onto a glass substrate. The thicknesses of the individual films typically lie between 200nm and 2000nm and the device essentially forms a *Fabry-Perot*[23] interferometer whereby interference occurs between radiation reflected across the successive layers. Fine adjustment of the layer thicknesses gives rise to a filter with a transmission curve approximating to that of the luminous spectrum shown in figure 1.1. Such a filter reflects back essentially all harmful U.V and I.R radiation emitted during the welding process irrespective of the state of the liquid crystal cells.

Note that due to the physical nature of operation for an I.F with radiation being reflected across successive layers of dielectric materials, a $2^{nd}$ ($3^{rd}$) transmission peak exists at shorter wavelengths corresponding to $\lambda/4$ ($\lambda/8$) layer thicknesses. However, due to the high U.V absorption of glass and other optically transparent materials, these peaks are rapidly absorbed and hence are not manifested in the overall optical properties of the glass pack as a whole.

The top transmission peak of an I.F typically lies between 40% and 70% when using alternate layers of *aluminium oxide* ( $Al_2O_3$ ) and *silver* ( $Ag$ ), although different optical parameters can be obtained via utilisation of other material combinations. This constitutes a whole area of research in order to attain the highest optical throughputs possible. However, such work falls outside the scope of this thesis and the optical properties of an eleven layer filter using alternate films of $Al_2O_3$ and $Ag$ are simply quoted in figure 1.7. The specific design of the system is detailed in table 1.6. This type of filter is used extensively throughout this report as the first element in an automatically darkening welding filter glass pack ensuring that the majority of harmful U.V and I.R radiation is reflected back at all times. Note that as a consequence of the device possessing a high optical transmittance over the green wavelengths, the reflectance spectrum is devoid of these wavelengths and the filter appears *pink-red* in reflection. This point is discussed further in chapter six.

**Figure 1.7: Optical properties of an eleven layer I.F using alternate layers of $Al_2O_3$ and $Ag$. The thicknesses of the individual sheets are indicated in table 1.6.**

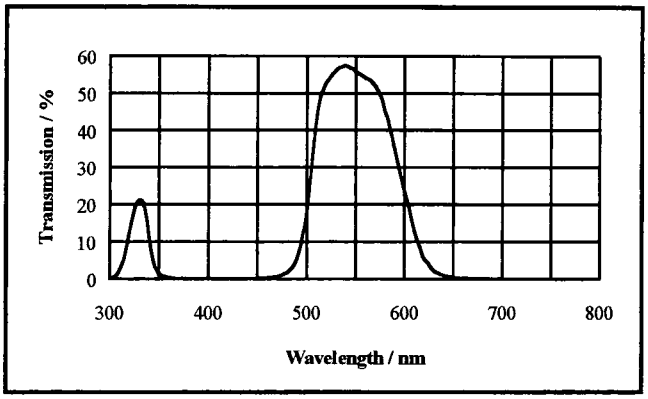


Note that the first and last layers of $Al_2O_3$ in this construction have no optical purpose but are present for mechanical strength reasons. Experiments indicate that an $Al_2O_3$ layer not only adheres better to glass than $Ag$, but is also less environmentally sensitive. In particular, many different types of films are destroyed by prolonged exposure to humidity, an effect that is exaggerated at elevated temperatures. In an attempt to alleviate these problems, different types of barrier films have been employed and research is continuing further in this area.

**Table 1.6: General construction of an eleven layer I.F that reflects both U.V and I.R radiation.**

| Eleven layer I.F | | |
|---|---|---|
| Layer number | Material | Layer thickness |
| layer 1 | $Al_2O_3$ | 170 nm |
| layer 2 | $Ag$ | 150 nm |
| layer 3 | $Al_2O_3$ | 1240 nm |
| layer 4 | $Ag$ | 320 nm |
| layer 5 | $Al_2O_3$ | 1280 nm |
| layer 6 | $Ag$ | 350 nm |
| layer 7 | $Al_2O_3$ | 1260 nm |
| layer 8 | $Ag$ | 320 nm |
| layer 9 | $Al_2O_3$ | 1250 nm |
| layer 10 | $Ag$ | 150 nm |
| layer 11 | $Al_2O_3$ | 815 nm |

The thin material layers can be deposited by a whole variety of different vacuum techniques, but it must be remembered that the final optical performance of the filter largely depends upon the refractive indexes of the individual sheets themselves. This in turn is a function of the quality of the stacking structure. Suitable deposition processes include ion-assisted vacuum deposition whereby the materials are evaporated either by electrical resistance heating or with an electron beam at pressures below that of $10^{-5}$ mm Hg.

### *1.7.6 Linearly Polarising Materials.*

Liquid crystal cells are usually used in conjunction with polarising sheets consisting of long, organic molecular chains uniaxially stretched in one direction so as to give uniform alignment. Light oscillating parallel to the molecular axis suffers partial absorption from loosely bound electrons that are free to move along the chemical chains, whilst radiation vibrating perpendicular to this axis passes through unaffected. This results in initially unpolarised light becoming predominantly linearly polarised upon traversing the polarising medium.

The two parameters that define the overall performance of a particular material are the *polarising efficiency*, defined as the percentage of light that becomes polarised along the major transmission axis of the device, and the total *transmission* throughput of the material for unpolarised incident radiation. An inescapable consequence of polariser operation is that a material possessing a high polarising efficiency invariably has a low overall optical transmittance and vice versa. Typical values for the polarising efficiency lie between 80% and 99.9%, whilst that for the total optical transmission lie between 50% and 30% respectively. The material used extensively throughout this report is the *LC81* polariser from *Dodwell*[24] manufacturers that has a polarising efficiency of 99.9% and an overall optical transmission throughput of 38%. This polariser comes as a pliable, durable plastic sheet capable of being heated up to 80°C before suffering permanent deformation.

Maximum light extinction is obtained from two polarisers positioned with their transmission axes lying perpendicular relative to each other and as this angle is reduced, the total transmittance of the system rises to a maximum for when the polarisers are aligned parallel. In general, the overall optical throughput of a pair of polarisers is given by *Malus' Law*[25], quoted in equation 1.5. Here, $I(0)$ is the maximum transmission of the device with parallel polarisers and $\theta$ the angle between the transmission axes of the two sheets.

$$I(\theta) = I(0)\cos^2\theta \qquad (1.5)$$

Figure 1.8 confirms the validity of Malus' Law for the *Dodwell* LC81 polarising material. Here, the measured luminous transmittance stated as a percentage is shown for two LC81 polarisers as a function of the angle between the transmission axes. The polarisers are placed together with an I.F possessing an optical response curve matching that of figure 1.7. This ensures that only luminous wavelengths pass

through the system and contribute to the total intensity measured by the light detector. The experimentally measured values are plotted over a $cos^2\theta$ mathematical function obtained via use of regression. There is good agreement between the two indicating the validity of equation 1.6, which is also in quantitative agreement to that of Malus' Law.

Integrated luminous transmittance, $I(\theta) = 3.6\ cos^2\theta$ (1.6)

**Figure 1.8: Luminous transmittance of two *LC81* polarisers crossed at an angle θ. Experimentally measured points are superimposed onto an "$I(\theta) = 3.6\ cos^2\theta$" function. An I.F is present.**

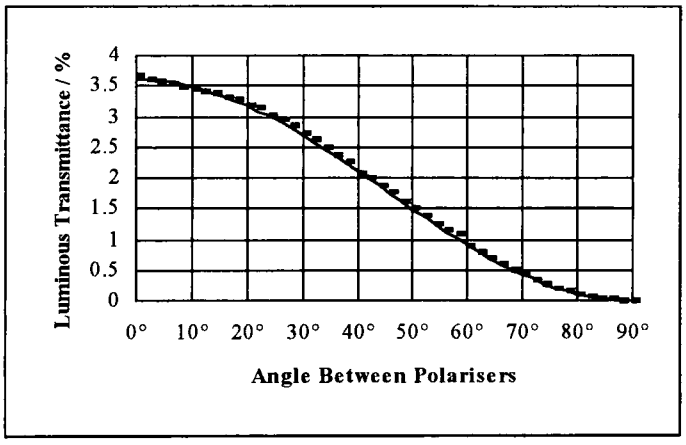


### *1.7.7 The Controlling Electronics.*

The controlling electronics have the function of detecting whether or not welding is in progress and to apply the appropriate voltages to the liquid crystal cells present in the glass pack. In principle, the electronics consist of three parts; the *detectors* that take information from the environment, the *logic circuits* that make decisions depending upon the input information and the *power supply* that operates the system and is connected or disconnected from the cells. It is beyond the scope of this thesis to go into detail concerning the specific circuit diagrams for the appropriate parts and just the basic principles will be mentioned in the proceeding sections.

There are usually several detectors placed around the welding helmet and oriented so as to cover the field of view. There are many different types of radiation detectors available on the market, each characterised by the wavelengths at which they react. U.V detectors appear most suitable for use in

automatically darkening welding filters due to the large quantities of electromagnetic radiation emitted at these frequencies. However, U.V light is rapidly absorbed by transparent, protective plastic covers making it impossible to prevent welding splatter and other sources of contamination from destroying the detector surface, hence reducing the sensitivity of detection after prolonged use.

In contrast to this, I.R detectors can be protected behind replaceable plastic sheets, but the large quantities of natural I.R radiation emitted by artificial incandescent lighting makes it difficult for logic circuits to distinguish between welding radiation and that from the ambient lighting conditions.

Other types of detectors are also available that are sensitive to the visible wavelengths or to *magnetic fields*. There is no perfect choice of detector that can cover all types of welding processes under all possible ambient lighting conditions and in principle a combination of several different types of detectors would give the best overall result.

To further improve the sensitivity of the unit to the welding conditions, a D.C filter is often connect to the electronics so that the device is only triggered by *fluctuating* radiation intensity levels characteristic of welding processes. This is referred to as *automatic* triggering and has the advantage over that of simply switching upon the magnitude of detected radiation in that the ambient lighting conditions becomes less critical. The latter type of operation is known as *manual* triggering since it is necessary for the welder to manually adjust the radiation level at which the unit should respond.

The most effective power supply for automatically darkening welding filters is a rechargeable battery supplied with current from a solar cell illuminated by radiation emitted from the welding process itself. Such designs enable the unit to be operated for many years without the requirement of any mechanical attention. However, the incorporation of a solar panel adds to the manufacturing costs and hence must be balanced up against the competitiveness of the final product from a marketing point of view.

### *1.7.8 Appropriate Driving Voltages for Liquid Crystal Cells.*

Liquid crystal materials are highly sensitive to impurities requiring the manufacturing processes to be carried out in an environmentally controlled *clean room* offering extremely low levels of contaminants. Impurities present in the cell destroy the helical stacking structure and in particular the ubiquitous nature of alkaline earth metal ions will cause a leakage current to flow across the cell gap giving rise to some power consumption when in the activated phase.

If driven with D.C voltage, any impurity ions present will migrate towards the alignment polymer layers under the action of the electric field and may become embedded at the cell surfaces. Upon removal of the stimulating voltage, an electrical field across the crystal may therefore persist due to the captured charges and hence hinder cell switching.

For this reason, liquid crystal cells are normally driven with square wave voltages of between ± 3.0 and ± 10 volts whereby the polarity is rapidly switched at speeds of up to 100Hz in order to prevent impurity ion migration from occuring. It might be expected that activation of the liquid crystal cell with A.C voltage would cause the molecules to rotate. However, the single molecular model considered so far in which each individual liquid crystal molecule interacts with the applied stimulating voltage is somewhat over simplified and in practice the interactions between the liquid crystal molecules themselves must also be considered.

Figure 1.9 depicts a TN liquid crystal cell in the activated phase in which the bulk molecules are oriented by the applied electric field and interact with each other so that adjacent molecular dipoles are aligned *anti-parallel*. An individual bulk molecule is therefore *screened* or shielded by the surrounding molecular dipoles and hence is not directly subjected to the externally applied voltage but only that due to the local environment.

**Figure 1.9: Diagram of an activated liquid crystal cell showing the intermolecular interactions.**

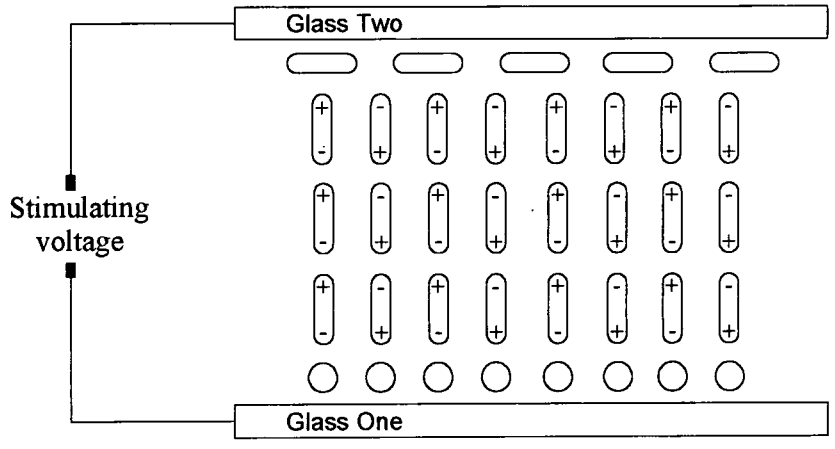


Polarity reversal of the driving electronics will therefore have no effect upon the local environment of the screened bulk molecules and the performance of the device is dependent upon the *RMS voltage* and not on the polarity of the external field.

However, during polarity reversal the liquid crystal cell must first be discharged before being charged up again in the opposite sense, resulting in the removal of the voltage across the liquid crystal material for a short period of time. This enables partial molecular relaxation back to the helical stacking structure to occur prior to the cell becoming fully charged again. The molecules are therefore able to *rock* to and fro with a frequency of twice that of the driving voltage resulting in the overall optical transmittance of the device to oscillate.

The human eye takes time to adapt to new illumination levels and if the intensity changes are faster than that of the adaptation period, the eye acts as an integrator perceiving the time-averaged luminance and preventing cell flickering from being observed. The critical value at which flickering becomes apparent depends upon the level of luminance, amplitude, size and wave form of the variation, but typical values lie between 35Hz and 45Hz for a square wave driving pulse. Since many artificial lamps operate at 50Hz / 100Hz, it is also necessary to avoid these frequencies to prevent stroboscopic effects from occurring.

Whilst preventing cell degradation, operation of the cell with an A.C voltage has the disadvantage in that the cell, which approximates to a parallel plate capacitor, must continually be charged and discharged upon polarity reversal. This produces a large power consumption when in the activated state. In general, the power consumption is a linear function of the cell capacitance which, to a first approximation is inversely proportional to the cell thickness. This is demonstrated in figure 1.10 which shows the current consumption of $70^{0}$ LT cells as a function of cell thickness. The cells are filled with the *Merck MLC-6096 + 0.1% ZLI-811 (6096)* liquid crystal mixture and driven with a ± 6 volt square wave at 42Hz. The current consumption is taken as being the mean, time-averaged current flowing through the device measured in milliamps. From this graph, equation 1.7 is confirmed. Reduction of the cell thickness together with an increase in the driving frequency hence produces a rise in the current consumption of the unit and reduces the operating life of the battery.

**Figure 1.10: Current consumption of $70^{0}$ LT cells as a function of cell thickness. The *Merck 6096* liquid crystal is used and the time-averaged, mean current flowing is measured in mA.**

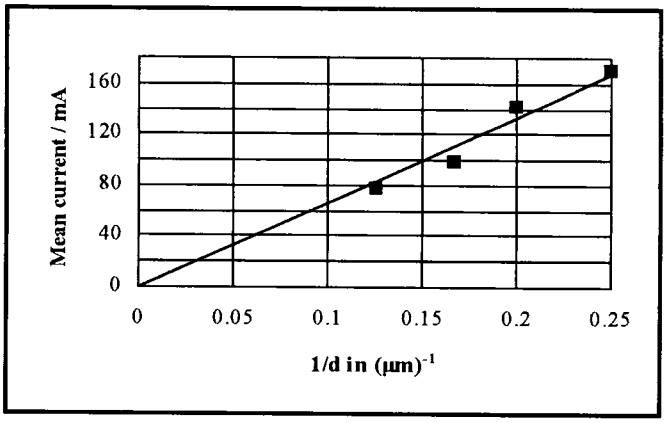


$$I_{mean} \propto \frac{1}{d} \qquad \text{(Constant frequency)} \qquad (1.7)$$

Recent work includes the investigation of utilising barrier coatings within the cell structure in order to prevent the capture of impurity ions at the surfaces and hence offering the possibility of lowering the driving frequency and reducing the number of charge / discharge cycles to below that of 0.1Hz[26]. Suitable materials include silicon dioxide layers[27] spun-deposited over the I.T.O films and hard baked at 300°C for several hours. Further research is being conducted in this area.

### *1.7.9 The Response Times of Liquid Crystal Cells.*

There are two switching speeds associated with a liquid crystal cell. The first involves switching the cell from the inactivated to the activated state upon application of a stimulating voltage and typically takes less 50ms for the crystal to react. The second is the reverse process whereby crystal *relaxation* occurs upon removal of the electric field and takes around 10 times longer. Optical shutters that require very fast response times from the light to the dark state are therefore restricted to using liquid crystal cells that operate in the normally *white* mode.

There are many parameters influencing the switching speeds of liquid crystal cells. In particular, intrinsic properties of the crystal such as viscosity and dielectric anisotropy play a major role. However, other factors such as cell thickness and the level of the driving voltage also have a significant bearing upon the final value. This is illustrated in figures 1.11 and 1.12 where the switching speeds of 60° LT cells filled with the *Merck 6096* liquid crystal mixture and operating in the normally white mode at room temperature are shown as a function of both the cell thickness and the stimulating voltage. The cells are reacting between the light and dark states upon application of the driving voltage and are positioned between perpendicular LC81 polarisers oriented at 0° and 90° respectively such that the working polariser is aligned perpendicularly to the entrance liquid crystal director vector.

**Figure 1.11: Stimulating switching speeds of 60° LT cells with the *Merck 6096* crystal operating in the normally white mode from the light to dark state as a function of cell thickness.**

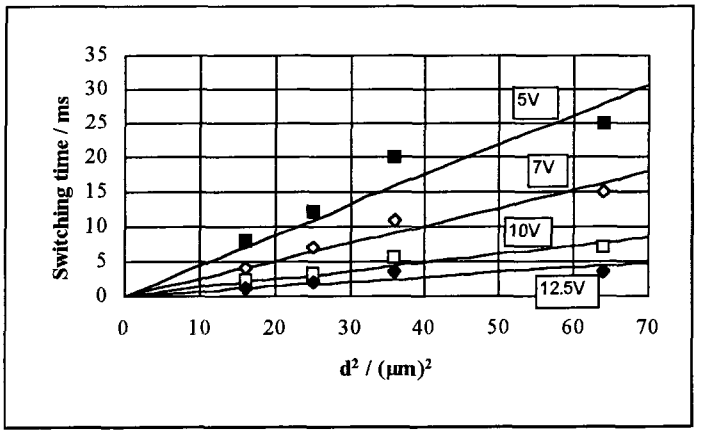

The test cells are driven with a 3Hz square wave voltage pulse operating from 0 volts up to a voltage of between + 5 and + 12.5 volts and the response time monitored by positioning of the samples between a 150 watts projector halogen lamp and a *silicon photodiode light detector*[28] and examining the voltage output variation from the detector with an oscilloscope. The switching time of the cell was taken to be the time period for the optical response to pass between the two extreme values of the dark and light states.

These graphs indicate that the stimulating switching speeds of liquid crystal cells operating in the normally white mode is a linear function of the square of the cell thickness and inversely proportional to the square of the stimulating voltage. This gives the following relationship shown in equation 1.8.

$$t_{stim} \propto \frac{d^2}{V^2} \tag{1.8}$$

**Figure 1.12: Stimulating switching speeds of 60$^0$ LT cells with the *Merck 6096* crystal operating in the normally white mode from the light to dark state as a function of the driving voltage.**

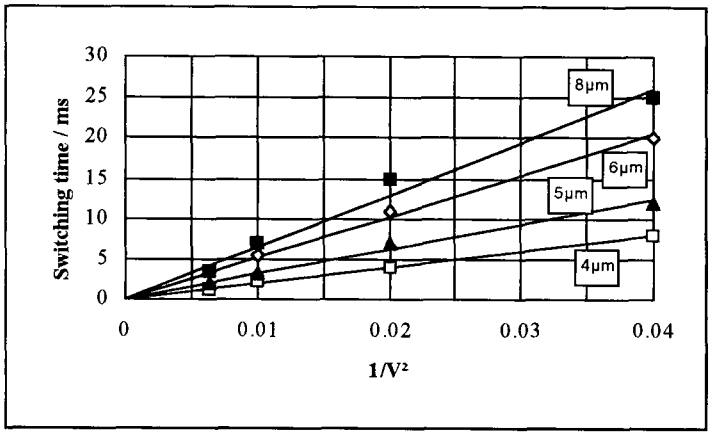


More explicit arguments are given elsewhere in the literature[29] which deduce the complete form of the switching time relationship formula, quoted in equation 1.9. Here, C is a material constant, $\eta$ the crystal viscosity, $\varepsilon_0$ the permittivity of free space and $\Delta\varepsilon$ the dielectric anisotropy. As a consequence of this dependence, a short, very high voltage pulse or *spike* can be used to *kick-start* the crystal in order to achieve very fast response times. Typical pulses lie in the range of up to 24 volts for a period of several milliseconds.

$$t_{stim} = \left( \frac{C\eta d^2}{\varepsilon_o \Delta\varepsilon V^2} \right) \tag{1.9}$$

So far, only the response times of liquid crystal cells upon activation with a stimulating voltage has been considered, this being the fastest mode of operation for such devices. For completeness, the *relaxation* switching times of $60^{0}$ LT cells filled with the *Merck 6096* mixture and operating in the normally white mode from the dark to the light state upon removal of the driving voltage are shown in figure 1.13. Whilst being independent of the initial driving voltage, the relaxation response time of a liquid crystal cell is a linear function of the cell thickness, yielding equation 1.10.

$$t_{relax} \propto d \tag{1.10}$$

**Figure 1.13: Relaxation switching speeds of $60^{0}$ LT cells in the normally white mode from the dark to light states filled with the *Merck 6096* liquid crystal mixture as a function of cell thickness.**

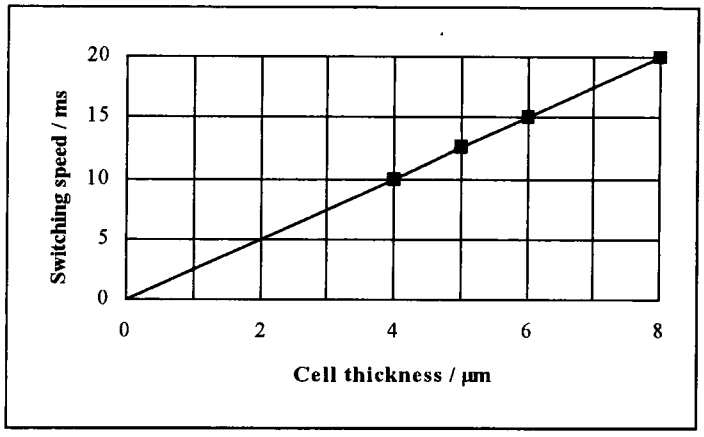


An inescapable consequence of liquid crystal operation is the rapid decrease of the switching speed at reduced temperatures due to the increase in crystal viscosity. At the other end of the scale, the operating range of a liquid crystal cell is limited by the clearing point temperature, above which the liquid crystal molecules possess excessive kinetic energy so that they no longer can form the helical stacking structure. Instead, they behave as an isotropic liquid possessing no medium or long range stacking order. The clearing point typically lies between $80^{o}$C and $120^{o}$C depending upon the liquid crystal mixture.

The quoted value of the response time for a liquid crystal cell depends upon the way in which the switching speed is defined. Many authors take the reaction time as being the period required for the optical transmittance of the device to pass between the 10% and 90% levels. However, the European Standard[30] defines the switching speeds of automatically darkening welding filters in a different manner and unless otherwise stated, this definition is followed throughout this report. The formula for the switching time calculation according to this standard is covered in section 3.5 of chapter three.

# *CHAPTER TWO*

*This chapter summarises the optical properties displayed by automatically darkening welding filters currently on the market that are based on liquid crystal technology and specifically analyses the characteristics of liquid crystal cells both when stimulated at reduced voltages and when in the inactivated phase. The poor angular dependence of such devices are indicated and the current techniques for alleviating these problems introduced. The final section deals with the inactivated state and highlights the necessity of optimising the pertinent parameters of liquid crystal cells in order to maximise the overall optical transmittance when functioning in the normally white mode.*

## *2.1 The Optical Properties of Welding Filters Based on Liquid Crystal Technology.*

The optical characteristics of the glass pack as a whole are dependent upon the properties of the individual elements themselves and the way in which they are combined together in order to form the complete unit. When considering the overall properties of such devices, a suitable place to start therefore is to reflect on those for the individual layers themselves. This includes the liquid crystal cells, the polarising sheets and the interference filter.

The electro-optic properties of a 4μm $90^0$ TN cell filled with the *Merck ZLI-3700-100 + 0.1% ZLI-811 (3700)* liquid crystal mixture in a direction lying parallel to the surface normal and placed between crossed LC81 polarisers aligned perpendicularly to both the entrance and exit liquid crystal molecules are shown in figure 2.1. A standard I.F is present and the cell is driven with a 50Hz square wave pulse.

**Figure 2.1: Electro-optic properties of a 4μm $90^0$ TN cell filled with the *Merck 3700* liquid crystal mixture with *LC81* polarisers oriented at $0^0$ and $90^0$ respectively. A standard I.F is present.**

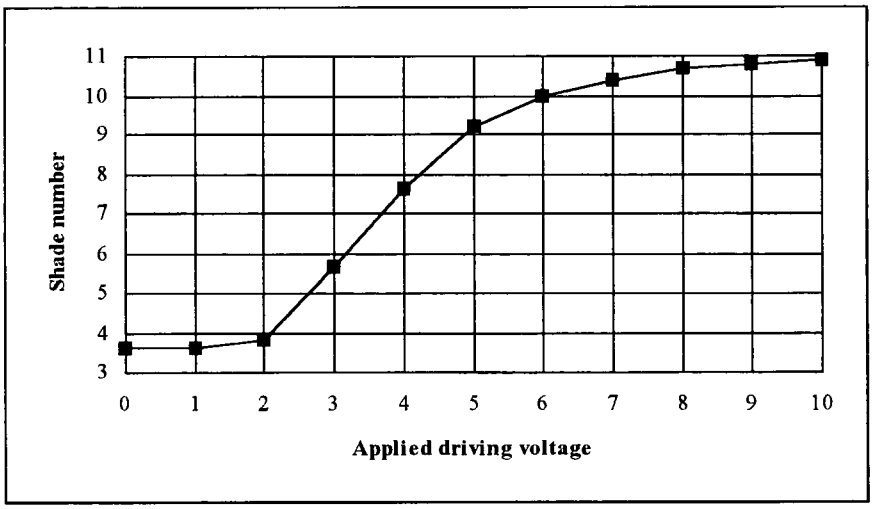

The cell is operating in the normally white mode and accordingly displays a high transmittance when in the inactivated phase. There is little change in the shade number of the device upon increment of the driving voltage until the threshold voltage for the specific liquid crystal material in use is exceeded, in this case being ± 2.0 volts. This voltage is defined as being the minimum field required in order to start the commencement of molecular alignment and is an inherent property of the crystal material itself, depending upon intrinsic parameters such as viscosity and the dielectric anisotropy.

Subsequent increase of the driving voltage beyond this point generates further alignment of the liquid crystal molecules until the saturation point is reached, where upon the majority of bulk molecules are predominantly oriented parallel with the electric field, hence destroying the helical stacking structure and essentially removing all remaining optical activity. The saturation voltage for the above example lies at around ± 8.0 volts where upon additional increment of the stimulating field has little further effect upon the shade number attained by the device.

The intermediate range between the threshold and saturation voltages is characterised by the liquid crystal molecules being only partially aligned with a balance being struck between the electric orientation forces and those due to the natural spontaneous stacking sequence of the crystal. In general, bulk molecules are relatively more free to rotate than those immediately adjacent to the polymer alignment surfaces and it is therefore in this region where the helical stacking structure is first destroyed. The partial remnants of optical activity present when in the intermediate voltage range facilitates the development of optical shutters possessing variable transmittances via utilisation of liquid crystal technology and it is therefore in this region that a variable shade, automatically darkening welding filter will operate.

### *2.1.1 The Optical Angular Properties of Liquid Crystal Cells.*

So far, only the electro-optic properties in a direction lying perpendicular to the sample surface have been considered. Despite a state in excess of shade number 11 being reached with a ± 10 volts pulse being applied to the 4μm $90^{O}$ TN cell when filled with the *Merck 3700* liquid crystal mixture, a rapid loss of contrast is observed when the cell is viewed at grazing inclination angles towards the far corners of the device. This is in fact a general problem of nematic type liquid crystal cells[31] that operate in the intermediate voltage region stimulated by reduced fields of less than ± 8 volts.

The origin of the angular dependence of shade number displayed by liquid crystal cells operating at reduced voltages is indicated in figure 2.2. Here, a schematic of the liquid crystal material is shown where the bulk molecules are only partially oriented with the applied field whilst those at the surface remain relatively unaffected. Two viewing angles are considered in the diagram, one being approximately parallel to the bulk molecules, the other making a significant angle with the director axis. Note that this diagram is greatly simplified and neglects the partial remnant molecular twisting present across the cell. This however does not significantly effect the physics involved and for the ease of illustration will generally be ignored in the proceeding discussions.

**Figure 2.2: Liquid crystal cell operating in the intermediate voltage region giving rise to the partial alignment of the bulk molecules. Two viewing angles are considered.**

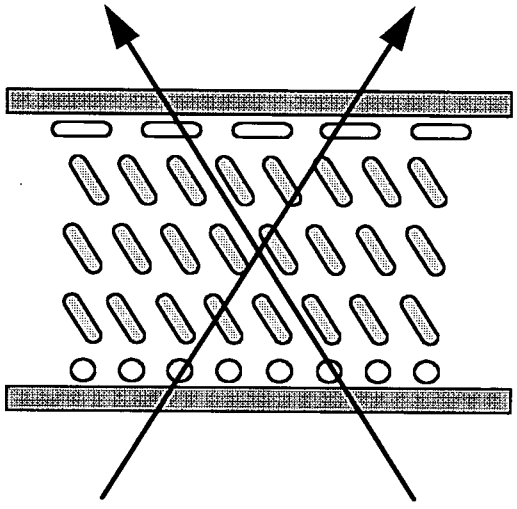

Light passing through the cell in a direction lying predominately parallel to the bulk molecular director experiences only one refractive index $n_o$, irrespective of the incident radiation polarisation. No retardation is therefore induced by the cell and the device becomes optically inert, appearing dark when viewed between crossed polarisers. However, light impinging on the macroscopic structure with components that are oscillating parallel to the molecular axis are exposed to both refractive indexes depending upon the direction of polarisation. Retardation between the ordinary and extra-ordinary rays therefore occurs and the cell possesses a degree of optical activity, giving rise to a high level of transmittance when viewed in this direction. This generates highly asymmetric angular properties for the single cell when operated at reduced voltages with one side appearing highly transparent whilst the other retains a large degree of cell contrast.

The angular variation of transmittance can be experimentally measured and displayed in a polar plot diagram using a colouring scheme in order to indicate the shade number as a function of viewing angle, shown in figure 2.3. As a standard, the z-axis is taken as being perpendicular to the sample surface and hence is represented by the central point in the polar chart. Points possessing identical inclination angles form concentric rings around the mid-point and the azimuth angle is represented by the magnitude of circular rotation anti-clockwise from the x-axis.

Test equipment built at *Hörnell Innovation A.B* was used in order to determine the optical angular properties of various samples. This consists of a fixed 150 watts projector halogen lamp focused by a series of lenses and apertures forming an intense parallel beam of diameter 5mm. This illuminates a *photopic light detector* connected to a *logarithmic amplifier* and a *sampling unit* giving out readings in shade number. By initial calibration of the amplifier to a value of 1.00, the shade number of samples placed in a fixture between the projector lamp and light detector can be determined. The specific details

concerning the experimental set-up of the apparatus together with an estimate of the numerical accuracy of the readings can be found in section 1.4 of chapter one.

**Figure 2.3: The optical angular properties of samples are displayed in polar plot diagrams using a colouring scheme in order to represent the shade number as a function of viewing angle.**

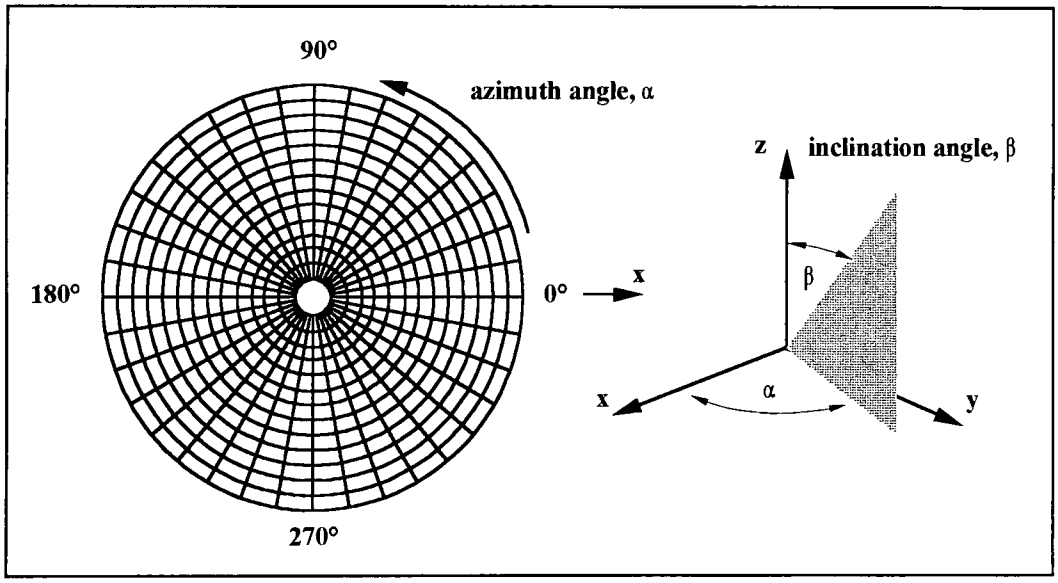


The orientation of the fixture holding the sample is controlled by two step-motors operated by computer, one governing the vertical rotation, the other the horizontal motion. As the sample is rotated through the various azimuth and inclination angle combinations, the shade number is plotted in a polar chart using a colouring scheme with unity shade number steps. As a standard, the transmittance of samples were measured with azimuth step angles of $10^{0}$ ranging from $0^{0}$ through to $360^{0}$ and with inclination steps of $2^{0}$ ranging from $0^{0}$ through to $30^{0}$ respectively.

Figure 2.4 shows the optical angular properties of a 4μm $90^{0}$ TN cell filled with the *Merck 3700* liquid crystal mixture operating in the normally *white* mode placed between crossed LC81 polarisers and driven with a ± 3.0 volt square wave at 50Hz. The polarisers are aligned parallel to the entrance and exit liquid crystal molecules and a standard I.F is present. The asymmetry in the cell retardation generates an off axis dark *cone* or band in the polar plot. Increasing the stimulating voltage improves the alignment of the bulk molecules and hence causes the dark cone to move towards the centre of the chart, indicating a reduction in the asymmetry of the cell. In the limiting case of full cell activation where the driving voltage exceeds that of the saturation point, the dark viewing cone becomes centrally symmetric around the surface normal, although it is noted that the single cell still appears significantly lighter when viewed at grazing angles.

**Figure 2.4: Optical angular properties of a 4μm 90° TN cell filled with the *Merck 3700* liquid crystal between crossed *LC81* polarisers. Cell driven with ± 3.0 volts. A standard I.F is present.**

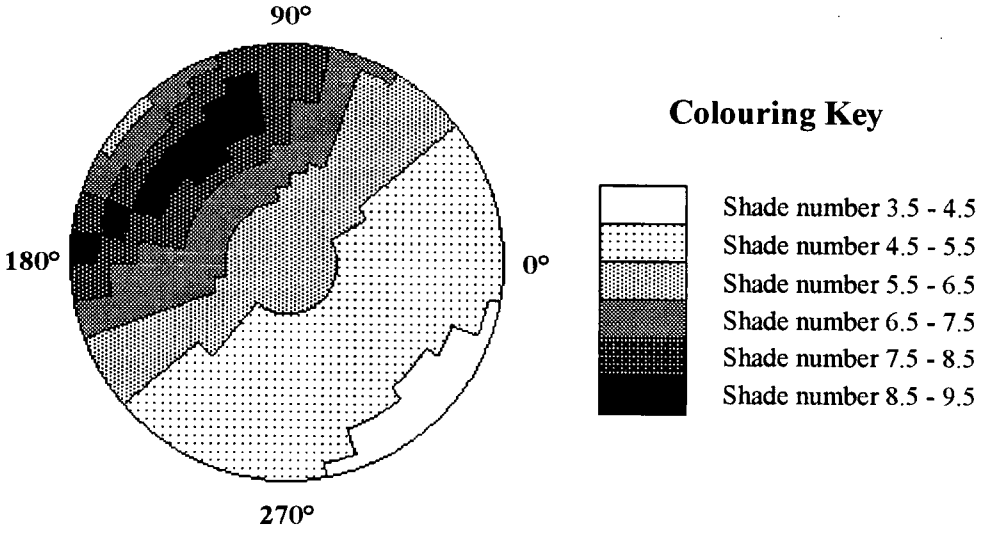


**4μm 90° TN cell with the Merck 3700 liquid crystal. 3.0 volts.**

In contrast to this, when in the inactivated phase the liquid crystal molecules are predominantly aligned parallel to the glass plates and hence there is little variation in the effective anisotropic index of refraction experienced by radiation traversing the device at different incident angles. This produces good optical angular properties that are generally centrally symmetric with large regions or domains in the polar chart encapsulating points that possess similar transmittance values. This is demonstrated in figure 2.5 which shows the optical angular properties for both a 4μm and 8μm 90° TN cell filled with the *Merck MLC-6096 + 0.1% ZLI-811 (6096)* liquid crystal mixture and operating in the normally *black* mode placed between parallel LC81 polarisers oriented parallel to the entrance molecular alignment director.

It is therefore only in the intermediate region with the cell activated at reduced voltages of less than ± 8 volts that the optical angular properties are highly asymmetric and therefore inadequate for use as a variable shade, optical shutter where a wide central viewing cone is required. Since it is in this range that liquid crystal cells are operated when in the glass pack of a variable shade, automatically darkening welding filter, the remaining sections of this report will concentrate on the optical angular properties of such cells with the view of developing a welding filter possessing enhanced optical properties accordingly.

It is the inherent asymmetric birefringence of a single cell generating poor optical angular properties that renders a one cell configuration unsuitable as a variable shade optical shutter where a wide viewing cone is required. In general, the birefringence variation of the standard 90° TN cell can be reduced to a minimum by use of both a thinner cell and a liquid crystal material possessing a lower anisotropic index of refraction; i.e. by reducing the Δn.d product of the device[32,33]. However, the requirement of maximising the overall optical transmittance of the cell when in the inactivated phase sets a lower limit to the minimum permissible value of the Δn.d and the optical angular properties of normally white, single cells operating in the intermediate voltage region remain inadequately asymmetric.

**Figure 2.5: Angular properties of inactivated 4μm and 8μm 90° TN cells with the *Merck 6096* liquid crystal and operating in the normally black mode with *LC81* polarisers. A standard I.F is present.**

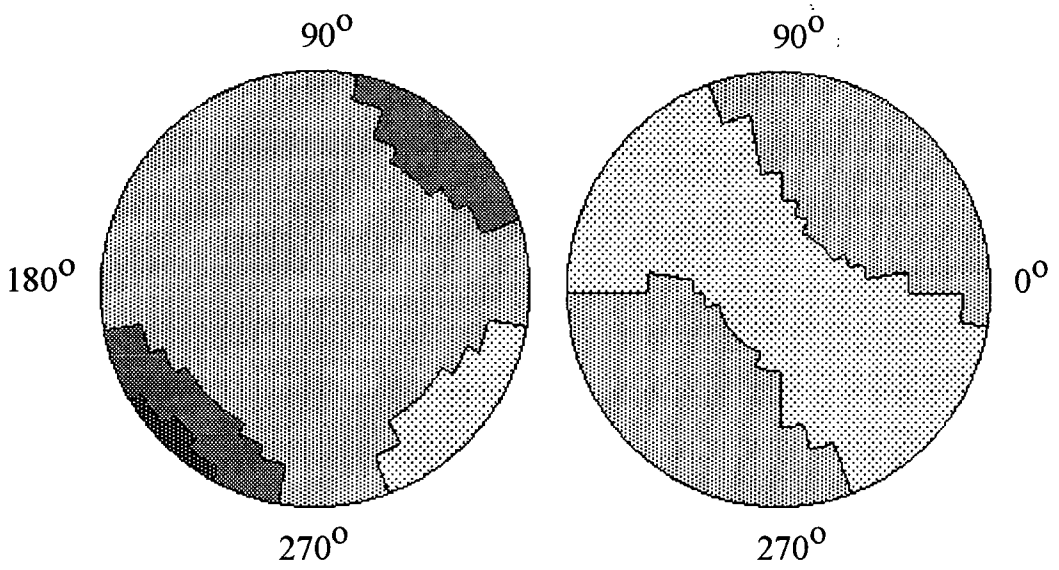


**4μm 90° TN cell with the Merck 6096 crystal and parallel LC81 polarisers. Inactivated phase**

**8μm 90° TN cell with the Merck 6096 crystal and parallel LC81 polarisers. Inactivated phase**

One way of helping to alleviate these problems is to construct a so-called *double-cell* arrangement whereby two cells operating in the normally white mode are placed together in opposite orientations such that the face-to-face rub directions are crossed, hence providing a certain degree of cell compensation. Such a design is shown in figure 2.6. Here, when one cell appears light at a specific viewing angle, the other displays a dark transmittance and vice versa. This greatly reduces the shade number variation of the device producing an optical shutter with an enhanced viewing cone. The optical properties of such a design are shown in figure 2.7 for various shade number states. Here, 4μm 90° TN cells filled with the *Merck 3700* liquid crystal mixture are used together with LC81 polarisers oriented at 0°; 90° and 0° respectively. A standard I.F is present and the cells are driven together with a 50Hz square wave.

Here, a so-called *iris* pattern is obtained in the polar chart as the dark viewing cones of the two cells placed in opposite orientations overlap. However, at larger inclination angles above that of 20°, the filter still appears very light. This problem is particularly evident at higher driving voltages when more contrast is required and the dark bands for the individual cells move towards the centre of the viewing cone. For good compensation to occur in a double-cell design, highly asymmetric liquid crystal cells are therefore required.

**Figure 2.6: Configuration of a double-cell structure giving rise to cell compensation.**

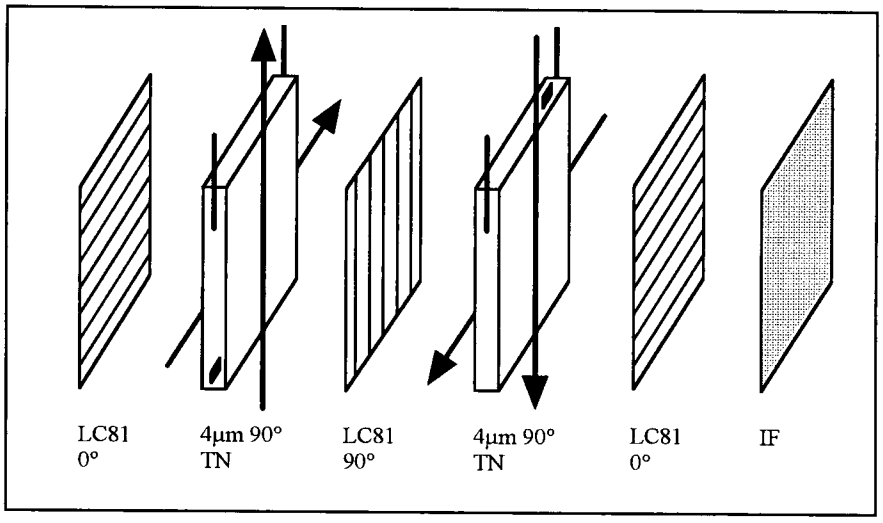


Despite the fact that liquid crystal technology offers the possibility of developing extremely fast automatically darkening welding filters possessing variable transmittances when in the dark state, this leads to poor optical angular properties when viewed at grazing angles towards the corners of the device, giving rise to a potential source of hazard and irritation for the welder.

**Figure 2.7: Optical angular properties of a double-cell structure using 4μm 90° TN cells with the *Merck 3700* liquid crystal and *LC81* polarisers cut at 0°, 90° and 0°. A standard I.F is present.**

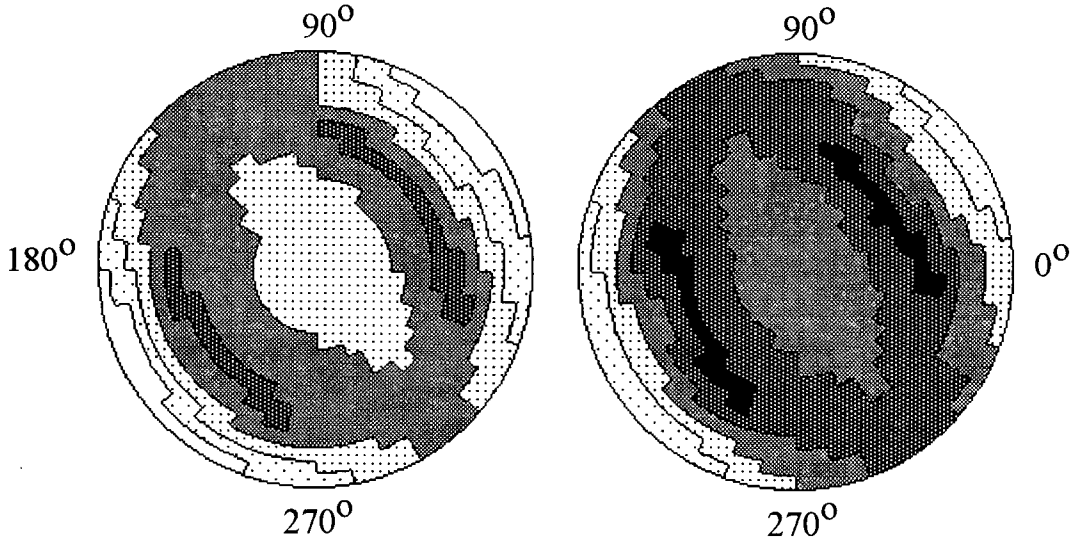


**Two 4μm 90° TN cells with the 3700 crystal and LC81 polarisers at 0°, 90° and 0°. Shade 10**

**Two 4μm 90° TN cells with the 3700 crystal and LC81 polarisers at 0°, 90° and 0°. Shade 11**

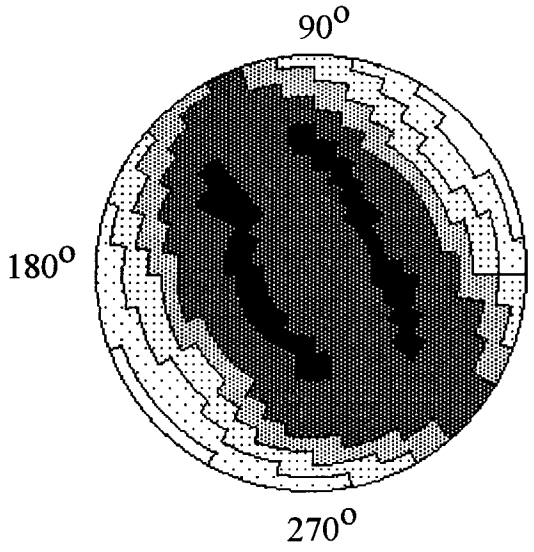


**Two 4μm 90° TN cells with the 3700 crystal and LC81 polarisers at 0°, 90° and 0°. Shade 12**

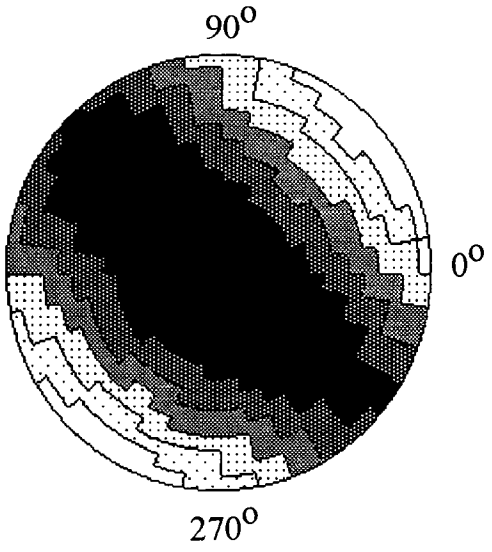


**Two 4μm 90° TN cells with the 3700 crystal and LC81 polarisers at 0°, 90° and 0°. Shade 13**

This is in fact a problem that afflicts the majority of automatically darkening welding filters currently on the market due to the necessity of operating normally white liquid crystal cells in the intermediate voltage range so as to give the possibility of providing a variable, dark state shade number. Use of the standard 90° TN cell functioning in the normally *black* mode between parallel polarisers somewhat alleviates these problems since the cell is inactivated when in the dark phase. However, this is at the expense of the cell response time to the dark, welding state and hence is of little interest as far as developing a fast, automatically darkening welding filter possessing a wide central viewing cone is concerned. The remaining sections of this thesis will therefore concentrate on techniques in order to improve the optical angular properties of welding filters using liquid crystal cells operating in the normally *white* mode.

### *2.1.2 The Optical Properties of Retardation Films.*

Birefringent films are passive optical phase retarders made from thin layers of plastics such as polycarbonate and are typically less than 5μm thick. The film is uniformly stretched in one or more directions so as to generate long chain molecular alignment. Such materials are more polarisable in directions lying parallel with the chains and hence display a higher index of refraction for radiation oscillating in these orientations. The film therefore possesses two or more unique refractive indexes depending upon the state of light polarisation. The structure of polycarbonate is shown below:

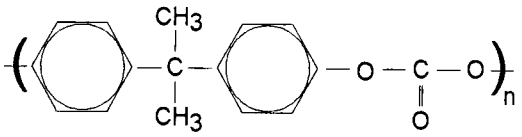

The simplest film to manufacture is one that is uniaxially stretched in a direction lying in the plane of the sheet forming the optic axis. Light transmitted parallel to this axis experiences only one refractive index irrespective of polarisation. However, other incident directions suffer retardation between components polarised in mutually perpendicular orientations due to the anisotropy in refractive index which, in general is a function of viewing angle.

Figure 2.8 shows the variation of refractive index as a function of viewing angle for a *uniaxially* stretched birefringent film lying in the x-y plane with the z-axis being parallel to the surface normal. The optic axis lies in the x direction and the refractive indexes for the ordinary and extra-ordinary components are shown. These parameters are represented by traces in a polar chart with the modulus length from the centre being proportional to the magnitude of the value whilst the argument angle gives the appropriate direction of radiation propagation through the film in the x-z plane. Note that the amount of birefringence generated by the film is determined from the difference between the two refractive indexes for the mutually perpendicularly polarised rays. This is also found to be wavelength dependent.

**Figure 2.8: Polar chart showing the variation of refractive index for the ordinary and extra-ordinary rays as a function of viewing angle for a uniaxially stretched retardation film.**

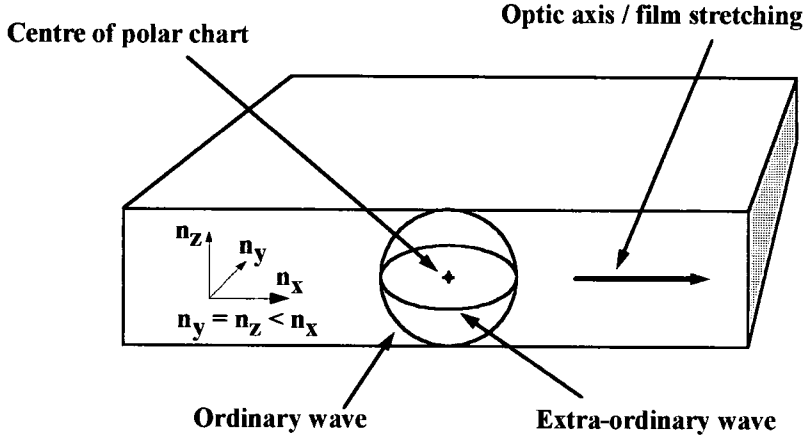


For this particular type of film, the refractive indexes along the three mutually perpendicular axes satisfy equation 2.1 and because retardation is defined as being $(n_e-n_o)$ where $n_o$ and $n_e$ are the refractive indexes for the ordinary and the extra-ordinary light components respectively, it is said to have a negative birefringence[34].

$n_y = n_z < n_x$ (Optic axis parallel to the x-direction) (2.1)

Such films are optically inert to radiation propagating in directions lying parallel to the optic axis and maximum retardation is experienced by light travelling parallel to the surface normal. It is this value expressed in units of nanometres that is used to describe the performance of the material and typically lies in the range of 300nm to 600nm for optical wavelengths of 570nm at a temperature of 20°C. However, the variation of retardation with viewing angle is also an important factor when considering the overall performance of the device.

**Figure 2.9: Variation of refractive index as a function of viewing angle for both the ordinary and extra-ordinary waves traversing through a uniaxially stretched retardation film.**

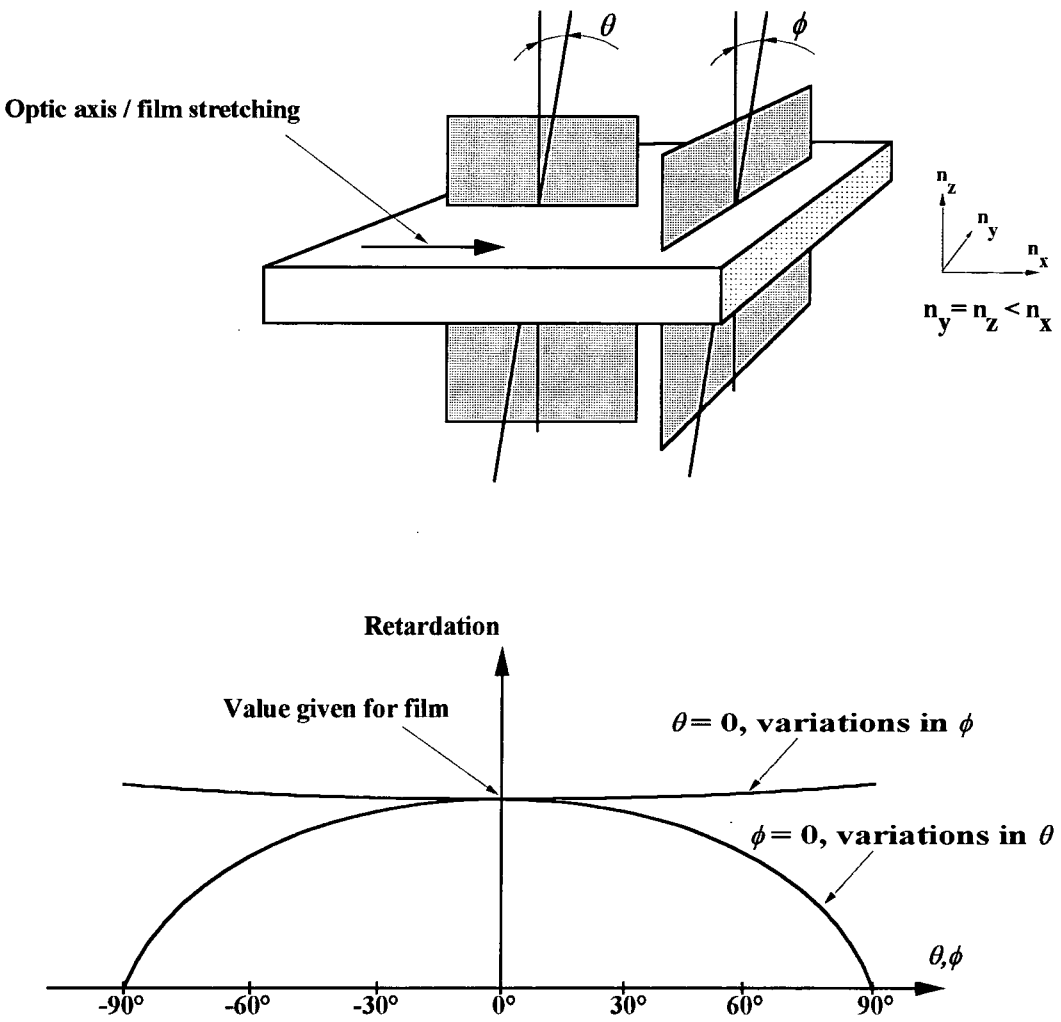

Figure 2.9 shows the retardation variation between the ordinary and extra-ordinary light components for a standard uniaxially stretched retardation film as a function of inclination angle away from the surface normal. For variations in $\theta$ with $\phi$ equal to zero, the overall birefringence is rapidly degraded at large inclination angles due to changes in the refractive index, approaching zero when $\theta$ is aligned parallel to the optic axis. This is in contrast to that for variations in $\phi$ where the velocity of light propagation through the material remains unaltered. However, increasing the value of $\phi$ enhances the optical path length traversed by radiation through the material, hence giving rise to small increases in the overall retardation generated by the film.

Other types of birefringent films currently on the market include *biaxial* films that are stretched in two mutually perpendicular directions lying in the plane of the film and hence possess unique refractive indexes along all three axes. Such films display larger variations in retardation especially as a function of $\phi$, although the centrally symmetric optical performance of the material around the surface normal remains essentially unaltered. Both *positive* and *negative* retardation films are also available where the refractive indexes of the stretched optic axes are respectively less than and greater than that of the unstretched directions.

Birefringent films have been successfully employed in order to compensate for the angular variation of retardation produced by both *super-twist devices*[35, 36, 37, 38] and by $90^{o}$ TN cells when in the inactivated phase[39]. Here, two or more films are usually placed together with the thin liquid crystal layer between the polarising media. In order to ease the utilisation of such films, polarisers are now available on the market[40] that come ready laminated together with birefringent layers. Note that the retardation displayed by both these systems is centrally symmetric.

Calculations indicate[41] that the optical angular properties displayed by $90^{o}$ TN cells operating in the normally *white* mode and driven with high voltages exceeding that of the saturation point can be enhanced upon positioning of a negative type retardation film together with the cell and with the optic axis lying perpendicular to the plane of the material. However, little research has been conducted into the use of retardation films together with such cells activated by *reduced* voltages of less than $\pm$ 8 volts, it being these cells that are of interest as far as manufacturing fast, variable shade welding filters is concerned.

Figure 2.10 shows the retardation produced by a 4μm $90^{o}$ TN cell filled with the *Merck 6096* liquid crystal mixture operating in the normally white mode placed between crossed LC81 polarisers oriented at $0^{o}$ and $90^{o}$ as a function of the viewing angle. The cell is driven with a $\pm$ 6.0 volt 50Hz square wave and the inclination angular variation in planes respectively parallel and perpendicular to the entrance liquid crystal molecules and encapsulating the surface normal is investigated. A wavelength of 633nm from a helium-neon laser is used.

Retardation is measured via use of the *Sénarmont*[42, 43] configuration whereby two polarisers are crossed together with a quarter wave plate with its fast axis aligned along the initial polarisation direction all placed between a laser and a light detector such that a minimum in transmission is observed. Upon addition of the specimen between the two polarising media, the second polariser is rotated so as to regain

the minimum transmittance state. The amount of birefringence introduced by the sample is then obtained from the required rotation of the analyser element, θ using equation 2.2. By definition, a negative sense of optical activity is taken as corresponding to a positive value of birefringence.

**Figure 2.10: Retardation at λ = 633nm for a 4μm 90° TN cell driven at ± 6 volts as a function of inclination angle in planes parallel and perpendicular to the entrance liquid crystal molecules.**

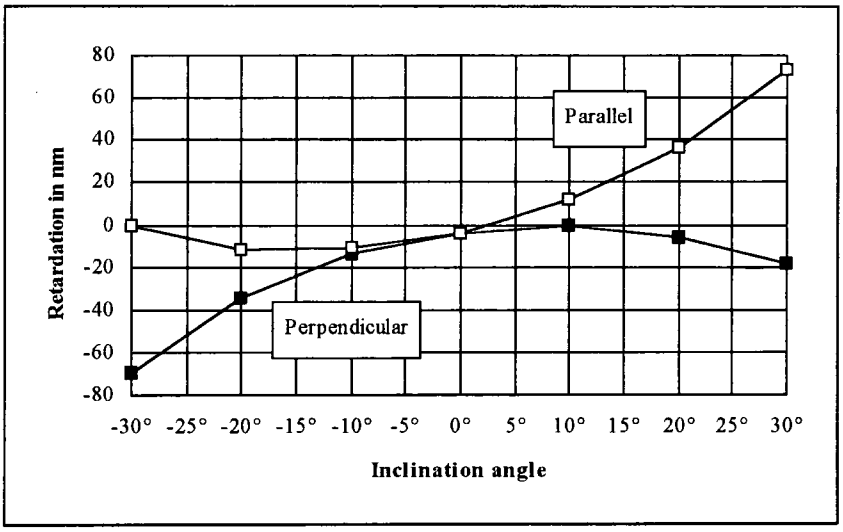


$$\text{Retardation} = \left(\frac{\theta.\lambda}{180}\right) \qquad (2.2)$$

Due to the incomplete orientation of the liquid crystal molecules with the cell activated at reduced voltages of less than ± 8 volts, the overall birefringence produced by the unit is strongly dependent upon the viewing angle and is highly asymmetric. Retardation films capable of offering a certain degree of compensation for this type of cell must therefore also reflect this symmetry.

The standard retardation films introduced above are all uniaxially or biaxially stretched in directions lying in the plane of the material and therefore possess predominantly symmetric birefringent properties centred around the surface normal. However, such a symmetry does not match that of the 90° TN cell when driven at reduced voltages and hence these films are not expected to offer any large degree of improvement as far as the overall optical angular properties of the cells are concerned. Note that at higher driving voltages exceeding that of the saturation voltage or with the 90° TN cell in the inactivated phase, complete molecular alignment generally occurs throughout the liquid crystal layer and hence the unit develops symmetric birefringent properties that more closely match those of the standard uniaxially or biaxially stretched retardation sheets introduced above. Use of such films might therefore offer some degree of improvement in such cases.

A type of retardation film that possesses optical properties corresponding more closely to the symmetry displayed by the 90° TN cell when in the partially activated state is introduced in figure 2.11. Here, the polycarbonate sheet is uniaxially stretched in a linear direction making an inclination angle of up to 20° with the surface normal. Such a material offers maximum birefringence when viewed at off-axis incident angles and hence would be capable of producing a certain amount of cell compensation for the poor optical angular properties displayed by the device. Note that due to current manufacturing difficulties, such films are not yet available on the market.

Other areas of development include liquid crystal polymer retarders[44] that can be customised with various values of twist and birefringence as well as films based on transparent pre-imidised polyimide materials spun deposited onto a substrate and cured by heating at 100°C in order to remove the solvent[45].

**Figure 2.11: Refractive index variation for the ordinary and extra-ordinary waves as a function of viewing angle for a sheet uniaxially stretched at an angle of 20° relative to the surface normal.**

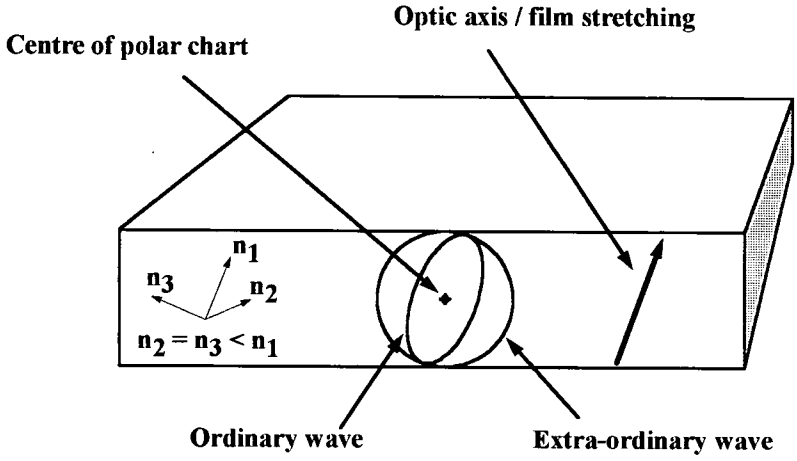


### *2.1.3 The Optical Angular Properties of Linear Polarisers.*

Note that it is not only the optical properties of the liquid crystal layer itself that are strongly dependent upon viewing angle, but also those of the polarising media. This is indicated in figure 2.12 which shows the optical angular properties of two crossed LC81 polarisers placed respectively parallel and perpendicular to the x-axis together with a standard I.F. It is seen that a *Maltese cross* pattern is obtained in the polar chart with the unit becoming significantly lighter when viewed at azimuth angles lying at 45° to the x and y-axes.

**Figure 2.12: Optical angular properties of two crossed *LC81* polarisers placed respectively parallel and perpendicular to the x-axis together with a standard I.F.**

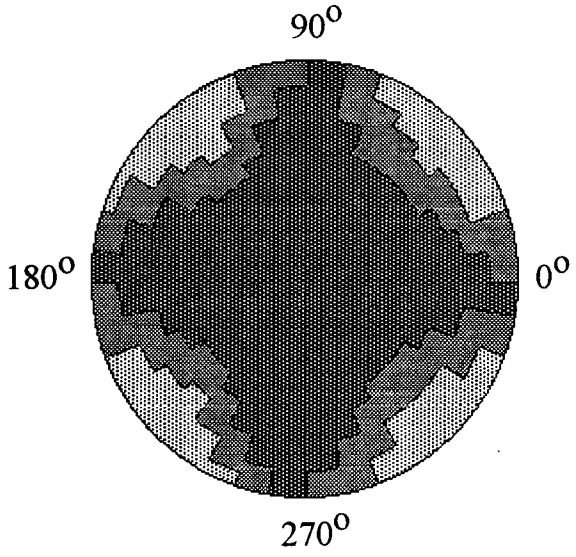


**Perpendicular LC81 polarisers together with a standard I.F. "Maltese Cross" pattern.**

These properties are best understood by considering the geometric arrangement outlined in figure 2.13. Here, mutually perpendicular axes are viewed from two different perspectives. The first corresponds to the system as seen along a direction lying normal to the axes plane, the second to that in which it is observed from a point lying above and to one side of this surface. In the latter case, the apparent perceived two dimensional angle between the axes is less than that of 90°. This results in a higher transmittance being observed for radiation incident upon crossed polarisers at such angles, producing the *Maltese cross* arrangement in the polar plot diagram. However, it is noted that although the polarisers themselves possess a certain degree of angular dependence due to such geometric effects, the variation in shade number as a function of viewing angle is very much less than that due to the liquid crystal layer itself and can therefore generally be ignored when considering the overall optical properties of complete welding filter designs.

Incidentally, the symmetry of the optical properties associated with crossed polarisers closely matches that displayed by standard uniaxially stretched birefringent films. It is therefore expected that the addition of such films together with the polarising sheets will produce a significant improvement in the angular properties displayed by the system.

**Figure 2.13: Geometric arrangement of mutually perpendicular axes observed from two different perspectives. The second angle perceives the axes as crossing at an angle of less than $90^{o}$.**

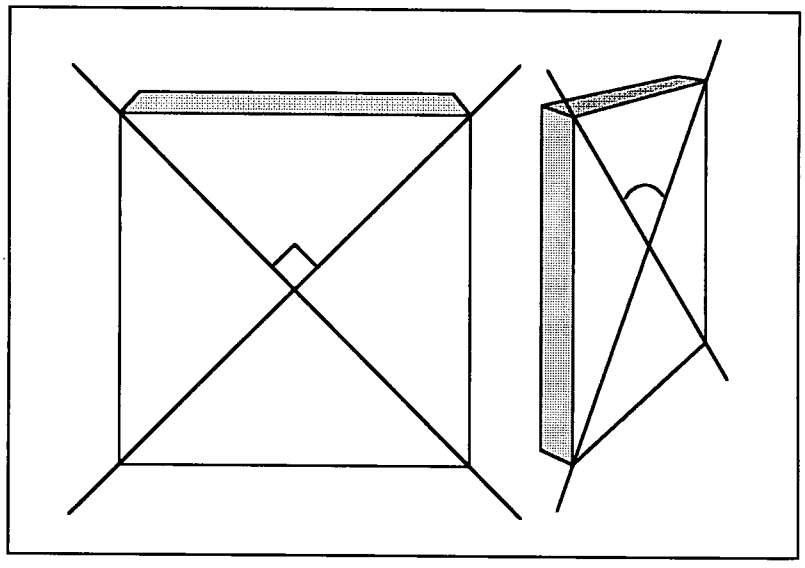

## *2.2 The Optical Properties of Liquid Crystal Cells when in the Inactivated Phase.*

When in the inactivated phase, light rotation occurs due to the inherent anisotropic index of refraction present in the twisted nematic liquid crystal material. The optical properties of such a system have been analysed by C.H. Gooch and H.A. Tarry[46] where the helical structure is considered as being a series of parallel, birefringent plates of thickness $\delta z$ lying in the $\underline{x}$-$\underline{y}$ plane. Each plate is rotated an angle $\delta\theta$ anti-clockwise around the $\underline{z}$-axis relative to the preceding one and light propagating through the system with components oscillating in two mutually perpendicular directions experiences retardation from the individual films. The net effect of the overall cell is found by summing the contributions from the separate layers and extrapolating to the limit of zero sheet thickness.

The original paper published by Gooch and Tarry considers the specific case of a twisted nematic liquid crystal cell operating in the normally *black* mode with the working polariser aligned parallel to the entrance liquid crystal molecules. This model is extended further in appendix two to cover the general case of a cell operating in the normally *white* mode placed between *crossed* polarisers oriented at an angle $\phi$ relative to the entrance molecular director. Only the main formulae used during the calculation are quoted in the following section and the reader is referred to appendix two for the specific details surrounding the calculation.

Incident light is represented by two mutually perpendicular components oscillating in the $\underline{x}'$ and $\underline{y}'$ local co-ordinate directions taken as being respectively parallel and perpendicular to the molecular axis present in each elemental layer. These components are described by the superposition of sinusoidal waves, indicated by equations 2.3 - 2.5.

$$E^{in}(\underline{r}) = E^{in}(\underline{x}')\ \underline{x}' + E^{in}(\underline{y}')\ \underline{y}' \quad (2.3)$$

$$E^{in}(\underline{x}') = f_A \sin \omega t + f_B \cos \omega t \quad (2.4)$$

$$E^{in}(\underline{y}') = f_C \sin \omega t + f_D \cos \omega t \quad (2.5)$$

A phase factor is introduced between the two components upon passage through the plate and with the assumption of zero energy absorption or light scattering taking place, equations can be obtained giving the evolution of the coefficients $f_A$, $f_B$, $f_C$ and $f_D$ as a function of $\underline{z}$ through the liquid crystal material. Applying the appropriate initial boundary conditions and recombining the components exiting the liquid crystal cell yields the overall optical throughput of the device.

With incident light initially polarised in a general direction making an angle $\phi$ relative to the entrance molecular director at $z = 0$, the boundary conditions of equations 2.6-2.8 apply giving the following equations in 2.11-2.14 for $f_A(z)$, $f_B(z)$, $f_C(z)$ and $f_D(z)$ respectively as a function of z. Here, $\theta$ is the overall twist-angle of the helical structure, $d$ the cell thickness, $\Delta n$ the anisotropy of the refractive index for the liquid crystal material, $\lambda$ the wavelength of radiation under consideration and $q$ an empirical function defined in equations 2.9 and 2.10.

$$\underline{E}^{initial}(\underline{r})_{z=0} = \cos\phi \,.\, \sin \omega t\ \underline{x}' + \sin\phi \,.\, \sin \omega t\ \underline{y}' \quad (2.6)$$

$$E^{initial}(\underline{x}')_{z=0} = \cos\phi \,.\, \sin \omega t\,, \qquad f_A^{z=0} = \cos\phi\,, \qquad f_B^{z=0} = 0\,, \quad (2.7)$$

$$E^{initial}(\underline{y}')_{z=0} = \sin\phi \,.\, \sin \omega t\,, \qquad f_C^{z=0} = \sin\phi\,, \qquad f_D^{z=0} = 0\,, \quad (2.8)$$

$$u = \left(\frac{\pi d \Delta n}{\theta \lambda}\right) \quad (2.9)$$

$$q = \left[1 + 2u^2 + 2u\sqrt{1 + u^2}\right]^{\frac{1}{2}} \quad (2.10)$$

$$f_A(z) = \left(\frac{1}{1+q^2}\right)\cos\left(\frac{q\theta z}{d}\right)\cos\phi + \left(\frac{-q}{1+q^2}\right)\sin\left(\frac{q\theta z}{d}\right)\sin\phi + \ldots\ldots$$

$$\ldots\ldots + \left(\frac{q^2}{1+q^2}\right)\cos\left(\frac{\theta z}{dq}\right)\cos\phi + \left(\frac{-q}{1+q^2}\right)\sin\left(\frac{\theta z}{dq}\right)\sin\phi \quad (2.11)$$

$$f_B(z) = \left(\frac{q}{1+q^2}\right)\cos\left(\frac{q\theta z}{d}\right)\sin\phi + \left(\frac{1}{1+q^2}\right)\sin\left(\frac{q\theta z}{d}\right)\cos\phi + \ldots\ldots$$

$$\ldots\ldots + \left(\frac{-q}{1+q^2}\right)\cos\left(\frac{\theta z}{dq}\right)\sin\phi + \left(\frac{-q^2}{1+q^2}\right)\sin\left(\frac{\theta z}{dq}\right)\cos\phi \qquad (2.12)$$

$$f_C(z) = \left(\frac{q^2}{1+q^2}\right)\cos\left(\frac{q\theta z}{d}\right)\sin\phi + \left(\frac{q}{1+q^2}\right)\sin\left(\frac{q\theta z}{d}\right)\cos\phi + \ldots\ldots$$

$$\ldots\ldots + \left(\frac{1}{1+q^2}\right)\cos\left(\frac{\theta z}{dq}\right)\sin\phi + \left(\frac{q}{1+q^2}\right)\sin\left(\frac{\theta z}{dq}\right)\cos\phi \qquad (2.13)$$

$$f_D(z) = \left(\frac{-q}{1+q^2}\right)\cos\left(\frac{q\theta z}{d}\right)\cos\phi + \left(\frac{q^2}{1+q^2}\right)\sin\left(\frac{q\theta z}{d}\right)\sin\phi$$

$$\ldots\ldots + \left(\frac{q}{1+q^2}\right)\cos\left(\frac{\theta z}{dq}\right)\cos\phi + \left(\frac{-1}{1+q^2}\right)\sin\left(\frac{\theta z}{dq}\right)\sin\phi \qquad (2.14)$$

The total luminous transmittance of the device, $T_{luminous}$ is found by integrating over the entire visible spectrum, shown in equation 2.15. Here, $y(\lambda)$ represents the standard relative sensitivity of the human eye and $T_{total}(d, \Delta n, \theta, \lambda, \phi)$ the wavelength dependent transmittance of the cell.

$$T_{luminous} = \frac{\int_{380}^{760} T_{total}(d, \Delta n, \theta, \lambda, \phi) * y(\lambda).d\lambda}{\int_{380}^{760} y(\lambda).d\lambda} \qquad (2.15)$$

For the specific case where the inactivated cell is operating in the normally *black* mode and where the working polariser is aligned *parallel* with the entrance liquid crystal molecules, the standard results introduced by Gooch and Tarry for the overall transmittance of the cell in directions lying respectively parallel and perpendicular to the exit liquid crystal molecules are obtained. These are reproduced in equations 2.16 and 2.17.

$$T_{parallel} = \frac{u^2 + \cos^2\left(\theta\sqrt{1+u^2}\right)}{1+u^2} \quad (2.16)$$

$$T_{perpendicular} = \frac{\sin^2\left(\theta\sqrt{1+u^2}\right)}{1+u^2} \quad (2.17)$$

These results indicate that it is only in the limit of large cell thickness where the *Mauguin* conditions[47] of equation 2.18 are satisfied that true light rotation occurs and that in general, the emerging radiation becomes elliptically polarised with components oscillating in directions lying both parallel and perpendicular to the exit molecular alignment director. These components suffer interference effects producing a series of fringes as the pertinent Δn.d parameter of the cell is changed. It therefore becomes necessary to optimise the cell thickness in order to maximise the overall optical transmittance of the device when in the inactivated phase.

$$\Delta n.d >> \frac{\theta.\lambda}{\Pi} \quad (2.18)$$

Figure 2.14 shows the magnitude of light components exiting a 90° TN cell aligned in directions respectively parallel and perpendicular to the exit liquid crystal molecules as a function of the Δn.d parameter. Incident radiation is taken as lying parallel to the entrance molecules and the assumption of no light absorption is reflected by peak transmittances approaching 100% for the parallel components in the limit of large cell thickness. Note that light absorption due to the presence of the polarisers is not taken into consideration and that a single wavelength of 550nm is used for the calculation.

The values of Δn.d giving maximum optical transmittance from a 90° TN cell operating in the normally *white* mode and when in the inactivated phase are predicted from equations 2.19 and 2.20. Due to the beneficial effects of minimising the Δn.d parameter of the device upon both the switching speed and the optical angular properties of the cell when in the activated state, it is therefore usual to manufacture liquid crystal cells that operate in the so-called *Gooch and Tarry first maximum* mode. For the standard 90° TN device, this lies at a Δn.d value of 0.476μm with a wavelength of 550nm and hence sets the lower limit for practical cell thicknesses when utilising this type of cell.

**Figure 2.14: Calculated transmittance of a 90° TN cell at a wavelength of 550nm in directions lying respectively parallel and perpendicular to the exit liquid crystal molecules as a function of Δn.d.**

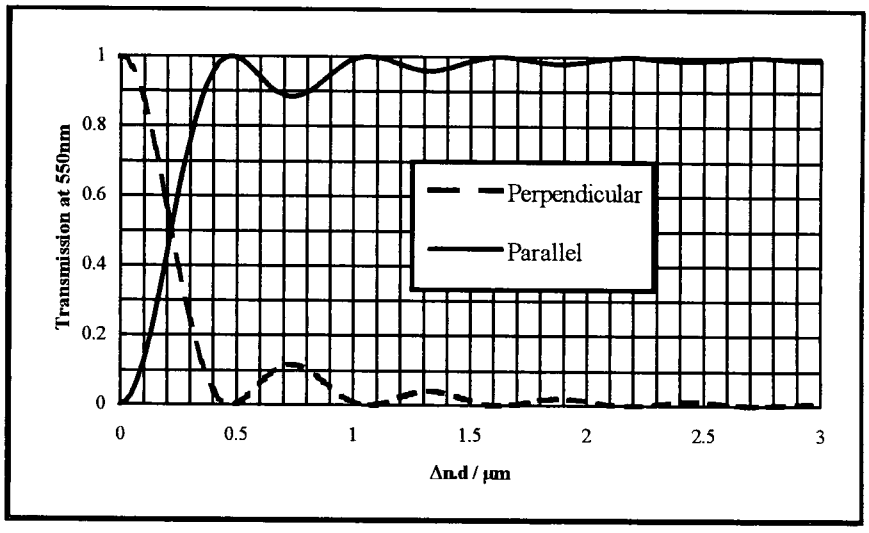


$$\Delta n.d_{maxima} = \left(\frac{\theta\lambda}{\pi}\right)\sqrt{\left(\frac{\pi m}{\theta}\right)^2 - 1} \qquad \text{for} \qquad \{n \in N\} \tag{2.19}$$

$$\Delta n.d_{maxima} = 0.275\sqrt{3}\ \mu m,\ 0.275\sqrt{15}\ \mu m,\ 0.275\sqrt{35}\ \mu m,\ 0.275\sqrt{63}\ \mu m,\ .....$$

$$\approx 0.476\ \mu m,\ 1.065\ \mu m,\ 1.627\ \mu m,\ 2.183\ \mu m,\ ..... \tag{2.20}$$

# *CHAPTER THREE*

*This chapter introduces the various international standards that regulate the manufacturing of automatically darkening welding filters in order to ensure their safety during operation. The newly compiled European Standard [4] is presented and the specific requirements as far as the optical properties are concerned are discussed in some detail. This standard builds the framework around which the engineer must design the glass pack and the desired performance of such devices are examined together with the short comings of filters that are currently on the market.*

## *3.1 Manufacturing Regulations of Automatically Darkening Welding Filters.*

Due to the absolute necessity to ensure the safety of workers carrying out welding processes and other related techniques, several national and international standards have been compiled in order to regulate the manufacturing of automatically darkening welding filters. These standards cover a wide range of aspects extending from the general mechanical strength of such filters to the specific optical characteristics required by the device. Whilst the robust nature of the filter is ensured by the material scientist and design engineers, these properties are not directly relevant as far as this thesis is concerned and hence little reference to this area will be made in the following sections. Instead, the *optical* requirements of the filters are analysed and information regarding this aspect is summarised in some detail.

A new European Standard[4] is presently being compiled that encapsulates information contained within the various individual standards currently circulated. It is expected that this standard will supersede all others in the next couple of years especially as far as the European markets are concerned and hence all data quoted in this report originates from this source.

## *3.2 The Transmittance Requirements of Welding Filters.*

The recommended shade numbers required for specific welding processes and other related techniques are summarised in table 1.5 of chapter one. Here, several different welding methods are investigated under various intensities of operation. It must be stressed that these values are for guidance only and that an adjacent shade number may be more appropriate depending upon the specific ambient lighting conditions of the working area.

Table 3.1 reproduces the information contained within section *EN 169: 1992* of the European Standard covering the transmittance of welding filters in the U.V, visible and I.R regions of the electromagnetic spectrum. These figures represent the maximum permissible optical throughputs at the relevant wavelengths for a temperature of $23^{o}C \pm 5^{o}C$ and apply for both automatically darkening and fixed shade

welding filters. However, it is also a requirement from section *EN 379: 1993* that a switchable shade filter satisfy the demands in both the light and dark optical states. In addition to this table, there are several other transmission requirements that are summarised below:

(a) For 210nm < $\lambda \leq$ 313nm, the spectral transmittance shall not exceed the value permitted for 313nm.
(b) For 313nm < $\lambda \leq$ 365nm, the spectral transmittance shall not exceed the value permitted for 365nm.
(c) For 365nm < $\lambda \leq$ 400nm, the spectral transmittance shall not exceed the luminous transmittance.
(d) For 400nm < $\lambda \leq$ 480nm, the spectral transmittance shall not exceed the value observed at 480nm.

**Table 3.1: Transmittance requirements of welding filters according to the European Standard.**

| Shade | U.V transmittance | | Luminous transmittance | | I.R |
|---|---|---|---|---|---|
| number | 313nm | 365nm | Maximum | Minimum | 780-1400nm |
| 2 | 0.0003 % | 14 % | 43.2 % | 29.1 % | 28 % |
| 2.5 | 0.0003 % | 6.4 % | 29.1 % | 17.8 % | 15 % |
| 3 | 0.0003 % | 2.8 % | 17.8 % | 8.5 % | 12 % |
| 4 | 0.0003 % | 0.95 % | 8.5 % | 3.2 % | 6.4 % |
| 5 | 0.0003 % | 0.3 % | 3.2 % | 1.2 % | 3.2 % |
| 6 | 0.0003 % | 0.1 % | 1.2 % | 0.44 % | 1.7 % |
| 7 | 0.0003 % | 0.05 % | 0.44 % | 0.16 % | 0.81 % |
| 8 | 0.0003 % | 0.025 % | 0.16 % | 0.061 % | 0.43 % |
| 9 | 0.0003 % | 0.012 % | 0.061 % | 0.023 % | 0.2 % |
| 10 | 0.0003 % | 0.006 % | 0.023 % | 0.0085 % | 0.1 % |
| 11 | 0.0003 % | 0.0032 % | 0.0085 % | 0.0032 % | 0.05 % |
| 12 | 0.0003 % | 0.0012 % | 0.0032 % | 0.0012 % | 0.027 % |
| 13 | 0.0003 % | 0.00044 % | 0.0012 % | 0.00044 % | 0.014 % |

Due to the fact that it is necessary for automatically darkening welding filters to fulfil these obligations in both the light and dark states, it becomes essential for the glass pack to contain some type of *interference filter (I.F)* that reflects back both U.V and I.R radiation at all times. The band width of such a filter must be limited to the luminous wavelengths making it difficult to manufacture filters possessing peak transmittances exceeding that of about 70%. In fact, this constitutes an area of continued research in an attempt to reach ever increasing overall optical throughputs. However, this work falls outside the scope of this thesis and the optical properties of the standard filter used throughout this report are merely quoted in figure 1.7 of chapter one.

The transmittance homogeneity across the surface of the filter when operating at a temperature of 23°C ± 5°C is also regulated by the European Standard. Here, the uniformity of the two visual areas for both the left and right eyes are determined. By definition, the visual areas consist of two 50mm circles centred on the horizontal halfway-line of the filter, 32mm each side of the mid-point. A 5mm nominal light beam is scanned across these areas measuring the luminous transmittance at each point. For each region, the largest absolute deviation from the central value is expressed as a percentage of that number, giving the factors $P_{left}$ and $P_{right}$. The percentage difference between the two visual centres is also calculated as a fraction of the largest value, yielding $P_{diff}$.

The maximum acceptable values for $P_{left}$, $P_{right}$ and $P_{diff}$ are given in section *EN 166: 1994* of the European Standard and are reproduced in table 3.2 for ease of reference. Manufacturers are obliged to mark their products according to the class specifications giving a big incentive for suppliers to develop the highest quality products possible. Note that the classification categories depend upon the overall optical throughput at the central point of the device and in general become broader as the transmittance of the filter is reduced.

**Table 3.2: Maximum permissible transmittance variation of welding filters over the two visual areas.**

| Central luminous transmittance | Variation of $P_{left}$ and $P_{right}$ | | | Variation of $P_{diff}$ | | |
|---|---|---|---|---|---|---|
| | Class 1 | Class 2 | Class 3 | Class 1 | Class 2 | Class 3 |
| 100 - 17.9 % | 5 % | 10 % | 15 % | 20 % | 20 % | 20 % |
| 17.8 - 0.44 % | 10 % | 15 % | 20 % | 20 % | 20 % | 20 % |
| 0.43 - 0.023 % | 15 % | 20 % | 30 % | 20 % | 20 % | 30 % |
| 0.022 - 0.0012 % | 20 % | 30 % | 40 % | 20 % | 30 % | 40 % |
| 0.0011 - 0.000023 % | 30 % | 40 % | 60 % | 30 % | 40 % | 60 % |

### *3.3 Lens Aberration Tolerances.*

The diffusion of light generated by welding filters is regulated by section *EN 166: 1994* of the European Standard and the method for measuring the spherical, astigmatic and prismatic aberrations is described in section *EN 167: 1994*. In principle, this is carried out with a telescope of magnification lying between ×10 and ×30 possessing an opening aperture of 20mm. The eye piece of the telescope incorporates a reticular and is focused onto the centre of an illuminated target positioned 4.60m ± 0.02m from the entrance aperture.

The target consists of an etched pattern shown in figure 3.1. The diameter of the two inner rings are 11.0mm ± 0.1mm and 23.0mm ± 0.1mm respectively with the line thicknesses being 0.6mm ± 0.1mm. The bars are of thickness 2.0mm and are 20.0mm long with a separation of 2.0mm.

**Figure 3.1: Illuminated target used to measure the optical aberration of lenses.**

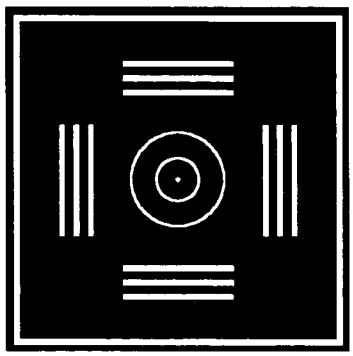

The test sample is introduced between the telescope and the target elements and the objective lens re-adjusted so as to obtain a clear image. The spherical refractive power of the device is determined from the amount of modification required. If astigmatism is present, the telescope is focused on each set of parallel bars in turn, giving the adjustment values $D_1$ and $D_2$. The spherical aberration is then taken as being the mean of these two values and the absolute difference gives the astigmatic power of the filter.

Upon placement of the sample between the telescope and target, the new position of the reticule is also noted. If this falls inside of the inner circle, the prismatic refractive power of the lens is less than that of $0.12 cm.m^{-1}$. A drifting of the reticule outside of the outer ring indicates that the filter has a prismatic aberration exceeding $0.25 cm.m^{-1}$. When analysing mounted oculars that cover both eyes, the difference in prismatic power for the two visual areas is determined. This is carried out with the unit mounted in front of the telescope as worn by the welder and the location of the reticule noted for each visual area. The horizontal and vertical displacements between the two positions are related to the variation in prismatic refractive power components along these axes. Note that there are two distinct values for the permissible horizontal difference in prismatic aberration depending upon whether the anisotropy between the left and right visual areas produces a focusing of incident parallel light before or after the plane of the eye retina. The spherical, astigmatic and prismatic aberrations of welding lenses are subject to the classification procedures outlined in section *EN 166:1994* of the European Standard, summarised in table 3.3.

**Table 3.3: Permissible tolerances for the optical aberration of lenses from the European Standard.**

| | Refractive Power | | Difference in Prismatic Power | |
|---|---|---|---|---|
| Optical Class | Spherical $(D1+D2)/2$ | Astigmatic $\lvert D1 - D2 \rvert$ | Horizontal (Before/After) | Vertical |
| 1 | $\pm 0.06\ m^{-1}$ | $0.06\ m^{-1}$ | $0.25 / 0.75\ cm.m^{-1}$ | $0.25\ cm.m^{-1}$ |
| 2 | $\pm 0.12\ m^{-1}$ | $0.12\ m^{-1}$ | $0.25 / 1.00\ cm.m^{-1}$ | $0.25\ cm.m^{-1}$ |
| 3 | $+0.12 / -0.25\ m^{-1}$ | $0.25\ m^{-1}$ | $0.25 / 1.00\ cm.m^{-1}$ | $0.25\ cm.m^{-1}$ |

### *3.4 Light Diffusion Requirements.*

The quantity of light scattering produced by an optical lens is regulated by section *EN 166: 1994*. Here, light diffusion is defined as the quantity of radiation that is deviated by an angle $\alpha$ upon passage through the device and is proportional to the incident light intensity. By dividing the ratio of these two by the overall transmittance of the lens in a direction lying parallel to the surface normal, the *reduced luminance* factor is obtained in units of candelas per square metre per lux ($cd.m^{-2}.lx^{-1}$).

The reduced luminance factor is a function of the deviation angle $\alpha$, and for optical filters possessing symmetrical scattering properties around the surface normal, the mean value is taken within angles limited by two cones of separation $\Delta\alpha$, indicated in figure 3.2. This average number varies with both $\alpha$ and $\Delta\alpha$ and as a standard, light scattered at angles of between $1.5^{o}$ and $2^{o}$ respectively is determined. The experimental apparatus used to make the measurements is not directly relevant to this report and the reader is directed to the above references if further information is required.

**Figure 3.2: Diffusion of light upon passage through an optical lens.**

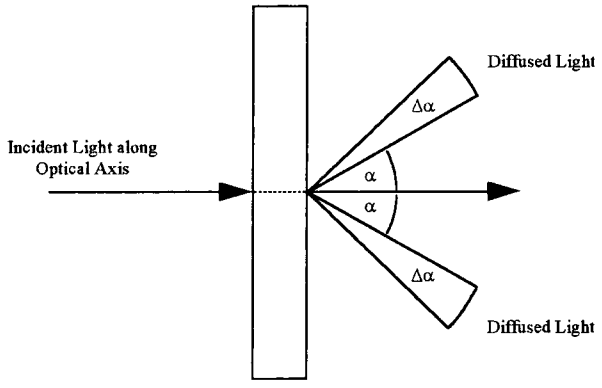


The quantity of diffused light is determined at both centres of the visual regions and are subject to the conditions of *EN 379:1993*, reproduced in table 3.4. Again, the manufacturer is obliged to clearly mark the product with the awarded grade for the optical properties of the unit.

**Table 3.4: Permissible quantity of light scattering generated by an optical lenses.**

| European Standard | Light Scattering |
|---|---|
| Class 1 | 1.00 $cd.m^{-2}.lx^{-1}$ |
| Class 2 | 2.00 $cd.m^{-2}.lx^{-1}$ |
| Class 3 | 3.00 $cd.m^{-2}.lx^{-1}$ |

The overall light scattering generated by a welding filter depends upon that produced by the individual elements themselves and in particular is highly sensitive to the cleanliness and quality of the sample surfaces as well as the type of liquid crystal cells in use. Any boundary between two media possessing different refractive indexes gives rise to a certain amount of radiation diffusion and since the refractive index is a function of the liquid crystal molecular orientation, the quantity of light scattering produced by the liquid crystal cell as a whole is a function of the driving voltage.

This is demonstrated in figure 3.3 which shows the magnitude of light diffusion generated by a double-cell construction using 4μm $90^0$ TN cells filled with the *Merck ZLI-4246 + 0.1% ZLI-811 (4246)* liquid crystal mixture and placed between LC81 polarisers oriented at $0^0$, $90^0$ and $0^0$ respectively. A standard I.F is present and the quantity of scattering measured as a function of the 50Hz square wave voltage applied to the cells. Two configurations are investigated, one with the cells placed in opposite orientations such that the face-to-face rub directions are crossed, the other with the two liquid crystal devices aligned similarly.

**Figure 3.3. Light scattering generated by double-cell structures as a function of driving electronics. 4μm $90^0$ TN cells filled with the *Merck 4246* liquid crystal are used together with a standard I.F.**

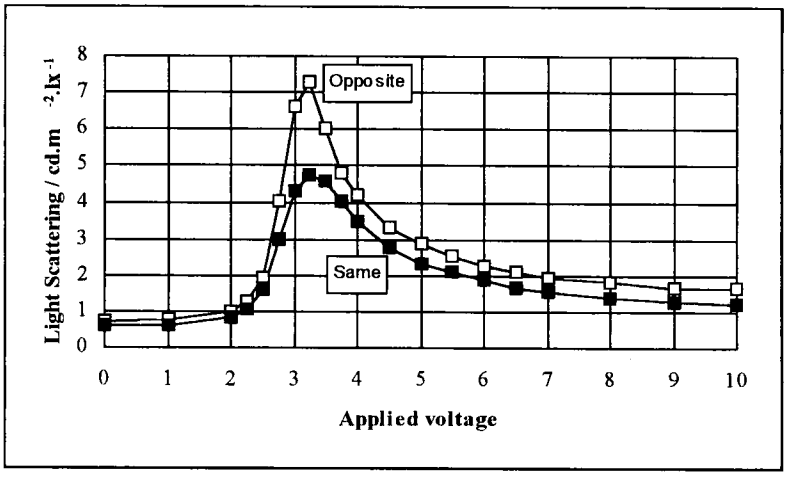


It is seen that there is a strong dependence of light scattering upon the driving voltage applied to the cells and in particular a large increase is observed with the cells operating at the lower end of the intermediate voltage range between ± 2.5 volts and ± 4 volts. Further increment of the electronics above this region produces a reduction in the overall light scattering of the unit. Experiments also indicate that the light scattering parameter is sensitive to the orientation of both the liquid crystal cells and the polarisers themselves making it imperative to develop theoretical models enabling the diffusion of radiation to be reduced to a minimum. This is an area of continued research that falls outside the scope of this thesis. Incidentally, the magnitude of light scattering is also shown to be independent of the driving *frequency* and hence is not related to the small rocking of the molecules upon polarity reversal of the liquid crystal cells themselves.

### *3.5 Response Times of Automatically Darkening Welding Filters.*

In the case of short term exposure to light, the perceived glare is approximately proportional to the product of the illuminance impinging on the eye and the duration of exposure. Since the darkening process of a liquid crystal shutter as a function of time is non-linear, it is therefore appropriate to define the switching speed of an automatically darkening welding filter as an integral of the optical transmittance over time and not merely by the time period taken for the unit to transmute between the two extreme states.

This is reflected in section *EN 379: 1993* of the European Standard and is re-iterated in figure 3.4. Here, the integrated area under the optical response curve between the 100% level and that possessing a transmittance of three times the lowest state achieved by the device is determined and divided by the maximum transmittance of the filter when in the light state in order to obtain units of time. Other definitions of switching speed also exist and many authors consider the period taken for the cell to pass between the 10% and 90% transmission levels as being representative of the reaction time for the device. However, this report will follow the guidelines set out by the European Standard and unless otherwise stated, all quoted values will be in accordance to this calculation.

**Figure 3.4: Switching time of a TN liquid crystal cell operating in the normally white mode from the light to the dark state according to the definition of the European Standard.**

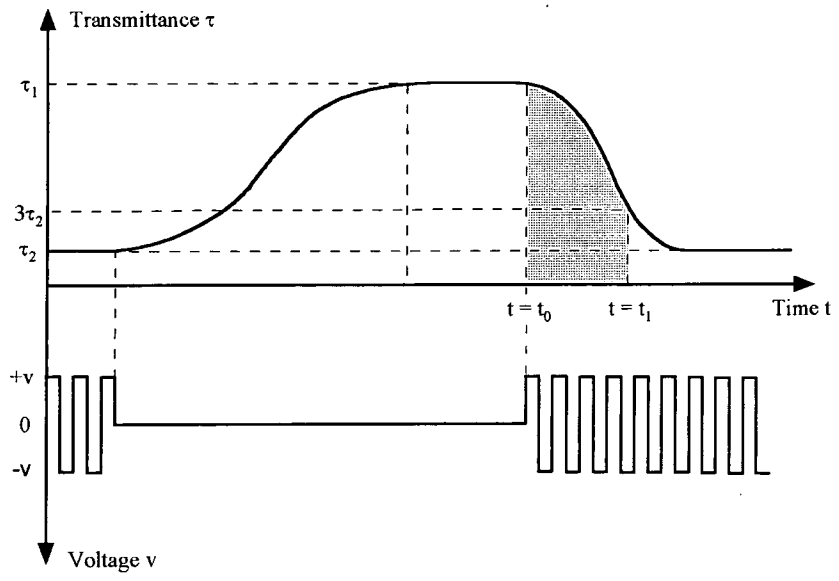

$$t_s = \frac{1}{\tau_1} * \int_{t=t_0}^{t=t_1(\tau=3*\tau_2)} \tau(t)\, dt$$

$t_s$ = switching time as defined by the European Standard.

$\tau_1$ = maximum transmittance when inactivated.

$\tau_2$ = minimum transmittance in the activated, state.

$t = t_0$ time at which cell activation begins.

$t = t_1$ time at which the transmittance reduces to $3\tau_2$.

The maximum permissible response times of automatically darkening welding filters operating from the light to the dark state are required to satisfy the stipulations set out in this section of the European Standard. These are reproduced in table 3.5 for ease of reference. These criteria apply at temperatures of both -5°C ± 2°C and at 55°C ± 2°C respectively. However, when utilising liquid crystal technology switching times become inflated at reduced temperatures. It is therefore only necessary to measure that for the lower temperature as compliance at this point ensures that the standard as a whole is satisfied. Note that if the unit fails the demands at -5°C but passes at 10°C, there is an option to market the product on the proviso that the device is not to be operated below this temperature.

**Table 3.5: Response time requirements of automatically darkening welding filters switching from the light to the dark state according to the European Standard.**

| Switching to dark state shade number | Switching from light state shade number | | | | | | |
|---|---|---|---|---|---|---|---|
| | 1.7 | 2 | 2.5 | 3 | 4 | 5 | 6 |
| 7 | 300 ms | 400 ms | 500 ms | 700 ms | 1000 ms | - | - |
| 8 | 100 ms | 150 ms | 200 ms | 300 ms | 500 ms | 1000 ms | - |
| 9 | 40 ms | 50 ms | 70 ms | 100 ms | 200 ms | 400 ms | 700 ms |
| 10 | 20 ms | 20 ms | 30 ms | 40 ms | 70 ms | 100 ms | 300 ms |
| 11 | 6 ms | 7 ms | 10 ms | 15 ms | 30 ms | 50 ms | 100 ms |
| 12 | 2 ms | 3 ms | 4 ms | 5 ms | 10 ms | 20 ms | 40 ms |
| 13 | 0.8 ms | 1 ms | 1.5 ms | 2 ms | 4 ms | 7 ms | 10 ms |
| 14 | 0.3 ms | 0.4 ms | 0.5 ms | 0.7 ms | 1 ms | 3 ms | 5 ms |
| 15 | 0.1 ms | 0.15 ms | 0.2 ms | 0.3 ms | 0.5 ms | 1 ms | 2 ms |
| 16 | 0.04 ms | 0.05 ms | 0.07 ms | 0.1 ms | 0.2 ms | 0.4 ms | 0.7 ms |

### *3.6 General Requirements of Automatically Darkening Welding Filters.*

The remaining pertinent requirements set out in the European Standard referring to mechanical strength and robustness of the filter are of little relevance to this report which, in general will concentrate only upon the optical properties of such devices. The reader is therefore directed towards the appropriate references if further information is required. The existence of this standard sets the frame work around which the design of the glass pack must be developed.

In order to manufacture a variable shade, automatically darkening welding filter based on liquid crystal technology, it is necessary to operate the cells in the intermediate voltage range where the transmittance is a function of the applied driving electronics. In addition to this, the switching time requirements ensures that at least one cell included in the construction is operating in the normally *white* mode, hence providing fast response times from the light to dark states. However, in doing so the poor optical angular properties afforded by such devices when stimulated at reduced voltages become apparent in the overall characteristics of the welding filter as a whole when in the dark state. Use of liquid crystal cells functioning in the normally *black* mode somewhat alleviates these problems, but this is at the expense of the switching speed and in general there is a trade off between the two.

In practice, due to the marketing requirements of manufacturing the fastest filters possible, the reaction time is not usually compromised and consequently the majority of welding filters currently on the market suffer significantly from their poor angular dependence. This subject is discussed further in chapters four and five where novel techniques in order to improve the overall optical angular properties of liquid crystal cells operating in the normally white mode and driven at reduced voltages are investigated.

The transmittance obligations in both the light and dark states also require the necessity for incorporating some type of static optical filter is incorporated into the design of the glass pack that is capable of reflecting back both U.V and I.R radiation at all times. For this purpose, an interference filter is generally used and due to the band width restrictions of such a device to that of the visible wavelengths only, it is difficult to obtain filters possessing luminous transmittances exceeding that of around 70%. The optical properties of a typical interference filter together with the details concerning their construction are covered in section 1.7.5 of chapter one. This sets a limit to the highest overall optical throughput attainable by the glass pack when in the light state.

An ongoing manufacturing goal is to develop welding filters possessing increasingly higher transmittances when in the light state, hence enhancing a worker's field of view prior to operation. The vast majority of filters currently on the market attain a shade number 4, although there is a move towards developing new glass packs capable of reaching down beyond a shade number 3. Use of polarisers possessing higher optical transmittance together with lighter interference filters helps towards this end, although it is also essential to optimise both the intrinsic parameters of the liquid crystal cell so that the *Gooch and Tarry first maximum* position is satisfied and the orientation alignment of the polarisers. This point is discussed further in chapter five.

Although not a requirement in the European Standard, from a marketing point of view it is desirable to ensure that upon malfunction of the controlling electronics, the glass pack is not left in a potentially hazardous, high transmittance state but reverts back to a fail-safe, darker situation. This also aids the operator by converting from the "*off*" state to that of the light phase prior to the commencement of usage, hence indicating that the unit is responding. The European Standard also stipulates that the maximum shade number difference between the inactivated condition and the dark, welding state must not exceed more than 9 shade numbers. A filter that attains a shade number 4 when in the inactivated phase can therefore only be used down towards a shade 13. However, a glass pack that reaches a shade number 3 instead would be unsuitable for operation below that of a shade number 12. The development of a fail-safe shade step would therefore help to alleviate these problems.

The fail-safe shade step is defined as being the shade number difference between the light state and that of the inactivated phase and is generally provided for via use of *Guest-Host (GH)* liquid crystal cells. However, this adds both expense and weight to the welding filter helmet and techniques to achieve a safe-state shade step without the incorporation of additional cells into the glass pack are investigated in chapter six.

Other general requirements to ensure the competitiveness of the product include battery life and pricing. The electronics and liquid crystal cells account for about 30% and 70% respectively of the overall power drain generated by the device. Whilst that of the electronics can be minimised via use of low voltage components, the current consumption of liquid crystal cells is proportional to the driving frequency, the reciprocal of the cell thickness and the applied voltage. The first two are limited by the onset of perceived cell flickering and the switching time requirements respectively. However, as far as the power consumption is concerned it is advantageous to keep the operating range of the liquid crystal elements to the lower part of the intermediate voltage region.

By overcoming the chemical degradation processes that occur when a liquid crystal cell is stimulated at low frequencies below that of 0.1Hz, the effective power drain of the cell is reduced to an absolute minimum giving rise to the possibility of operating cells at voltages exceeding that of ± 10 volts. This offers advantages in terms of both the optical angular properties of the device and the light scattering generated by the filter. Further research is being conducted in this area.

In order to maximise cell contrast enabling the filter to achieve dark welding states in excess of shade number 13 and also to keep the working voltage to a minimum, it is necessary to sandwich the cells between polarisers that are oriented exactly perpendicularly relative to each other when operating in the normally white mode. Note that this is in fact the only constraint introduced into the theoretical model expanded in appendix two for the general transmittance of liquid crystal cells when in the inactivated phase.

Finally, by simplifying the voltages necessary in order to operate the glass pack, the complexity of the controlling electronics can be reduced to a minimum in order to keep prices low. Use of the double-cell arrangement introduced in figure 2.6 of chapter two not only enables the cells to be driven together from the same electrical output, but also facilitates the overall manufacturing processes of the filter by reducing

the number of unique liquid crystal elements incorporated into the design. Indeed, the vast majority of automatically darkening, variable shade welding filters that currently command a significant portion of the World's market are based on this concept and consequently are afflicted by the poor optical angular properties afforded by such systems. This will be the subject of chapters four and five.

# CHAPTER FOUR

*This chapter investigates the optical angular properties displayed by the standard 90$^{o}$ TN cell when operating in the normally white mode and shows that a large degree of improvement can be obtained by rotation of the crossed polarisers away from the orthodox configuration whereby they are oriented either parallel or perpendicular to the entrance and exit liquid crystal molecules of the cell. However, this is at the expense of the light state transmittance when the cell is in the inactivated phase, an effect that is highly undesirable as far as developing automatically darkening welding filters is concerned. The final sections introduce the concept of low-twist (LT) cells and their beneficial effects upon the angular dependence of a double-cell structure is shown. However, once again an increase in the light state shade number is observed when the polarisers are held in the standard 0$^{o}$/90$^{o}$ arrangement.*

## *4.1 The Optical Angular Properties of 90$^{o}$ TN Cells.*

The optical angular properties of a conventional double-cell arrangement are shown in figure 2.7 of chapter two. Here, 4μm 90$^{o}$ TN cells filled with the *Merck 3700* liquid crystal mixture are used and are placed between crossed LC81 polarisers oriented either parallel or perpendicular to the entrance and exit liquid crystal molecules of the two cells. Here, an *iris* pattern is observed in the polar plot diagram, this being characteristic of such designs wherein the dark viewing cones for the two oppositely oriented cells overlap. However, at larger inclination angles exceeding that of 20$^{o}$, the filter still becomes significantly lighter, a problem that is particularly apparent upon application of a higher driving voltage in order to obtain more cell contrast. This is rationalised by remembering that the dark viewing cone for a single cell moves towards the centre of the polar chart as the stimulating voltage is increased, hence becoming more centrally symmetric. Glass packs based on this design therefore inherently possess poor optical angular properties.

Two schemes exist in order to improve the attributes of such an arrangement. The first involves making the optical angular properties of a single cell as centrally symmetric as possible before building the double-cell construction, thereby producing an overall filter possessing a large central viewing cone. The second involves making the characteristics of a single cell as asymmetric as possible and then connecting two such devices together in such a way so as to provide a large degree of cell compensation. The first technique can be achieved by reduction of the pertinent Δn.d parameter of the liquid crystal cell and maximising the applied voltage, but in practice the results still remain inadequate. However, that of the second scheme appears more promising and will therefore be the subject of investigation in the proceeding sections of chapters four and five.

The standard design uses 90$^{o}$ TN cells placed together with high efficient polarisers oriented at either 0$^{o}$ and 90$^{o}$ or at 90$^{o}$ and 180$^{o}$ so as to be respectively perpendicular or parallel to the entrance and exit

liquid crystal molecules. Note that in practice there is little difference between the optical angular properties displayed by these two configurations and that for the perpendicular case is shown in figure 4.1.

**Figure 4.1: Negative twisting 90$^0$ TN cell placed between crossed polarisers oriented at 0$^0$ and 90$^0$.**

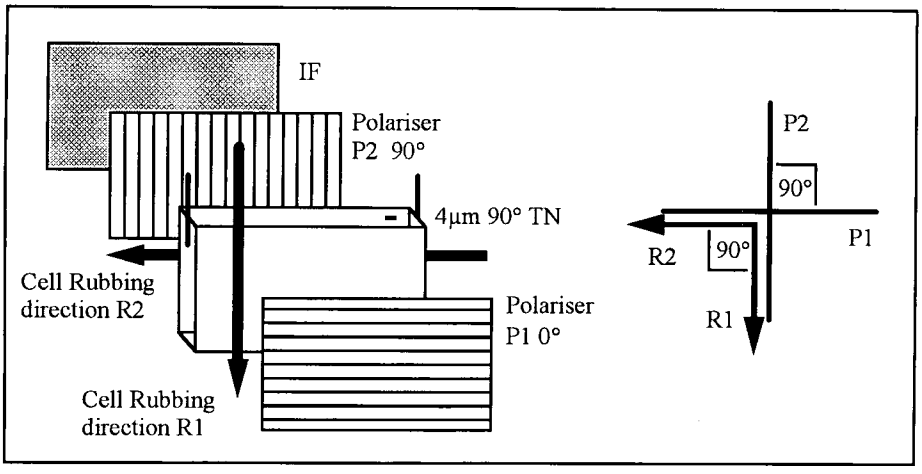


The use of two polarisers, P1 and P2, placed perpendicularly relative to each other ensures that maximum cell contrast is obtained from the device. The effect of rotating the crossed polarisers relative to the cell upon the optical angular properties of the system is shown in figure 4.2. Here, 4μm 90$^0$ TN cells filled with the *Merck 3700* liquid crystal mixture are used and are driven with a ± 4 volt square wave operating at 50Hz. The LC81 polarising material is employed and a standard I.F is present.

**Figure 4.2: Effect of rotating the crossed polarisers upon the optical angular properties of a 4μm 90$^0$ TN cell with the *Merck 3700* crystal. The cell is driven with a ± 4 volts 50Hz square wave.**

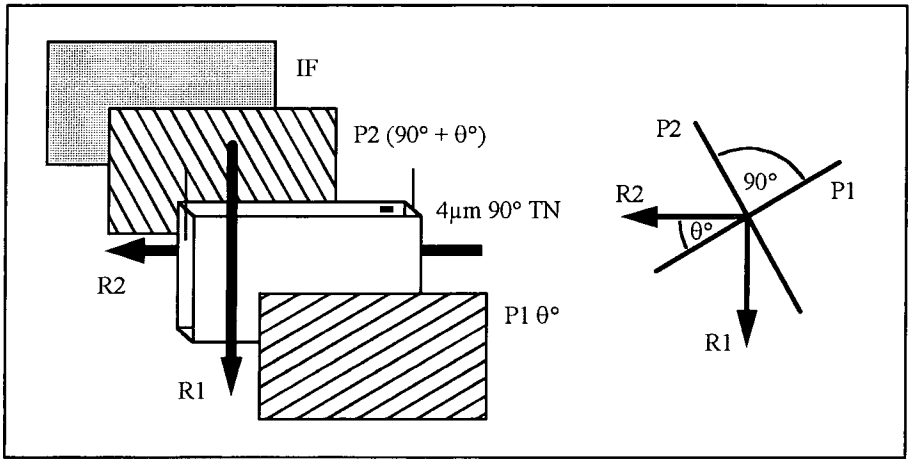

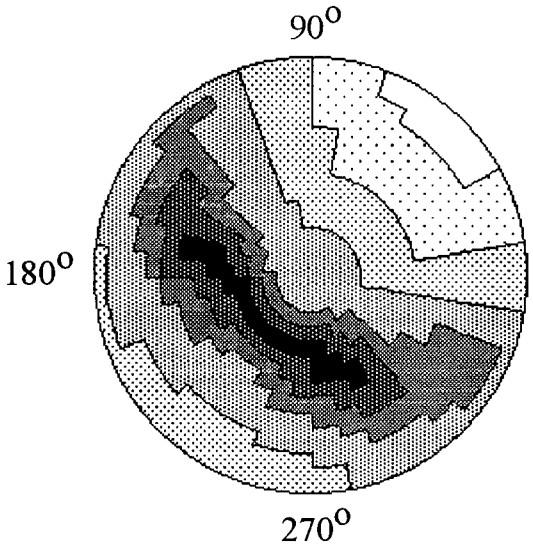


**4μm 90° TN cells crossed between 2 LC81 polarisers cut at 0° and 90°**

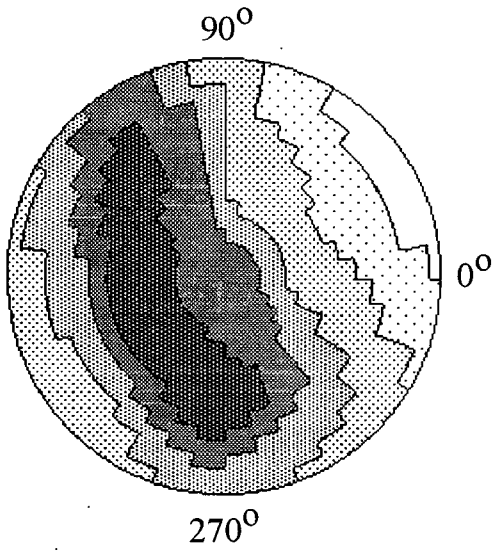


**4μm 90° TN cells crossed between 2 LC81 polarisers cut at 10° and 100°**

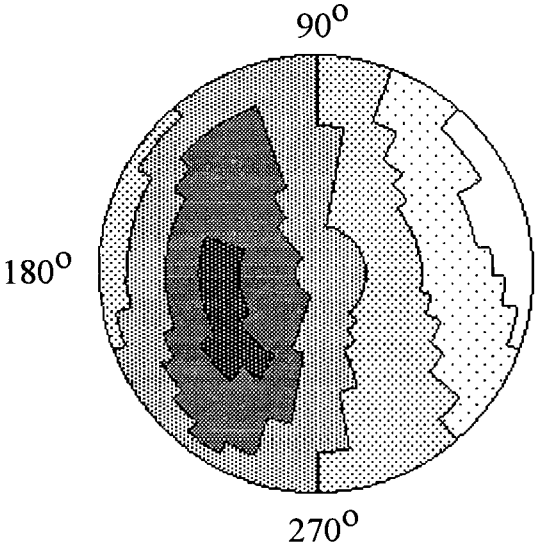


**4μm 90° TN cells crossed between 2 LC81 polarisers cut at 20° and 110°**

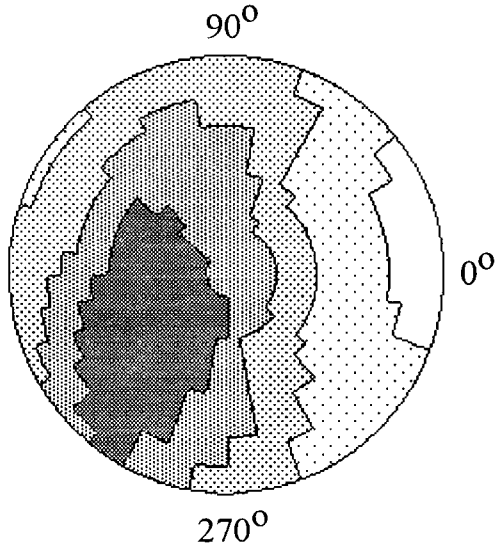


**4μm 90° TN cells crossed between 2 LC81 polarisers cut at 30° and 120°**

Rotation of the polarisers away from the conventional $0^{o}/90^{o}$ arrangement towards a $20^{o}/110^{o}$ configuration reduces the intensity and increases the overall area depicting the dark viewing cone in the polar plot diagram. Further movement beyond this point causes the dark band to reduce in length and develop across one corner of the cell, thereby making the device less suitable for incorporation into a double-cell design in which a large degree of cell compensation is required. Polariser rotation over the $45^{o}/135^{o}$ mark essentially reverses the process so that the angular properties of the $90^{o}/180^{o}$ configuration are identical to those for the $0^{o}/90^{o}$ arrangement. A certain degree of improvement in the angular dependence of an automatically darkening welding filter is therefore acquired upon rotating the polarisers approximately $20^{o}$ away from the standard orientation.

The contrast obtained in a direction lying parallel to the surface normal from a 4μm 90$^{0}$ TN cell filled with the *Merck 3700* liquid crystal mixture as a function of the polariser orientation is shown in figure 4.3. Here, contrast is defined as the shade number step observed upon switching of the cell between 0 volts and a ± 10 volts 50Hz square wave. The angle between the first polariser and the entrance molecular alignment director is recorded and the LC81 polarising material is used. A standard I.F is present.

**Figure 4.3: Cell contrast obtained from a 4μm 90$^{0}$ TN cell filled with the *Merck 3700* liquid crystal mixture as a function of the crossed *LC81* polariser orientation. A standard I.F is present.**

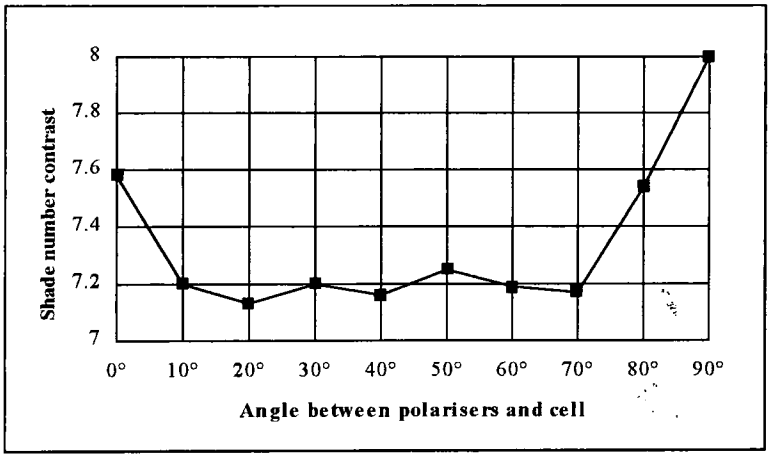


Maximum contrast is obtained with the polarisers aligned *parallel* to the entrance and exit liquid crystal molecules, although sufficiently high contrast is still maintained with the polarisers oriented *perpendicularly* to these axes. At intermediate angles, small losses of contrast are observed although a shade number step of over 7.2 is nevertheless achieved for the 45$^{0}$/135$^{0}$ configuration. Note that this still remains at adequate levels for incorporation into fully functional welding filter designs.

The light state shade number attained by the 4μm 90$^{0}$ TN cell operating in the normally white mode and when in the inactivated phase is displayed in figure 4.4 as a function of the polariser orientation. It is shown that the cell becomes steadily darker as the polarisers are moved away from the standard configuration whereby they are aligned either parallel or perpendicular to both the entrance and exit liquid crystal molecules and the light state shade number rises 0.14 shade numbers in going from the 0$^{0}$/90$^{0}$ to a 45$^{0}$/135$^{0}$ arrangement. Since an on-going manufacturing goal is to improve the overall optical throughput of automatically darkening welding filters when in the light state, such a loss in overall transmission is highly undesirable.

**Figure 4.4: Light state shade number as a function of the crossed *LC81* polariser orientation for a 4μm 90° TN cell with the *Merck 3700* liquid crystal mixture. A standard I.F is present.**

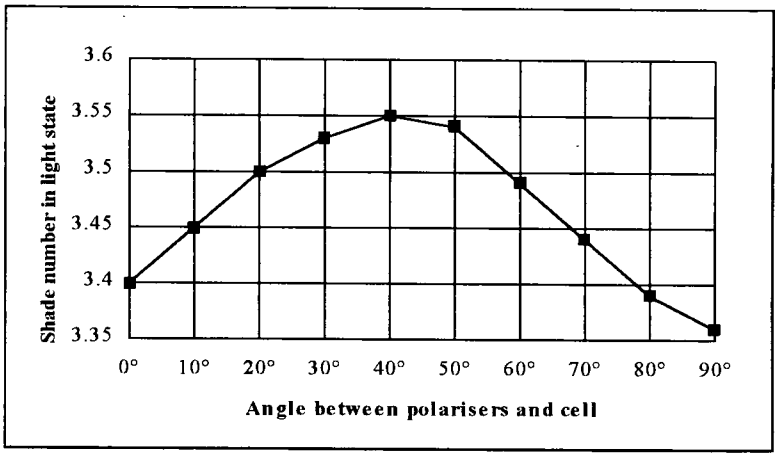


Figure 4.5 compares the optical angular properties of double-cell structures using 4μm 90° TN cells filled with the *Merck 3700* liquid crystal mixture with various polariser orientations. Crossed LC81 polarisers are used in order to maximise cell contrast. The cells are driven together with a 50Hz square wave voltage so as to obtain a shade number 10 and a standard I.F is present. As predicted, a strong improvement in the overall optical angular properties of the filter as a whole is observed for the 20°/110°/20° design. However, this is at the expense of the overall light state transmittance of the device.

**Figure 4.5: Effect of polariser rotation upon the optical angular properties of double-cell structures using 4μm 90° TN cells filled with the *Merck 3700* liquid crystal. Shade number 10.**

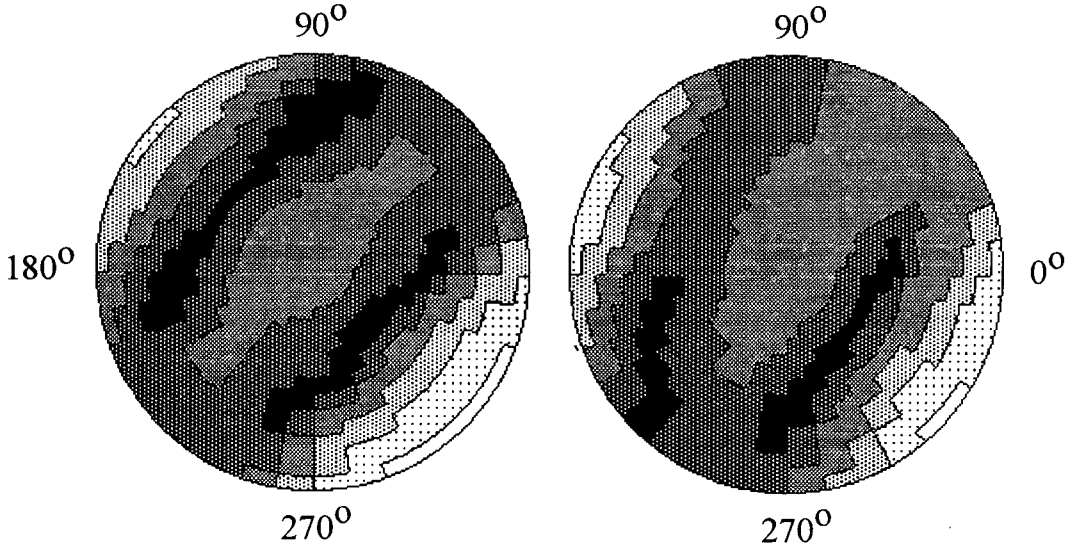


**Double cell structure using 4μm 90° TN cells crossed between polarisers cut at 0°, 90° and 0°**

**Double cell structure using 4μm 90° TN cells crossed between polarisers cut at 10°, 100° and 10°**

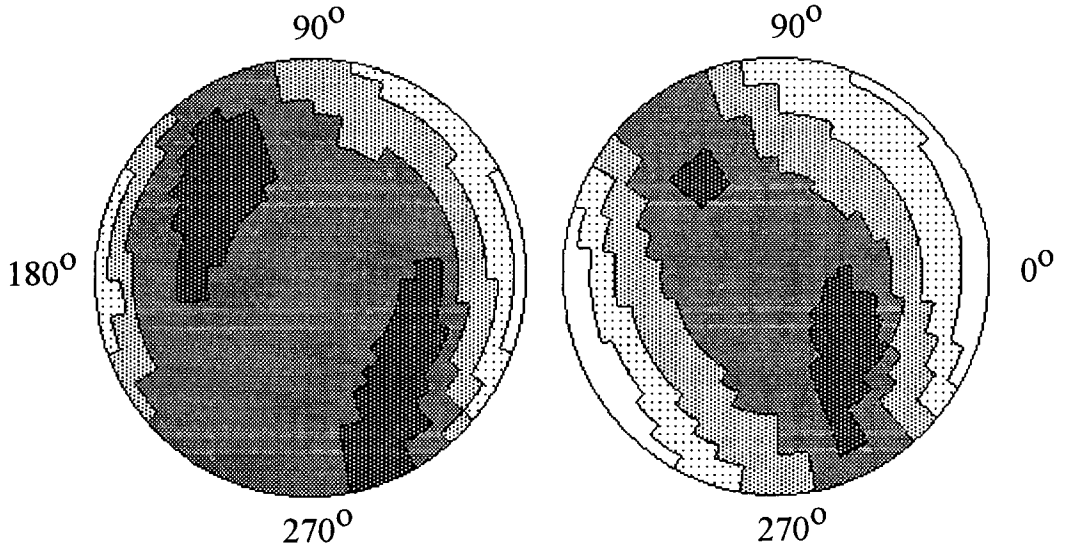


**Double cell structure using 4μm 90° TN cells crossed between polarisers cut at 20°, 110° and 20°**

**Double cell structure using 4μm 90° TN cells crossed between polarisers cut at 30°, 120° and 30°**

This effect is analysed further in figure 4.6 where the $20^0/110^0/20^0$ design is compared to that of the standard $0^0/90^0/0^0$ arrangement. Here, complete welding filter designs are investigated using double-cell structures consisting of 4μm $90^0$ TN cells filled with the *Merck 3700* liquid crystal mixture together with both a standard GH cell and an I.F. The two $90^0$ TN cells are driven together so as to attain a shade number 10. Note that the GH cell is inactivated when in the dark, low transmittance state.

**Figure 4.6: Optical properties of welding filters using 4μm $90^0$ TN cells with the *Merck 3700* crystal and polarisers cut at $0^0/90^0/0^0$ and $20^0/110^0/20^0$. A GH cell and I.F are present. Shade 10.**

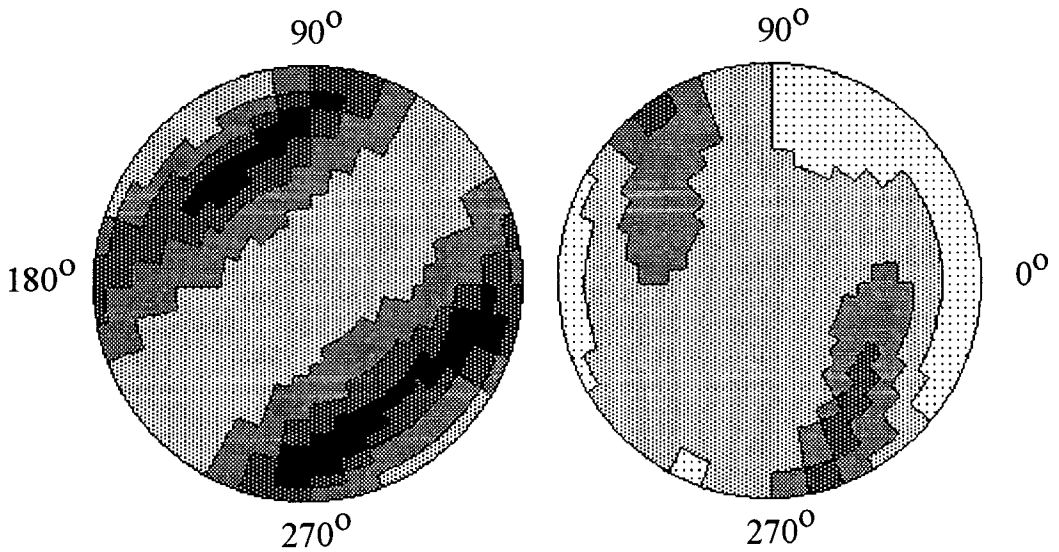


**Double cell structure using 4μm 90° TN cells with LC81 polarisers at 0°, 90°, 0°. A GH cell and IF are present**

**Double cell structure using 4μm 90° TN cells with LC81 polarisers at 20°, 110°, 20°. A GH cell and IF are present**

A strong improvement in the optical angular properties of the unit are observed upon formation of the non-standard design. However, due to the increase in shade number when in the *inactivated* phase upon rotation of the polarisers away from the $0^o/90^o$ alignment, the welding filter is up to 0.40 shade numbers darker when in the light state than that of the standard arrangement. This is clearly unacceptable if a competitive product is to be developed.

### *4.2 The Optical Angular Properties of Low-Twist (LT) Cells.*

The standard liquid crystal cells used in the vast majority of automatically darkening welding filters currently on the market possess a helical twist-angle of $90^o$ when in the inactivated phase. However, by careful control of the manufacturing processes, other twist angles can also be induced. The structure of a *low-twist (LT)* cell that boasts a twist-angle of less than that of $90^o$ was introduced in figure 1.2 of chapter one. The effect of using such cells upon the optical angular properties of the system are investigated in figure 4.7. Here, 4μm cells filled with the *Merck 3700* liquid crystal mixture and possessing twist angles ranging from $90^o$ down towards $60^o$ are studied. The cells are placed between crossed LC81 polarisers oriented at $0^o$ and $90^o$ respectively so that the working polariser is aligned perpendicularly to the *entrance* liquid crystal molecules and the cell is driven with a ± 4 volts square wave pulse operating at 50Hz. A standard I.F is present.

**Figure 4.7: Optical Properties of 4μm LT cells with the *Merck 3700* crystal placed between *LC81* polarisers at $0^o$ and $90^o$ as a function of twist-angle. Cell driven with ± 4 volts square wave.**

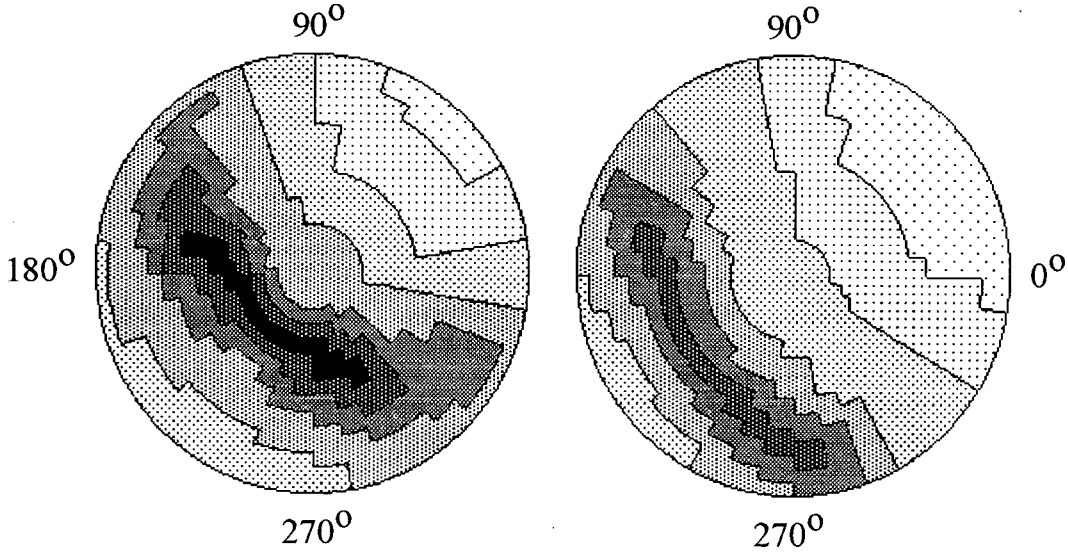


**4μm 90° TN cell crossed between 2 LC81 polarisers cut at 0° and 90°**

**4μm 80° LT cell crossed between 2 LC81 polarisers cut at 0° and 90°**

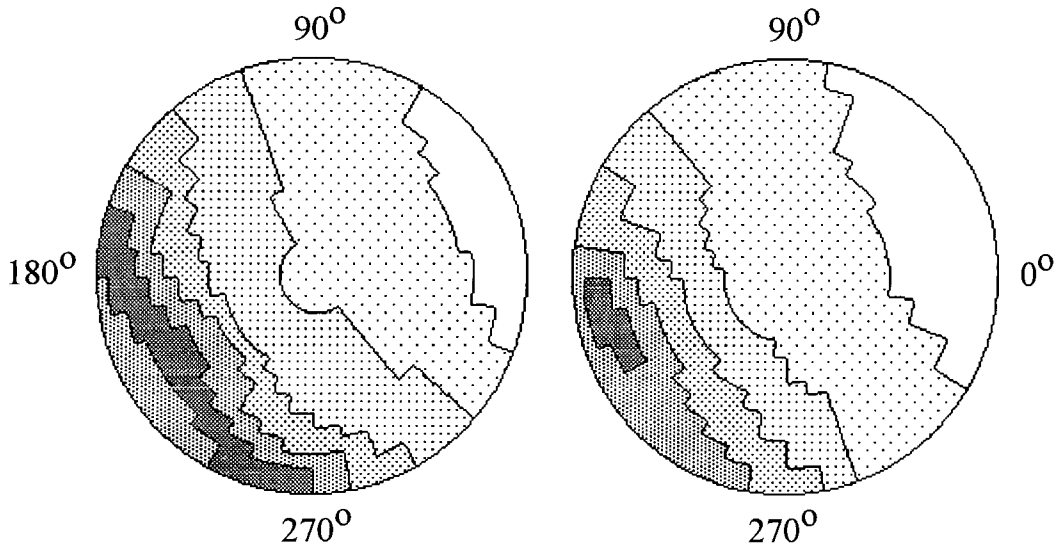


**4μm 70° LT cell crossed between 2 LC81 polarisers cut at 0° and 90°**

**4μm 60° LT cell crossed between 2 LC81 polarisers cut at 0° and 90°**

A reduction of the twist-angle causes the dark, off-axis viewing cone to reduce in intensity and shift away from the centre of the polar chart, producing highly asymmetric cells. This is particularly apparent for cells possessing twist-angles of below $60^{o}$ and when driven with low voltages of under $\pm$ 4 volts. As is also the case for the $90^{o}$ TN device, the dark band displayed by LT cells moves towards the centre upon increment of the stimulating voltage, although the cell becomes significantly less sensitive to this effect upon twist-angle reduction.

This phenomenon is quite general for nematic type liquid crystal cells activated at reduced voltages irrespective of both the liquid crystal component and the nature of the polarising material in use. The dark band in the polar chart arises due to the incomplete alignment of the bulk liquid crystal molecules parallel with the electric field when stimulated at low voltages. Instead, they remain tilted with some angle away from the surface normal and it is only in this direction that the unit possesses minimal retardation. Increment of the driving electronics enhances the molecular alignment forces resulting in a reduction in the tilt angle away from the surface normal and the dark cone is therefore seen to move towards the centre of the polar chart.

Such asymmetric cells are ideal candidates for incorporation into double-cell designs whereby a large degree of cell compensation is required. This is demonstrated in figure 4.8 where the optical angular properties of complete welding filter glass packs are shown as a function of the twist-angle in the cell. A standard I.F and GH cell are present. The 4μm LT cells are driven together with a 50Hz square wave so as to attain a shade number 13 and the LC81 polarisers are held at $0^{o}$, $90^{o}$ and $0^{o}$ respectively. Note that the GH cell is in the inactivated phase when the unit is in the dark state.

Reduction of the twist-angle causes the optical properties of the single cell to become more asymmetric, hence the overall angular dependence of the fully compensated welding filter design using two such cells placed in opposite orientations is improved. The progress step is relatively small in moving from a twist-angle of $90^{o}$ down to that of $80^{o}$, the largest developments coming from hopping between $80^{o}$ and $70^{o}$ and again from $70^{o}$ down to $60^{o}$. The optical properties of the filter with the $60^{o}$ and the $50^{o}$ cells are found to be largely similar indicating that the cells become less sensitive to this effect at lower twist-angles.

**Figure 4.8: Optical angular properties of complete welding filter glass packs using 4μm cells filled with the *Merck 3700* liquid crystal as a function of twist-angle in the cell. Shade number 13.**

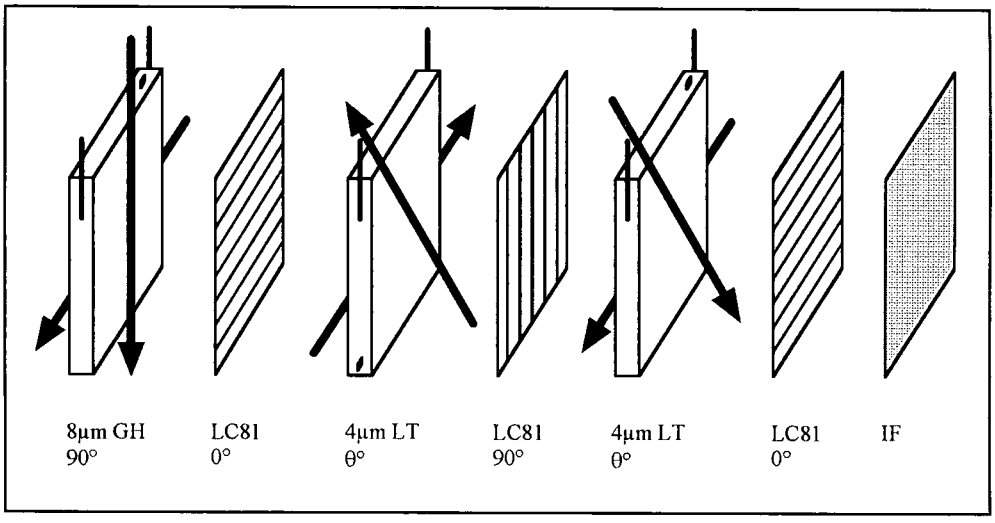


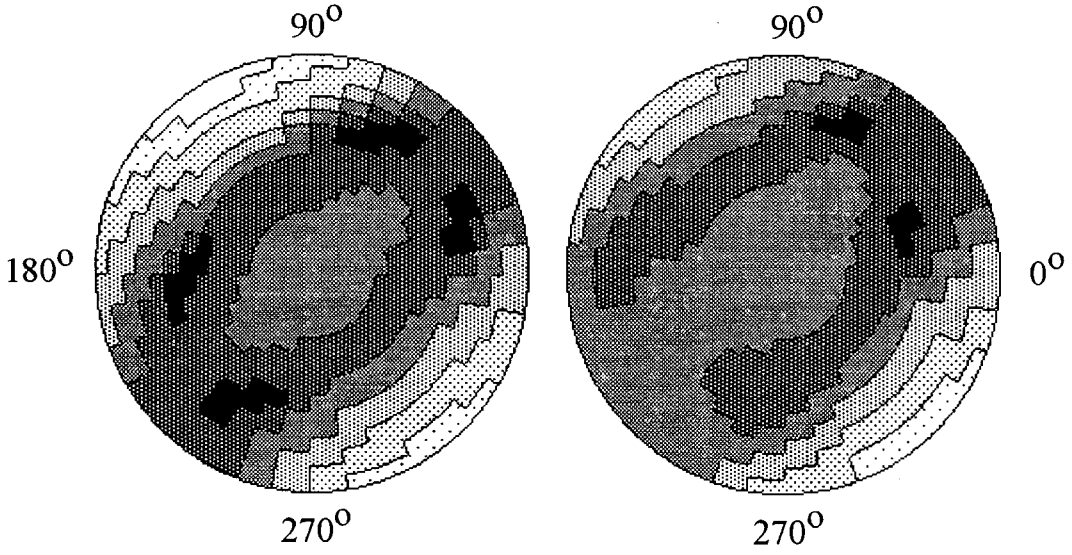


**Welding filter using two 90° TN cells with LC81 polarisers cut at 0°, 90° and 0°. Shade 13**

**Welding filter using two 80° LT cells with LC81 polarisers cut at 0°, 90° and 0°. Shade 13**

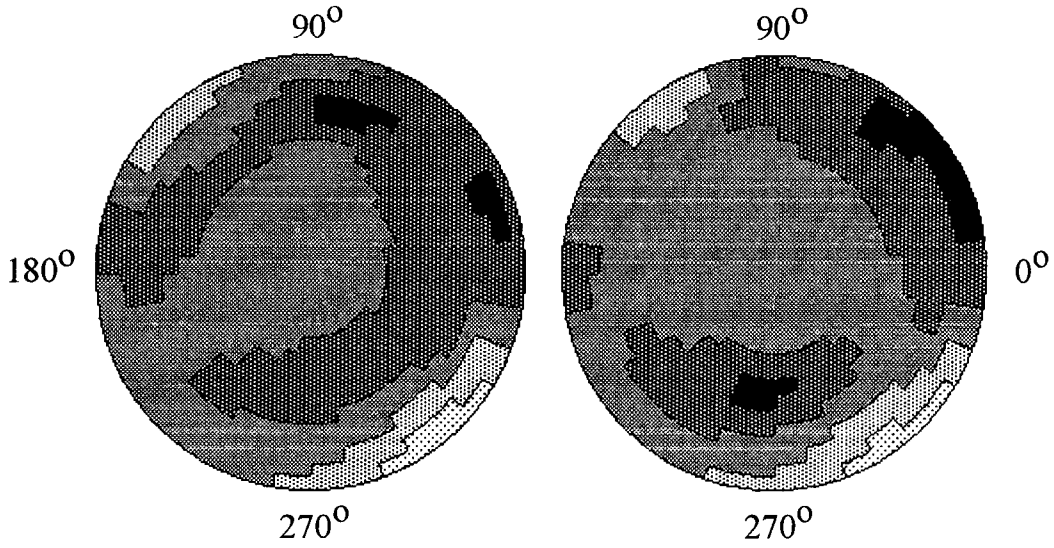


**Welding filter using two 70° TN cells with LC81 polarisers cut at 0°, 90° and 0°. Shade 13**

**Welding filter using two 60° LT cells with LC81 polarisers cut at 0°, 90° and 0°. Shade 13**

The electro-optic response of the double-cell welding filter introduced above in a direction lying parallel to the surface normal is shown in figure 4.9 as a function of the twist-angle. The GH cell is inactivated and a standard I.F is present.

**Figure 4.9: Electro-optic properties of welding filter designs as a function of twist-angle present in the LT cells. The *LC81* polarisers are oriented at $0^0$, $90^0$ and $0^0$ and the GH cell is inactivated.**

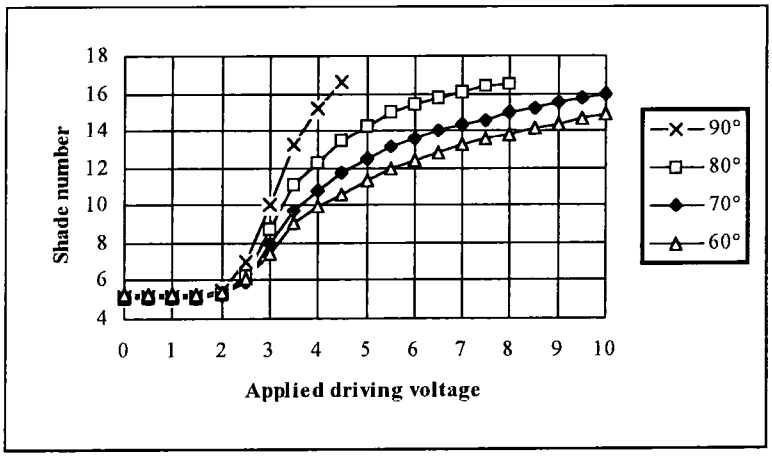

Reduction of the twist-angle causes the dark viewing cone to move away from the central axis and hence the optical angular properties of the device become more asymmetric. However, this also has the effect of reducing the shade number attained in a direction lying parallel to the surface normal for a given driving voltage, necessitating a higher voltage in order to reach a desired degree of darkness. This manifests itself by the loss of cell contrast upon reduction of the twist-angle. Nevertheless, a dark state exceeding that of shade number 14 with an applied driving voltage of ± 10 volts is still obtained from the complete welding filter design when using twist-angles as low as $60^{o}$, indicating that sufficient contrast is still available.

The loss of cell contrast upon twist-angle reduction is understood by considering the arrangement shown in figure 4.10. Here, a $90^{o}$ TN cell is activated at reduced voltages lying below that of the saturation point for the device. Despite the fact that the bulk molecules are predominately aligned parallel with the applied electric field, the liquid crystal molecules immediately adjacent to the cell surfaces remain unperturbed and hence maintain the low energy helical stacking structure. This means that the two layers of liquid crystal material in contact with the cell sides can be represented by perpendicular, birefringent layers that are similar in structure to that of uniaxially stretched retardation sheets.

**Figure 4.10: Surface liquid crystal molecules of a $90^{o}$ TN cell remain unperturbed upon application of a reduced voltage and hence can be represented by two crossed retardation films.**

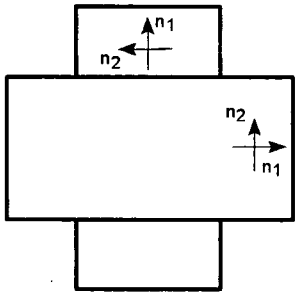


With such an arrangement, the phase factor induced between two mutually perpendicular light components upon passage through the first sheet is counteracted by that introduced upon transmittance through the second birefringent layer. The net effect is total cancellation and the cell possesses minimal retardation, hence displays a high cell contrast. Reduction of the twist-angle reduces the compensation phenomenon and inflates the residual optical activity of the unit, hence degrading the dark state shade number attained by the system.

This is in fact an intrinsic problem that afflicts all LT cells and in particular increases the operating voltage of both a $0^{o}$ LT cell and the closely related π-cell to that of over ± 30 volts. However, use of a positive retardation film together with the π-cell such that the optic axis lies perpendicular to the

molecular director vector, results in the device only requiring stimulation to the point where the residual birefringence equals that of the compensation film. Such techniques have succeeded in reducing the operating voltage of the π-cell to below that of ± 6 volts[48]. Further research is also continuing in this area with regard to LT cells.

The light state shade number of the double-cell welding filters introduced above are displayed in figure 4.11 as a function of the twist-angle in the 4μm LT cells. The cells are filled with the *Merck 3700* liquid crystal mixture and LC81 polarisers cut at $0^o$, $90^o$ and $0^o$ respectively are utilised. Note that in order to obtain the high transmittance state, the GH cell is stimulated with a ± 6 volts 50Hz square wave and that both the LT cells are in the inactivated phase. A standard I.F is present.

**Figure 4.11: Light state shade numbers of double-cell welding filters using *LC81* polarisers cut at $0^o$, $90^o$ and $0^o$ respectively as a function of twist-angle in the LT cells. A GH cell and I.F are present.**

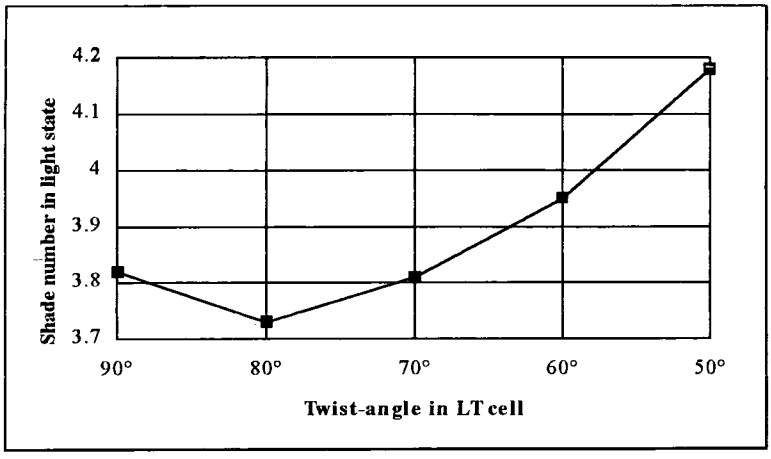


A minimum is observed in the overall optical throughput of the device with a twist-angle of $80^o$. Further reduction beyond this point improves the optical angular properties displayed by the unit but also has a detrimental effect upon the light state shade number. With a polariser configuration of $0^o$, $90^o$, and $0^o$ respectively, the optimum performance of the device is therefore obtained with this twist-angle. Theoretical explanations for this are presented in chapter five together with a novel technique in order to improve the overall optical transmittance obtained from the LT cells when in the inactivated phase and operating in the normally *white* mode. Such methods are capable of maintaining the enhanced optical angular properties afforded by such devices whilst inflating the light state shade number of the unit.

# *CHAPTER FIVE*

*This chapter utilises the theoretical model introduced in appendix two in order to optimise the overall luminous transmittance of LT cells when in the inactivated phase and operating in the normally white mode. It is shown that the performance of such a device is maximised by positioning of the crossed polarisers symmetrically around the molecular directors on each side of the cell. Such a configuration together with an optimisation of the twist-angle yields light state transmittances approaching 100% over a wide range of Δn.d values down towards the theoretical limit of 0.27μm. This prediction is experimentally confirmed and it is shown that the enhanced optical angular properties afforded by LT cells are not adversely affected by this polariser arrangement. Finally, the angular dependence of such cells are investigated as a function of the Δn.d value and it is found that although a significant improvement can be obtained upon reduction of this parameter when employing the standard 90° TN cell, that for the LT case is dramatically less sensitive to this effect. The final sections introduce a complete automatically darkening welding filter design based on this technology and analyses the optical performance of such a system.*

## *5.1 The Theoretical Transmittance of LT Cells when in the Inactivated Phase.*

Chapter four showed that a reduction of the twist-angle present in a liquid crystal cell has beneficial effects upon the overall optical angular properties of welding filters based on the double-cell design where a large degree of cell compensation occurs. However, when using the 4μm cells filled with the *Merck 3700* liquid crystal mixture and placed between *crossed* polarisers oriented in the 0°/90° arrangement such that the working polariser is aligned perpendicular to the entrance liquid crystal molecules, a loss of light state transmittance is observed for twist angles less than that of 80°. This chapter investigates the possibility of optimising the twist-angle, polariser configuration and the pertinent Δn.d parameter of the cell in order to maximise the overall optical throughput of the device when in the inactivated phase whilst maintaining the enhanced angular properties exhibited by LT cells when in the activated state.

Chapter two illustrated that the *Gooch and Tarry first maximum* for the 90° TN device operating in the normally white mode and with the polarisers oriented either parallel or perpendicular to the entrance and exit liquid crystal molecules occurs with a Δn.d value of 0.48μm for a wavelength of 550nm. It is therefore this value that maximises the overall light state optical throughput for the 90° TN cell.

The effect of reducing the twist-angle upon the position of the *Gooch and Tarry first maximum* is investigated in figure 5.1. Here, the integrated luminous transmittance of the cell is calculated as a function of the Δn.d parameter for cells possessing various twist-angles and operating in the normally white mode placed between polarisers oriented at 0° and 90° respectively. The theoretical model used for the calculation is expanded in appendix two together with a schematic of the specific arrangement being shown in figure B1 of that section. The numerical analysis is carried out using *Mathcad 'for Windows*[49].

**Figure 5.1: Integrated luminous transmittances of cells possessing various twist-angles operating between crossed polarisers cut at $0^0$ and $90^0$ as a function of the Δn.d parameter.**

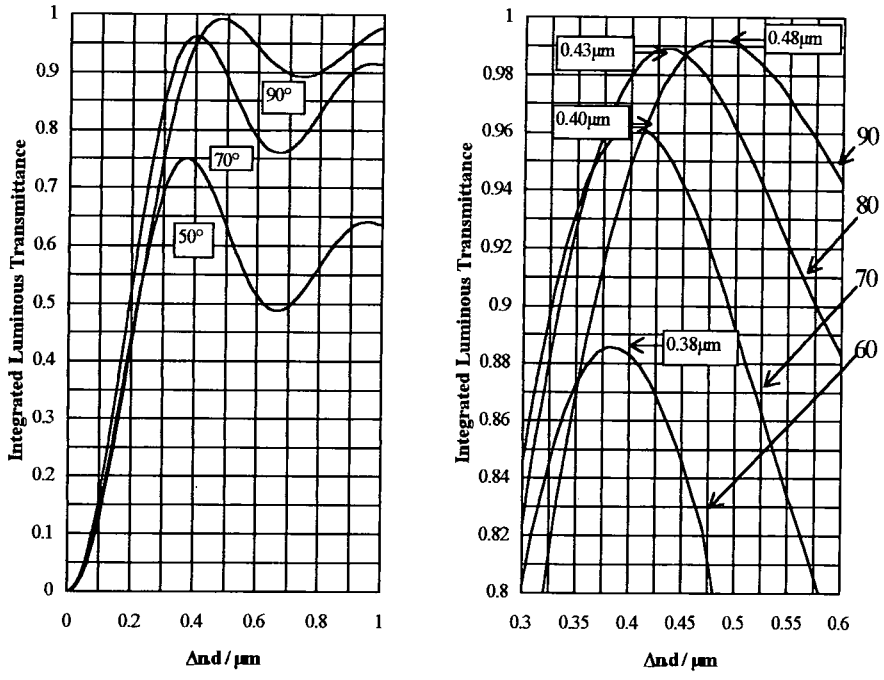


Reduction of the twist-angle generates a shift of the *first maximum* towards lower Δn.d values as well as a diminishing of the peak transmittance due to a miss-match between the exit molecular alignment and the analysing polariser. There is therefore an optimum twist-angle that maximises the light state luminous transmittance dependent upon the relevant Δn.d parameter under consideration. This is illustrated in figure 5.2 for three different Δn.d values ranging from 0.30μm through to 0.50μm. In the latter case, the required twist-angle is seen to be close to that of $90^0$ and an overall transmittance approaching 100% is achieved. This can be compared to that of only 85% for a cell possessing a Δn.d value of 0.30μm and a twist-angle of $72^0$.

The effect of rotating the crossed polarisers away from the standard $0^0/90^0$ configuration where the working polariser is aligned perpendicular to the entrance liquid crystal molecules is investigated in figure 5.3. Here, two values of Δn.d are examined with cells possessing twist-angles ranging from $50^0$ through to $90^0$. The first graph shows the fully optimised $90^0$ TN cell operating in the *first maximum* mode. This basic $90^0$ TN unit achieves maximum light state transmittance with the polarisers oriented at $0^0$ and $90^0$ respectively and in fact there is only little variation in transmission upon polariser rotation for this cell type, although the cell does become more sensitive at lower twist-angles. The second corresponds to a very thin liquid crystal layer operating well below the conventional limits for a $90^0$ TN device. Despite this, reduction of the twist-angle together with an optimisation of the polariser arrangement is still able to generate a high light state transmittance approaching 100%.

**Figure 5.2: Integrated luminous transmittance of cells possessing various Δn.d values operating in the normally white mode between polarisers cut at $0^0$ and $90^0$ as a function of twist-angle.**

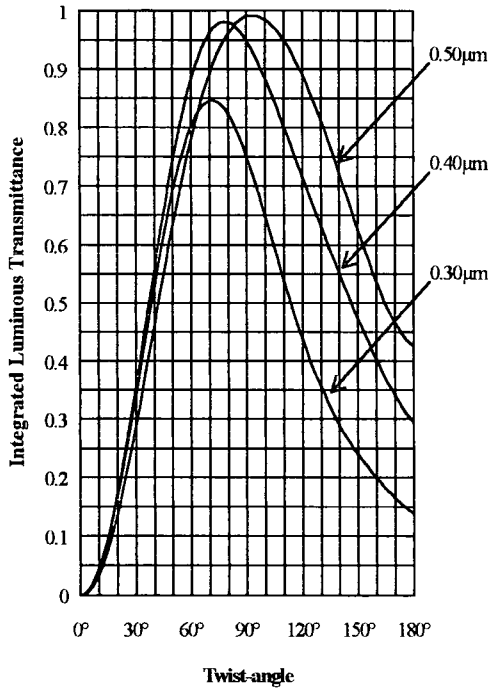


**Figure 5.3: Luminous transmittance of LT cells placed between crossed polarisers oriented at various angles relative to the entrance molecular director. Two values of Δn.d are shown.**

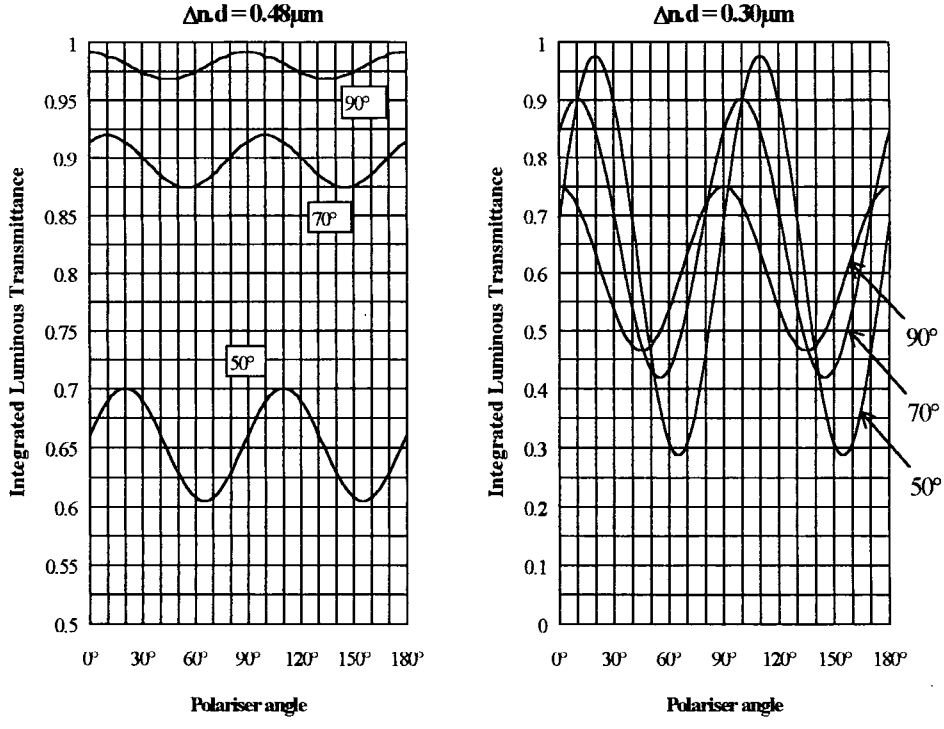

The optimum polariser configuration required in order to maximise the luminous transmittance displayed by LT cells when in the inactivated phase is investigated in figure 5.4. Here, the overall optical throughput at a wavelength of 550nm for nematic type cells possessing a Δn.d value of 0.40μm and with twist-angles ranging from $90^{o}$ down to $50^{o}$ are calculated as a function of the angle between the working polariser and the entrance molecular alignment director.

**Figure 5.4: Calculated transmittance at a wavelength of 550nm for liquid crystal cells operating in the normally white mode with a Δn.d value of 0.40μm as a function of the polariser configuration.**

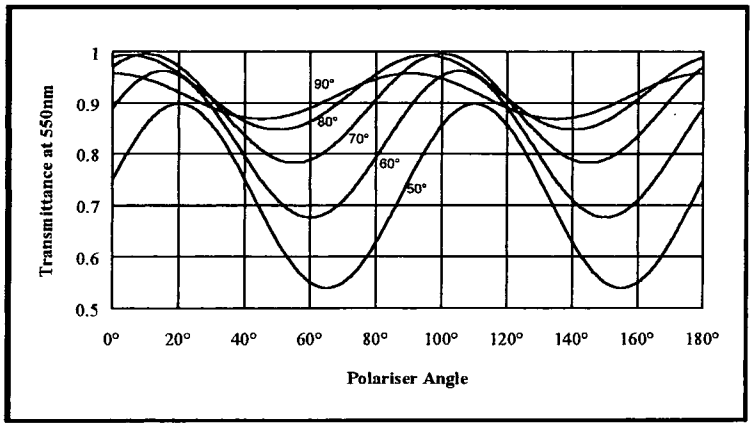


There are several points apparent from this graph. The first is that with a Δn.d value of 0.40μm appropriate for a 4μm cell filled with the *Merck 3700* liquid crystal mixture, an overall transmittance approaching 100% is obtained with a twist-angle of between $70^{o}$ and $80^{o}$. This is in quantitative agreement to the experimental observations displayed in figure 4.11 of chapter four. The second is that in general, there are two polariser arrangements that are of particular interest with regard to liquid crystal cells operating in the inactivated phase. The first orientation *maximises* the overall optical transmittance generated by the device, whilst that of the second *minimises* this value.

Consideration of these two arrangements reveals that both designs require the polarisers to be placed symmetrically in some fashion around the alignment directors on each surface of the cell, hence are referred to as the *Symmetric A* and *Symmetric B* orientations accordingly. Calculations indicate that these configurations are applicable irrespective of both the twist-angle present in the cell and the Δn.d parameter. Note that this also encapsulates cells possessing twist-angles exceeding that of $90^{o}$. These two novel designs are depicted in figure 5.5 and by definition, the *Symmetric A* orientation is taken as being that which *maximises* the overall optical transmittance of the device. Note that for the standard $90^{o}$ TN liquid crystal cell, the *Symmetric A* arrangement corresponds to the trivial case where the polarisers are

placed in the $0^{o}/90^{o}$ orientation and that the variation in transmittance as a function of polariser orientation becomes more apparent as both the twist-angle and the $\Delta n.d$ value of the device are reduced.

**Figure 5.5: Symmetric polariser arrangements that respectively maximise (a) and minimise (b) the optical transmittance displayed by LT cells when in the inactivated phase.**

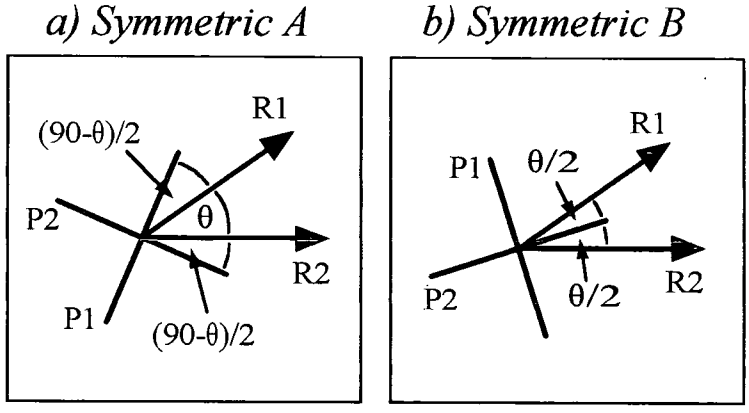


This is analysed further in figures 5.6 through to 5.8. Here, the integrated luminous transmittances of different cell types are displayed as a function of both the twist-angle and the polariser orientation in surface plot diagrams. The polarisers are held perpendicular relative to each other and the angle between the working polariser and the entrance molecular director is recorded. The overall transmittance is represented by contour lines with the tops defining points of maximum optical throughput. Such graphs enable the intrinsic properties of nematic type liquid crystal cells to be quickly optimised by considering the variation of two parameters simultaneously.

Figure 5.6 represents that for the fully optimised $90^{o}$ TN cell operating in the *Gooch and Tarry first maximum* mode whereby the $\Delta n.d$ parameter is equal to $0.48\mu m$. Here, there is little effect upon polariser rotation and both the $0^{o}/90^{o}$ and $90^{o}/180^{o}$ configurations which correspond to where the polarisers are respectively perpendicular to and parallel with the entrance and exit liquid crystal molecules give rise to a maximum light state transmittance.

The effect of reducing the cell thickness is investigated in figures 5.7 and 5.8. With a $\Delta n.d$ value of $0.40\mu m$, the twist-angle necessary in order to maintain maximum optical performance is reduced to $74^{o}$ with the polarisers oriented at $8^{o}$ and $98^{o}$ respectively relative to the input molecular director. With such a design, a luminous transmission approaching 100% is obtained. Note that the same diagrams are reproduced at two different scales in figures 5.7 and 5.8 in order to increase resolution.

**Figure 5.6: Integrated optical transmittance shown in a surface plot for a cell possessing a Δn.d value of 0.48μm placed between crossed polarisers and in the inactivated phase.**

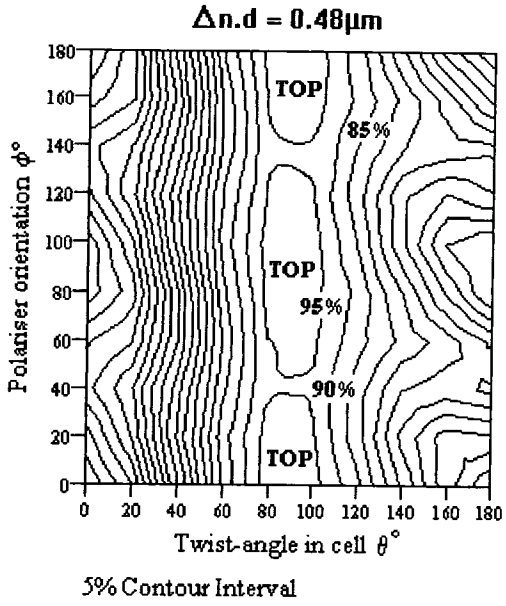


**Figure 5.7: Integrated optical transmittance shown in a surface plot for a cell possessing a Δn.d value of 0.40μm placed between crossed polarisers and in the inactivated phase.**

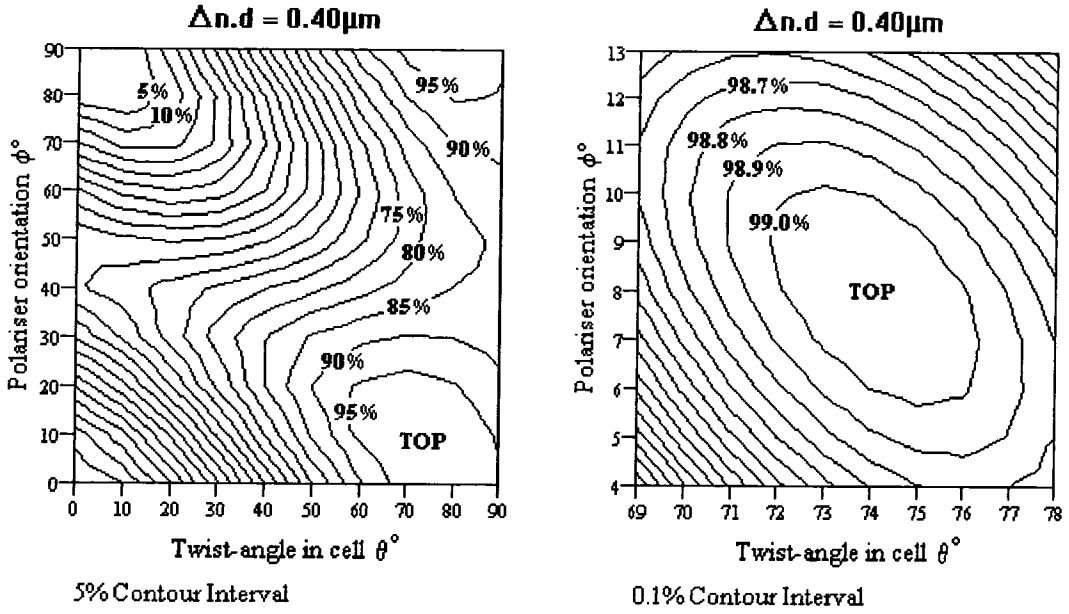

Figure 5.8 shows the calculated optical performance of a thin liquid crystal layer operating well below the standard level for a $90^{o}$ TN cell with a pertinent $\Delta n.d$ value of 0.30μm. Here too, a high light state optical throughput approaching 100% is obtained by twist-angle reduction down to $38^{o}$ and rotation of the crossed polarisers surrounding the device to a $26^{o}/116^{o}$ configuration corresponding to the *Symmetric A* orientation.

**Figure 5.8: Integrated optical transmittance shown in a surface plot for a cell possessing a $\Delta n.d$ value of 0.30μm placed between crossed polarisers and in the inactivated phase.**

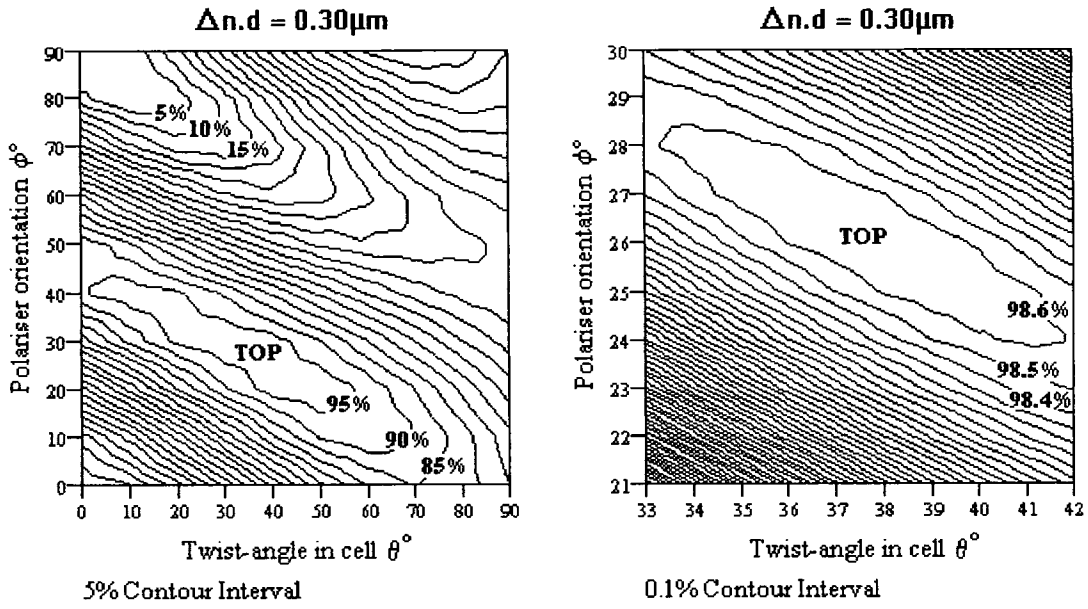


Having established the polariser arrangements necessary in order to optimise the transmittances when utilising LT cells in the inactivated phase and operating in the normally white mode, we are now in a position to investigate both the maximum optical throughput available from a cell and the optimum twist-angle required, both as functions of the $\Delta n.d$ parameter. This involves use of the *Symmetric A* polariser configuration and we will be returning to that of the *Symmetric B* orientation later in chapter six.

Figure 5.9 shows the optimum twist-angle required in order to maximise the light state transmittances of LT cells at a wavelength of 550nm, given as a function of the $\Delta n.d$ parameter. The cells are in the inactivated phase and placed between crossed polarisers oriented in the *Symmetric A* arrangement. This information is complimented by that contained within figure 5.10 which shows the maximum integrated luminous transmittances available from fully optimised nematic type cells with the twist-angles indicated in figure 5.9, also as a function of the $\Delta n.d$ parameter.

**Figure 5.9: Optimum twist-angle maximising the light state transmittances of cells placed between crossed polarisers with the "Symmetric A" polariser arrangement as a function of Δn.d.**

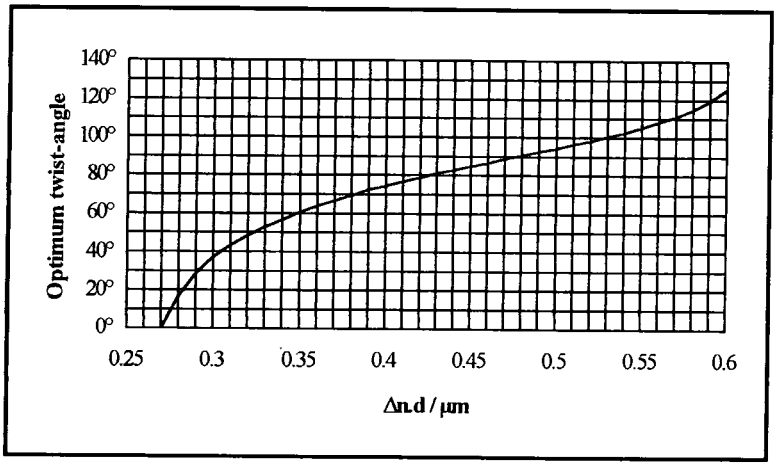


Cell optimisation therefore enables a total light state luminous transmittance approaching 100% to be obtained from cells operating in the normally white mode over a wide range of Δn.d values down towards the theoretical limit of 0.27μm. At this point, the liquid crystal layer forms a *half-wave plate* with the value of Δn.d approximating to half the wavelength of the central part of the visible spectrum. This sets the lower limit for which optical activity occurs and further reduction of the Δn.d parameter beyond this point generates a rapid loss of optical transmittance.

**Figure 5.10: Integrated luminous transmittances of cells placed between crossed polarisers oriented in the "Symmetric A" arrangement as a function of the Δn.d parameter.**

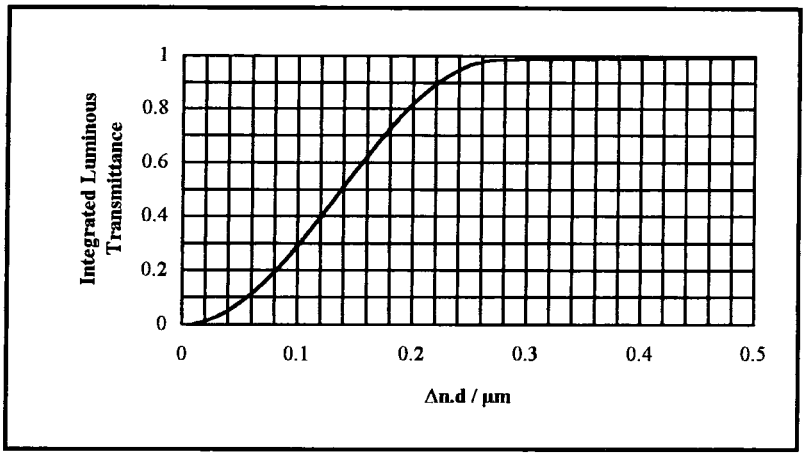

Careful control of both the polariser orientations and the Δn.d value of the device therefore enables LT cells to be manufactured that maintain high optical throughputs when in the inactivated phase. The final sections of this chapter experimentally confirm these theoretical predictions and analyses the optical angular properties displayed by such devices in order to develop complete automatically darkening welding filter designs based on this technology.

### *5.2 Experimentally Determined Optical Properties of LT Cells in the Inactivated Phase.*

Figure 5.11 shows the experimentally determined light state shade numbers of liquid crystal cells operating in the normally white mode and with a Δn.d value of 0.39μm as a function of the polariser orientation. 4μm LT cells filled with the *Merck 3700* liquid crystal mixture and possessing various twist-angles ranging from $90^{o}$ down to $50^{o}$ are investigated and placed between crossed LC81 polarisers. A standard I.F is present.

**Figure 5.11: Experimentally determined light state shade numbers as a function of polariser orientation for liquid crystal cells with a Δn.d value of 0.39μm. A standard I.F is present.**

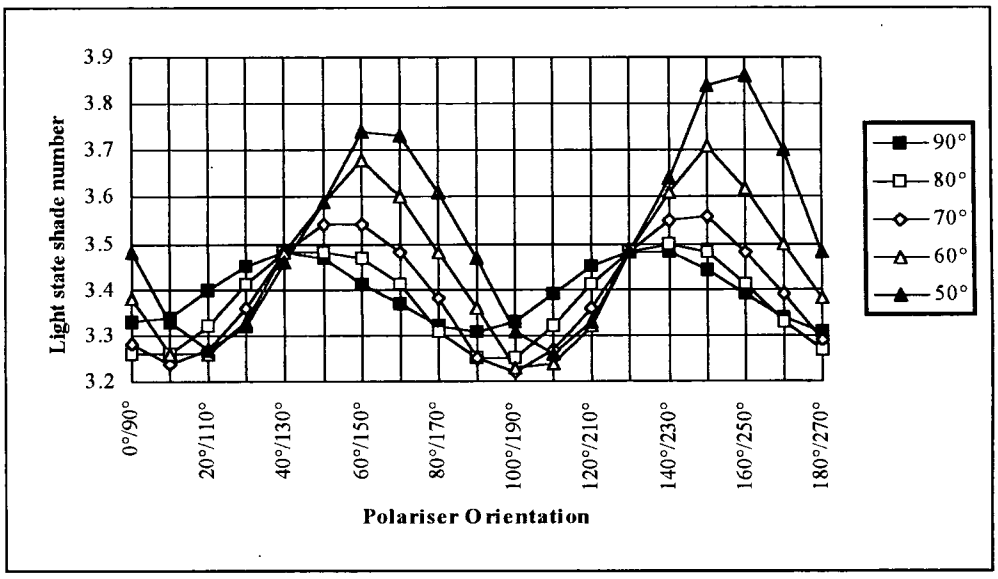


It is seen that the polariser configuration giving rise to a maximum optical transmittance with the cell in the inactivated phase is indeed the *Symmetric A* orientation and that the curves display sinusoidal oscillations with maxima occurring for the *Symmetric B* arrangement. The optimum twist-angle for this value of Δn.d is also seen to lie close to $70^{o}$, this being in quantitative agreement with the $72^{o}$ predicted for this cell type in figure 5.9. Similar curves are obtained for other liquid crystal materials possessing

different Δn.d values indicating that the optimum polariser arrangement is applicable irrespective of the thickness and type of liquid crystal component under consideration.

Figure 5.12 shows the experimentally measured light state shade numbers of different cell types possessing Δn.d values ranging from 0.20μm through to 0.39μm as a function of the twist-angle in the cell. The cells are placed between crossed LC81 polarisers oriented in the *Symmetric A* arrangement and a standard I.F is present. The different Δn.d values investigated correspond to the following cells; 2.1μm cell filled with the *Merck 3700* liquid crystal mixture (Δn.d = 0.20μm), 2.1μm cell with the *Merck ZLI-3949 + 0.2% ZLI-811 (3949)* mixture (Δn.d = 0.30μm), a 4μm cell with the *Merck ZLI-3376* crystal (Δn.d = 0.35μm) and a 4μm device filled with the *Merck 3700* liquid crystal component (Δn.d = 0.39μm).

**Figure 5.12: Light-state shade numbers of various cells placed in the "Symmetric A" configuration possessing Δn.d values ranging from 0.20μm through to 0.39μm as a function of the twist-angle.**

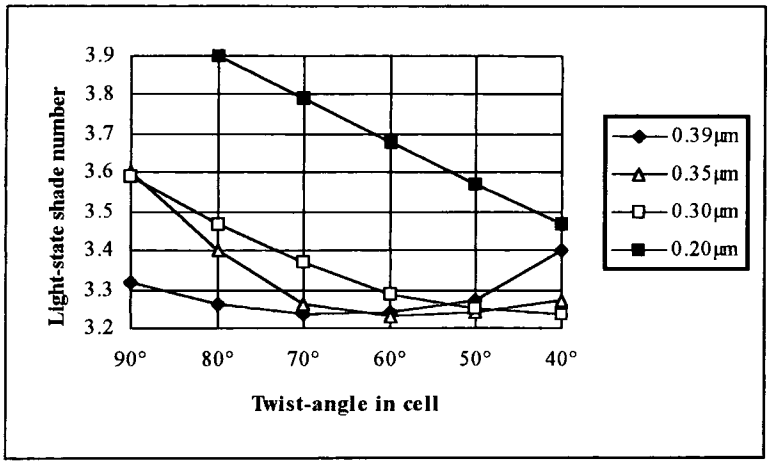


It is noted that an optimum twist-angle exists that maximises the overall transmittance of the device when inactivated and operating in the normally white mode, dependent upon the Δn.d parameter of the cell. Such optimisation produces integrated luminous throughputs approaching 100% for all values of Δ n.d down towards 0.27μm. Note that the shade number displayed by two parallel LC81 polarising sheets together with a standard I.F is 3.11, it being this value that corresponds to 100% cell transmittance. However, in practice reflections from the glass surfaces inevitably increases this value to some extent.

Having established that the optimum light state transmittance of liquid crystal cells possessing a Δn.d value of 0.39μm occurs with a twist-angle of $72^{o}$, the contrast available from such a system will now be investigated. Figure 5.13 shows the cell contrast obtained from a 4μm $70^{o}$ LT device filled with the *Merck 3700* liquid crystal mixture as a function of the angle between the working polariser and the entrance molecular director vector. Crossed LC81 polarisers are used and the contrast is defined as being the shade number step obtained with a voltage jump from 0 volts up to a ± 10 volts 50Hz square wave. A standard I.F is present.

**Figure 5.13: Contrast obtained from various cell types placed between crossed *LC81* polarisers as a function of the polariser orientation. A standard I.F is present.**

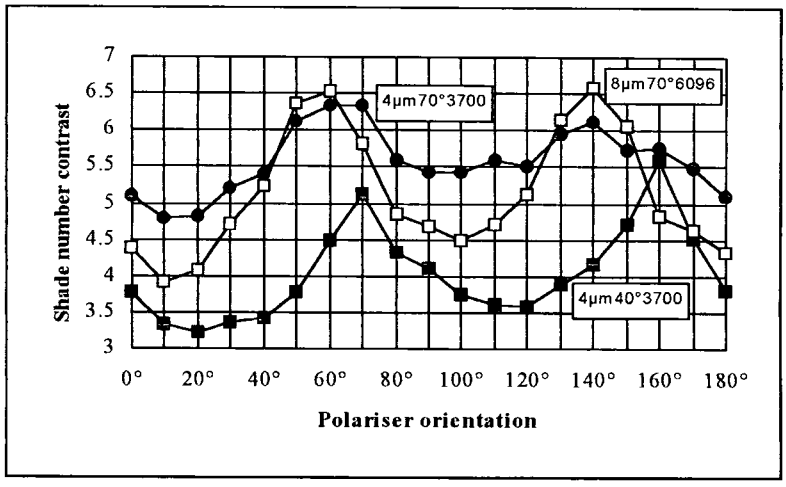


Those for a 4µm 40$^{o}$ LT cell filled with the *Merck 3700* liquid crystal component and an 8µm 70$^{o}$ LT cell with the *Merck 6096* mixture are also shown for comparison. Note that for the latter case, contrast is defined in a slightly different manner. Here, the shade number step between the lightest available state and the dark state obtained with an applied voltage of ± 10 volts is determined. In practice, a small stimulating voltage of between ± 2.0 volts and ± 3.0 volts is required in order to reach the highest transmittance state. The reasons for this are discussed further in chapter six.

Several points are apparent from these curves. The first is that cell contrast is highly dependent upon the polariser orientation and is maximised upon utilisation of the *Symmetric B* arrangement, whilst that for the *Symmetric A* configuration generates a minimum in the curve. This is quite general irrespective of the nature of the liquid crystal cell in use. A contrast of over 6.3 shade numbers is obtained from the 4µm 70$^{o}$ LT cell when operating in the *Symmetric B* arrangement, a value that plummets nearly 1.6 shades upon rotation into the *Symmetric A* polariser design. Note however, that a contrast step of over 5.4 shade numbers is still available from the 4µm 70$^{o}$ LT cell with such a configuration, this remaining adequate for incorporation into an automatically darkening welding filter unit. As far as the cell contrast is concerned, it is therefore preferable, but not essential, to place the polarisers in the *Symmetric B* design.

The second point to note is that the contrast curves are periodic with a repetition length corresponding to a polariser rotation of 90$^{o}$. This indicates that at least to a first approximation, the electro-optic properties of a cell with a polariser arrangement of $\theta^{o}$ and $(90 + \theta)^{o}$ are identical to those with the polarisers aligned at $(90 + \theta)^{o}$ and $(180 + \theta)^{o}$ respectively, although subtle improvements in both the light state shade number and cell contrast are observed upon positioning of the major transmission axes of the polarisers symmetrically around the cell rubbing directions according to figure 5.5 rather than that of the alignment vectors lying perpendicular to these transmission axes. Note that these differences are generally small in comparison to the gross overall effects being investigated in this thesis and are therefore regarded

as being insignificant. The electro-optic properties of a cell with the polarisers aligned *parallel* to the molecular directors at the surface of the glass plates are thus considered to be identical to those with the polarisers oriented *perpendicularly* to these vectors.

The final point to note is that the electro-optic properties of liquid crystal cells become more sensitive to the polariser orientation upon both reduction of the twist-angle and increment of the pertinent Δn.d value. In general, reducing the twist-angle also generates a loss in cell contrast. Since it is the *Symmetric A* polariser configuration that is expected to maximise the light state shade number when in the inactivated phase, it is therefore this design that appears most promising as far as developing automatically darkening welding filters is concerned. This arrangement is therefore investigated further in the proceeding sections.

The electro-optic properties of liquid crystal cells operating in the normally white mode as a function of both the twist-angle and the cell thickness are analysed in figure 5.14. Here, both 4μm and 2.1μm cells filled with the *Merck 3700* liquid crystal mixture and possessing twist-angles ranging from $80^{o}$ down to $50^{o}$ respectively are investigated. The LC81 polarising material placed in the *Symmetric A* configuration is used and a standard I.F is present.

**Figure 5.14: Electro-optic properties of LT cells using the *Merck 3700* liquid crystal as a function of both the twist-angle and cell thickness. *LC81* polarisers in the "Symmetric A" configuration.**

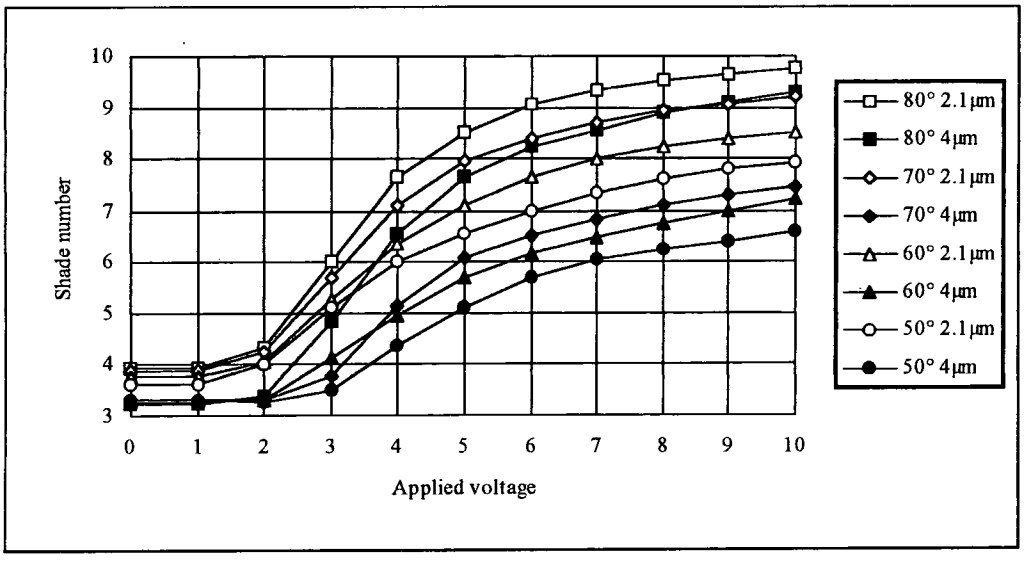


Several points are apparent from these curves, the first being the effect of twist-angle reduction upon cell contrast. The operating voltage of the cell steadily rises upon lowering of the twist-angle and hence a higher electric field is required in order to reach a specific shade number. This point is illustrated further in figure 5.15 which shows the driving voltage necessary in order to attain a shade number 6 as a function of the twist-angle for different cell types. Once again, the cells are placed in the *Symmetric A* polariser configuration using the LC81 material and a standard I.F is present. A square wave voltage operating at 50Hz is used.

**Figure 5.15: Voltage necessary in order to attain a shade number 6 as a function of the twist-angle for different cell types placed in the "Symmetric A" configuration. A standard I.F is present.**

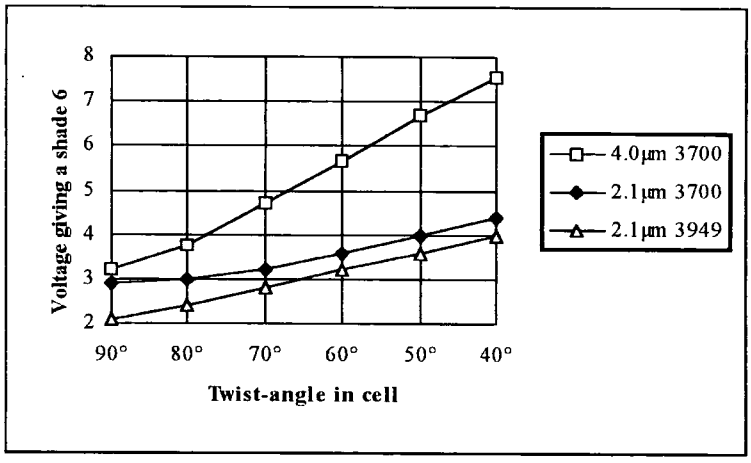


It is seen that the operating voltage increases from ± 3.2 volts for the 4μm 90° TN cell filled with the *Merck 3700* liquid crystal mixture to that of over ± 7.4 volts for the 40° LT case using the same crystal. This effect is quite general irrespective of both the cell thickness and the type of liquid crystal material in use. Such a phenomenon produces an undesirable increase in the overall power consumption of the filter upon twist-angle reduction. Incidentally, this will also have the effect of helping to slide the operating voltage of the unit away from the lower end of the intermediate voltage region of between ± 3.0 volts and ± 4.0 volts and hence help to minimise the total *light scattering* generated by the system.

The second point to note is the effect of reducing the cell thickness upon the observed contrast. A significant drop is seen in the required driving voltage as the liquid crystal width is lowered, hence producing a rise in cell contrast. The voltage necessary in order to yield a shade number 6 with a 90° TN cell filled with the *Merck 3700* liquid crystal mixture is cut from ± 3.2 volts with a 4μm cell to below that of ± 2.8 volts for the 2.1μm case. The operating voltage of thinner cells is also less sensitive to twist-angle reduction, a decrease of 3 volts being observed in the field required to produce a shade number 6 with a 40° LT device filled with the *Merck 3700* liquid crystal mixture in going from a 4μm to a 2.1μm cell.

The final observation from figure 5.15 is that different liquid crystal mixtures naturally possess distinct operating voltage ranges depending upon the intrinsic properties of the material itself such as the threshold voltage and the dielectric anisotropy. The *Merck ZLI-3949* liquid crystal component operates at between 0.5 and 1.0 volts below that of the *Merck 3700* liquid crystal mixture depending upon the twist-angle present in the cell, the difference becoming less apparent at reduced angles.

It has been demonstrated that despite it being only in the short wavelength limit that the liquid crystal helical structure can be considered as producing true rotation of linearly polarised light, the phase difference between the elliptically polarised components of the exiting radiation gives rise to a series of maxima in the overall optical transmission throughput of the device when plotted as a function of the Δn.d parameter. Very thin cells can therefore be manufactured possessing Δn.d values well below that of the

standard 0.48μm limit for the conventional 90° TN unit whilst maintaining the light state transmittance at high levels by reduction of the twist-angle together with a rotation of the crossed polarisers relative to the liquid crystal molecular alignment directors into the *Symmetric A* configuration. Overall optical transmissions approaching 100% can hence be obtained for liquid crystal devices covering a wide range of Δn.d values down towards the theoretical limit of 0.27μm whereupon the cell transforms into a half-wave plate for optical wavelengths and a rapid loss of transmittance is observed. Note that it is also this polariser arrangement that *minimises* the cell contrast obtained from the unit.

Reduction of the twist-angle has the effect of increasing the operating voltage of the liquid crystal device due to a diminishing of the cancellation effects between the residual retardation present in the two layers of liquid crystal material immediately adjacent to the sides of the cell, hence lowering the gradient of the electro-optic response curve. An increase in the driving voltage has adverse consequences for the current consumption but may offer advantages in terms of the overall light scattering generated by the unit. This problem can be alleviated to a certain extent via use of thinner cells, but since the power expenditure is inversely proportional to the cell thickness (equation 1.7, chapter one), the problem of battery life remains largely unresolved.

Another area as yet uninvestigated is the effect of using different alignment layers during the manufacturing procedure that naturally induce higher liquid crystal molecular tilt angles at the contact surfaces when in the inactivated phase. This may provide a further reduction in the operating voltage of the device and hence reduce the current consumption of the cell. It may also be possible to employ uniaxially stretched retardation sheets to compensate for the residual birefringence present in the cell when in the activated phase and further research is continuing in this area.

### *5.3 The Optical Angular Properties of LT Cells Activated at Reduced Voltages.*

So far, only the transmittance of inactivated LT cells in a direction lying perpendicular to the sample surface have been considered. The optical angular properties of such devices when stimulated at reduced voltages and operating in the normally white mode will now be investigated. Figure 5.16 shows the effect of rotating the crossed polarisers relative to the cell rubbing directions for a 4μm 70° LT cell filled with the *Merck 3700* liquid crystal mixture. The cell is stimulated with a ± 4 volts 50Hz square wave and a standard I.F is present.

In general, the optical angular properties of the system are largely dependent upon the asymmetric birefringence present in the liquid crystal layer itself when stimulated by reduced voltages of less than ± 8 volts. The main effect of polariser rotation therefore is to cause the optical response of the cell represented in the polar plot diagram to simply rotate in harmony without any other significant changes being observed over a wide range of polariser configurations. However, one exception exists when the crossed polarisers hit the *Symmetric B* orientation. Here, the standard *streak* or *cone* pattern in the polar plot diagram is replaced by one that is *wrapped* around the central viewing cone of the device and offset to one side.

**Figure 5.16: Effect of polariser rotation upon the optical angular properties of 4µm 70° LT cells with the *Merck 3700* liquid crystal activated with ± 4 volts and placed between crossed polarisers.**

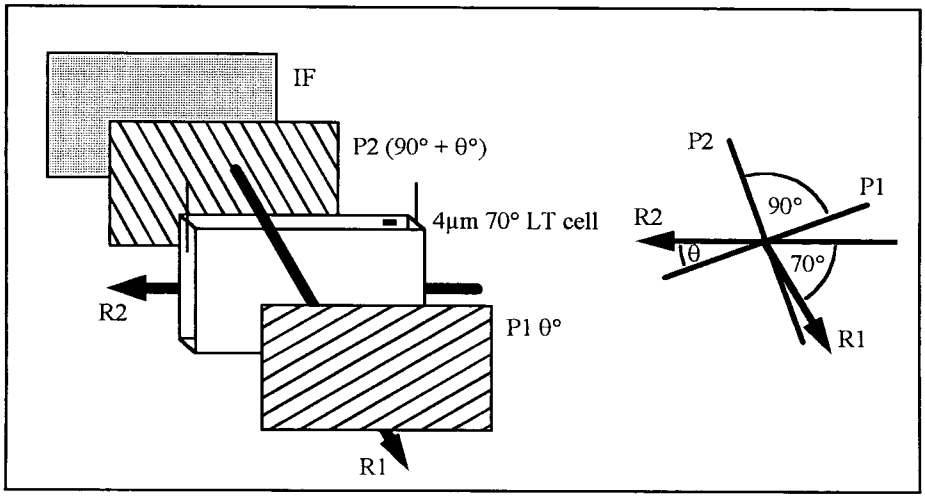


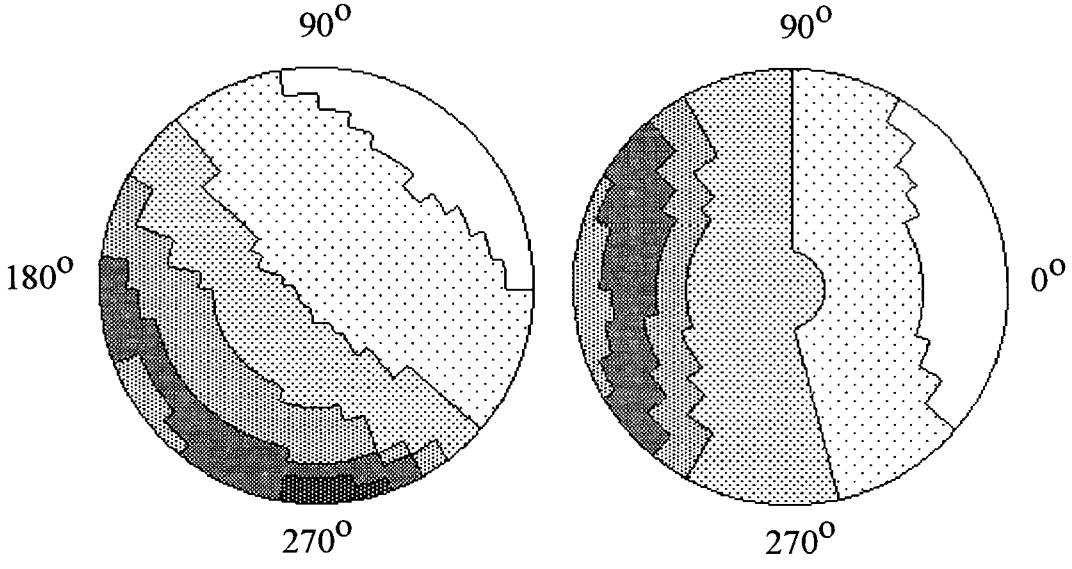


**4µm 70° LT cell with LC81 polarisers oriented at 0° and 90°. ± 4 volts to the cell. "Streak" pattern.**

**4µm 70° LT cell with LC81 polarisers oriented at 30° and 120°. ± 4 volts to the cell. "Streak" pattern.**

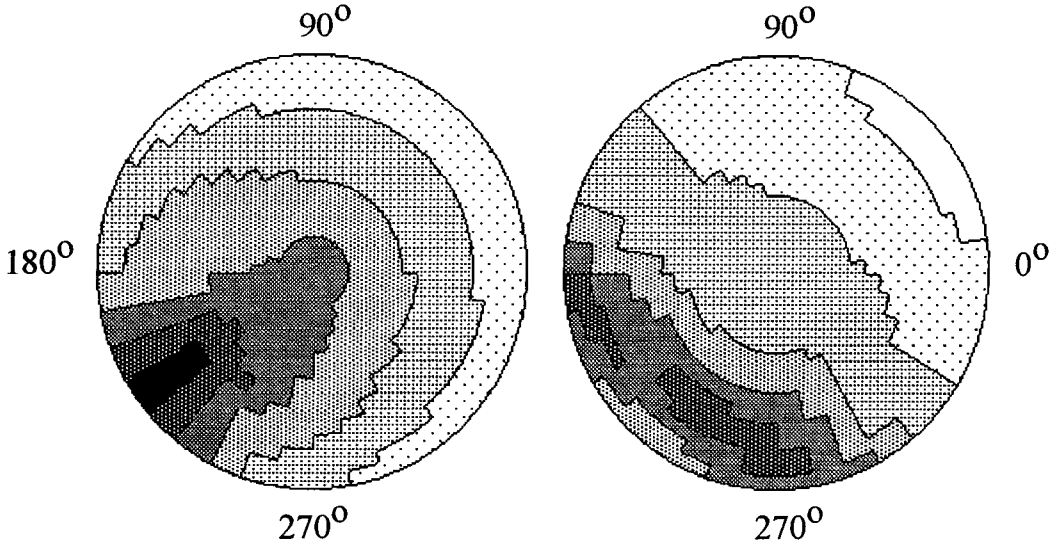


**4μm 70° LT cell with LC81 polarisers oriented at 60° and 150°. ± 4 volts to the cell. "Wrapped" pattern.**

**4μm 70° LT cell with LC81 polarisers oriented at 90° and 180°. ± 4 volts to the cell. "Streak" pattern.**

The asymmetric *streak* pattern characteristic for the majority of polariser configurations including both the standard $0^{o}/90^{o}$ and the *Symmetric A* polariser arrangements is ideal for incorporation into double-cell designs whereby a large degree of cell compensation occurs, giving rise to a glass pack possessing a wide central viewing cone. This is in contrast to that which is *wrapped* around the centre of the polar plot chart which, due to the geometry of the optical response, leads to welding filters possessing inferior optical angular properties when viewed at grazing inclination angles towards the far corners of the device.

This phenomenon is quite general irrespective of the type of liquid crystal cell in use, although a lowering of both the twist-angle and the pertinent Δn.d value of the device makes the effect less obtrusive. Figure 5.17 displays the effect for an 8μm $90^{o}$ TN cell filled with the *Merck 6096* liquid crystal mixture giving a Δn.d value of 0.80μm. The cell is placed between crossed LC81 polarisers and driven with a 50Hz square wave voltage in order to realise a shade number 8. A standard I.F is present.

In general, the optical angular properties of liquid crystal cells operating in the normally white mode and driven at reduced voltages of less than ± 8 volts remain highly asymmetric when utilising the *Symmetric A* configuration, hence are suitable for incorporation into double-cell structures wherein a large degree of cell compensation is required. However, when functioning in the *Symmetric B* arrangement, the characteristics of the angular properties dramatically change becoming unsuitable for applications in areas where a wide central viewing cone is required. This point is discussed further in chapter six.

**Figure 5.17: Optical angular properties of an 8μm 90° TN cell with the *Merck 6096* liquid crystal mixture as a function of the *LC81* polariser orientation. A standard LF is present. Shade 8.**

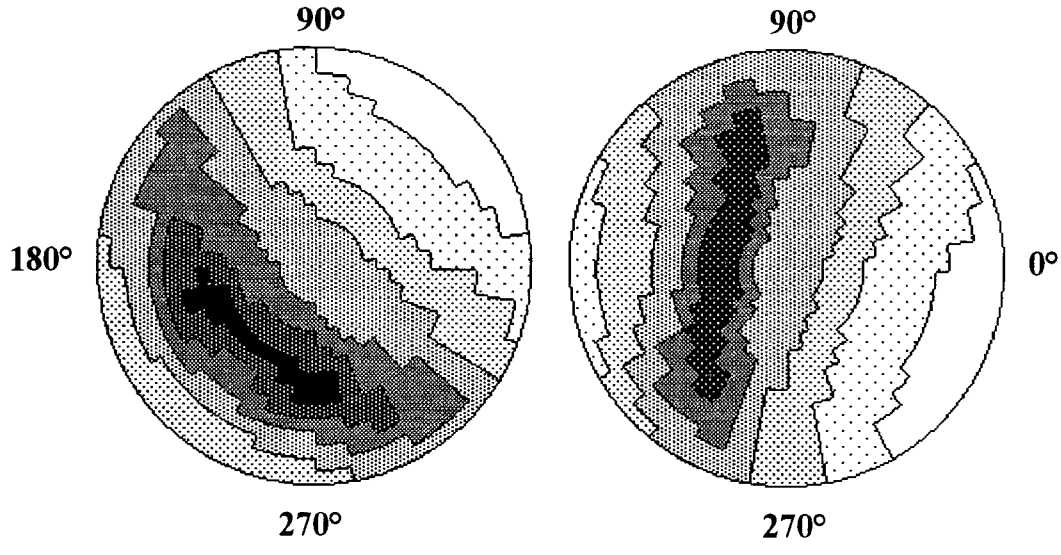


**8μm 90° TN cell with the 6096 crystal and LC81 polarisers at 0° and 90°. Shade number 8. "Streak" pattern**

**8μm 90° TN cell with the 6096 crystal and LC81 polarisers at 20° and 110°. Shade number 8. "Streak" pattern**

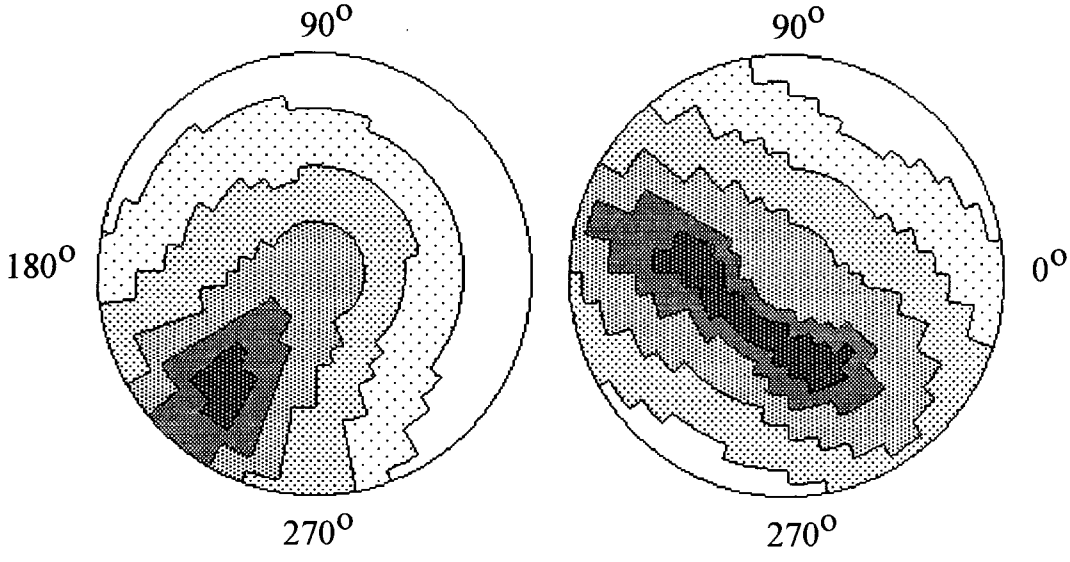


**8μm 90° TN cell with the 6096 crystal and LC81 polarisers at 45° and 135°. Shade number 8. "Wrapped" pattern**

**8μm 90° TN cell with the 6096 crystal and LC81 polarisers at 70° and 160°. Shade number 8. "Streak" pattern**

Having established that the enhanced optical angular properties afforded by LT cells are maintained upon utilisation of the *Symmetric A* polariser configuration, the effect of reducing the twist-angle will now be investigated. Figure 5.18 shows the optical angular properties of 2.1μm cells filled with the *Merck ZLI-*

*3949* liquid crystal mixture as a function of this parameter. Here, the relevant Δn.d value lies at 0.30μm and the LC81 polarising material is held in the *Symmetric A* arrangement for all applicable twist-angles. The stimulating voltage is adjusted so as to give a shade number 8 and a standard I.F is present.

**Figure 5.18: Angular properties of LT cells in the "Symmetric A" configuration with Δn.d equal to 0.30μm as a function of twist-angle. The cell is in the shade 8 state and a standard I.F is present.**

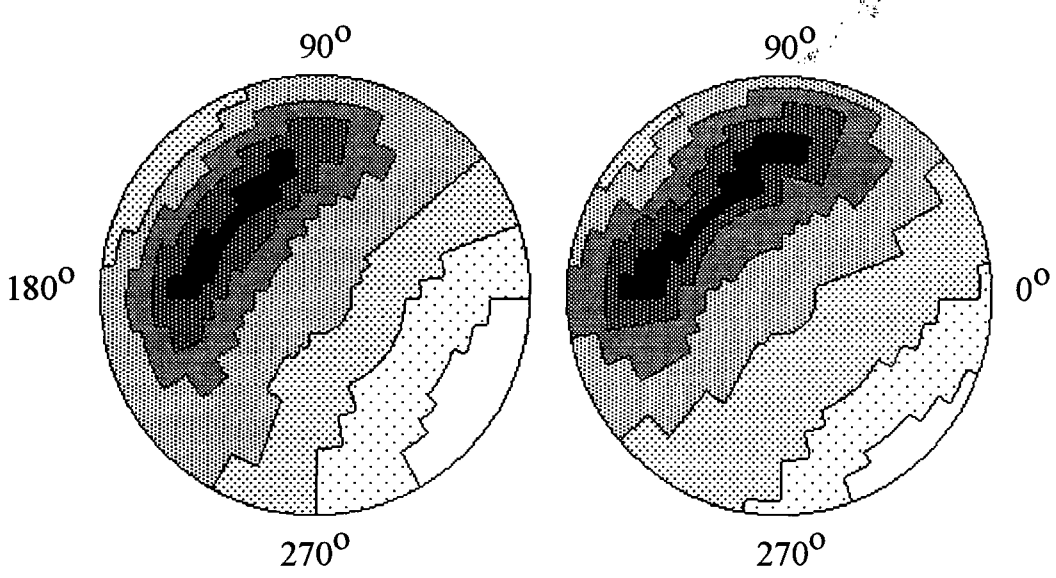


**90° TN cell with a Δn.d value of 0.30μm operating in the "Symmetric A" arrangement. Shade number 8**

**80° LT cell with a Δn.d value of 0.30μm operating in the "Symmetric A" arrangement. Shade number 8**

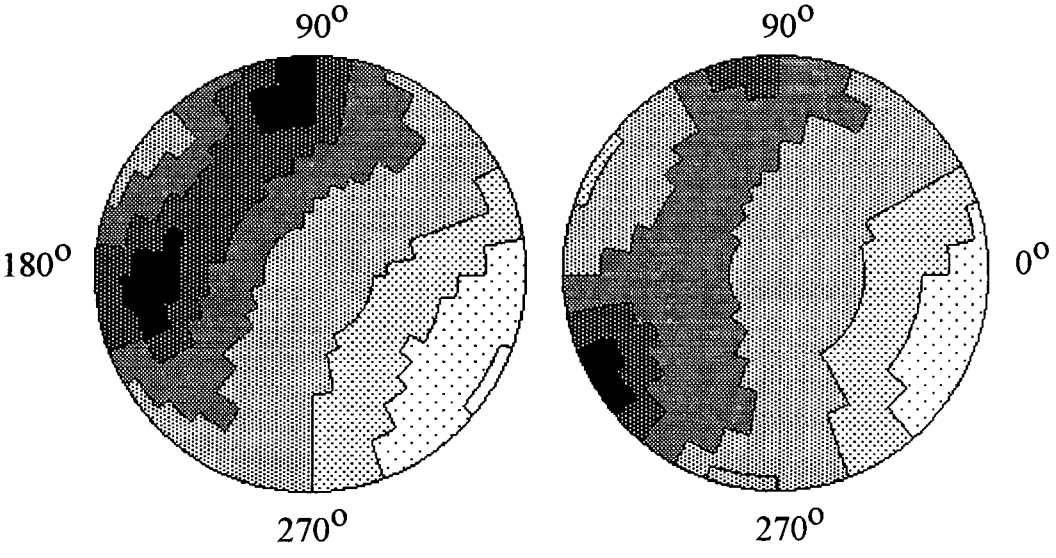


**70° LT cell with a Δn.d value of 0.30μm operating in the "Symmetric A" arrangement. Shade number 8**

**60° LT cell with a Δn.d value of 0.30μm operating in the "Symmetric A" arrangement. Shade number 8**

As is the case for the conventional $0^{o}/90^{o}$ polariser orientation where the working polariser is aligned perpendicular to the entrance liquid crystal molecules, the effect of reducing the twist-angle in the cell is to disperse the dark, off-axis viewing cone and to increase the area depicting this region in the polar plot diagram. In general, the lower the twist-angle present in the cell, the more diffuse is the off-axis viewing cone and the larger are the areas representing points of equal transmission in the polar chart. This gives rise to the possibility of utilising LT cells in double-cell designs in order to improve the optical angular properties of such systems whilst maintaining the overall optical throughput of the device when in the inactivated phase.

Figure 5.19 shows the optical angular properties of double-cell structures using 4μm cells filled with the *Merck 3700* liquid crystal mixture and placed in the *Symmetric A* polariser configuration as a function of the twist-angle in the cell. The pertinent Δn.d value for the device is 0.39μm and the LC81 polarising material is employed. A standard I.F is present and the cells are driven together with a 50Hz square wave so as to realise a shade number 13.

In general, the lower the twist-angle in the cell, the better are the optical angular properties of the double-cell shutter arrangement. Use of liquid crystal cells possessing Δn.d values well below that of 0.48μm for the standard $90^{o}$ TN device naturally require reduced twist-angles in order to maximise the overall optical transmittance when in the inactivated phase, hence will display improved dark state optical angular properties accordingly. For example, a cell possessing a Δn.d value of 0.39μm has an optimum twist-angle of $72^{o}$, whilst that for a 0.30μm device requires a twist-angle of only $38^{o}$.

**Figure 5.19: Angular properties of double-cell filters using 4μm cells with the *Merck 3700* liquid crystal as a function of twist-angle. *LC81* polarisers are used in the "Symmetric A" configuration.**

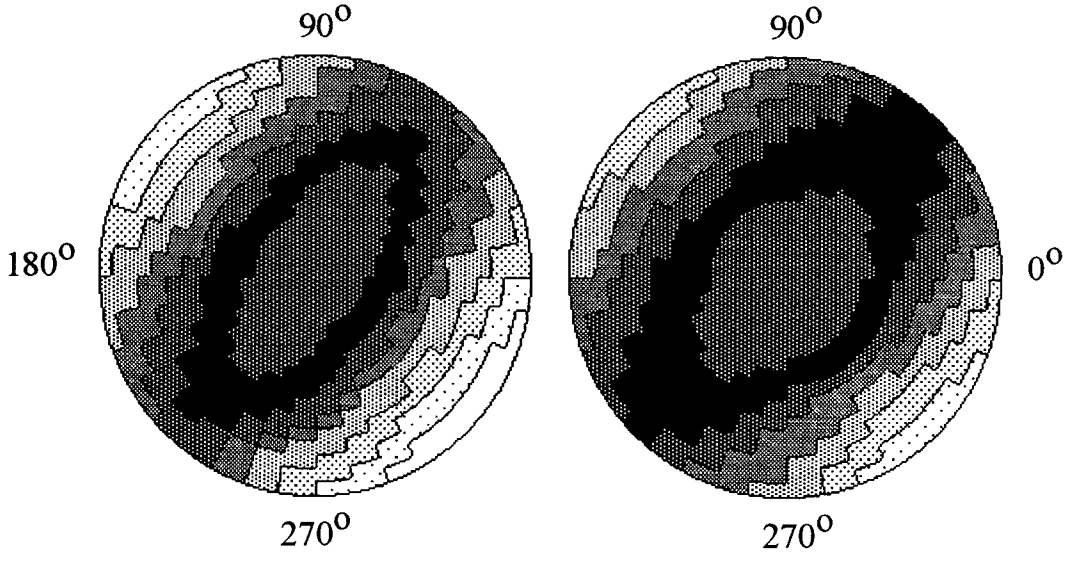


**Double-cell structure using 4μm 90° TN cells operating in the "Symmetric A" arrangement. Shade number 13**

**Double-cell structure using 4μm 80° LT cells operating in the "Symmetric A" arrangement. Shade number 13**

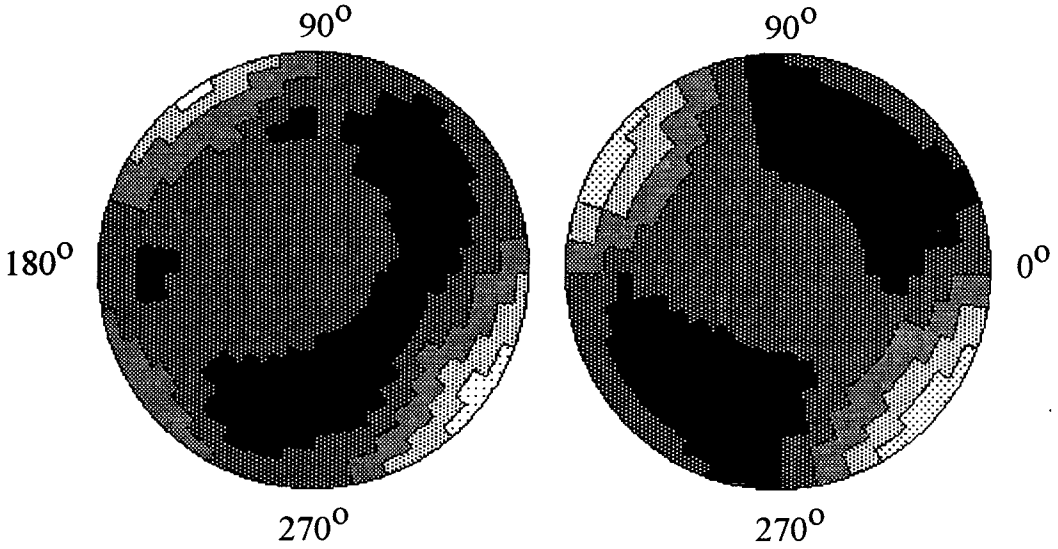


**Double-cell structure using 4μm 70° LT cells operating in the "Symmetric A" arrangement. Shade number 13**

**Double-cell structure using 4μm 60° LT cells operating in the "Symmetric A" arrangement. Shade number 13**

The dependence of the optical angular properties of liquid crystal cells upon the pertinent Δn.d value are investigated in figure 5.20 for the 90° TN case and figure 5.21 for the 70° LT device. Both use the *Symmetric A* polariser configuration and the cells are driven so as to give a shade number 9 with the 90° TN cells and a shade number 7 for the 70° LT case respectively. The specific cell designs giving the appropriate Δn.d values are indicated in table 5.1. Note that a standard I.F is present.

**Table 5.1: Specific cell designs giving the appropriate values of Δn.d.**

| Value of Δn.d | Liquid crystal type |
|---|---|
| 0.80μm | 8μm MLC-6096 |
| 0.60μm | 6μm MLC-6096 |
| 0.40μm | 4μm MLC-6096 |
| 0.39μm | 4μm ZLI-3700 |
| 0.30μm | 2.1μm ZLI-3949 |
| 0.20μm | 2.1μm ZLI-3700 |

**Figure 5.20: Optical angular properties of 90° TN cells as a function of the Δn.d value. The cells are in the "Symmetric A" polariser configuration and a standard I.F is present. Shade number 9.**

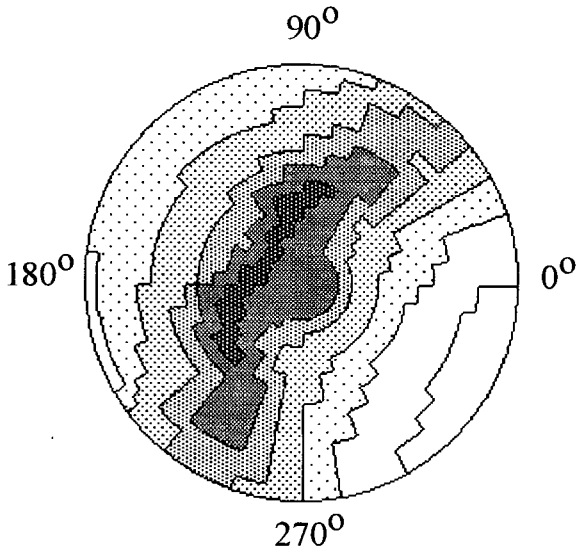


**90° TN Cell. Shade number 9.**
**Δn.d = 0.80μm**

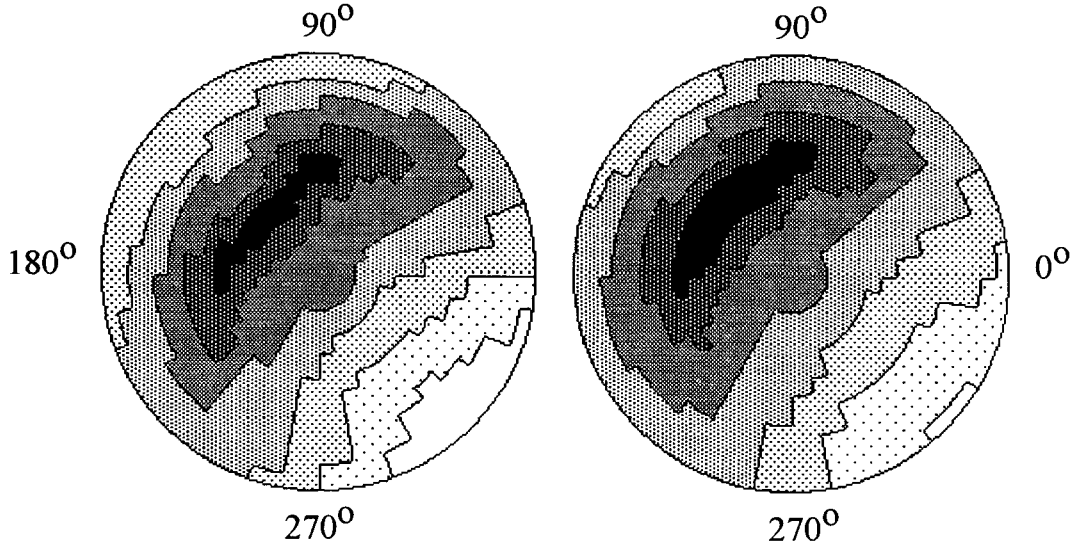


**90° TN Cell. Shade number 9.**
**Δn.d = 0.39μm**

**90° TN Cell. Shade number 9.**
**Δn.d = 0.30μm**

Figure 5.20 indicates that for the 90° TN case, there is a strong dependence of the optical angular properties upon the specific Δn.d value of the cell. Reduction of this parameter increases the area of the off-axis dark viewing cone and reduces the shade number drop observed at acute viewing angles. This is rationalised by remembering that the asymmetric birefringence generated by a liquid crystal cell when in the activated state is caused by incident light striking the partially aligned molecules at an angle, hence

being subjected to the remnant retardation present in the molecules at such orientations. Reduction of the intrinsic Δn.d parameter reduces this effect and hence improves the overall angular properties of the system. It is therefore preferable to use as low a Δn.d value as possible when dealing with the conventional $90^{o}$ TN cell as far as the optical angular properties of the unit are concerned. For this purpose, most $90^{o}$ TN cells are operated in the *Gooch and Tarry first maximum* mode.

**Figure 5.21: Optical angular properties of $70^{0}$ LT cells as a function of the Δn.d value. The cells are in the "Symmetric A" polariser configuration and a standard I.F is present. Shade number 7.**

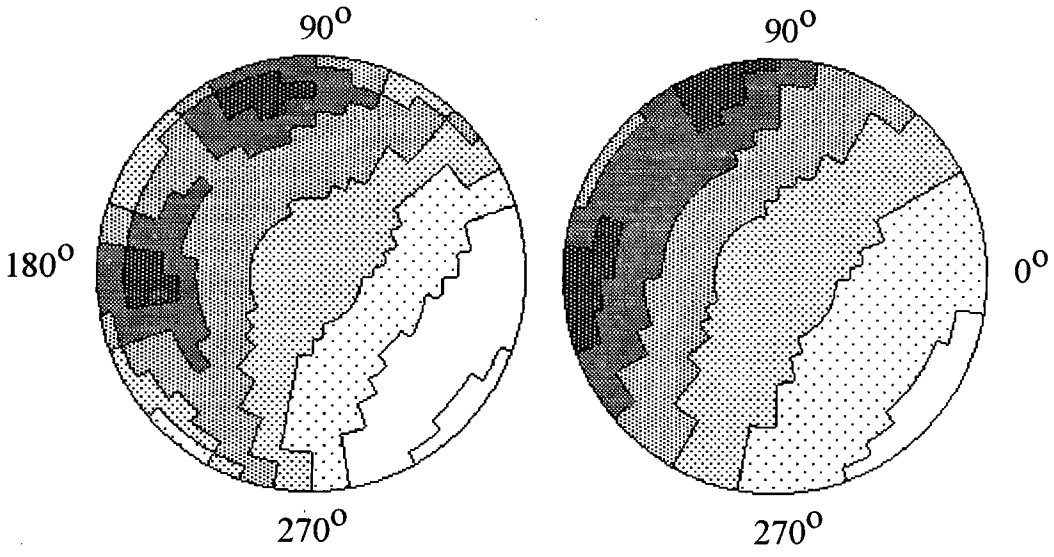


**70° LT Cell. Shade number 7.**
**Δn.d = 0.60μm**

**70° LT Cell. Shade number 7.**
**Δn.d = 0.40μm**

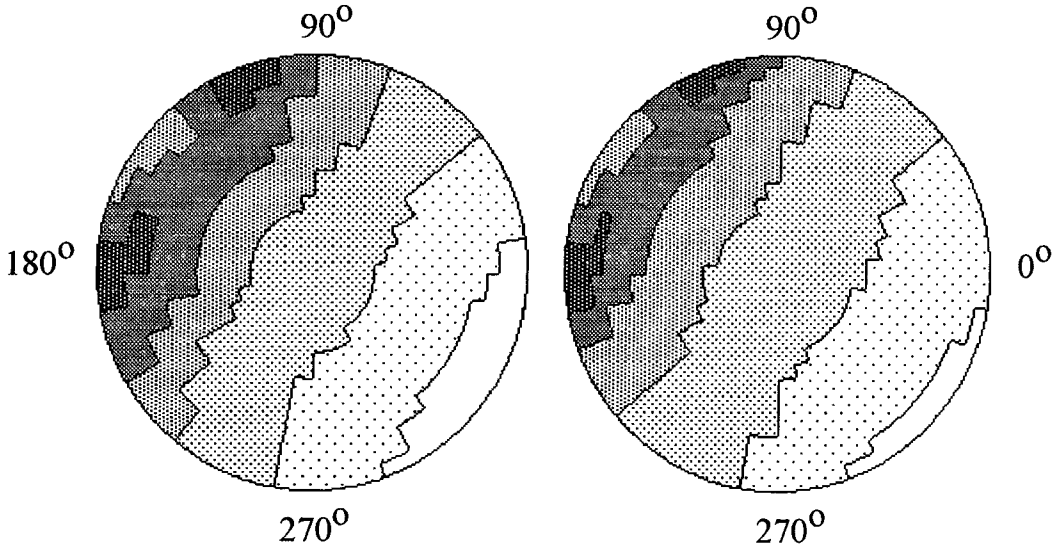


**70° LT Cell. Shade number 7.**
**Δn.d = 0.30μm**

**70° LT Cell. Shade number 7.**
**Δn.d = 0.21μm**

This is in stark contrast to that observed for the $70^{o}$ LT cells shown in figure 5.21. Here, after small initial improvements when dropping from a value of 0.60μm down towards 0.40μm, there is little further effect upon continued reduction beyond this point within the inclination viewing range of ± 30°.

### *5.4 Welding Filter Designs Using Low-Twist (LT) Cells.*

It has been demonstrated that the asymmetric optical angular properties afforded by LT cells operating in the normally white mode are not adversely affected upon rotation of the crossed polarisers into the *Symmetric A* configuration, this being the arrangement required in order to maximise the overall optical throughput of the device when in the inactivated phase. By controlling the Δn.d parameter of the cell, transmissions approaching 100% can thus be achieved over a wide range of values down towards the theoretical limit of 0.27μm. Despite it being this design that minimises the contrast available from the filter, the contrast remains at adequate levels suitable for incorporation into a welding filter unit.

As far as the optical angular properties of the unit are concerned, the lower the twist-angle, the better are the results. However, the amount of freedom in designing automatically darkening welding filter glass packs is restricted by the associated rise in operating voltage, limiting the life of the battery. A construction using $90^{o}$ TN cells may require voltages in the region of ± 4.0 volts, compared to that of ± 8.0 volts for a unit functioning with $50^{o}$ LT cells instead. A point of compromise therefore has to be reached dependent upon the marketability of the complete product and in general, the highest acceptable voltage first ascertained giving the minimum obliging twist-angle.

Welding filters based on double-cell structures can be manufactured using LT cells placed in the *Symmetric A* configuration so as to maximise the overall transmittance when in the inactivated phase whilst maintaining the improved optical angular properties afforded by the utilisation of such devices. A structure using LT cells possessing a general twist-angle of $\theta^{o}$ is shown in figure 5.22 where a GH cell and an I.F are also present[50].

The optical angular properties of such a design are shown in figure 5.23 as a function of the twist-angle. Here, 4μm cells filled with the *Merck 3700* liquid crystal mixture are placed in the *Symmetric A* configuration together with the LC81 material. The pertinent Δn.d value for the device is 0.39μm. A standard GH cell and I.F are also present and the cells are driven together so as to obtain a shade number 12. The improvement in the angular dependence of the welding filter upon twist-angle reduction is apparent from these figures.

**Figure 5.22: Welding filter design using LT cells with a general twist-angle operating in the "Symmetric A" configuration so as to maximise the transmittance when in the light state.**

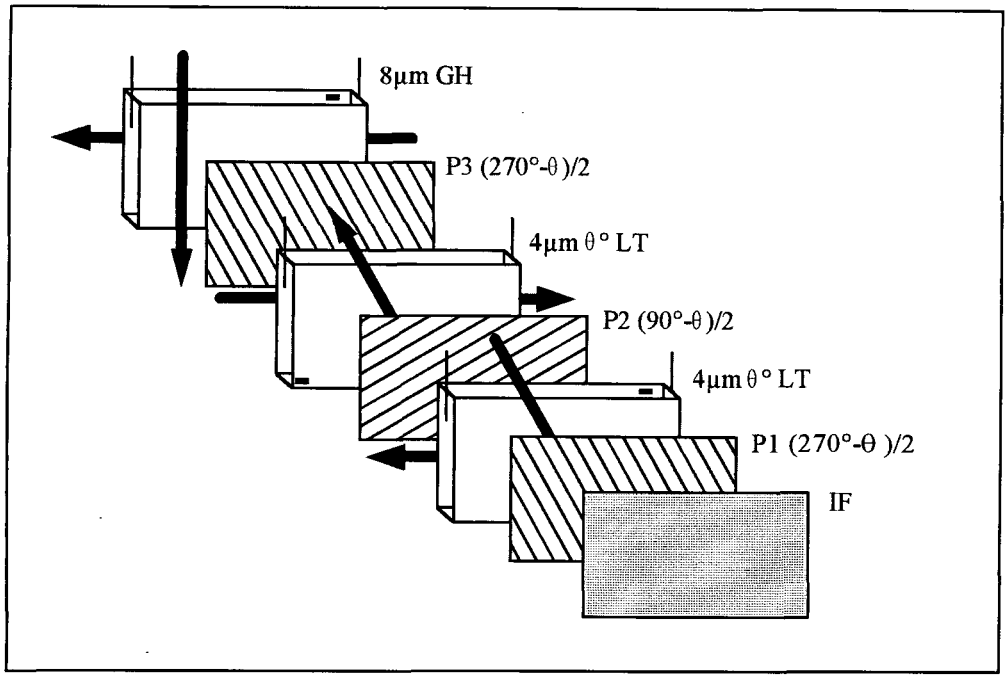


**Figure 5.23: Optical angular properties of welding filters using LT cells of varying twist-angles placed in the "Symmetric A" configuration with *LC81* polarisers. A GH cell and I.F are present.**

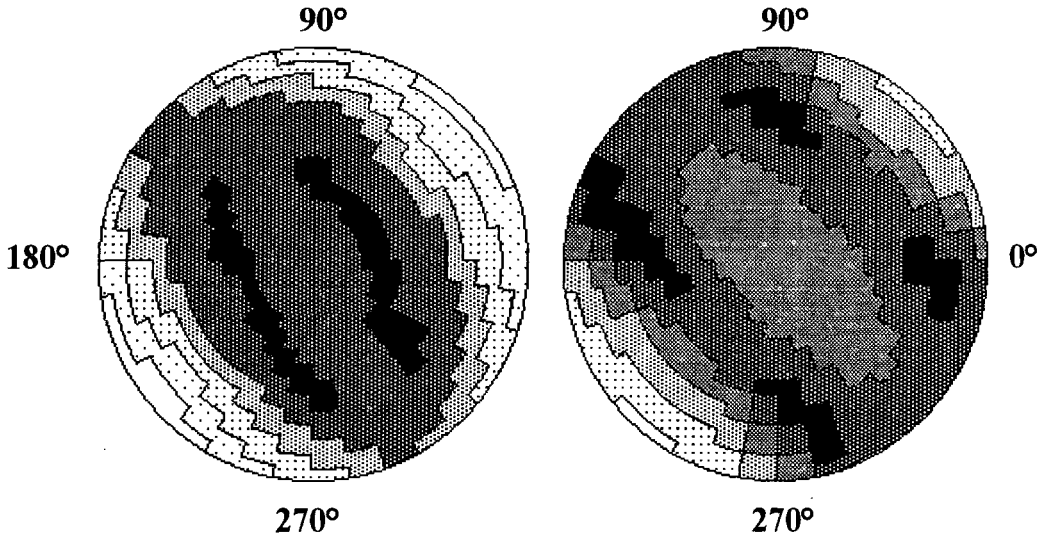


**Welding filter using 4μm 90° TN cells operating in the "Symmetric A" configuration. Shade number 12**

**Welding filter using 4μm 80° LT cells operating in the "Symmetric A" configuration. Shade number 12**

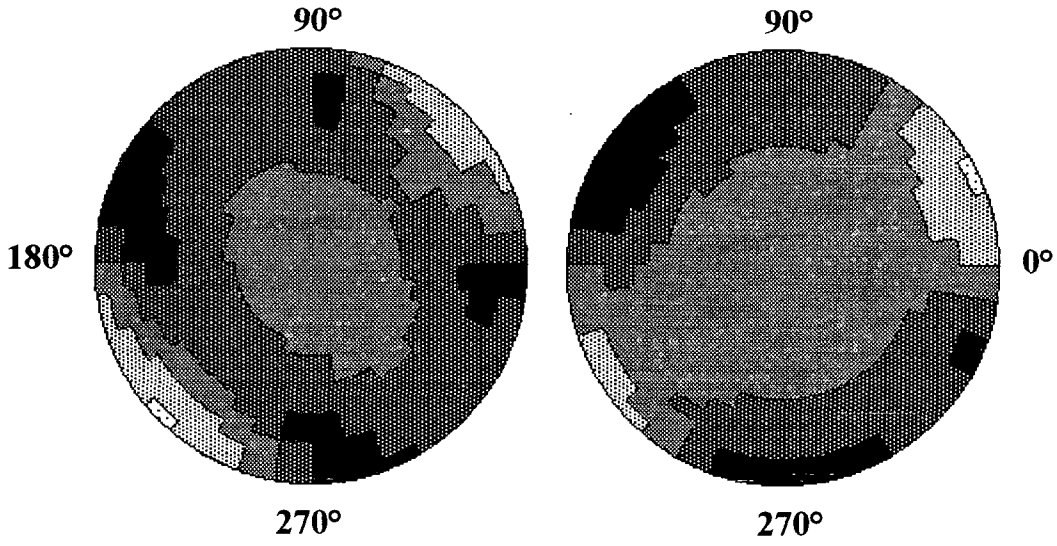


**Welding filter using 4μm 70° LT cells operating in the "Symmetric A" configuration. Shade number 12**

**Welding filter using 4μm 60° LT cells operating in the "Symmetric A" configuration. Shade number 12**

Some of the electro-optic properties associated with this complete welding filter design are displayed in table 5.2 as a function of the twist-angle present in the LT cells. The 4μm LT cells are filled with the *Merck 3700* liquid crystal mixture and are driven together with a 50Hz square wave. Here, GH cell contrast is defined as the shade number step obtained upon switching of the cell from the inactivated to the stimulated state with an applied driving voltage of ± 6.0 volts at 50Hz. As expected from the geometry of the system, this contrast is degraded upon depreciation of the twist-angle due to the diminishing component of radiation polarised parallel to the entrance molecular director of the GH device. To alleviate this problem, the alignment orientation of the entrance liquid crystal molecules present in the GH cell must be oriented parallel with the preceding polariser.

**Table 5.2: Electro-optic properties of welding filter designs using LT cells with various twist-angles placed in the "Symmetric A" configuration between *LC81* polarisers. A GH cell and I.F are present.**

| Twist-angle in LT cells | Light state shade number | GH cell contrast | Voltage to attain shade number 12 |
|---|---|---|---|
| $90^0$ | 3.82 | 1.34 | ± 3.8 volts |
| $80^0$ | 3.66 | 1.33 | ± 3.9 volts |
| $70^0$ | 3.63 | 1.25 | ± 5.1 volts |
| $60^0$ | 3.64 | 1.16 | ± 6.5 volts |

### *5.5 Using Reverse-Twist Cells in Welding Filter Designs.*

The nematic type liquid crystal cells considered so far have all been of the *negative* twisting sense or *left-handed* and hence filled with a liquid crystal mixture that is appropriately doped with a chiral component possessing a natural twisting helix with this direction of rotation. This ensures that the required spiralling orientation is induced throughout the entire liquid crystal layer and prevents the formation of domains where the crystal is twisting in the opposite sense. The cholesteric component exclusively used for this purpose throughout this thesis is the *Merck ZLI-811* material at the 0.1% by volume doping level.

However, the manufacturing of *positive* twisting or *right-handed* cells is readily achieved via suitable cell assembly together with doping of the crystal element with a *positive* cholesteric component such as the *Merck ZLI-3786* material. This gives rise to the possibility of placing two oppositely twisting devices together forming a double-cell arrangement and may offer advantages in terms of the optical angular properties of the system due to an increase in cell compensation.

Figure 5.24 shows the optical angular properties of two double-cell designs using 4μm 70° LT cells filled with the *Merck 3700* liquid crystal material and operating in the *Symmetric A* configuration between LC81 polarisers. The cells are driven together with a 50Hz square wave so as to attain a shade number 10 and a standard I.F is present. The first shows that for two negatively twisting cells in which the crystal is doped with the *Merck ZLI-811* chiral component. It is noted that in order to obtain compensation with such an arrangement, it is necessary to orient the cells in *opposite* directions and position one cell *upside down* as indicated in figure 2.6 of chapter two.

**Figure 5.24: The optical properties of double-cell structures using 4μm 70° LT cells with the *Merck 3700* crystal in the "Symmetric A" arrangement. The use of reverse twist cells is investigated.**

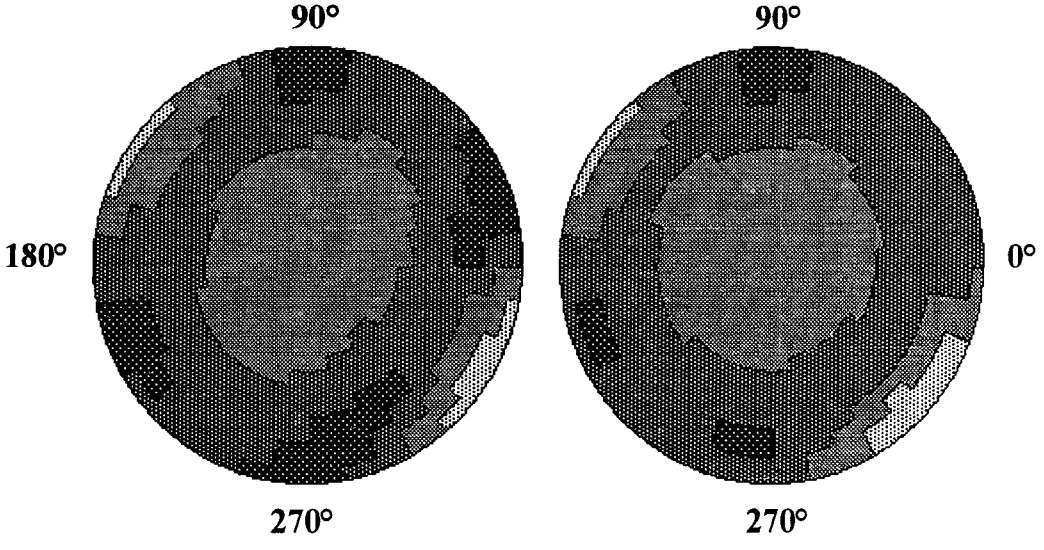


**Two -'ve twisting 4μm 70° LT cells operating in the "Symmetric A" configuration. Shade number 10**

**Two 4μm 70° LT cells with opposite twists placed in the "Symmetric A" configuration. Shade number 10**

The second polar plot corresponds to the case where both a negative and a positive twisting 4μm 70° LT cell is used. The cells are still driven together but this time it is essential to position the cells in the *same* orientation with one cell being upside down in order to gain good cell compensation. This arrangement is schematised in figure 5.25. Note that if the cells are not correctly oriented, the dark viewing cones of each individual cell re-reinforce each other in the polar chart and an overall system possessing exaggerated asymmetry is obtained.

**Figure 5.25: Required arrangement in order to generate cell compensation in a double-cell design using two 4μm 70° LT cells of opposite twists and operating in the "Symmetric A" configuration.**

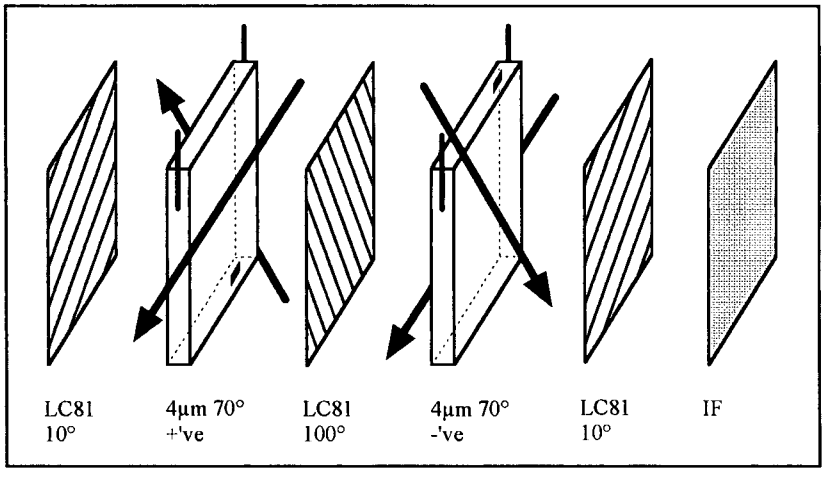


From figure 5.24 it is apparent that there is little significant improvement in the optical angular properties displayed by double-cell designs upon utilisation of two cells possessing opposite senses of rotation when in the activated phase, although there is a small subtle increase in the central symmetry of these properties. This however, must be balanced up against the extra manufacturing costs involved in the production of two cell types instead of only one unique design and in general far out weighs that of the small improvements observed above. Note that this is also applicable for other twist-angles including that of the standard 90° TN device and it is therefore concluded that the use of oppositely twisting cells offers no great advantage in terms of the angular dependence of automatically darkening welding filters based on liquid crystal cells operating in the normally white mode and with the *Symmetric A* polariser configuration.

*This chapter has shown that despite optimisation of both the Δn.d parameter and the polariser configuration in order to maximise the overall optical transmittance of LT cells when in the inactivated phase and operating in the normally white mode, the enhanced asymmetric optical angular properties afforded by such devices is maintained. This gives rise to the possibility of developing automatically darkening welding filters based on double-cell structures possessing improved angular properties accordingly. The only compromise comes from the requirement of increasing the operating voltage of the unit upon twist-angle reduction, producing adverse effects upon the current consumption of the system. Although further optical improvements can be obtained upon reduction of the pertinent Δn.d value when utilising the standard $90^{o}$ TN unit, LT cells are far less sensitive to this factor. No significant advantage was observed upon incorporation of cells possessing twist-angles with opposite senses of rotation into the glass pack and the extra manufacturing costs involved upon production of such designs makes this system far less attractive.*

# *CHAPTER SIX*

*This chapter introduces a new mode of operation for a twisted nematic liquid crystal cell placed between crossed polarisers such that the device displays a dark state when inactivated and placed together with an interference filter possessing a high optical transmittance over the central part of the visible spectrum. A small stimulating voltage of between ± 2.0 and ± 3.0 volts is required in order to attain the light state and further increment of the driving voltage beyond this point reverts the unit back to a dark condition. Such a device offers advantages over that of the normally white mode of operation in that a fail safe, dark state is provided should the controlling electronics malfunction, a property often associated with the normally black mode of operation, whilst the fast response time from the light to the dark state associated with the normally white mode of operation is maintained. It is shown that there are only two cell types that display this phenomenon and the optical properties of these two systems are investigated in some detail with the view of developing an automatically darkening welding filter based on this technology.*

## *6.1 A Novel Mode of Operation for a Twisted-Nematic Liquid Crystal Cell.*

When linearly polarised light passes through a twisting liquid crystal helical structure, the plane of the major axis is rotated by the cell and the emerging radiation becomes elliptically polarised with components oscillating in directions both parallel and perpendicular to the exit liquid crystal molecules. The phase difference between these two components produces a whole variety of colours dependent upon the twist-angle in the cell, the cell thickness and the type of liquid crystal material in use. By careful manufacturing control, it is therefore possible to produce cells that display virtually any desired colouration when in the inactivated phase and placed between two polarising media. Application of a low stimulating voltage to the cell partially destroys the spiralling structure and hence removes the colouration.

The first element in an automatically darkening welding filter glass pack is usually a passive *interference filter (I.F)* that reflects both U.V and I.R radiation at all times and possesses a transmission spectrum matching that for the sensitivity curve of the human eye. Typical optical properties for the standard I.F used throughout this report are shown in figure 1.7 of chapter one. A natural consequence of this filter having a high optical transmittance over the central part of the visible spectrum is that *reflected* radiation from the surface of the device is devoid of green radiation. This gives the I.F a *pink-red* appearance when observed in reflection.

By using liquid crystal cells that possess a low optical throughput when in the inactivated phase at wavelengths matching those at which the passive I.F transmits, a welding filter is obtained that is relatively dark (shade number 7) in the absence of any stimulating voltage. Application of a small electric

field (typically ± 2.5 volts) removes the colouration of the cell and hence the unit becomes light. If, in addition the cell is placed between *crossed* polarisers, further increment of the stimulating voltage reverts the device back to a dark state as the remaining optical activity of the cell is removed. The unit is therefore operated typically between a highly transparent ± 2.5 volt and an opaque ± 8.0 volt state.

Such a device offers several advantages over that of the normally white mode of operation where the cell is optimised so as to give maximum transmittance when in the light state with the Δn.d parameter corresponding to one of the *Gooch and Tarry maximum* positions. The first comes from the safety requirement that an automatically darkening welding filter be in a dark state should the driving electronics malfunction. Most designs currently on the market achieve this via utilisation of GH cells that are in a dark phase when inactivated. However, this not only increases the production costs but also adds to the overall weight of the protection helmet. Employment of the novel mode of operation introduced above would remove the necessity for GH cell incorporation into the glass pack and hence alleviate these problems.

The second advantage comes from the fact that the cell requires a small electric field in order to attain the light state. Here, the bulk molecules are already partially oriented and further transformation to the dark state occurs primarily due to the rotation of the surface molecules only upon additional increment of the driving electronics. The nematic type cell is thus akin to that of a *Surface-Mode-Device (S.M.D)*[51] and is therefore expected to possess enhanced switching speeds accordingly.

The desired criteria for this phenomenon to be observed is that the optical *transmittance* spectrum of the cell be devoid of green wavelengths when placed between crossed polarisers and in the inactivated phase. The proceeding sections determine suitable cell types that satisfy this requirement and investigate the optical properties of such systems.

### *6.2 Cell Types Displaying this Mode of Operation.*

Figure 6.1 shows the calculated transmittance curves obtained from LT cells when in the inactivated phase and placed between crossed polarisers oriented in the *Symmetric A* configuration for three different twist-angles of $50^{o}$, $70^{o}$ and $90^{o}$ respectively. The cells are optimised in terms of both the Δn.d parameter and the polariser orientations in order to maximise the overall optical throughput of the device. Note that this requires the Δn.d values given according to figure 5.9 in chapter five.

The transmittance curves display maxima centred at a wavelength of 550nm corresponding to the centre of the luminous spectrum and the overall optical throughputs in the near U.V and I.R regions decrease upon reduction of the twist-angle in the cell.

In order that a liquid crystal cell achieves a dark state when placed together with the standard I.F, the transmittance curve for the single cell should be devoid of green radiation and hence display a pink-red colouration. Figure 6.2 shows the calculated transmittances at a wavelength of 550nm for LT cells placed between crossed polarisers as a function of both the twist-angle and the pertinent Δn.d parameter. Twist-

angles of between $0^{o}$ and $90^{o}$ are investigated together with $\Delta n.d$ values of up to 0.80μm for both the *Symmetric A* and *Symmetric B* polariser configurations. The transmittance values are displayed in a surface plot diagram with a 5% contour interval.

**Figure 6.1: Transmission spectrums of optimised LT cells in the inactivated phase as a function of twist-angle. The "Symmetric A" polariser configuration is used giving maximum transmittance.**

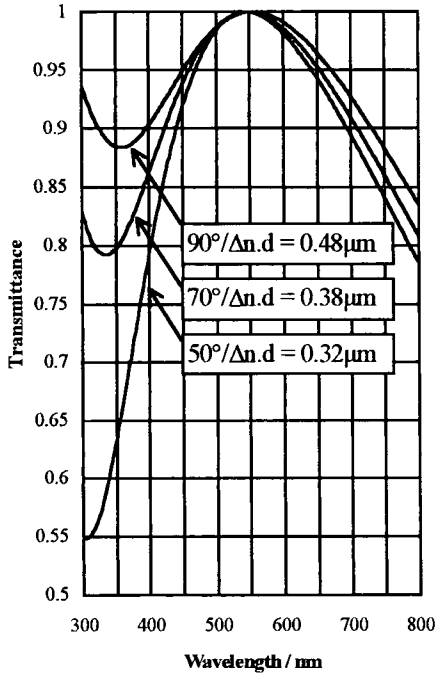


**Figure 6.2: Optical transmittance at 550nm for LT cells with the "Symmetric A" and "Symmetric B" polariser configurations as a function of both the twist-angle and the $\Delta n.d$ parameter.**

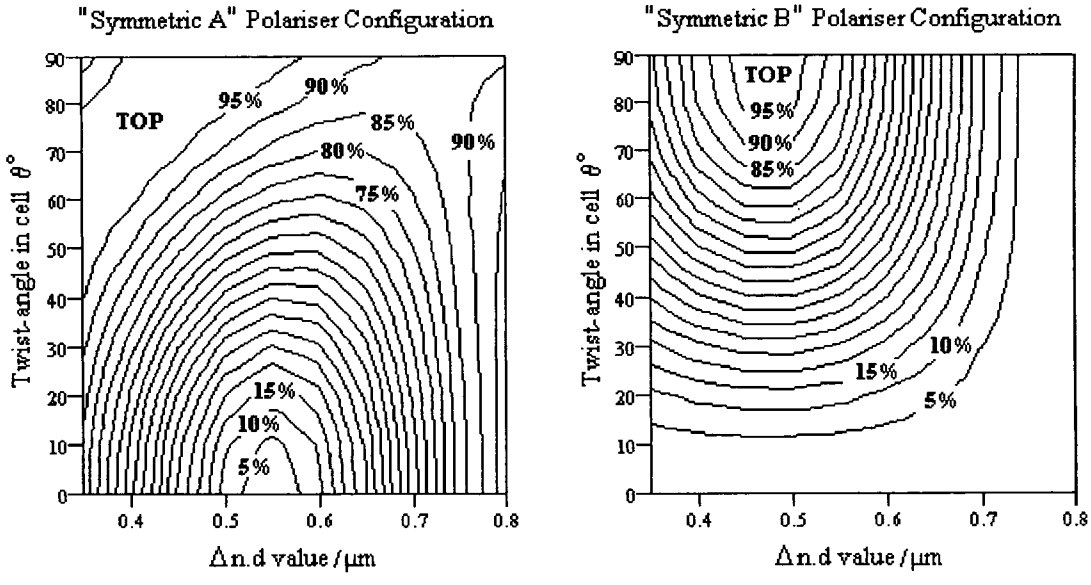

There are two liquid crystal cell types that are seen to fulfil the requirements when in the inactivated phase and placed between crossed polarisers, indicated by points of depression in figure 6.2. This is illustrated more clearly in figure 6.3 where the crossed polarisers are held at $45^{o}$ and $135^{o}$ respectively relative to the entrance molecular alignment director. The first solution corresponds to a $0^{o}$ LT cell possessing a $\Delta$n.d value of 0.55μm with the polarisers oriented in the *Symmetric A* configuration, whilst that of the second represents a $90^{o}$ TN cell with a value of 0.78μm and polarisers placed in the *Symmetric B* arrangement. Note that due to the geometry of these two systems, both solutions require the polarisers to be positioned at $45^{o}$ and $135^{o}$ respectively relative to the entrance molecular director vector.

**Figure 6.3: Calculated transmittance at 550nm for LT cells placed between crossed polarisers oriented at $45^{o}$ and $135^{o}$ respectively as a function of both the twist-angle and the $\Delta$n.d parameter.**

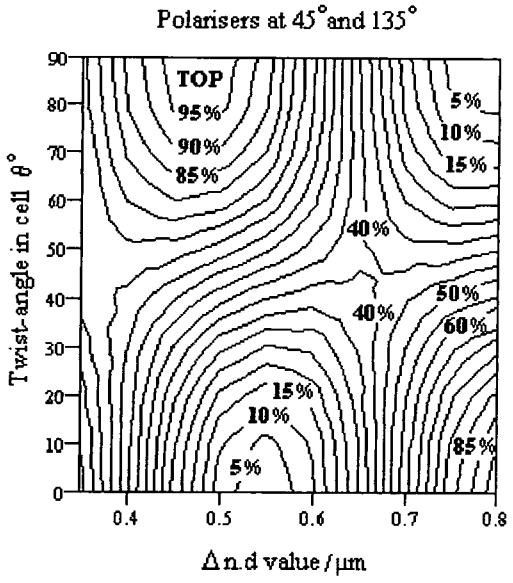


Other cell types that satisfy the criteria of displaying a low optical transmittance over the green wavelengths indicated in figure 6.2 for the *Symmetric B* polariser configuration represent the trivial cases for which the LT cell possesses a low transmittance over the entire visible spectrum and hence are of little relevance here. The proceeding sections will therefore investigate the optical properties of these two cell types with the view of developing an automatically darkening welding filter glass pack that provides a safe-state shade step should the electronics malfunction whilst maintaining the fast response time from the light to the dark state associated with the normally white mode of operation.

### *6.3 $0^o$ LT Cell with Δn.d equal to 0.55μm.*

The first cell to be considered is a 4μm $0^o$ LT cell filled with the *Merck ZLI-4246 (4246)* liquid crystal mixture giving a Δn.d value of 0.52μm, this being sufficiently close to the optimised value of 0.55μm for the desired phenomenon to be observed. Here, LC81 polarisers oriented at $45^o$ and $135^o$ respectively are used. The calculated transmission curve for such a device is shown in figure 6.4.

**Figure 6.4: Calculated optical transmittance of a $0^o$ LT cell placed between crossed polarisers possessing a Δn.d value of 0.52μm as a function of the polariser orientation.**

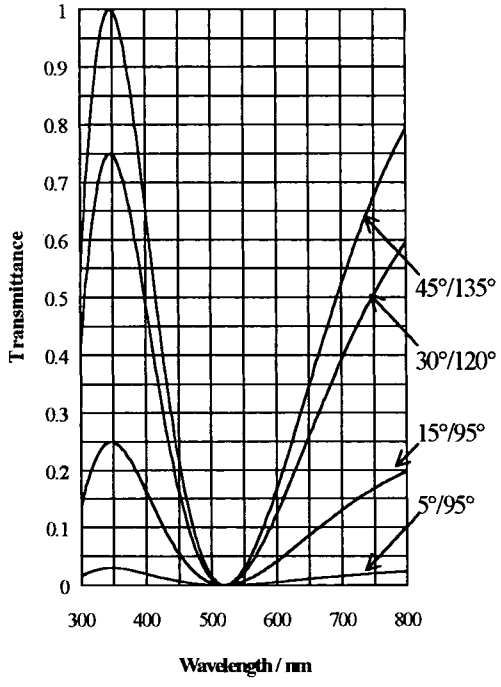


The most intense pink-red colouration is obtained with the polarisers oriented in the *Symmetric A* configuration and whilst rotation of the polarisers away from this arrangement does not alter the position of the minima centred around a wavelength of 520nm, the total integrated luminous transmittance of the device is reduced.

The electro-optic properties of such a device placed together with a standard I.F and with crossed LC81 polarisers oriented at $45^o$ and $135^o$ respectively are shown in figure 6.5. Here, shade number is displayed as a function of the applied 50Hz square wave driving voltage. The cell achieves a shade number of 5.3 in the inactivated phase and as required, becomes first lighter before reverting back to a dark state upon increment of the stimulating voltage. A ± 2.4 volt square wave is required in order to obtain the lowest shade number of less than 3.4. However, the contrast available from the cell with a voltage step from the light state to a ± 10 volt square wave is only 3.1 shade numbers, clearly inadequate if the cell is to provide the main contrast ramp in an optical shutter element.

**Figure 6.5: Electro-optic properties of a 4μm $0^0$ LT cell filled with the *Merck 4246* liquid crystal mixture with *LC81* polarisers at $45^0$ and $135^0$ respectively. A standard I.F is present.**

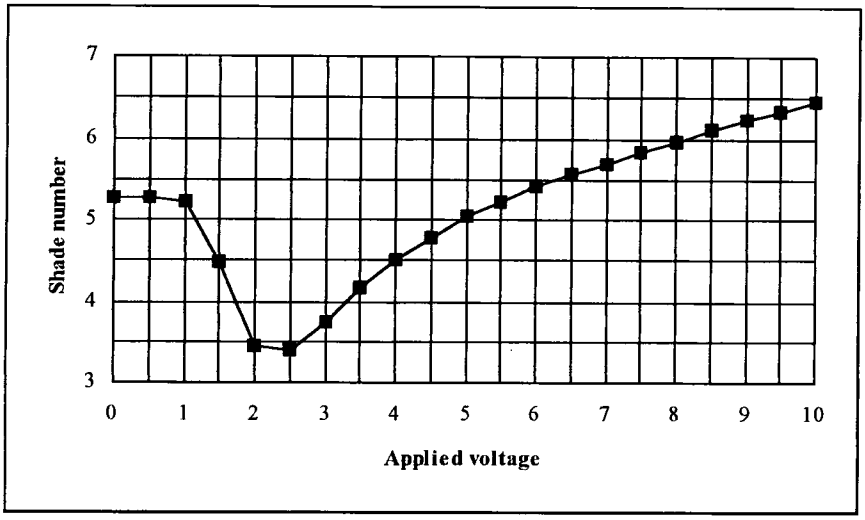


The contrast obtained from the 4μm $0^0$ LT cell filled with the *Merck 4246* liquid crystal mixture as a function of the polariser configuration is shown in figure 6.6. Here, contrast is defined as the shade number step obtained in going from the lightest state available to that reached with a ± 10 volt square wave operating at 50Hz. Crossed LC81 polarisers are used and a standard I.F is present. The contrast obtained from several other cell types are also shown for comparison. This includes a 4μm $90^0$ TN cell, a 4μm $70^0$ LT device and a 4μm $40^0$ LT unit all filled with the *Merck 3700* liquid crystal mixture as well as an 8μm $90^0$ TN cell and an 8μm $50^0$ LT unit filled with the *Merck 6096* component.

**Figure 6.6: Contrast from various cell types placed between crossed polarisers as a function of angle between the first polariser and the entrance molecular director. A standard I.F is present.**

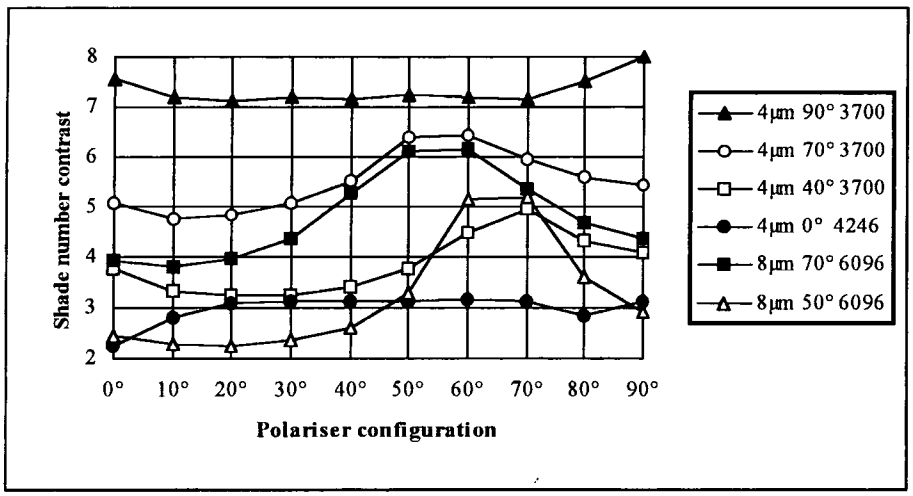

The large contrast available from the higher twisting cells remains essentially unaltered upon rotation of the crossed polarisers relative to the cell rubbing directions, the 4μm $90^{o}$ TN cell giving a drop of only 0.5 shade numbers as the polarisers are moved away from the standard $0^{o}/90^{o}$ configuration into the intermediate $45^{o}/135^{o}$ orientation. However, the electro-optic properties of the lower twisting cells are characteristic of such devices where it is essential to reach the *Symmetric B* polariser configuration in order to maximise cell contrast. Reduction of the twist-angle together with an increase in the Δn.d parameter also has the effect of making the unit more sensitive to this phenomenon.

The 4μm $0^{o}$ LT cell forms a birefringent device and due to the low twist-angle present in the cell, little compensation occurs between the remnant retardation present in the two layers of unperturbed liquid crystal material immediately adjacent to the cell sides when in the partially activated phase. This prevailing birefringence generates an associated loss of cell contrast and dramatically increases the operating voltage of the unit. This is manifested by the severe degradation of the dark state shade number reached by the $0^{o}$ LT cell with an applied voltage of ± 10 volts, which at best only attains a contrast step of 3.1 shade numbers. Such a cell therefore possesses insufficient contrast in order to provide the major transmittance step in an automatically darkening welding filter design. Note that it may be possible to compensate for the retardation produced by the surface liquid crystal molecules via use of low-value retardation films and research is continuing in this area.

Figure 6.7 shows the electro-optic properties of a 4μm $0^{o}$ LT cell as a function of the polariser orientation. Crossed LC81 polarisers are used and a standard I.F is present The device displays a dark state in excess of a shade number 9 with the polarisers placed in the standard $0^{o}/90^{o}$ configuration irrespective of the driving voltage. However, for intermediate polariser arrangements a higher overall optical throughput is obtained. It must be noted however, that the available cell contrast from the device remains largely independent of the polariser orientation relative to the cell.

**Figure 6.7: Electro-optic properties of a 4μm $0^{o}$ LT cell with the *Merck 4246* liquid crystal as a function of the polariser orientation. *LC81* polarisers are used and a standard I.F is present.**

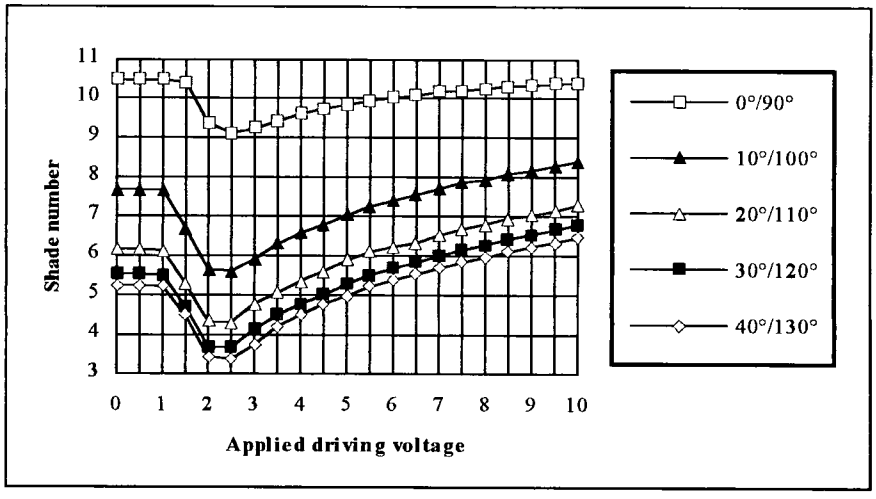

The optical angular properties of a 4μm $0^{o}$ LT cell filled with the *Merck 4246* liquid crystal mixture are shown in figure 6.8 for the light and dark states. The cells are placed between crossed LC81 polarisers oriented at $45^{o}$ and $135^{o}$ respectively in order to maximise the light state transmittance and a standard I.F is present. It can be seen that the single cell possesses highly asymmetric angular properties due to both the low twist-angle present in the cell and utilisation of the *Symmetric A* polariser configuration. These properties make the cell highly suitable for incorporation into a double-cell structure whereby a large degree of cell compensation occurs.

Whilst possessing optical angular properties that are highly asymmetric due to both the low twist-angle present in the cell and employment of the *Symmetric A* polariser configuration, the contrast available from the $0^{o}$ LT cell is insufficient for incorporation into a welding filter design that is required to attain a dark state in excess of a shade number 13. A certain degree of improvement may be obtained via use of thinner cells down towards 2μm, but this will also have adverse effects upon the manufacturing ease of the device as well as increasing the power consumption of the unit. These problems may be alleviated via utilisation of low-value retardation films and further research is continuing in this area.

**Figure 6.8: Optical angular properties of a 4μm $0^{o}$ LT cell with the *Merck 4246* liquid crystal placed between *LC81* polarisers oriented at $45^{o}$ and $135^{o}$ respectively. A standard I.F is present.**

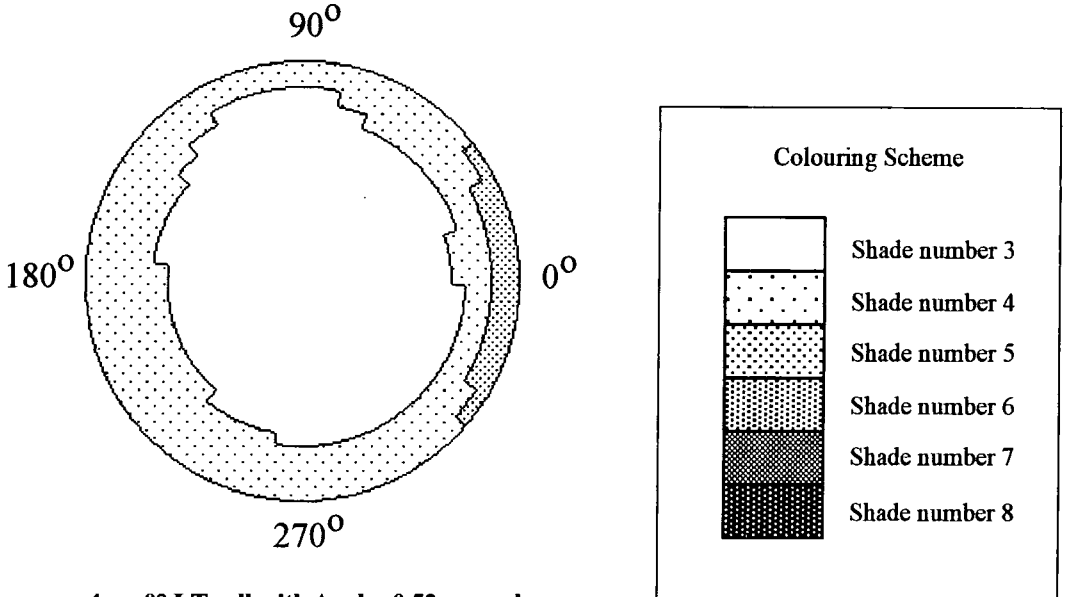


**4μm 0° LT cell with Δn.d = 0.52μm and LC81 polarisers cut at 45° and 135°. An I.F is present. ± 2.5 volts giving light state.**

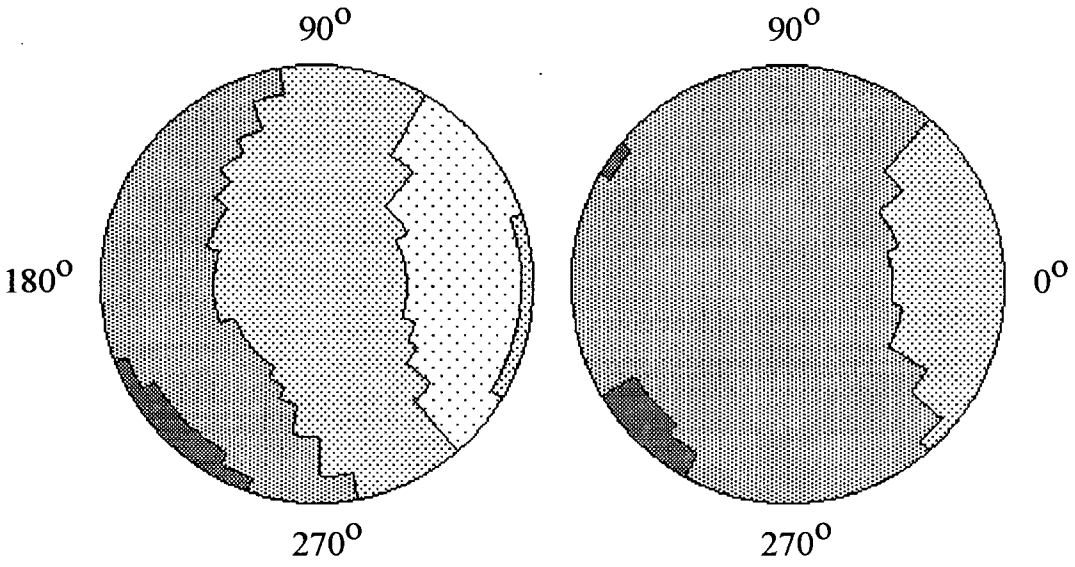


**4μm 0° LT cell with Δn.d = 0.52μm and LC81 polarisers cut at 45° and 135°. An I.F is present. ± 5 volts for shade 5.**

**4μm 0° LT cell with Δn.d = 0.52μm and LC81 polarisers cut at 45° and 135°. An I.F is present. ± 10 volts for shade 6.**

### *6.4 90° TN cell with Δn.d equal to 0.78μm.*

The second cell type that displays the required phenomenon corresponds to a 90° TN cell possessing a Δ n.d value of 0.78μm with crossed polarisers oriented in the *Symmetric B* configuration at 45° and 135° respectively. An 8μm 90° TN cell filled with the *Merck 6096* liquid crystal mixture fulfils this requirement, giving a Δn.d value of 0.80μm. The calculated optical transmittance for such a device is displayed in figure 6.9 as a function of the polariser arrangement. With the polarisers arranged in the standard 0°/90° configuration, the unit maintains a high luminous transmittance over the entire visible spectrum and hence appears colourless. However, rotation of the polarisers away from this orientation generates a reduction in the optical transmittance for radiation centred around the green wavelengths, hence developing the desired pink-red colouration. The most intense tone appears with the polarisers placed in the *Symmetric B* configuration and is slowly dissipated upon rotation of the polarisers away from this point.

The electro-optic properties of an 8μm 90° TN cell filled with the *Merck 6096* liquid crystal mixture and placed between crossed LC81 polarisers is shown in figure 6.10 as a function of the polariser arrangement. A standard I.F is present and a 50Hz square wave is used. It is noted that good cell contrast is obtained irrespective of the polariser configuration.

**Figure 6.9: Calculated optical transmittance of a 90$^0$ TN cell placed between crossed polarisers with a Δn.d value of 0.80μm as a function of the polariser orientation.**

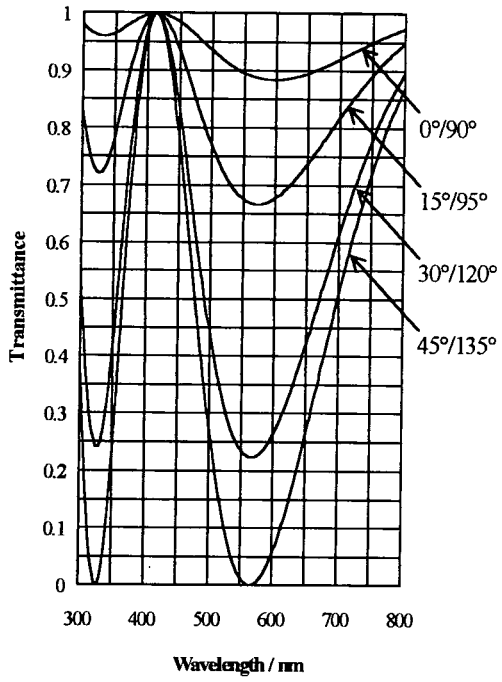


**Figure 6.10: Electro-optic properties of an 8μm 90$^0$ TN cell filled with the *Merck 6096* liquid crystal mixture as a function of the *LC81* polariser orientation. A standard I.F is present.**

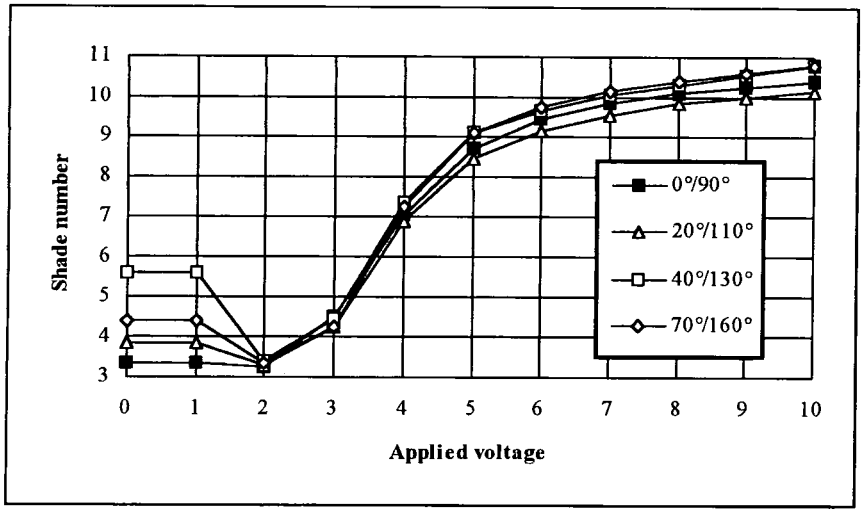


When in the inactivated phase and with the standard 0$^0$/90$^0$ and 90$^0$/180$^0$ polariser configurations, the 90$^0$ TN cell possesses a relatively high transmittance of under 3.5 shade numbers, remaining constant until the liquid crystal threshold voltage is exceeded whereupon the unit rapidly becomes darker upon further increment of the driving electronics. However, the non-standard intermediate polariser

configurations produce the desired pink-red colouration when in the inactivated phase, necessitating a small driving voltage of between ± 2.0 and ± 3.0 volts in order to switch the unit into the lightest state. Raising the voltage beyond this point causes the cell to rapidly become darker again. This provides the required degree of safety whereby in the event of the electronics malfunctioning, the unit switches into an intermediate dark state rather than holding in a potentially hazardous lighter condition.

The safe-state shade step is defined as being the shade number difference between the inactivated, dark state and the lightest transmittance reached by the unit upon application of a small stimulating voltage. Figure 6.11 shows the magnitude of the safe-state shade step obtained from an 8μm 90° TN cell filled with the *Merck 6096* liquid crystal mixture as a function of the angle between the crossed polarisers and the cell rubbing directions. The LC81 polarising material is used and a standard I.F is present. It is shown that a minimum is observed with the polarisers oriented in either the standard 0°/90° or 90°/180° configurations and that a maximum of 2.2 shade numbers is obtained with the polarisers aligned at 45° and 135° respectively.

**Figure 6.11: Safe-state shade step from an 8μm 90° TN cell with the *Merck 6096* liquid crystal as a function of the angle between the first polariser and the entrance molecular director.**

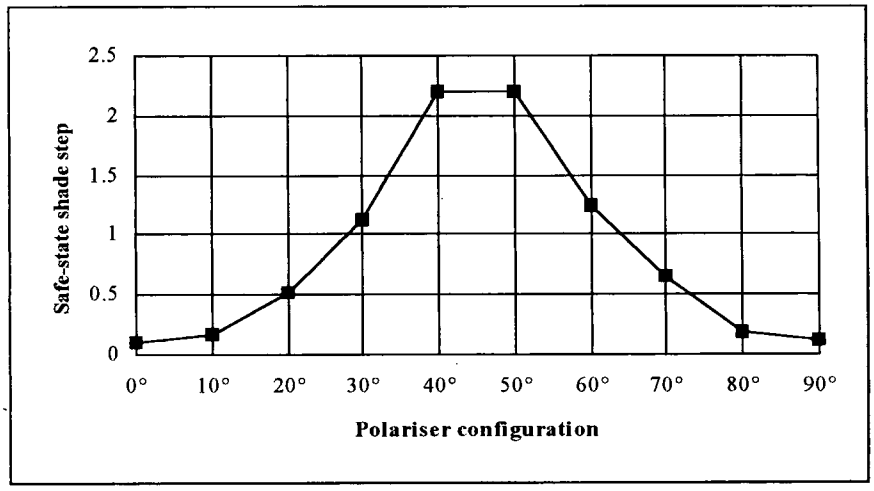


With the polarisers placed in the *Symmetric B* configuration, good cell contrast and a large safe-state shade step is obtained for viewing angles lying parallel to the surface normal. However, it has been demonstrated in chapter five that the poor optical angular properties associated with this polariser arrangement generates a rapid loss of cell contrast at large inclination angles exceeding that of 20°. This is reiterated in figure 6.12 which shows the angular dependence of two cell types operating in the *Symmetric B* configuration. Both a 4μm 70° LT cell filled with the *Merck MLC-6080 + 0.1% Merck ZLI-*

*811 (6080)* liquid crystal mixture and an 8μm 90° TN cell with the *Merck 6096* material are investigated and crossed LC81 polarisers are used. The first is activated with a ± 4.0 volts 50Hz square wave, the second driven so as to attain a shade number 8. A standard I.F is present in both cases.

This effect is quite general upon utilisation of the *Symmetric B* design irrespective of the type of liquid crystal cell employed and devices based upon such structures therefore possess poor optical angular properties accordingly. Since it is this arrangement that is necessary in order to produce the pink-red colouration when exploiting 90° TN cells placed between crossed polarisers and with a Δn.d value of 0.80μm, this cell is also subjected to this ailment.

**Figure 6.12: Angular properties of 4μm 70° LT cells with the *Merck 6080* crystal and 8μm 90° TN cells with the *Merck 6096* material in the "Symmetric B" configuration. A standard I.F is present.**

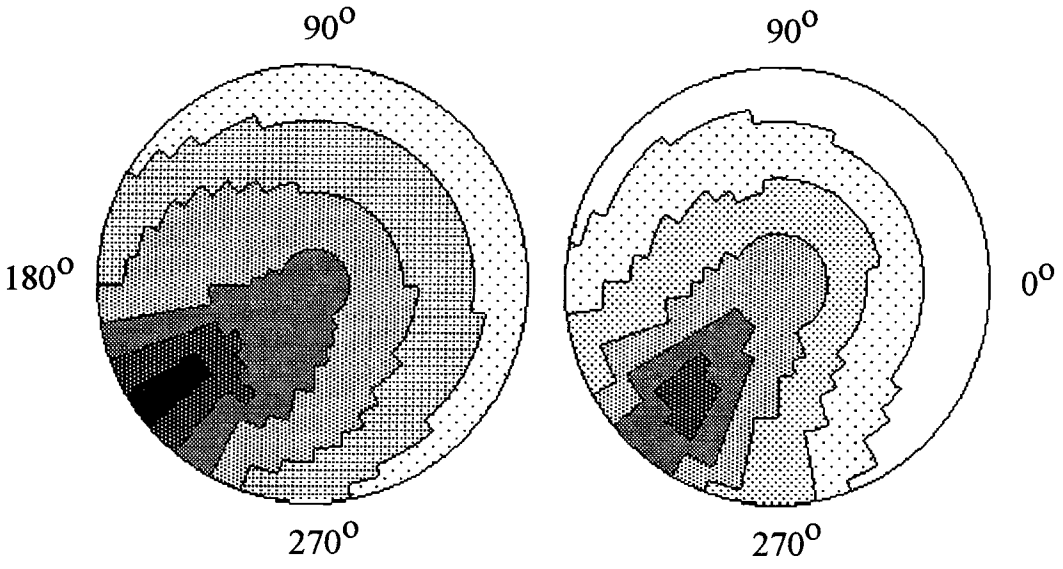


**4μm 70° LT cell with the 6080 crystal operating in the "Symmetric B" configuration. ± 4 volts to the cell**

**8μm 90° TN cell with the 6096 crystal operating in the "Symmetric B" configuration. Shade number 8**

Figure 6.13 shows the optical angular properties of an 8μm 90° TN cell filled with the *Merck 6096* liquid crystal mixture placed between crossed LC81 polarisers oriented in the *Symmetric B* configuration as a function of the applied voltage. A 50Hz square wave is used and a standard I.F is present.

When in the inactivated phase, the optical angular properties of the device are highly symmetric over a wide range of viewing angles with large domains or regions in the polar plot encapsulating points possessing similar transmittance values. However, upon application of the ± 2.4 volts required in order to attain the light state, a filter with a restricted viewing cone is obtained wherein the cell becomes gradually darker when viewed at acute angles away from the normal incident direction.

As a consequence of the *Symmetric B* polariser arrangement being used, the optical angular properties of the cell when stimulated by reduced voltages of less than ± 8 volts form the so-called *wrapped* pattern in the polar chart, making the system less suitable for incorporation into an automatically darkening welding filter design whereby a large central viewing cone is required.

**Figure 6.13: Optical angular properties of 8µm 90° TN cells with the *Merck 6096* material operating in the "Symmetric B" arrangement as a function of applied voltage. A standard I.F is present.**

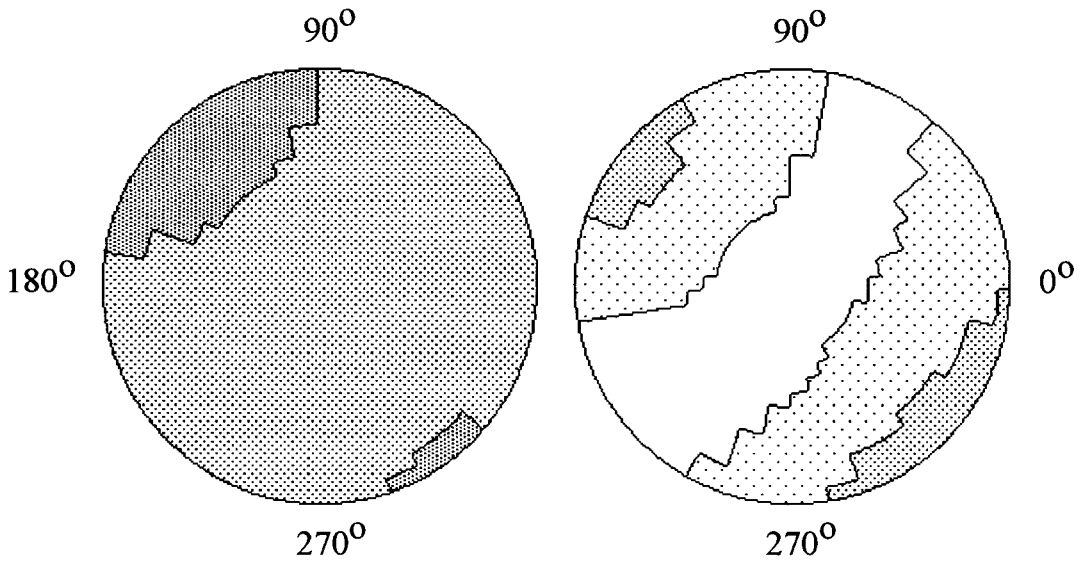


**8µm 90° TN cell with the 6096 crystal operating in the "Symmetric B" configuration. 0 volts to the cell**

**8µm 90° TN cell with the 6096 crystal operating in the "Symmetric B" configuration. ± 2.4 volts to the cell**

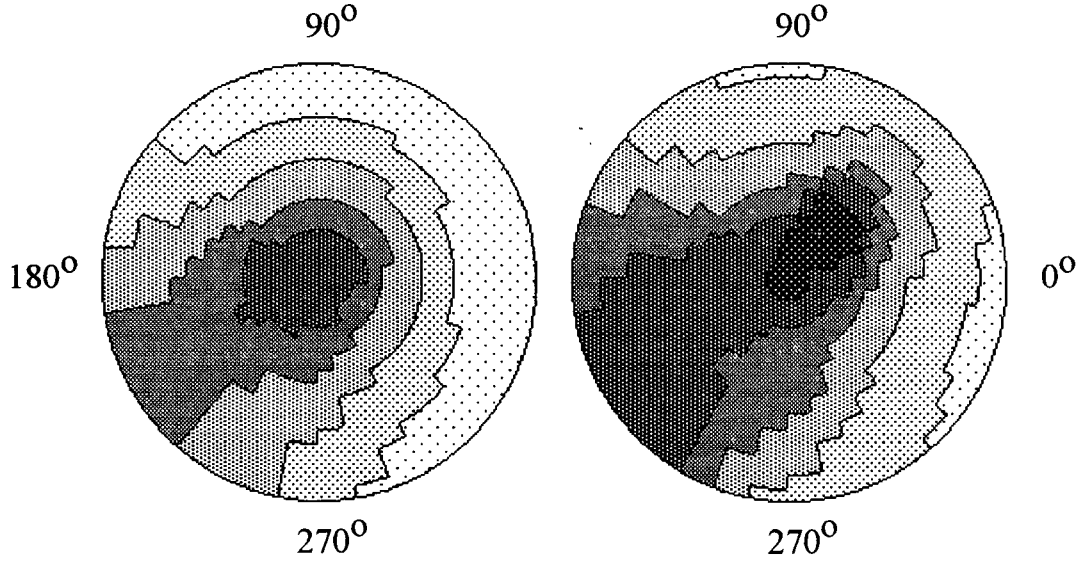


**8µm 90° TN cell with the 6096 crystal operating in the "Symmetric B" configuration. ± 5.0 volts to the cell**

**8µm 90° TN cell with the 6096 crystal operating in the "Symmetric B" configuration. ± 7.5 volts to the cell**

Figure 6.14 shows the optical angular properties of an 8μm 90° TN cell filled with the *Merck 6096* liquid crystal mixture in the light state as a function of the polariser configuration. The LC81 polarising material is used and a standard I.F is present. Note that in order to achieve the highest transmittance state, a small stimulating voltage of between ± 2.0 volts and ± 3.0 volts is applied to the cell.

**Figure 6.14: Optical angular properties of an 8μm 90° TN cell filled with the *Merck 6096* liquid crystal as a function of the *LC81* polariser configuration. A standard I.F is present. Light state.**

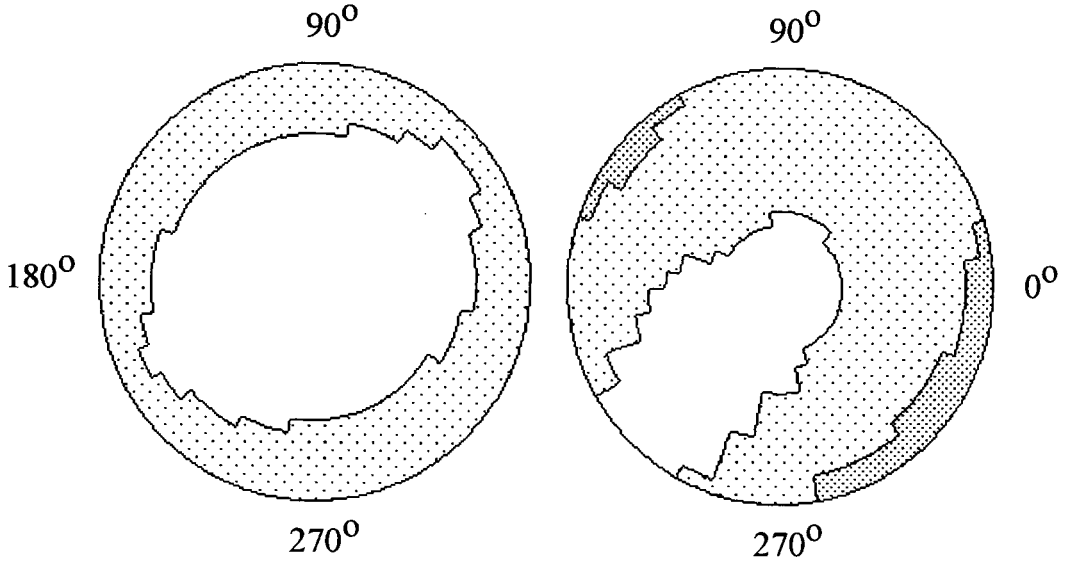


**8μm 90° TN cell with the 6096 crystal together with an I.F. LC81 polarisers cut at 0° and 90°. Light state**

**8μm 90° TN cell with the 6096 crystal together with an I.F. LC81 polarisers cut at 30° and 120°. Light state**

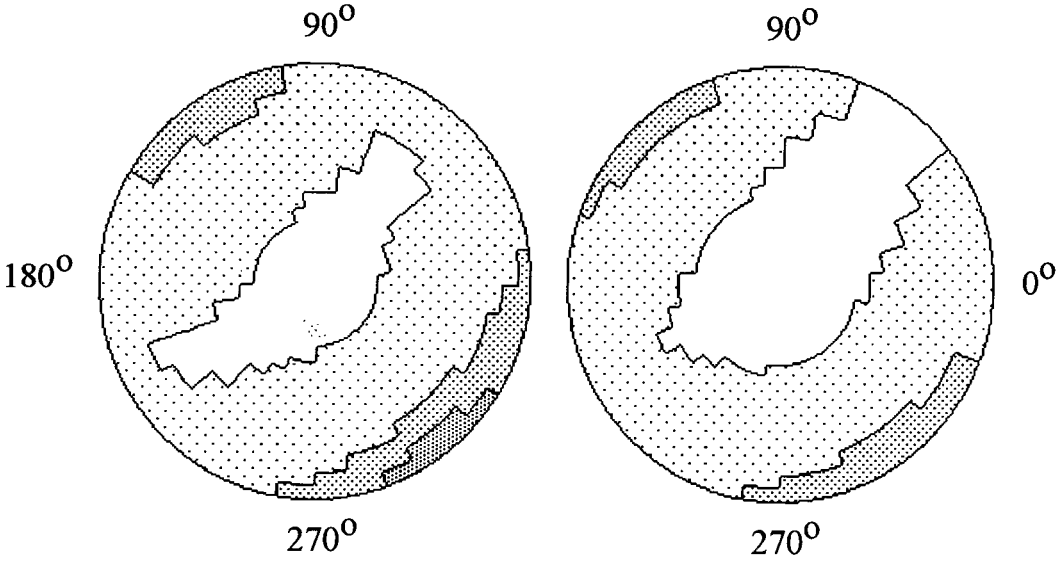


**8μm 90° TN cell with the 6096 crystal together with an I.F. LC81 polarisers cut at 45° and 135°. Light state**

**8μm 90° TN cell with the 6096 crystal together with an I.F. LC81 polarisers cut at 60° and 150°. Light state**

It is shown that the filter possesses a wide, centrally symmetric viewing cone when operating in the standard $0^0/90^0$ polariser mode, but that this region decreases in area as the *Symmetric B* arrangement is reached. At this point, an optical shutter possessing a restricted field of view is obtained. This is quite general for the *Symmetric B* polariser system.

A certain amount of improvement in the optical angular properties of the device can be obtained via use of *retardation* or *birefringent* films that are capable of offering some compensation for the centrally symmetric retardation generated by the liquid crystal layer itself when operating in the *Symmetric B* configuration. In particular, the addition of two uniaxially stretched 570nm retardation films[40] together with the 8μm $90^0$ TN cell filled with the *Merck 6096* liquid crystal mixture and placed between crossed LC81 polarisers oriented at $45^0$ and $135^0$ respectively is found to have beneficial effects upon the optical angular properties of the device. The arrangement of such a system is shown in figure 6.15. Note that the orientation of the individual filter elements is critical requiring careful manufacturing control. The optical angular properties of this unit are shown in figure 6.16 as a function of the driving voltage.

**Figure 6.15: Using uniaxially stretched retardation films to improve the optical angular properties of 8μm $90^0$ TN cells with the *Merck 6096* crystal and placed in the "Symmetric B" configuration.**

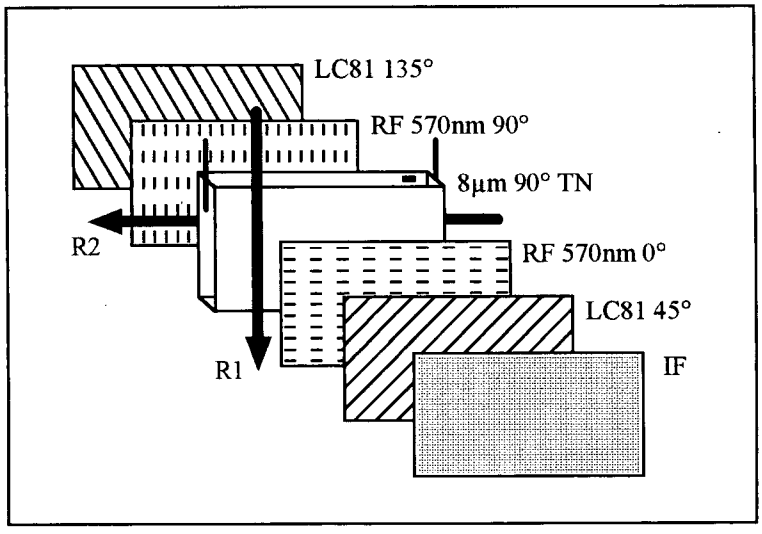


The optical angular properties of the single cell together with the retardation films become more symmetric with larger regions in the polar plot possessing similar transmission values. However, the cell still becomes inadequately lighter when viewed at large inclination angles away from the surface normal producing an optical shutter with a poor angular dependence. The symmetry of this device also makes it unsuitable for incorporation into a double-cell design whereby a large degree of cell compensation occurs.

**Figure 6.16: Optical angular properties of 8μm 90° TN cells filled with the *Merck 6096* crystal and *LC81* polarisers at 45° and 135°. Two 570nm retardation films are present together with an I.F.**

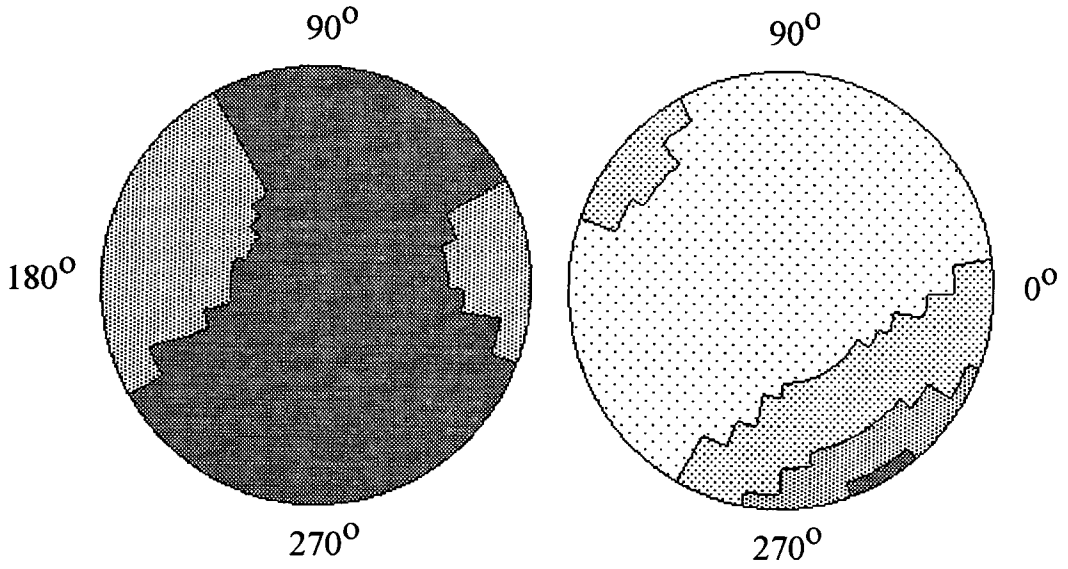


**8μm 90° TN cell with the 6096 crystal in the "Symmetric B" configuration. Two 570nm R.F's are used. 0 volts**

**8μm 90° TN cell with the 6096 crystal in the "Symmetric B" configuration. Two 570nm R.F's are used. ± 2.4 volts**

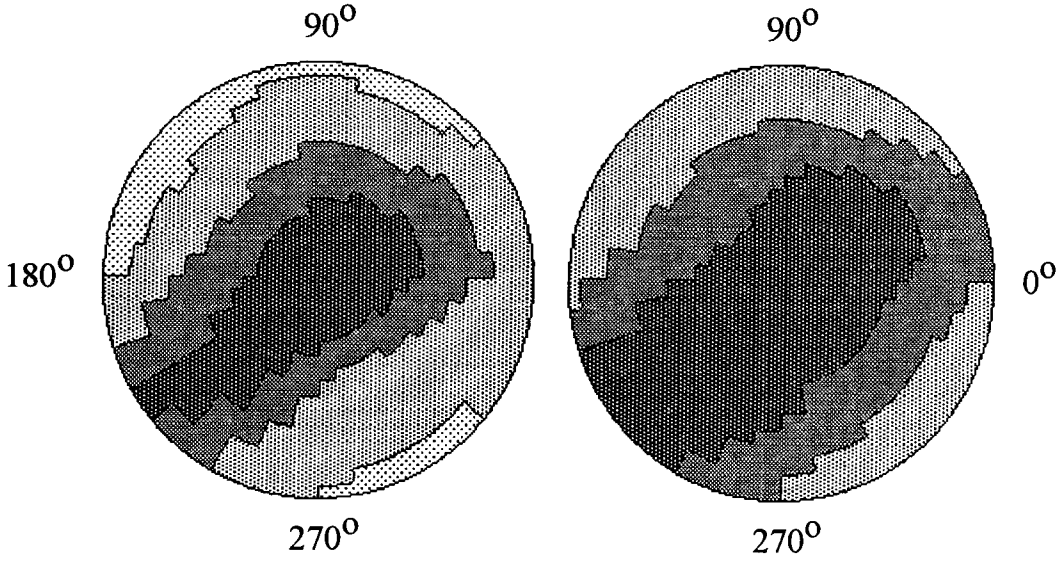


**8μm 90° TN cell with the 6096 crystal in the "Symmetric B" configuration. Two 570nm R.F's are used. ± 5.0 volts**

**8μm 90° TN cell with the 6096 crystal in the "Symmetric B" configuration. Two 570nm R.F's are used. ± 7.5 volts**

The addition of retardation films to the liquid crystal layer also has adverse effects upon the cell contrast. This is indicated in figure 6.17 which shows the electro-optic properties of an 8μm 90° TN cell filled with the *Merck 6096* liquid crystal mixture and operating in the *Symmetric B* polariser

configuration with and without the retardation sheets. It is seen that the contrast drops over 1.3 shade numbers upon addition of the retardation films when the cell is activated by a 50Hz square wave driving voltage of ± 10 volts. However, sufficient contrast is still maintained making the system suitable for incorporation into an optical shutter design as far as the electro-optic properties are concerned. Incidentally, the shade number when in the inactivated phase is also increased via use of retardation films, hence enhancing the safe-state shade step generated by the unit.

**Figure 6.17: Electro-optic properties of an 8μm 90$^{0}$ TN cell filled with the *Merck 6096* liquid crystal with and without the presence of two 570nm retardation sheets. A standard I.F is present.**

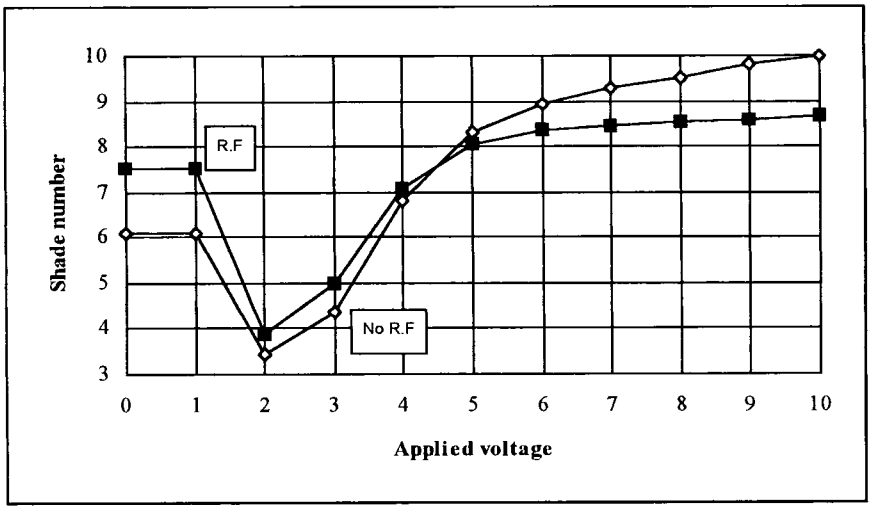


Despite the 8μm 90$^{0}$ TN cell displaying good cell contrast and a sufficient safe-state shade step of over 2.2 shade numbers being available from the single cell upon employment of the *Symmetric B* polariser configuration, the optical angular properties of the device remain inadequate both in the light state and when activated by reduced voltages. Although a certain degree of improvement can be obtained via use of uniaxially stretched 570nm retardation films, the symmetry of the cell still renders it unsuitable for incorporation into a double-cell design wherein a large degree of cell compensation occurs.

### *6.4.1 The Effect of Twist-Angle Reduction With Δn.d equal to 0.80μm.*

The effect of reducing the twist-angle upon the electro-optic properties of the device is investigated in figure 6.18. Here, the safe-state shade step obtained from 8μm LT cells filled with the *Merck 6096* liquid crystal mixture and possessing twist-angles ranging from 50$^{0}$ up to 90$^{0}$ respectively are shown as a function of the polariser orientation. A standard I.F is present.

It is shown that the *Symmetric B* polariser configuration maximises the safe-state shade step generated by the cell irrespective of the twist-angle present in the device. This shade step is also only weakly sensitive to the magnitude of the twist-angle and a maximum of 2.8 shade numbers is obtained for cells possessing twist-angles of between $50^{o}$ and $80^{o}$. This is to be compared to that of only 2.2 shade numbers obtained from the $90^{o}$ TN cell.

**Figure 6.18: Safe-state shade steps for 8μm LT cells with the *Merck 6096* liquid crystal and crossed polarisers as a function of angle between the first polariser and the entrance molecular director.**

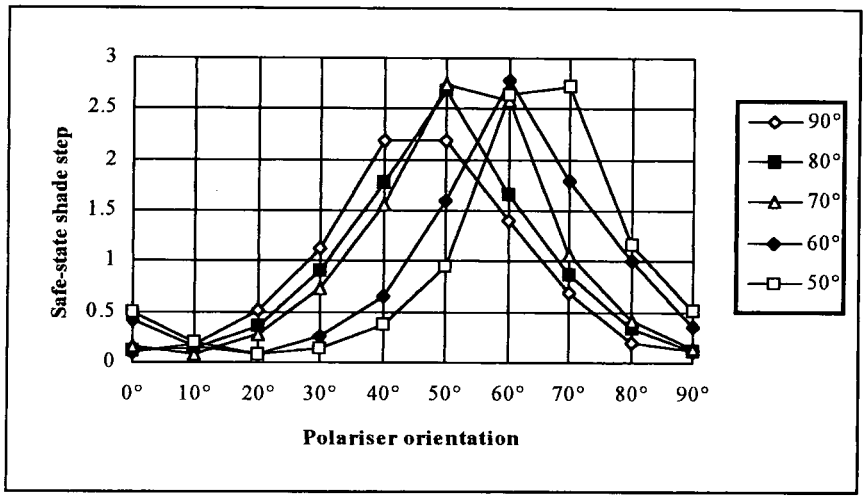


It is also this arrangement that produces both the lowest overall optical transmittance with the LT cell in the inactivated phase and the maximum cell contrast. This is illustrated in figure 6.19 for 8μm LT cells filled with the *Merck 6096* liquid crystal mixture possessing twist-angles ranging from $50^{o}$ through to $90^{o}$. Here, contrast is defined as the shade number difference obtained by the single cell from the lightest state available upon application of a small stimulating voltage of between ± 2.0 and ± 3.0 volts and the dark state attained with a 50Hz driving voltage of ± 10 volts.

It is seen that a maximum contrast of over 8.2 shade numbers is obtained from the $90^{o}$ TN device and that there is little change for this specific cell type upon rotation of the crossed polarisers relative to the cell. However, the lower twisting variants are significantly more sensitive to the polariser orientation making it imperative to utilise the *Symmetric B* configuration as far as cell contrast is concerned.

Twist-angle reduction lowers the available cell contrast. A value of only 5.2 shade numbers is accessible from the $50^{o}$ LT cell compared to that of 8.2 shade numbers for the $90^{o}$ TN case. This represents an average drop of 0.075 shade numbers per degree. However, even the $50^{o}$ LT unit still possesses sufficient contrast upon polariser optimisation in order to be suitable for incorporation into an automatically darkening welding filter design.

**Figure 6.19: Contrast from 8μm cells with various twist-angles placed between crossed polarisers as a function of the angle between the first polariser and the entrance molecular director.**

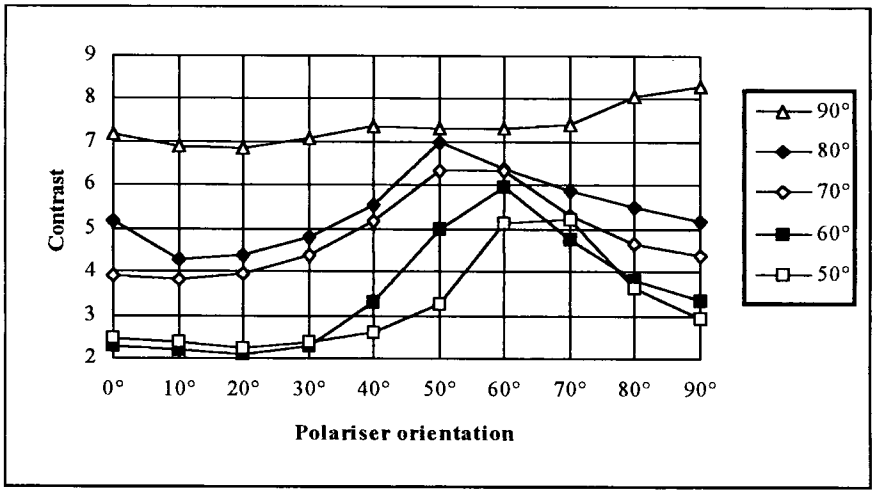


Figure 6.20 shows the light-state shade numbers attained by 8μm LT cells upon application of a small stimulating voltage of between ± 2.0 and ± 3.0 volts. Here, the effect of rotating the crossed polarisers is investigated for three different twist-angles. It is shown that the highest light-state transmittance is obtained when the cells are in the *Symmetric A* configuration with all three reaching a state of less than 3.27 shade numbers. This is to be compared to that of the *Symmetric B* arrangement that maximises both the safe-state shade step and the cell contrast but which also produces the lowest overall light-state optical transmittance. The most susceptible cell to this effect is that which possesses a twist-angle of $50^{o}$ where the *Symmetric B* configuration is nearly 0.34 shade numbers darker than that for the *Symmetric A* polariser arrangement.

**Figure 6.20: Light-state shade numbers of 8μm LT cells with the *Merck 6096* liquid crystal as a function of the angle between the first polariser and the entrance molecular director.**

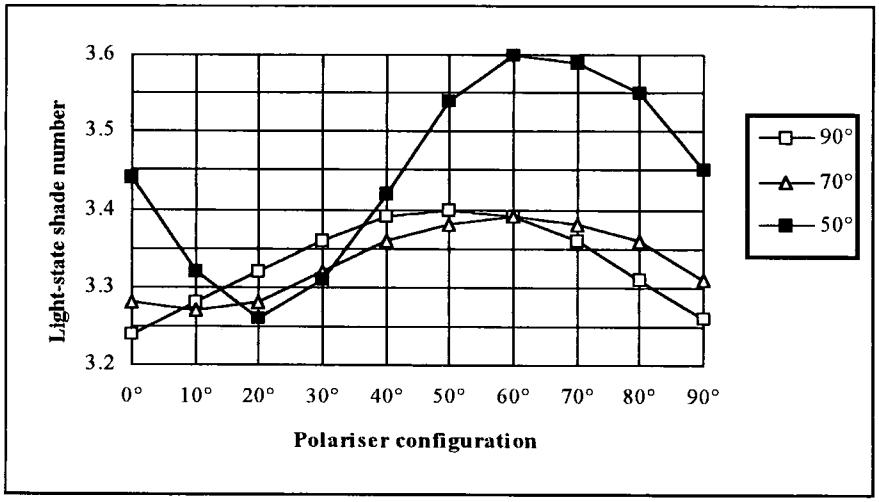

In general, this phenomenon is exaggerated via use of cells possessing low twist-angles of less than that of 60°. An ongoing manufacturing goal is to develop welding filters that display higher overall optical throughputs when in the light-state. Any reduction in light-state transmittance should therefore be avoided at all costs and hence the higher twisting variants appear more favourable as far as this point is concerned.

The importance of optimising the polariser orientations as far as the electro-optic properties of the cell are concerned is demonstrated in figure 6.21 where those for an 8μm 60° LT cell filled with the *Merck 6096* liquid crystal mixture are shown as a function of the polariser arrangement. The LC81 polarising material is used and the cells are stimulated with a 50Hz square wave voltage. A standard I.F is present. It is shown that it is not only the safe-state shade step that is highly sensitive to the polariser arrangement but also the available contrast from the cell. Note that for a 60° LT cell, the *Symmetric B* configuration lies at 60°/150°.

It has been demonstrated that in order to maximise both the safe-state shade step and the cell contrast, it is imperative to utilise the *Symmetric B* polariser configuration. It is therefore this arrangement that appears most promising for incorporation into optical shutter designs as far as the electro-optic properties are concerned and hence will be investigated further in the proceeding sections.

**Figure 6.21: Electro-optic properties of 8μm 60° LT cells with the *Merck 6096* liquid crystal placed between crossed *LC81* polarisers at various angles relative to the cell. A standard I.F is present.**

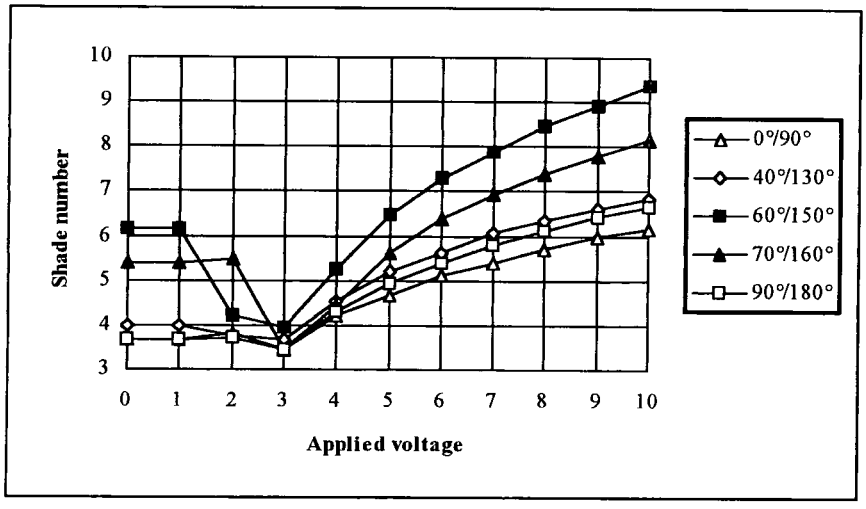


### *6.4.2 The Optical Properties of the "Symmetric B" configuration.*

Figure 6.22 shows the electro-optic properties of 8μm LT cells with various twist-angles and placed between crossed LC81 polarisers oriented in the *Symmetric B* configuration. The cells are filled with the *Merck 6096* liquid crystal mixture and are driven with a 50Hz square wave. A standard I.F is present.

**Figure 6.22: Electro-optic properties of 8μm cells with the "Symmetric B" polariser arrangement and twist-angles of $50^{o}$, $70^{o}$ and $90^{o}$. The *Merck 6096* crystal is used. A standard I.F is present.**

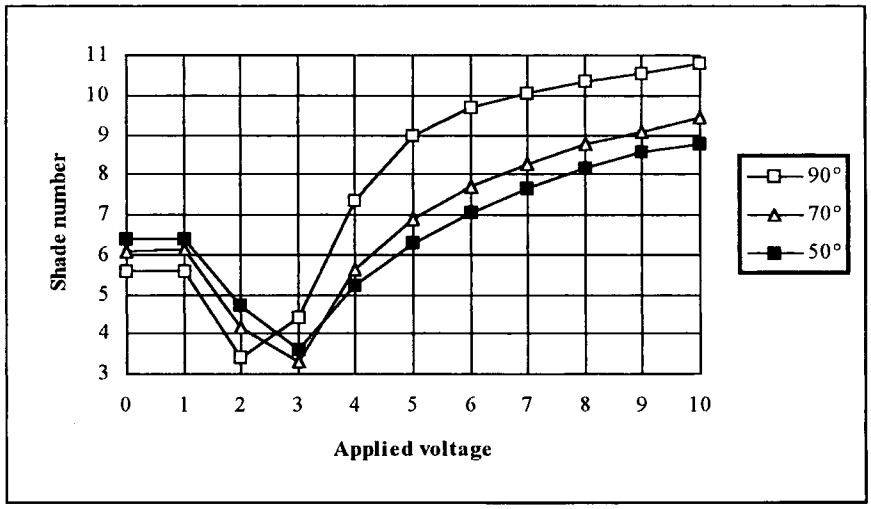


The loss of cell contrast upon reduction of the twist-angle manifests itself by the fact that the 8μm $90^{o}$ TN device reaches a shade number of 10.7 with an applied driving voltage of ± 10 volts, whilst that for the $50^{o}$ LT case only attains a shade number 8.7. This gives an average dark state shade number drop of 0.05 shade numbers per degree. Despite good contrast still being available with the $50^{o}$ twisting cell, a reduction of the twist-angle therefore produces an increase in the operating voltage of the device and inflates the power consumption of the system.

**Figure 6.23: Shade numbers of 8μm cells with the *Merck 6096* liquid crystal in the inactivated phase placed in the "Symmetric B" configuration as a function of twist-angle. A standard I.F is present.**

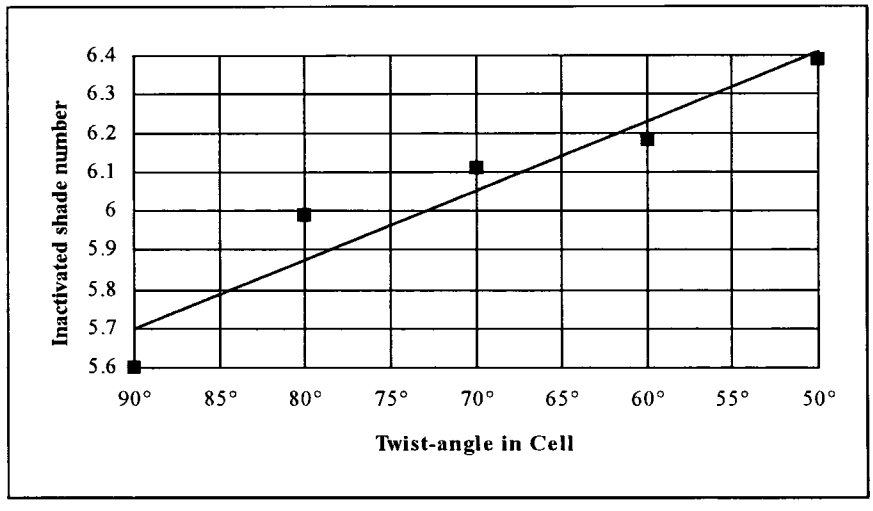

The overall transmittance of liquid crystal cells when in the *inactivated* phase and with the *Symmetric B* polariser configuration together with an I.F is a function of the twist-angle present in the cell. This is illustrated in figure 6.23 which shows the shade numbers of 8μm cells filled with the *Merck 6096* liquid crystal component. The LC81 polarising material is used and a standard I.F is present. Here, a shade number of 5.7 is obtained with a twist-angle of 90°, linearly increasing approximately 0.02 shade numbers per degree to reach a shade number 6.4 for the 50° twisting case. A lowering of the twist-angle therefore produces an increase in the shade number attained when in the inactivated phase.

Figure 6.24 shows the light state shade numbers of 8μm cells filled with the *Merck 6096* liquid crystal mixture and placed between crossed LC81 polarisers oriented in the *Symmetric B* configuration together with a standard I.F. The cells are driven with a small stimulating voltage of between ± 2.0 and ± 3.0 volts in order to attain the highest transmittance state. The lowest light state shade number of 3.31 is obtained with a twist-angle of between 70° and 80°, some 0.08 shade numbers below that reached with the 90° TN cell. With twist-angles lower than this, the light state transmittance rapidly declines approaching a shade number of 3.6 for the 50° twisting case. As far as the overall light state transmittance is concerned, twist-angles of between 70° and 80° are therefore preferable with this type of cell.

**Figure 6.24: Light state shade numbers of 8μm cells filled with the *Merck 6096* liquid crystal and placed in the "Symmetric B" configuration between *LC81* polarisers. A standard I.F is present.**

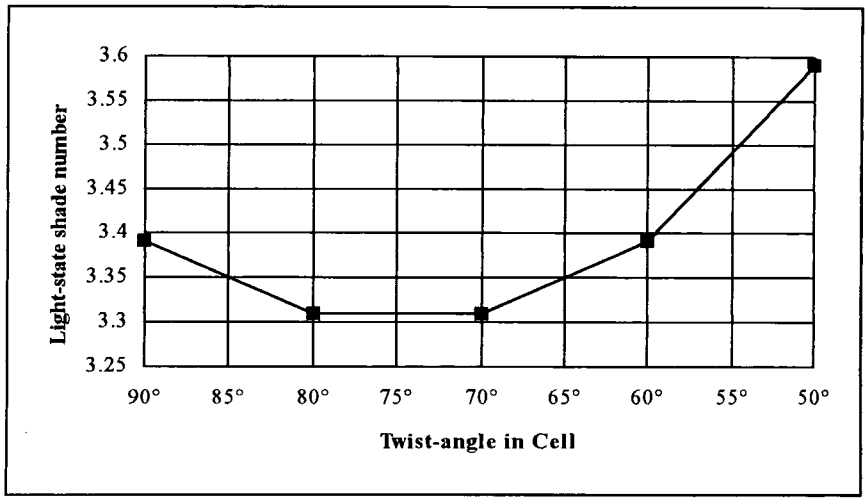


So far, only the electro-optic properties in a direction lying parallel to the surface normal have been considered. This has demonstrated that in order to maximise both the safe-state shade step and the cell contrast, twisted nematic cells should be operated in the *Symmetric B* polariser configuration. In addition to this, the lightest optical shutters are obtained via use of 8μm LT cells possessing twist angles of between 70° and 80° when filled with the *Merck 6096* liquid crystal component, giving a Δn.d value of 0.80μm. The optical *angular* properties of these cells will now be considered in order to examine how the transmittance of the cells vary as a function of viewing angle.

Figure 6.25 shows the optical angular properties of 8μm cells filled with the *Merck 6096* liquid crystal mixture and placed between crossed LC81 polarisers oriented in the *Symmetric B* configuration as a function of the twist-angle in the cell. The cells are driven with a 50Hz square wave so as to attain a shade number 8 and a standard I.F is present.

**Figure 6.25: The optical angular properties of 8μm cells with the *Merck 6096* liquid crystal and the "Symmetric B" configuration as a function of the twist-angle in the cell. A standard I.F is present.**

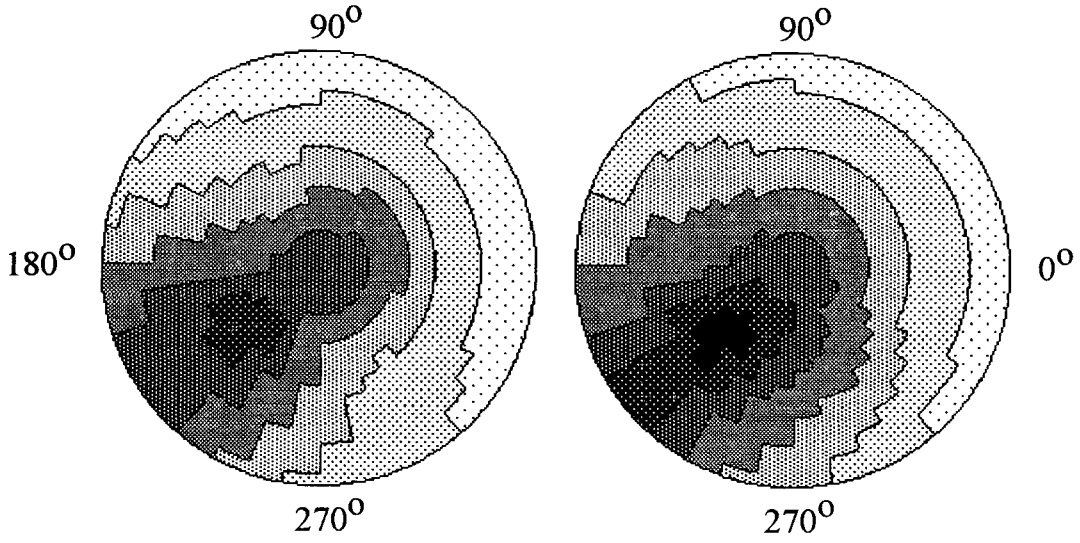


**8μm 90° TN cell with the 6096 liquid crystal and LC81 polarisers cut at 45° and 135°. Shade number 8**

**8μm 80° LT cell with the 6096 liquid crystal and LC81 polarisers cut at 50° and 140°. Shade number 8**

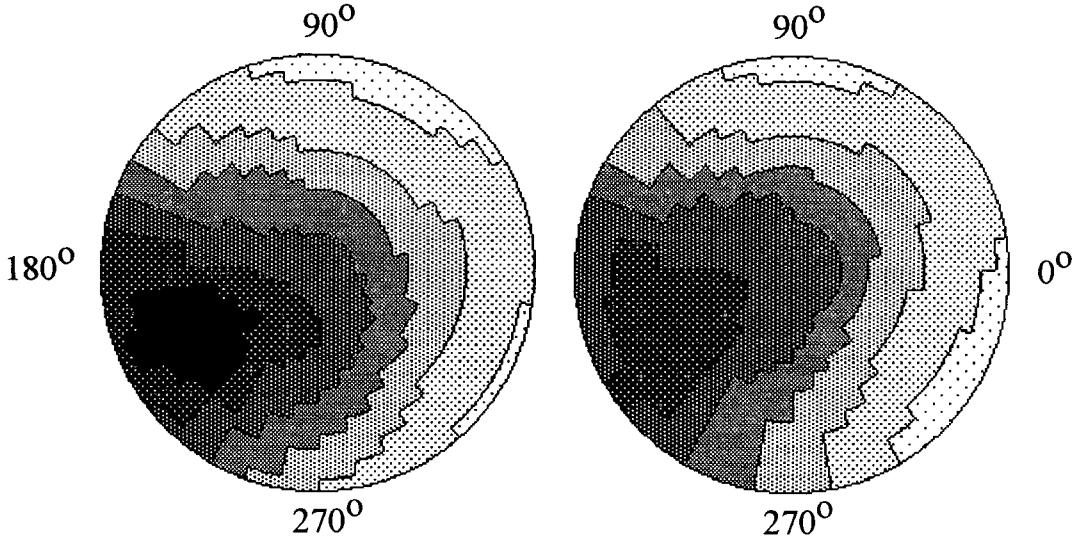


**8μm 70° LT cell with the 6096 liquid crystal and LC81 polarisers cut at 55° and 145°. Shade number 8**

**8μm 60° LT cell with the 6096 liquid crystal and LC81 polarisers cut at 60° and 150°. Shade number 8**

Such properties are characteristic of the *Symmetric B* polariser configuration whereby the darkest regions in the polar chart appear to be *wrapped* around the central viewing point and *skewed* off to one side. In general, there is only a small effect upon reduction of the twist-angle and the position of the darkest viewing cone remains relatively unchanged, maintaining the off axis symmetry of the device.

**Figure 6.26: The optical angular properties of 8µm LT cells with the *Merck 6096* liquid crystal and *LC81* polarisers in the "Symmetric B" arrangement as a function of the twist-angle. Light state.**

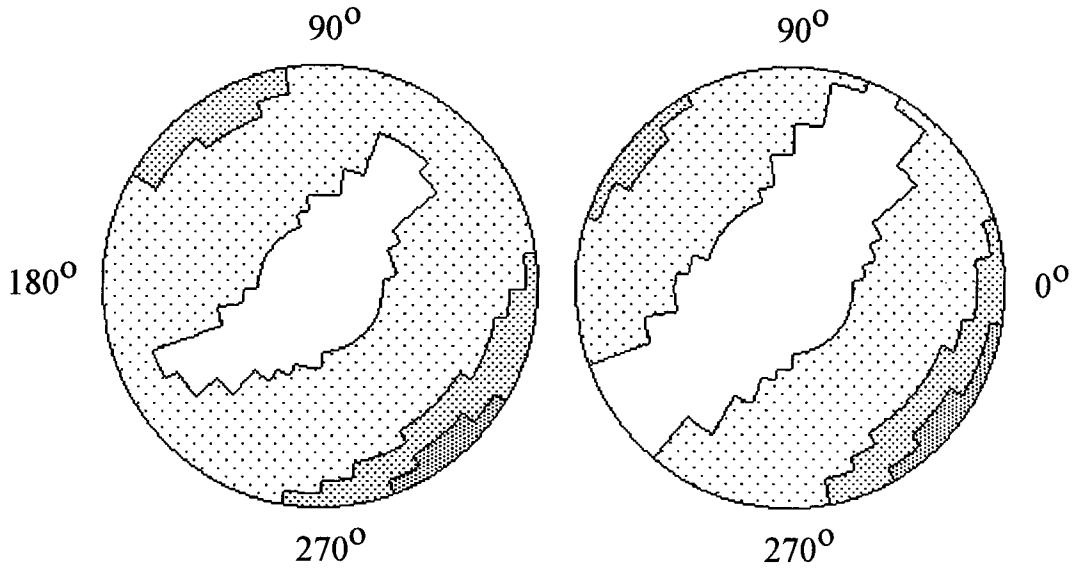


**8µm 90° TN cell with the 6096 crystal operating in the "Symmetric B" mode. An I.F is present. Light state**

**8µm 80° LT cell with the 6096 crystal operating in the "Symmetric B" mode. An I.F is present. Light state**

**8µm 70° LT cell with the 6096 crystal operating in the "Symmetric B" mode. An I.F is present. Light state**

**8µm 60° LT cell with the 6096 crystal operating in the "Symmetric B" mode. An I.F is present. Light state**

However, the area of this region is somewhat enhanced, producing subtle improvements in the overall optical angular properties displayed by the cell. Note that this is in stark contrast to that for LT cells operating in the *Symmetric A* polariser arrangement whereby a reduction of the twist-angle causes the dark cone both to move outwards away from the centre of the polar chart and to expand in area.

The optical angular properties of 8μm cells filled with the *Merck 6096* liquid crystal component when in the light state are shown in figure 6.26. LC81 polarisers oriented in the *Symmetric B* configuration are used and a standard I.F is present. A small stimulating voltage of between ± 2.0 volts and ± 3.0 volts is applied to the cells in order to achieve the highest transmittance state.

It is shown that the diminished field of view associated with the *Symmetric B* polariser configuration is somewhat alleviated upon reduction of the twist-angle and hence the $60^{o}$ LT device possesses an enlarged viewing cone compared to that of the $90^{o}$ TN cell. Further reduction beyond this point degrades the overall transmittance of the filter when in the light state according to figure 6.24 and hence is not directly of interest as far as developing optical shutters possessing a high light state transmittance is concerned. The optimum twist-angle therefore lies close to $70^{o}$ when employing 8μm cells filled with the *Merck 6096* liquid crystal component as far as the light state angular properties are concerned.

**Figure 6.27: Optical angular properties of double-cell structures using both $50^{o}$ and $90^{o}$ 8μm cells with the *Merck 6096* liquid crystal and *LC81* polarisers in the "Symmetric B" configuration.**

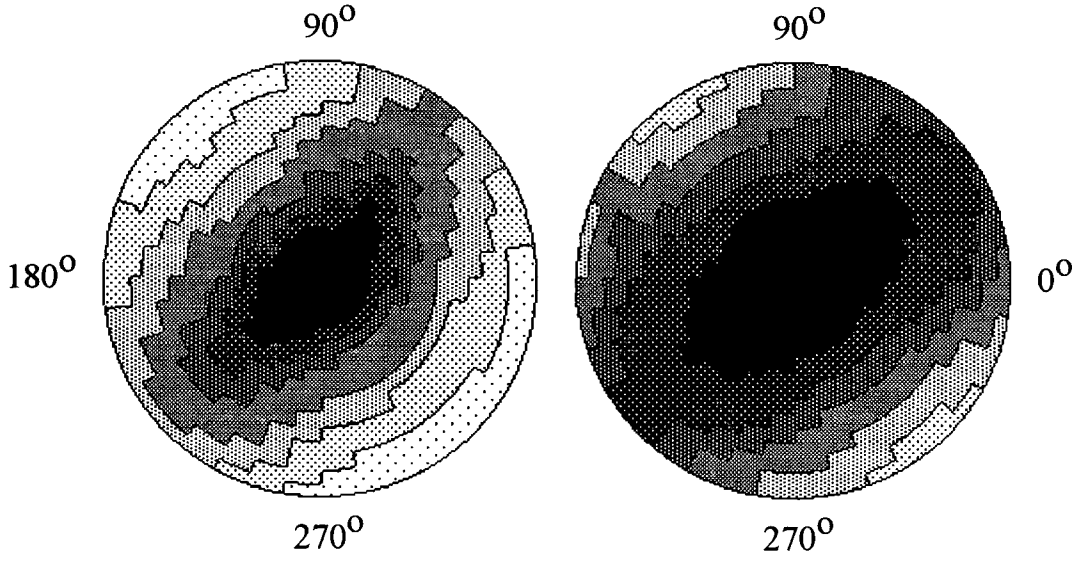


**Two 8μm 90° TN cells with the 6096 crystal crossed between polarisers cut at 45°, 135° and 45°. Shade number 12**

**Two 8μm 50° LT cells with the 6096 crystal crossed between polarisers cut at 65°, 155° and 65°. Shade number 12**

Figure 6.27 shows the optical angular properties of a double-cell structure based on 8μm cells filled with the *Merck 6096* liquid crystal component and LC81 polarisers oriented in the *Symmetric B* arrangement. Here, two twist-angles of $50^{o}$ and $90^{o}$ respectively are investigated and the cells are driven together with a 50Hz square wave so as to attain a shade number 12. Note that the cells are placed together in opposite

orientations with one cell being upside down such that the face-to-face rub directions are crossed in order to generate cell compensation. A standard I.F is present.

It is seen that the optical angular properties of such systems are centrally symmetric with the welding filter gradually becoming lighter when viewed at large inclination angles away from the surface normal. The subtle changes in the properties of a single cell upon reduction of the twist-angle manifests itself by producing small improvements in the overall characteristics of the full optical shutter design. However, the general symmetry of the shutter as a whole remains essentially unaltered and the unit still possesses inadequate optical properties when viewed at large inclination angles.

**Figure 6.28: Optical angular properties of 8μm 50° LT cells filled with the *Merck 6096* liquid crystal component as a function of the polariser orientation. A standard I.F is present. Shade number 6.**

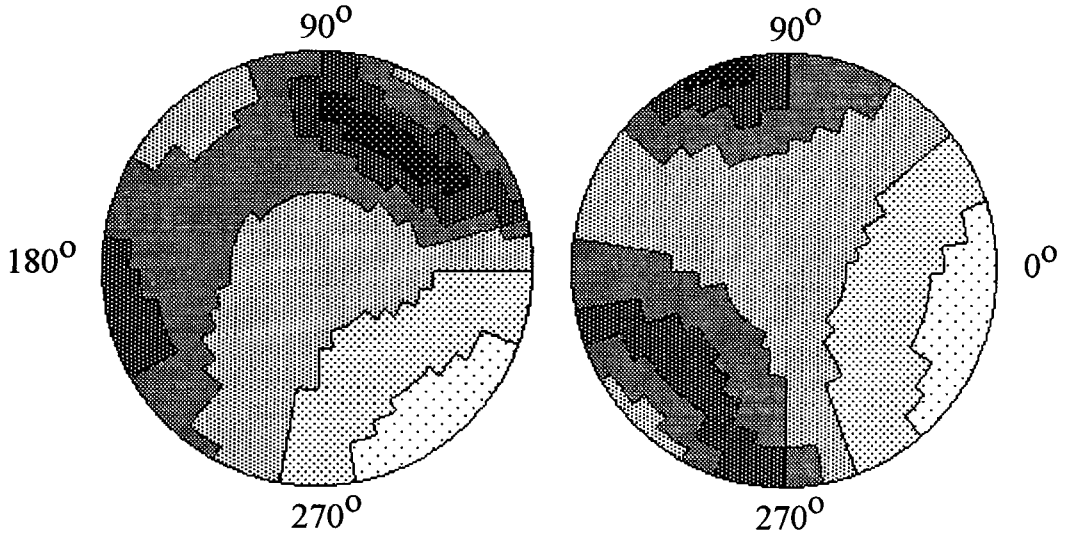


**8μm 50° LT cell with the 6096 liquid crystal and polarisers cut at 0° and 90°. Shade number 6**

**8μm 50° LT cell with the 6096 liquid crystal and polarisers cut at 30° and 120°. Shade number 6**

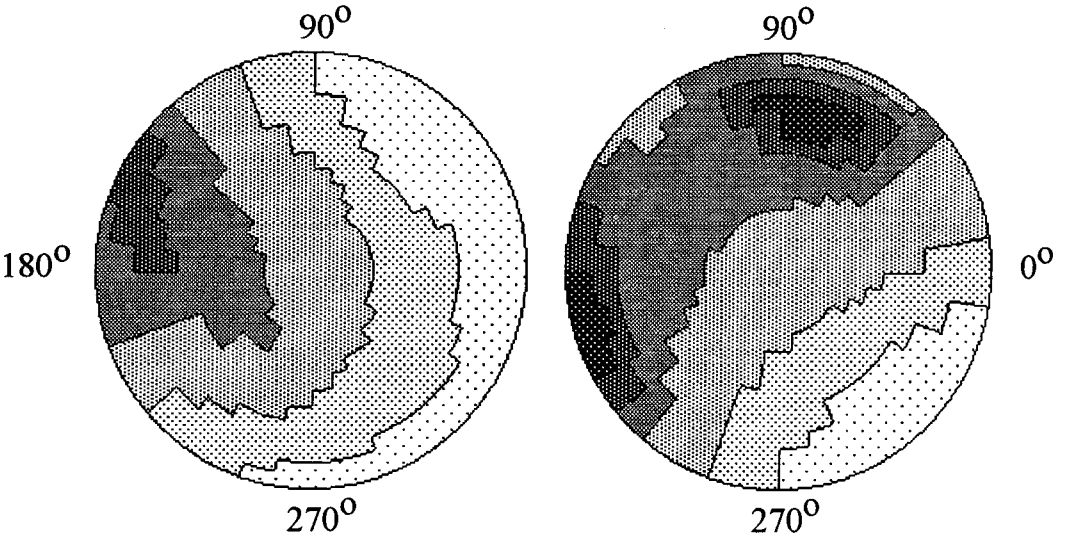


**8μm 50° LT cell with the 6096 liquid crystal and polarisers cut at 60° and 150°. Shade number 6**

**8μm 50° LT cell with the 6096 liquid crystal and polarisers cut at 90° and 180°. Shade number 6**

The effect of polariser rotation upon the optical angular properties of LT cells is investigated in figure 6.28. Here, the angular dependence of an 8μm 50° LT cell filled with the *Merck 6096* liquid crystal mixture and placed between crossed LC81 polarisers are shown as a function of the polariser orientation. A 50Hz square wave driving voltage is applied to the cell and adjusted so as to give a shade number 6. A standard I.F is present. Note that the *Symmetric B* polariser configuration for a 50° LT cell lies at 65° and 155° respectively.

Rotation of the crossed polarisers away from the *Symmetric B* configuration removes the inadequate optical angular properties associated with this arrangement and the polar plot diagram reverts back to the *streak* pattern characteristic for the majority of polariser arrangements including both the standard 0°/90° orientation and the *Symmetric A* configuration. In general, the gross overall symmetry of the LT cell remains essentially unchanged upon further rotation of the polarisers beyond this point and is therefore largely dependent upon the birefringence generated within the liquid crystal layer itself. Since it is the symmetry of the optical properties that determine the suitability of a cell for incorporation into a double-cell structure whereby a large degree of cell compensation is required, it is therefore expected that a significant improvement in the optical angular properties of an optical shutter design can be achieved upon moving away from the *Symmetric B* polariser arrangement. Note however, that it is this design that optimises the electro-optic properties of the cell in a direction lying parallel to the surface normal, hence a certain amount of compromise is therefore required.

Experiments indicate that in order to remove the *wrapped* pattern in the polar plot diagram representing the optical angular properties of the 8μm 90° TN cell filled with the *Merck 6096* liquid crystal mixture and operating in the *Symmetric B* configuration, the crossed polarisers must be rotated nearly 30° away forming a 15°/105° or a 75°/165° arrangement. However, the associated drop in the safe-state shade step makes these designs unsuitable for incorporation into an automatically darkening welding filter whereby a large, fail-safe shade step is required should the driving electronics malfunction. However, in contrast to this LT cells are far more sensitive to polariser orientations and only a relatively small rotation away from the *Symmetric B* configuration is required in order to dissipate the undesirable *wrapped* pattern in the polar chart. Such changes are capable of maintaining both the safe-state shade step and the cell contrast at adequate levels, making these systems suitable for incorporation into a double-cell optical shutter design.

The optical angular properties of a double cell structure based on 4μm 70° LT cells filled with the *Merck 6080* liquid crystal mixture and placed between crossed LC81 polarisers oriented at 30°, 120° and 30° respectively are shown in figure 6.29. The pertinent Δn.d value for this cell type lies at 0.81μm and hence the device satisfies the required criteria for demonstrating this mode of operation when placed between crossed polarisers. This polariser arrangement is sufficiently far away from the *Symmetric B* configuration in order to remove the undesirable *wrapped* pattern in the polar plot diagram displayed by the single cell, whilst both the cell contrast and the safe-state shade step are maintained at adequate levels. The optical angular properties of this system are therefore a significant improvement to those obtained with the 4μm 70° LT cell placed in the *Symmetric B* configuration and a wide, centrally symmetric viewing cone is obtained.

**Figure 6.29: Optical angular properties of a double-cell structure using 4μm 70° LT cells with the *Merck 6080* crystal and *LC81* polarisers placed at 30°, 120° and 30°. A standard LF is present.**

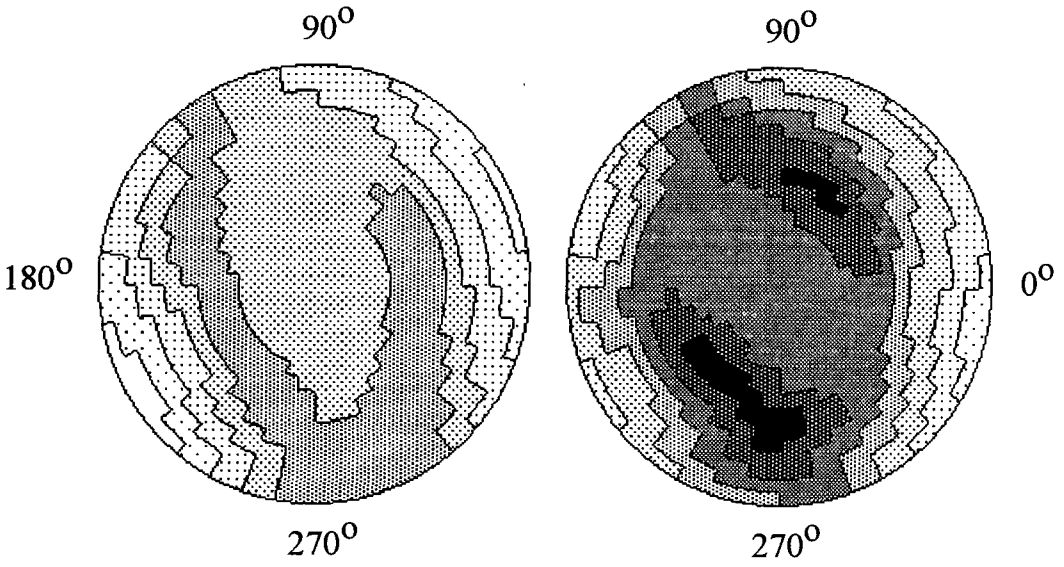


**Two 4μm 70° LT cells with the 6080 liquid crystal and LC81 polarisers cut at 30°, 120° and 30°. ± 5.0 volts for shade 6**

**Two 4μm 70° LT cells with the 6080 liquid crystal and LC81 polarisers cut at 30°, 120° and 30°. ± 7.0 volts for shade 12**

The electro-optic properties of this cell arrangement in a direction lying parallel to the surface normal are shown in figure 6.30. These are compared to those for a double-cell arrangement using the 4μm 70° LT cells placed in the *Symmetric B* polariser configuration. The cells are filled with the *Merck 6080* liquid crystal mixture and driven together with a 50Hz square wave. A standard I.F is present.

It is shown that the effect of rotating the crossed polarisers away from the *Symmetric B* configuration is to compromise on both the cell contrast and the safe-state shade step offered by the device. In the dark state, the shade number attained with a driving voltage of ± 10 volts drops from 15.5 with the *Symmetric B* polariser configuration to that of only 13.3 shade numbers for the 30°/120°/30° polariser arrangement. The safe-state shade step is also simultaneously degraded by up to 3.0 shade numbers to that of only 1.2 shades upon polariser rotation.

However, this system demonstrates how the optical angular properties of this cell type can be optimised upon rotation of the crossed polarisers away from the *Symmetric B* configuration whilst maintaining the remaining pertinent electro-optic properties at adequate levels for use in an automatically darkening welding filter glass pack.

**Figure 6.30: Electro-optic properties of double-cell structures using 4μm 70$^{0}$ LT cells filled with the *Merck 6080* liquid crystal as a function of the polariser orientation. A standard I.F is present.**

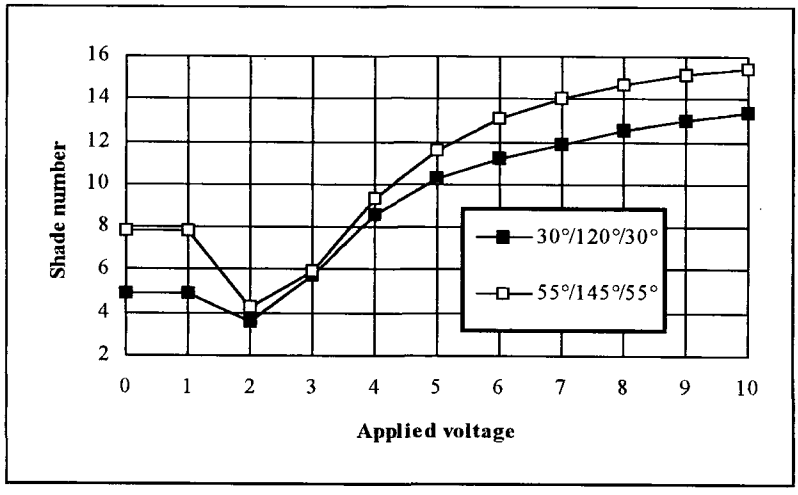


### *6.4.3 The Response Time for this Mode of Operation.*

The response time from the light to the dark state for an 8μm 90$^{0}$ TN cell filled with the *Merck 6096* liquid crystal mixture and operating in both the *Symmetric A* and *Symmetric B* arrangements respectively is shown in figure 6.31 as a function of the driving voltage. For the *Symmetric A* case, the unit is in the light state when inactivated, whilst that for the *Symmetric B* configuration requires the application of a small stimulating voltage of between ± 2.0 and ± 3.0 volts in order to attain the highest transmittance state. The LC81 polarising material is used and a standard I.F is present.

**Figure 6.31: Switching speeds of 8μm 90$^{0}$ TN cells with the *Merck 6096* liquid crystal operating in both the "Symmetric A" and "Symmetric B" configurations as a function of the driving voltage.**

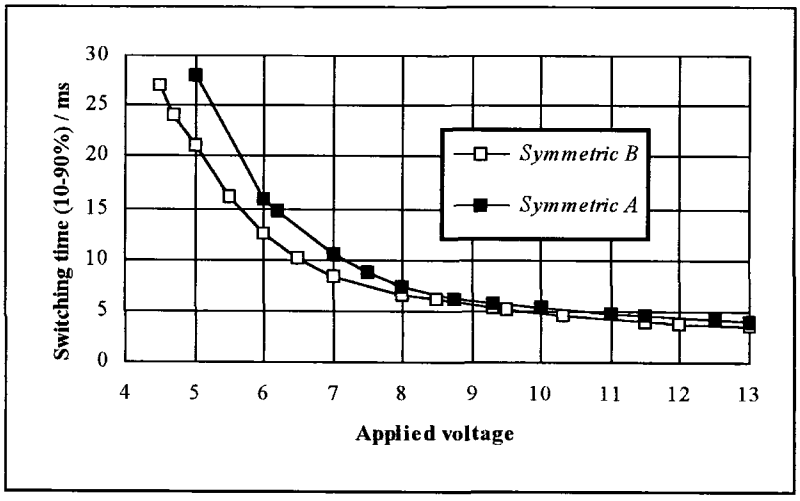

The cells are driven with a 3Hz square wave pulse from a frequency generator modulated between the light state voltage and the relevant test voltage, causing the unit to oscillate between the dark and light phases. By positioning of the device between a 150 watts halogen projector lamp driven at 24 volts D.C and a *silicon photodiode light detector*[28] connected directly to an oscilloscope, the response time of the system can be monitored. An *HP54501A Digitising Oscilloscope*[52] was used in order to measure the rise time of the filter. Here, the response time is taken as being that required by the system to change between the 10% and 90% transmission levels and hence the given values do not adhere to the definition of switching speed according to the *Deutsches Institut för Normung*[7] .

Both lines follow a $1/V^2$ type curve where the switching speed increases as the stimulating voltage is raised. It is also noted that the response time of the cell when operating in the *Symmetric B* design is marginally faster than that for the *Symmetric A* configuration. This effect is particularly apparent at low voltages but becomes progressively masked as the applied voltage is elevated. With a voltage exceeding that of 12 volts, little apparent difference is observed.

This effect is quite general irrespective of the cell thickness and the characteristics of the liquid crystal material in use. Figure 6.32 shows that for a 4μm $90^0$ TN cell filled with the *Merck 6080* liquid crystal component and again operating in both the *Symmetric A* and *Symmetric B* configurations respectively. Here, the value of Δn.d lies close to 0.81μm and hence a small stimulating voltage of between ± 2.0 and ± 3.0 volts is required in order to attain the highest transmitting phase when functioning in the *Symmetric B* arrangement. Note that the response time of the 4μm cell is up to four times faster than that of the 8μm device due to a halving of the cell thickness. In general, the response time of a liquid crystal cell is inversely proportional to the square of the cell thickness.

**Figure 6.32: Switching speeds of a 4μm $90^0$ TN cell with the *Merck 6080* liquid crystal operating in both the "Symmetric A" and "Symmetric B" configurations as a function of the driving voltage.**

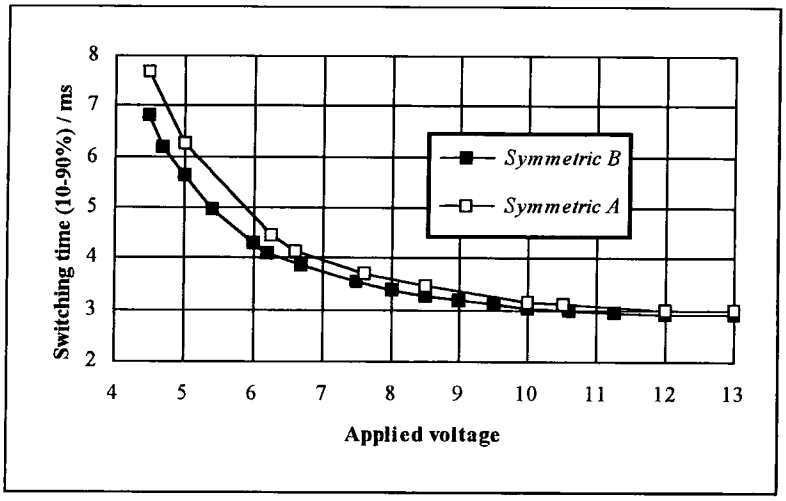

Operation of a TN liquid crystal cell between crossed polarisers together with an I.F such that the unit displays a dark state when in the inactivated phase produces a marginal increase in the switching speed of the device from the light to the dark state as compared to that when operating in the normally white mode. However, this effect is only small and becomes less apparent at high stimulating voltages exceeding that of 12 volts. In practice, the switching speed is more sensitive to both the cell thickness and the intrinsic parameters of the liquid crystal material itself. Utilisation of this mode of operation therefore maintains the fast response time from the light to the dark state associated with the normally *white* mode whilst providing a fail-safe, dark state should the controlling electronics malfunction, an effect often associated with the normally *black* mode of operation. Note that experiments also indicate that there is no significant effect upon the stimulating response time as the twist-angle is reduced and that the relaxation switching speed is independent of the driving voltage.

*This chapter has introduced a new mode of operation for a twisted-nematic liquid crystal cell placed between crossed polarisers whereby a pink-red colouration is displayed by the unit when in the inactivated phase. When operating together with a standard I.F that possesses a high optical transmittance over the central part of the visible spectrum, a dark state is obtained. Application of a small electric field removes the colouration and the unit transposes into the light state. Further increment of the voltage beyond this point reverts the filter back to a darker phase. Such a device offers advantages over that of the standard normally white mode of operation in that a fail-safe, low transmittance state is provided should the controlling electronics malfunction, whilst the fast response time of the normally white mode from the light to the dark state is maintained.*

*Calculations indicate that there are only two cell types that fulfil the criteria of displaying the pink-red colouration when placed between crossed polarisers and in the inactivated phase. The first corresponds to a $0^{o}$ LT birefringent device with a $\Delta n.d$ value of $0.55\mu m$ and polarisers placed in the "Symmetric A" configuration, whilst that of the second represents a $90^{o}$ TN cell with $\Delta n.d$ equal to $0.78\mu m$ together with the "Symmetric B" arrangement. Note that due to the geometry of these two systems, both solutions require the polarisers to be oriented at $45^{o}$ and $135^{o}$ respectively relative to the entrance molecular director vector.*

*The first system possesses excellent optical angular properties characteristic of a low-twisting liquid crystal cell. However, the unit also displays a poor cell contrast due to the lack of compensation between the remnant birefringence present in the two unperturbed liquid crystal layers immediately adjacent to the cell sides. Rotation of the polarisers away from the "Symmetric A" configuration has little effect upon cell contrast, making the unit unsuitable for providing the main contrast ramp in an optical shutter design. However, it may be possible to alleviate this problem via use of low-value retardation films and further research is continuing in this area.*

*The second cell type that satisfies the desired criteria possesses good optical properties in a direction lying perpendicular to the sample surface, but is unsatisfactory when viewed at large inclination angles away from the surface normal. This is due to both the large $\Delta n.d$ parameter and employment of the "Symmetric B" polariser configuration necessary in order to maximise the electro-optic properties of the device. These properties were analysed in some detail with the view of developing an automatically darkening welding filter based on such technology. It was found that although a certain degree of optimisation can be obtained, the optical performance of this device falls somewhat short of that for LT cells functioning in the "Symmetric A" polariser mode.*

# *CONCLUSIONS*

This thesis demonstrates that the use of liquid crystal technology enables automatically darkening welding filters to be developed that offer both a variable level of radiation protection in order to cater for all possible types of welding processes, together with a fast reaction time from the light to the dark state providing a high level of safety. The first point requires that the cell is functioning in the *reduced voltage* region whereby the liquid crystal molecules are only partially aligned with the applied electric field and hence retain a certain degree of birefringence, whilst that of the second demands that the unit is operating in the normally *white* mode and is therefore sandwiched between crossed polarisers.

However, the optical angular properties of such devices when driven in this manner are generally lacking and a loss of cell contrast is observed when the unit is viewed at large inclination angles away from the surface normal. This is in fact a problem that afflicts the majority of automatically darkening welding filters currently on the market that are based on liquid crystal technology. In order to help alleviate this ailment, most glass packs are based on a *double-cell* design whereby two identical cells are laminated together in opposite orientations with one cell being upside down such that the face-to-face rub directions of the two cells are crossed in order to generate a certain degree of cell compensation. This significantly improves the optical angular properties of the system although the characteristics of the unit still remains inadequate when viewed at acute angles.

Despite the fact that *retardation films* have been successfully employed in order to improve the poor optical angular properties displayed by both *super-twist* liquid crystal cells and those that function in the normally *black* mode, it is shown that the symmetry of the birefringence generated by cells operating in the normally *white* mode and driven at reduced voltages is asymmetric and hence does not match those of the standard retardation sheets that are uniaxially or biaxially stretched along directions lying in the plane of the material. Little improvement is therefore obtained upon utilisation of such sheets together with liquid crystal cells operating in this fashion. However, the concept of a new type of film that is drawn out in a linear direction making an angle of up to $20^{o}$ with the surface normal is introduced. Such films possess an optical symmetry that matches more closely that of the liquid crystal cell and hence is capable of generating a larger amount of improvement in the optical angular properties of the system. These layers are not yet available on the market but it is hoped that they will come on line in the not too distant future.

When in the activated phase and placed between crossed polarisers, the optical angular properties of a single cell generate a dark, off-axis cone in the polar plot diagram encapsulating viewing angles where the system displays a minimum in cell transmittance. For a $90^{o}$ TN cell, rotation of the polarisers away from the standard $0^{o}/90^{o}$ or $90^{o}/180^{o}$ configurations whereby they are aligned respectively perpendicular or parallel to the entrance and exit liquid crystal molecules, increases the area of this region and hence reduces the angular variation in transmittance. This enables double-cell structures to be designed that possess enhanced optical angular properties accordingly. However, this is at the expense of the light state transmittance so is less attractive as far as developing automatically darkening welding filters is concerned.

Reduction of the twist-angle in the cell causes the dark viewing cone displayed by a single cell to increase in area and to move outwards away from the centre of the polar chart, hence the unit becomes more asymmetric appearing dark when viewed at some incident angles whilst retaining a high transmittance at others. Such asymmetric cells are highly attractive for incorporation into double-cell structures whereby a large degree of cell compensation is required. In general, the lower the twist-angle, the better are the results. However, twist-angle reduction also has the effect of degrading the cell contrast due to a diminishing of the compensation effect between the remnant retardation present in the two layers of unperturbed liquid crystal material immediately adjacent to the cell sides. This results in a higher driving voltage being required in order to attain a specific shade number, an effect that is detrimental to the power consumption of the system.

With the polarisers held in the standard $0^{o}/90^{o}$ arrangement whereby the working polariser is aligned *perpendicular* to the entrance molecular director vector, twist-angle reduction also affects the light state transmittance in a way that depends upon the magnitude of the $\Delta n.d$ parameter. With a value of $0.39\mu m$, maximum light state transmittance is obtained for a twist-angle of $72^{o}$ and further reduction beyond this point generates a rapid deterioration in the light state transmittance. Use of LT cells may therefore offer advantages in terms of the optical angular properties of the device, but with the polarisers held in the standard arrangement a diminishing of both the cell contrast and the light state transmittance is observed.

The theoretical model introduced by *Gooch* and *Tarry* in 1975 analysing the optical transmittance of twisted nematic liquid crystal cells when in the inactivated phase and applicable to the specific case whereby the working polariser is aligned *parallel* to the entrance liquid crystal director vector, is extended to encapsulate the general situation whereby the polariser is oriented at some angle $\phi$ relative to this vector. This model is utilised in order to calculate the theoretical transmittance of LT cells with various polariser combinations. From these calculations, it is apparent that there are two polariser configurations of interest, both of which require the major transmission axes to be placed symmetrically in some fashion around the alignment directors at the cell sides. One arrangement *maximises* the overall optical throughput of the device when in the inactivated phase, whilst that of the second *minimises* this value. These two systems are referred to as the *Symmetric A* and *Symmetric B* polariser configurations respectively and by definition, the *Symmetric A* design is taken as being that which *maximises* the overall optical transmittance of the unit.

It is shown that use of the *Symmetric A* polariser arrangement together with an optimisation of both the twist-angle and the $\Delta n.d$ parameter enables optical transmittances approaching 100% to be obtained over a wide range of $\Delta n.d$ values down towards the theoretical limit of $0.27\mu m$. At this point, the liquid crystal layer forms a *half-wave plate* with $\Delta n.d$ approximating to half the wavelength of the central part of the visible spectrum and a rapid loss of cell transmittance is predicted. A curve displaying the optimum twist-angle for a given $\Delta n.d$ value is deduced.

These predictions are experimentally confirmed for a variety of cell types and it is shown that the available cell contrast is also sensitive to the polariser orientation. In general, it is the *Symmetric B* configuration that maximises the total contrast obtained from the device, whilst that for the *Symmetric A*

arrangement produces a minimum in the curve. This effect becomes more stark as both the twist-angle is reduced and the Δn.d parameter is increased, although the *Symmetric A* system is still able to offer adequate contrast over a wide range of twist-angles down towards $60^{o}$ with a Δn.d value of 0.39μm. It is also shown that the contrast curves plotted as a function of the polariser orientation are periodic with a repetition length of $90^{o}$, indicating that to a first approximation, the electro-optic properties of a LT cell are similar with the polarisers aligned either at $\phi^{o}$ and $(90 + \phi)^{o}$ or at $(90 + \phi)^{o}$ and $(180 + \phi)^{o}$.

Experiments indicate that the contrast is also dependent upon the width of the cell and in general, a reduction of the thickness generates a rise in the shade number attained for a given applied voltage. This phenomenon is particularly apparent for liquid crystal cells with low twist-angles. Although such an effect suppresses the operating voltage of the unit, the overall power consumption of the device is not favourably affected since the associated rise in cell capacitance increases the charge required in order to load up the cell. However, reduction of the driving frequency to below that of 0.1Hz alleviates this problem by lowering the number of charge/discharge cycles and further research is continuing in this area. In particular, the chemical degradation processes that occur inside the cell layers themselves when driven in such a fashion must be prevented.

Another area of study as yet unexplored is the effect of using different types of polyimide alignment materials within the cell structure that spontaneously induce higher molecular tilt angles at the surface. This may produce a reduction in the stimulating voltage required in order to generate a given amount of molecular alignment, hence lower the operating voltage of the device. It might also be possible to increase the cell contrast via use of low-value uniaxially stretched retardation films and further research is being carried out in this area.

Measurements of the optical angular properties of LT cells activated at reduced voltages indicate that in general, the angular variation of transmittance remains largely unaffected by rotation of the crossed polarisers relative to the cell. These properties are therefore predominantly governed by the liquid crystal layer itself. However, one exception exists when the polarisers hit the *Symmetric B* arrangement. Here, the off-axis dark cone is replaced by one that is *wrapped* around the central point of the polar chart and skewed off to one side. The symmetry of this pattern means that this system is not directly suitable for incorporation into double-cell structures whereby a large degree of cell compensation is required. This is in fact a general effect of the *Symmetric B* configuration and is independent of the nature of the specific liquid crystal cell under investigation.

The symmetry of the optical angular properties displayed by liquid crystal cells functioning in the *Symmetric A* polariser configuration enables two such cells to be placed together, forming a double-cell structure giving rise to a large amount of cell compensation. Welding filters can therefore be developed that possess the enhanced optical angular properties displayed by LT cells whilst maximising the light state optical throughput when in the inactivated phase. Although this is at the expense of the cell contrast, use of twist-angles above $60^{o}$ with a Δn.d value of 0.39μm maintains this quantity at acceptable levels.

Experiments indicate that the optical angular properties of a liquid crystal cell are also a function of the Δn.d parameter and that a certain amount of improvement can be achieved via reduction of this value.

This effect is particularly apparent for the standard 90° TN cell but becomes less critical as the twist-angle is lowered. For the 70° LT case, after initial improvements upon reduction from a value of 0.60μm to 0.40μm, little further effect is observed by pressing down towards the theoretical limit of 0.27μm within the viewing inclination angles of ± 30°.

A complete automatically darkening welding filter design based on this technology is introduced and it is shown to possess enhanced optical angular properties accordingly whilst maintaining the remaining pertinent electro-optic properties such as the light state shade number and the cell contrast at a high level. This design is patent protected by *Hörnell Innovation A.B* of Sweden.

It might be expected that the use of liquid crystal cells possessing opposite senses of helical rotation would offer an increased level of cell compensation in a double-cell design, hence further improve the optical angular properties of the filter. However, experiments indicate that there is in fact little significant improvement upon utilisation of oppositely twisting LT cells and when balanced up against the extra manufacturing costs involved with the production of two unique liquid crystal elements, such systems become far less attractive.

The second part of the experimental section deals with a novel mode of operation for a twisted nematic liquid crystal cell placed together with an interference filter that naturally appears *pink-red* when viewed in reflection. The system is in a dark state when in the inactivated phase and a small stimulating voltage of between ± 2.0 and ± 3.0 volts is required in order to attain the high transmittance condition. Further increment of the driving voltage beyond this point reverts the unit back to a darker phase.

Such systems offer advantages over that of the normally *white* mode of operation in that a dark, fail-safe state is provided should the controlling electronics malfunction, an effect usually characteristic of the normally *black* mode, whilst maintaining the fast response time from the light to the dark state associated with the normally *white* mode of operation.

Calculations indicate that there are only two cell types that display this phenomenon and the optical properties of these cells are investigated accordingly. The first corresponds to a 0° LT birefringent device possessing a Δn.d value of 0.55μm, whilst that of the second is a 90° TN unit with Δn.d being equal to 0.78μm. Both cells require the crossed polarisers to be positioned at 45° relative to the surface alignment directors. Experiments indicate that while the first device exhibits excellent optical angular properties due to employment of both the *Symmetric A* polariser arrangement and the low twist-angle present in the cell, the associated loss of cell contrast upon twist-angle reduction degrades the contrast to unacceptable levels. However, that for the second design possesses good electro-optic properties in a direction lying parallel to the surface normal and is therefore examined further in some detail.

The contrast available from an 8μm 90° TN cell filled with the *Merck 6096* liquid crystal component giving a Δn.d value of 0.80μm is found to be largely independent of the polariser configuration. However, the safe-state shade step is significantly more sensitive to the orientation of the polarisers and ranges from zero with the standard 0°/90° design, to that of over 2.2 shade numbers with a 45°/135° polariser system. In order to optimise both the safe-state shade step and the cell contrast of the device, it is necessary to employ the *Symmetric B* polariser design. However, the optical angular properties of the device are then

found to be inadequate and hence unsuitable for incorporation into a double-cell design whereby a large central viewing cone is required. The angular properties in the *light* state are also found to be lacking, with the unit becoming darker when observed at large inclination angles away from the surface normal, producing a welding filter with a restricted field of view.

It is noted that since the birefringence generated by such systems when activated at reduced voltages possesses a large degree of central symmetry, they are more suited for operation together with retardation films that are uniaxially or biaxially stretched in directions lying in the plane of the material. A certain amount of improvement is therefore obtained upon incorporation of two uniaxially stretched 570nm retardation sheets placed on either side of the cell between the polarisers. Note that it is critical to align the optic axes of the birefringent layers perpendicularly to the molecular alignment directors on each surface of the device in order to optimise the compensation effect. However, this also results in a small loss of cell contrast and the gross overall optical angular properties of the unit remain inferior to those displayed by LT cells operating in the *Symmetric A* polariser arrangement.

Experiments with low twist cells indicate that it is indeed the *Symmetric B* arrangement that is required in order to optimise the electro-optic properties of this mode of operation. Twist-angle reduction is again found to decrease the cell contrast, although the light state transmittance is maximised with a twist-angle of between $70^{o}$ and $80^{o}$ when utilising 8μm cells filled with the *Merck 6096* liquid crystal component and placed in the *Symmetric B* polariser configuration.

It is demonstrated that the optical angular properties of the 8μm $90^{o}$ TN cell are generally improved upon twist-angle reduction, although the gross overall angular dependence remains characteristic for the *Symmetric B* combination and hence is inadequate for incorporation into automatically darkening welding filter designs that require a large field of view. Small improvements in the optical angular properties of the device when in the light state are also apparent upon reduction of the twist-angle, although the unit still possesses a restricted viewing cone. Experiments using retardation films in order to further enhance the optical angular properties of this mode of operation based on LT cells proved largely unsuccessful and an additional loss of cell contrast was observed.

By compromising the electro-optic properties of the cell and allowing the polarisers to be moved away from the *Symmetric B* configuration, the optical angular properties of the unit can be improved. Experiments indicate that for the 8μm $90^{o}$ TN cell filled with the *Merck 6096* liquid crystal material, the polarisers must be rotated by up to $30^{o}$ away from this arrangement, hence having disastrous effects upon both the safe-state shade step and the cell contrast. However, the lower twisting variants are far more sensitive to the polariser orientations and it is found that for the 8μm $70^{o}$ LT case, a polariser arrangement of $30^{o}/120^{o}/30^{o}$ removes the inadequate *wrapped* pattern in the polar chart whilst maintaining the remaining pertinent optical properties at a suitable level.

Experiments indicate that there is little significant difference between the switching speeds from the light to the dark state for twisted nematic liquid crystal cells operating in either the normally white mode or with this new mode of operation, especially when activated with elevated voltages exceeding that of 12 volts. This mode of operation is therefore successful in providing a fail-safe, shade step whist maintaining the fast response time associated with the normally *white* mode of operation.

## *DISCUSSIONS*

The use of twisted-nematic liquid crystal cells enables automatically darkening welding filters to be developed that are capable of offering a variable level of radiation protection in order to accommodate all types of welding techniques. In addition to this, the operation of the cells in the normally *white* mode ensures that a fast response time from the light to the dark state is obtained upon commencement of welding, guaranteeing that a maximum level of safety is achieved. However, the poor optical angular properties afforded by such cells when in the activated phase afflicts the majority of welding filters currently on the market, rendering the optical performance of such products largely inadequate. It is therefore in this area that the bulk of research contained within this thesis has concentrated.

The experimental work is split into two sections. The first introduces a novel *polariser-cell* assembly that makes use of two *low-twisting* liquid crystal devices placed together in opposite orientations such that a large degree of cell compensation occurs. The net result is an optical shutter possessing enhanced optical angular properties accordingly whilst maintaining the remaining pertinent parameters at a high level. The only compromise comes from the associated loss of cell contrast upon twist-angle reduction, necessitating the requirement of a higher stimulating voltage and hence increasing the overall power consumption of the device.

The second part of the experimental section introduces a new mode of operation for a twisted-nematic liquid crystal cell placed between crossed polarisers together with an *interference filter* that naturally appears *pink-red* when observed in reflection. By fine adjustment of the intrinsic parameters of the cell, a device is obtained that displays a dark state when in the inactivated phase. Application of a small stimulating voltage removes the colouration of the cell and the unit transmutes into the highest transmittance phase. Further increment of the driving electronics beyond this point reverts the unit back to a dark condition.

Such devices offer several advantages over that of the normally *white* mode of operation. In particular, the unit provides a higher level of safety should the controlling electronics malfunction by reverting to a dark state rather than holding in a potentially hazardous lighter condition, a property usually correlated with the normally *black* mode, whilst the fast response time from the light to the dark state associated with the normally *white* mode of operation is maintained. However, experiments indicate that the optical angular properties of twisted nematic liquid crystal cells utilising this mode of operation fall somewhat short of those for optimised low-twist cells employing the *Symmetric A* polariser configuration and hence such devices appear less attractive as far as developing fast, automatically darkening welding filters is concerned.

Looking towards the future, the development of suitable retardation films that are capable of offering a large degree of compensation for the asymmetric birefringence generated by a liquid crystal cell when stimulated at reduced voltages and the utilisation of interference filters that naturally possess an angular dependent transmittance, becoming darker when viewed at large inclination angles away from the surface normal, will ensure that the problem of the poor angular dependence displayed by automatically

darkening welding filters based on liquid crystal technology will largely be eliminated. Research into other types of liquid crystal materials such as ferroelectric devices may also prove fruitful in the not too distant future.

Finally, I would like to thank Kristina Danielsson, Dr. Åke Hörnell and Professor Claes Granqvist for attempting to keep me sane whilst carrying out the research contained within this thesis. I also very much appreciated the continued support received from *Hörnell Innovation AB* in terms of access to the various production lines and test equipment.

# *REFERENCES*

[1]T.L Lyon et al., U.S Army Environment Hygiene Agency, AD/A-033 768: "Evaluation of the potential hazards from actinic ultraviolet radiation generated by electric welding and cutting arcs"

[2]Commission Internationale de L'Eclairage (CIE) Publication no. 15 (E-1.3.1) 1971, The CIE 1931 Standard Colorimetric Observer for day time viewing: "Colorimetry"

[3]Lichtmeßtechnik, Helmholtzstraße 9, Berlin 10, Germany.

[4]European Standard EN 169: 1992 "Personal eye protection - Filters for welding and related techniques - Transmittance Requirements and Recommended Utilisation"

[5]International Standard ISO 4850: 1979 "Personal eye protectors for welding and related techniques - Filters - Utilisation and transmittance requirements"

[6]American Standard ANSI Z87.1: 1989, American national standards Institute Inc., (American Society of Safe Engineers, Illinois): "Practice for Occupational and Educational Eye and face Protection"

[7]Deutsches Institut für Normung (D.I.N) Standards, Westliche 56, 7530 Pforzheim, Germany.

[8]Hörnell Elektrooptik A.B, Ernst Hedlunds Väg 35, 780 41 Gagnef, Sweden.

[9]Hörnell Elektrooptik A.B Market Research, Ernst Hedlunds Väg 35, 780 41 Gagnef, Sweden.

[10]M Schadt and W Helfrich, "Voltage-dependent Optical Activity of a Twisted Nematic Liquid Crystal", Appl. Phys. Lett. 18, page 127-128 (1971)

[11]Merck, Postfach 41 19, 6100 Darmstadt 1, Frankfurter Straße 250, Germany.

[12] E Guyon, P Pieranski and M Boix, Lett. Appl. Sci. E., Vol 1, No. 19, (1972)

[13]T.J Scheffer and J Nehring, "A New, Highly Multiplexable Liquid Crystal Display", Appl. Phys. Lett. 45, page 1021-1023 (1984)

[14]Birendra Bahadur, "Liquid Crystals: Applications and uses" (World Scientific Publishing Co. Pte. Ltd., Singapore, 1990) Volume 1, chapter 2.3

[15]Birendra Bahadur, "Liquid Crystals: Applications and uses" (World Scientific Publishing Co. Pte. Ltd., Singapore, 1990) Volume 1, chapter 12.2.3

[16]Donnelly Applied Film Corporation, 797 Winchester Circle, Boulder, Colorado 80301, U.S.A.

[17]Balzers, Bereich SF, FL-9496 Balzers, Liechtenstein.

[18]K.L Chopra, S Major and K Pandya, "Transparent Conductors - a Status Review", Thin Solid Films, volume 102, page 1 (1983)

[19]Rhodeftal 200, Rhone-Poulenc Chimie, 92499 Courbevoie Cedex 29, France.

[20]Textil Miljö, Box 1122, Hållingsgatan 15, 501 11 Borås, Sweden.

[21]Catalysts and Chemicals Industries, Nippon Building, Ohtemachi 2-Chome, Chiyoda-KU, Tokyo, Japan.

[22]Norland Products Inc., New Brunswick, 08902 New Jersey, U.S.A.

[23]H.A Macleod, "Thin Film Optical Filters" (Adam Hilger Ltd., Bristol, 1986) Second Edition, chapter 5

[24]Dodwell Hi-Tech KK, KOWA No. 16 Annex, 9-20 Akasaka 1-Chome, Minato-ku, Tokyo 107, Japan.

[25]Étienne Malus, 1809

[26]European patent no. EP 0 550 384 A1: 7th July 1993, "Blendschutzvorrichtung": Xelux AG, Zugerstaße 80, 8820 Wädenswil, Switzerland.

[27]U.S.A patent no. 3, 700 306: 24th October 1972, "Electro-optic Shutter Having a Thin Silicon Oxide Layer Between the Electrodes and the Liquid Crystal", J Cartmell, D Churchill and D Koopman, Dayton, Ohio, U.S.A.

[28]BPW 21 Silicon Photodiode, Seimens AG, LZW 85, Postfach 2348, W-8510 Fürth 2, Germany.

[29]Birendra Bahadur, "Liquid Crystals: Applications and uses" (World Scientific Publishing Co. Pte. Ltd., Singapore, 1990) Volume 2, chapter 8.7.6

[30]European Standard EN 379:1993, section 3.5, "Specification for Welding Filters with Switchable Luminous Transmittance and Welding Filters with Dual Luminous Transmittance"

[31]T Credelle, "Thin Film Transistors for Video Applications", Proceedings of the 8th International Display Research Conference, page 208-214 (1988)

[32]U.S.A Patent no. 4, 398 803: 16th August 1983, "Liquid Crystal Display Element", L Pohl, G Weber, R Eidenschink, G Baur and W Fehrenbach, Merck, Postfach 41 19, 6100 Darmstadt 1, Frankfurter Straβe 250, Germany.

[33]L Pohl, G Weber, R Eidenschink, G Baur and W Fehrenbach, "Low-Δn-Twisted Nematic Cell with Improved Optical Properties", Appl. Phys. Lett. 38, page 497-499 (1981)

[34]Y Fujimura, T Nagatsuka, H Yoshimi, S Umemoto and T Shimomura, "Optical Properties of Retardation Films", SID92 International Symposium Digest of Technical Papers XXIII, page 397-400 (1992)

[35]M Ohgawara, T Kuwata, H Hasebe, M Akatsuka, H Koh, K Matsuhiro, Y Souda and K Sawada, "A Colour STN Display with Two Retardation Compensating Films", SID89 Digest of Technical Papers XX, page 390-393 (1989)

[36]I Fukuda, Y Kotani and T Uchida, "Achromatic Super-Twisted Nematic LCD Using Birefringent Film", Proceedings of the 8th International Display Research Conference, page 159-160 (1988)

[37]H Odai, T Hanami, M Hara, K Iwasa and N Tatsumi, "Optical Compensation of Super Twisted Nematic LCD Applied by Polymer Retardation Film", Proceedings of the 8th International Display Research Conference, page 195-198 (1988)

[38]S Matsumoto, H Hatoh, A Murayama, T Yamamoto, S Kondo and S Kamagami, "A Single Cell high-Quality Black and White ST-LCD", Proceedings of the 8th International Display Research Conference, page 182-183 (1988)

[39]N Yamagishi, H Watanabe and K Yokoyama, "Wide Viewing Angle LCD Using Retardation Films", Proceedings of the 9th International Display Research Conference (Japan Display), page 316-319 (1989)

[40]Nitto Denko Corporation, 1-1-2 Shimohozumi, Ibaraki, Osaka, Japan.

[41]H.L Ong, "New Normally White Negative Birefringence Film Compensated Twisted-Nematic LCD's with Largest Viewing Angle Performance", Proceedings of the 12th International Display Research Conference (Japan Display), page 247-250 (1992)

[42]H.J Jerrard, J. Opt. Soc. Am., Volume 38(1), page 35 (1948)

[43]A.R Johnston and J.M Weingart, J, Opt. Soc. Am., Volume 55, page 7 (1965)

[44]J Mukai, T Kurita, T Kaminade, H Hara, T Toyooka and H Itoh, "A Liquid Crystal Polymer Film for Optical Applications", SID94 International Symposium Digest of Technical Papers XXV, page 241-244 (1994)

[45]F Harris, S Cheng and F Li, University of Akron, (to be published - for information contact S Cheng: Tel: 216-972-6931)

[46]C.H Gooch and H.A Tarry, "The Optical Properties of Twisted Nematic Liquid Crystal Structures with Twist Angles less than 90°", J. Phys, D: Appl. Phys., Volume 8, page 1575-1584 (1975)

[47]C Mauguin, "Sur les cristaux liquides de Lehmann", Bull. Soc. Franç. Mineral, Volume 34, page 71-117 (1911)

[48]S.T Wu and A.M Lackner, "Mylar-film Compensated π and Parallel Aligned Liquid Crystal Cells for Direct-View and Projection Displays", Appl. Phy. Let 64, page 2047 (1994)

[49]MathSoft Inc., 201 Broadway, Cambridge, Massachusetts 02139, U.S.A.

[50]Swedish patent no. SE 9401423-0: 26th April 1994, Å Hörnell and S Palmer, "Welding Filter with Improved Angular Properties", Hörnell Innovation A.B, Tunavägen 281, 781 73 Borlänge, Sweden.

[51]U.S.A patent no. 4,385,806 Serial no. 121,071: 13th February 1980, J. Fergason, Optical Shields Inc., 1390 Willow Road, Menlo Park, CA 94025, U.S.A.

[52]Hewlett Packard, Box 19, 164 93 Kista, Stockholm, Sweden

# *APPENDIX ONE*

*This appendix reproduces the information released by Merck[11] covering the pertinent intrinsic parameters of the liquid crystal materials used throughout this thesis. The data is purely quoted and the measurement techniques employed in order to obtain the figures is not covered. The reader is therefore referred to the relevant manufacturer if further information is required. Unless otherwise stated, all liquid crystal mixtures are doped with 0.1% by volume of the ZLI-811 negative twisting cholesteric component to induce the desired handiness of the cell.*

***The Physical Properties of Liquid Crystal Materials Used in this Thesis.***

| MERCK | ZLI-3376 | ZLI-3700 | ZLI-3949 | ZLI-4246 | ZLI-5035/4 | MLC-6080 | MLC-6096 |
|---|---|---|---|---|---|---|---|
| | | | | | | | |
| Development Date | Jan-86 | Aug-87 | Apr-87 | May-88 | - | Feb-93 | May-93 |
| | | | | | | | |
| Smetic-Nematic ($^{o}$C) | - 40$^{o}$C | - 40$^{o}$C | - 40$^{o}$C | - 40$^{o}$C | - 40$^{o}$C | - 30$^{o}$C | - 40$^{o}$C |
| Clearing Point ($^{o}$C) | + 100$^{o}$C | + 105$^{o}$C | + 85$^{o}$C | + 95$^{o}$C | + 97$^{o}$C | + 95$^{o}$C | + 93$^{o}$C |
| | | | | | | | |
| Viscosity ($mm^2s^{-1}$) | | | | | | | |
| 20$^{o}$C | 20 | 21 | 22 | 22 | 22 | 18 | 17 |
| 0$^{o}$C | 60 | 66 | 78 | 69 | 61 | 69 | 48 |
| - 20$^{o}$C | 290 | 320 | 460 | 340 | - | 490 | 220 |
| - 30$^{o}$C | 825 | 990 | 1760 | 1100 | - | 2730 | 620 |
| - 40$^{o}$C | 3000 | 3850 | 9870 | 4950 | - | - | 2370 |
| | | | | | | | |
| $\Delta\varepsilon$ (1 kHz, 20$^{o}$C) | + 4 | + 5.4 | + 11.3 | + 8.3 | + 5.7 | + 7.2 | + 5.4 |
| $\varepsilon_{parallel}$ | 7.6 | 9.4 | 15.6 | 12.5 | 9.1 | 11.1 | 9.0 |
| $\varepsilon_{perpen}$ | 3.6 | 4.0 | 4.3 | 4.2 | 3.4 | 3.9 | 3.6 |
| | | | | | | | |
| Voltage $V_{Threshold}$ | 2.51 | 2.1 | 1.77 | 2.05 | - | 2.23 | 1.82 |
| Voltage $V_{Saturation}$ | 3.79 | 2.5 | 2.52 | 2.87 | - | 3.05 | 2.87 |
| | | | | | | | |
| $\Delta V_{Threshold}$ / $\Delta$T (mV/$^{o}$C) | 8.25 | 2.6 | 7.0 | 2.6 | - | 2.88 | 3.69 |
| | | | | | | | |
| $\Delta$n (589nm, 20$^{o}$C) | + 0.0874 | + 0.0980 | + 0.1415 | + 0.1294 | + 0.1315 | + 0.2024 | + 0.1003 |
| $n_o$ (589nm, 20$^{o}$C) | 1.4804 | 1.4859 | 1.5027 | 1.4997 | 1.5012 | 1.5076 | 1.4852 |
| $n_e$ (589nm, 20$^{o}$C) | 1.5678 | 1.5839 | 1.6442 | 1.6291 | 1.6327 | 1.7100 | 1.5855 |
| | | | | | | | |
| $\Delta$n (633nm, 20$^{o}$C) | - | - | - | - | - | + 0.1984 | + 0.098 |
| $n_o$ (633nm, 20$^{o}$C) | - | - | - | - | - | 1.5041 | 1.4838 |
| $n_e$ (633nm, 20$^{o}$C) | - | - | - | - | - | 1.7025 | 1.5818 |

# *APPENDIX TWO*

*A theoretical model for the liquid crystal helical structure when in the inactivated phase was developed by C. H Gooch and H. A Tarry*[46] *in 1975 and applied to the specific case of a twisted nematic liquid crystal cell operating between polarisers oriented respectively parallel and perpendicular to the entrance and exit liquid crystal molecules. This model is extended further to cover the general case where the working polariser is oriented at an angle $\phi$ relative to the entrance molecular director vector, enabling the overall transmittance of the device to be calculated given the particular parameters appropriate for the system under consideration.*

***The Theoretical Transmittance of Liquid Crystal Cells in the Inactivated Phase.***

We consider a model of the nematic type liquid crystal cell introduced by Gooch and Tarry[46] where the helical molecular stacking structure is represented by a series of birefringent, parallel plates of thickness $\delta$ z lying in the $\underline{x}$-$\underline{y}$ plane. Each plate is rotated by an angle $\delta 6$ clockwise around the $\underline{z}$-axis relative to the preceding one and we define the local right-handed co-ordinate axis for each layer to be $\underline{x}'$ and $\underline{y}'$ which are respectively parallel and perpendicular to the local optic axis in each sheet.

The light emerging from the $m^{th}$ plate is given by:

$$E^{out}(\underline{r})_m = E^{out}(\underline{x}')_m \, \underline{x}' + E^{out}(\underline{y}')_m \, \underline{y}' \qquad (B1)$$

$$E^{out}(\underline{x}')_m = A_m \sin \omega t + B_m \cos \omega t \qquad (B2)$$

$$E^{out}(\underline{y}')_m = C_m \sin \omega t + D_m \cos \omega t \qquad (B3)$$

Upon passage into the $(m+1)^{th}$ plate, the light enters a region represented by another local co-ordinate system rotated by an angle $\delta 6$ clockwise around the $\underline{z}$-axis. This gives the equation for the incident radiation in the new layer as:

$$E^{in}(\underline{r})_{m+1} = E^{in}(\underline{x}')_{m+1} \, \underline{x}' + E^{in}(\underline{y}')_{m+1} \, \underline{y}' \qquad (B4)$$

$$E^{in}(\underline{x}')_{m+1} = A_m \sin \omega t \cos \delta\theta - C_m \sin \omega t \sin \delta\theta + B_m \cos \omega t \cos \delta\theta - D_m \cos \omega t \sin \delta\theta \qquad (B5)$$

$$E^{in}(\underline{y}')_{m+1} = A_m \sin \omega t \sin \delta\theta + C_m \sin \omega t \cos \delta\theta + B_m \cos \omega t \sin \delta\theta + D_m \cos \omega t \cos \delta\theta \qquad (B6)$$

Upon traversing through the $(m+1)^{th}$ plate, the $E(\underline{y}')$ component gains a phase factor relative to $E(\underline{x}')$ due to the birefringence of the liquid crystal sheet. This phase shift is given by $\delta\phi$, where we have:

$$\delta\phi = \frac{2\pi\Delta n\,\delta z}{\lambda} \qquad \text{(B7)}$$

The light emerging from the $(m+1)^{th}$ plate is now represented by:

$$E^{out}(\underline{x}')_{m+1} = A_{m+1}\sin\omega t + B_{m+1}\cos\omega t \qquad \text{(B8)}$$

$$E^{out}(\underline{y}')_{m+1} = C_{m+1}\sin(\omega t+\delta\phi) + D_{m+1}\cos(\omega t+\delta\phi) \qquad \text{(B9)}$$

Assuming that no light absorption or scattering occurs, energy conservation applies, giving:

$$E^{out}(\underline{x}')_{m+1} = E^{in}(\underline{x}')_{m+1} \qquad \text{(B10)}$$

$$E^{out}(\underline{y}')_{m+1} = E^{in}(\underline{y}')_{m+1} \qquad \text{(B11)}$$

Equating the coefficients of *sin ωt* and *cos ωt* for $E^{out}(\underline{x}')_{m+1}$ gives:

$$A_{m+1} = A_m\cos\delta\theta - C_m\sin\delta\theta \qquad \text{(B12)}$$

$$B_{m+1} = B_m\cos\delta\theta - D_m\sin\delta\theta \qquad \text{(B13)}$$

For $E^{out}(\underline{y}')_{m+1}$, the coefficient equating of *sin ωt* and *cos ωt* produces:

$$C_{m+1} = (A_m\sin\delta\theta + C_m\cos\delta\theta)\cos\delta\phi - (B_m\sin\delta\theta + D_m\cos\delta\theta)\sin\delta\phi \qquad \text{(B14)}$$

$$D_{m+1} = (B_m\sin\delta\theta + D_m\cos\delta\theta)\cos\delta\phi + (A_m\sin\delta\theta + C_m\cos\delta\theta)\sin\delta\phi \qquad \text{(B15)}$$

Formulae for $A_{m-1}$, $A_m$, $A_{m+1}$ and $A_{m+2}$ can now be written following the structure of equation B12 where we have:

$$A_{m-1} = A_{m-2}\cos\delta\theta - C_{m-2}\sin\delta\theta \qquad \text{(B16)}$$

$$A_m = A_{m-1}\cos\delta\theta - C_{m-1}\sin\delta\theta \qquad \text{(B17)}$$

$$A_{m+1} = A_m\cos\delta\theta - C_m\sin\delta\theta \qquad \text{(B18)}$$

$$A_{m+2} = A_{m+1}\cos\delta\theta - C_{m+1}\sin\delta\theta \qquad \text{(B19)}$$

Following some rather lengthy algebraic manipulations involving the substitutions of equations B12-B15 and derivatives thereof for $B_{m-1}$, $C_{m-1}$, and $D_{m-1}$ etc., into equations B16-B19, expressions can be found for $A_{m-2}$, $A_{m-1}$, $A_m$, $A_{m+1}$ and $A_{m+2}$ in terms of $A_m$, $B_m$, $C_m$ and $D_m$. This enables a difference equation in "$A$" to be deduced whereby the parameters $B_m$, $C_m$ and $D_m$ are eliminated:

$$A_{m-2} - 2A_{m-1}(1 + \cos\delta\phi)\cos\delta\theta + 2A_m\left[(1 + \cos\delta\phi)\cos^2\delta\theta + \cos\delta\phi\right] - \ldots\ldots$$

$$\ldots\ldots - 2A_{m+1}(1 + \cos\delta\phi)\cos\delta\theta + A_{m+2} = 0 \qquad \text{(B20)}$$

By defining $f_A(z)$ to be a function of $z$ describing the magnitude of "$A$" and $z_m$ to be the distance along the z-axis from the origin to the $m^{th}$ plate, given by $z_m = m * \delta z$, the terms in equation B20 can be expanded into a *Taylor's series* around $z_m$ to describe the evolution of "$A$" with $z$. This expansion gives the following terms:

$$A_{m-2} = f_A(z_m - 2\delta z) \approx f_A(z_m) + \sum \frac{(-2\delta z)^n}{n!} f_A^{(n)}(z_m) \qquad \text{(B21)}$$

$$A_{m-1} = f_A(z_m - \delta z) \approx f_A(z_m) + \sum \frac{(-\delta z)^n}{n!} f_A^{(n)}(z_m) \qquad \text{(B22)}$$

$$A_m = f_A(z_m) \qquad \text{(B23)}$$

$$A_{m+1} = f_A(z_m + \delta z) \approx f_A(z_m) + \sum \frac{(\delta z)^n}{n!} f_A^{(n)}(z_m) \qquad \text{(B24)}$$

$$A_{m+2} = f_A(z_m + 2\delta z) \approx f_A(z_m) + \sum \frac{(2\delta z)^n}{n!} f_A^{(n)}(z_m) \qquad \text{(B25)}$$

$$\cos\delta\theta \approx 1 - \frac{(\delta\theta)^2}{2!} + \frac{(\delta\theta)^4}{4!} - \frac{(\delta\theta)^6}{6!} + \ldots\ldots \qquad \text{(B26)}$$

$$\cos\delta\phi \approx 1 - \frac{(\delta\phi)^2}{2!} + \frac{(\delta\phi)^4}{4!} - \frac{(\delta\phi)^6}{6!} + \ldots\ldots \qquad \text{(B27)}$$

This allows the terms in equation B20 to be expanded to second order, giving the evolution of the function $f_A(z)$ across the discontinuous layer structure about $z_m$. For the continuous, smoothly twisting nematic structure, we apply the following limits as $\delta z \rightarrow 0$, where $d$ is the overall thickness of the liquid crystal layer and $\theta$ the total twist angle of the cell.

$$\delta\theta \rightarrow \left(\frac{\theta}{d}\right) \tag{B28}$$

$$\delta\phi \rightarrow \left(\frac{2\pi\Delta n}{\lambda}\right) \tag{B29}$$

This gives a differential equation describing the propagation of the function $f_A(z)$ through the liquid crystal structure, which in turn yields the magnitude of the "$A_m$" component of radiation defined in equation B2 above.

$$\left(\frac{d^4A}{dz^4}\right) + \left[2\left(\frac{\theta}{d}\right)^2 + 4\left(\frac{\pi\Delta n}{\lambda}\right)^2\right]\left(\frac{d^2A}{dz^2}\right) + \left(\frac{\theta}{d}\right)^4 = 0 \tag{B30}$$

This differential equation can be solved to give the function $f_A(z)$, where the parameters $u$ and $q$ are defined in equations B32-B33:

$$f_A(z) = a_1 \cos\left(\frac{q\theta z}{d}\right) + a_2 \sin\left(\frac{q\theta z}{d}\right) + a_3 \cos\left(\frac{\theta z}{dq}\right) + a_4 \sin\left(\frac{\theta z}{dq}\right) \tag{B31}$$

$$u = \left(\frac{\pi d\Delta n}{\theta\lambda}\right) \tag{B32}$$

$$q = \left[1 + 2u^2 + 2u\sqrt{1 + u^2}\right]^{\frac{1}{2}} \tag{B33}$$

Applying the appropriate initial boundary conditions yields the values of the coefficients $a_1$, $a_2$, $a_3$ and $a_4$. So far, we have concentrated only on the "$A$" component of radiation traversing through the system. Similar mathematical procedures generate identical equations describing the $f_B(z)$, $f_C(z)$ and $f_D(z)$ functions. Taken together, these components completely describe the propagation of radiation through the liquid crystal helical layer.

With incident radiation initially polarised along the x-direction at $z = 0$, we have:

$$E^{initial}(x')_{z=0} = \sin \omega t, \qquad A_{z=0} = 1, \qquad B_{z=0} = 0, \tag{B34}$$

$$E^{initial}(y')_{z=0} = 0, \qquad C_{z=0} = 0, \qquad D_{z=0} = 0, \tag{B35}$$

and $f_A(z)^2 + f_B(z)^2 + f_C(z)^2 + f_D(z)^2 = 1$, giving: (B36)

$$f_A(z) = \left(\frac{q^2}{1+q^2}\right)\cos\left(\frac{\theta z}{dq}\right) + \left(\frac{1}{1+q^2}\right)\cos\left(\frac{q\theta z}{d}\right) \tag{B37}$$

$$f_B(z) = \left(\frac{-q^2}{1+q^2}\right)\sin\left(\frac{\theta z}{dq}\right) + \left(\frac{1}{1+q^2}\right)\sin\left(\frac{q\theta z}{d}\right) \tag{B38}$$

$$f_C(z) = \left(\frac{q}{1+q^2}\right)\sin\left(\frac{\theta z}{dq}\right) + \left(\frac{q}{1+q^2}\right)\sin\left(\frac{q\theta z}{d}\right) \tag{B39}$$

$$f_D(z) = \left(\frac{q}{1+q^2}\right)\cos\left(\frac{\theta z}{dq}\right) + \left(\frac{-q}{1+q^2}\right)\cos\left(\frac{q\theta z}{d}\right) \tag{B40}$$

For the specific case where the first polariser is aligned parallel to the entrance liquid crystal molecules, the intensity of radiation emerging in directions respectively parallel and perpendicular to the exit molecules are given by equations B41-B42 with the amplitude functions evaluated for $z = d$, where $d$ is the thickness of the liquid crystal layer.

$$T_{parallel} = f_A^2(d) + f_B^2(d) \tag{B41}$$

$$T_{perpendicular} = f_C^2(d) + f_D^2(d) \tag{B42}$$

This yields the standard results introduced by *Gooch and Tarry* that are applicable for twisted nematic liquid crystal cells with the working polariser aligned parallel to the entrance molecular director vector.

$$T_{parallel} = \frac{u^2 + \cos^2\left(\theta\sqrt{1+u^2}\right)}{1+u^2} \quad \text{(B43)}$$

$$T_{perpendicular} = \frac{\sin^2\left(\theta\sqrt{1+u^2}\right)}{1+u^2} \quad \text{(B44)}$$

With incident radiation polarised at an angle $\phi$ to the entrance liquid crystal molecules at $z = 0$, the following equations are obtained for the amplitude functions:

$$\underline{E}^{initial}(\underline{r}) = \cos\phi \sin\omega t\, \underline{x}' + \sin\phi \sin\omega t\, \underline{y}' \quad \text{(B45)}$$

$$E^{initial}(\underline{x}')_{z=0} = \cos\phi \sin\omega t, \quad A_{z=0} = \cos\phi, \quad B_{z=0} = 0, \quad \text{(B46)}$$

$$E^{initial}(\underline{y}')_{z=0} = \sin\phi \sin\omega t, \quad C_{z=0} = \sin\phi, \quad D_{z=0} = 0, \quad \text{(B47)}$$

$$f_A(z) = \left(\frac{1}{1+q^2}\right)\cos\left(\frac{q\theta z}{d}\right)\cos\phi + \left(\frac{-q}{1+q^2}\right)\sin\left(\frac{q\theta z}{d}\right)\sin\phi + \ldots\ldots$$

$$\ldots\ldots + \left(\frac{q^2}{1+q^2}\right)\cos\left(\frac{\theta z}{dq}\right)\cos\phi + \left(\frac{-q}{1+q^2}\right)\sin\left(\frac{\theta z}{dq}\right)\sin\phi \quad \text{(B48)}$$

$$f_B(z) = \left(\frac{q}{1+q^2}\right)\cos\left(\frac{q\theta z}{d}\right)\sin\phi + \left(\frac{1}{1+q^2}\right)\sin\left(\frac{q\theta z}{d}\right)\cos\phi + \ldots\ldots$$

$$\ldots\ldots + \left(\frac{-q}{1+q^2}\right)\cos\left(\frac{\theta z}{dq}\right)\sin\phi + \left(\frac{-q^2}{1+q^2}\right)\sin\left(\frac{\theta z}{dq}\right)\cos\phi \quad \text{(B49)}$$

$$f_C(z) = \left(\frac{q^2}{1+q^2}\right)\cos\left(\frac{q\theta z}{d}\right)\sin\phi + \left(\frac{q}{1+q^2}\right)\sin\left(\frac{q\theta z}{d}\right)\cos\phi + \ldots\ldots$$

$$\ldots\ldots + \left(\frac{1}{1+q^2}\right)\cos\left(\frac{\theta z}{dq}\right)\sin\phi + \left(\frac{q}{1+q^2}\right)\sin\left(\frac{\theta z}{dq}\right)\cos\phi \quad \text{(B50)}$$

$$f_D(z) = \left(\frac{-q}{1+q^2}\right)\cos\left(\frac{q\theta z}{d}\right)\cos\phi + \left(\frac{q^2}{1+q^2}\right)\sin\left(\frac{q\theta z}{d}\right)\sin\phi$$

$$\ldots\ldots + \left(\frac{q}{1+q^2}\right)\cos\left(\frac{\theta z}{dq}\right)\cos\phi + \left(\frac{-1}{1+q^2}\right)\sin\left(\frac{\theta z}{dq}\right)\sin\phi \qquad \text{(B51)}$$

We now consider the general arrangement outlined in figure B1. Here, the only system constraint is that the liquid crystal cell is placed between crossed polarisers. This ensures that maximum cell contrast is maintained together with a fast response time from the light to the dark state upon application of a stimulating voltage. There are no other demands placed upon the remaining parameters of the system.

**Figure B1: General arrangement of a liquid crystal cell placed between crossed polarisers.**

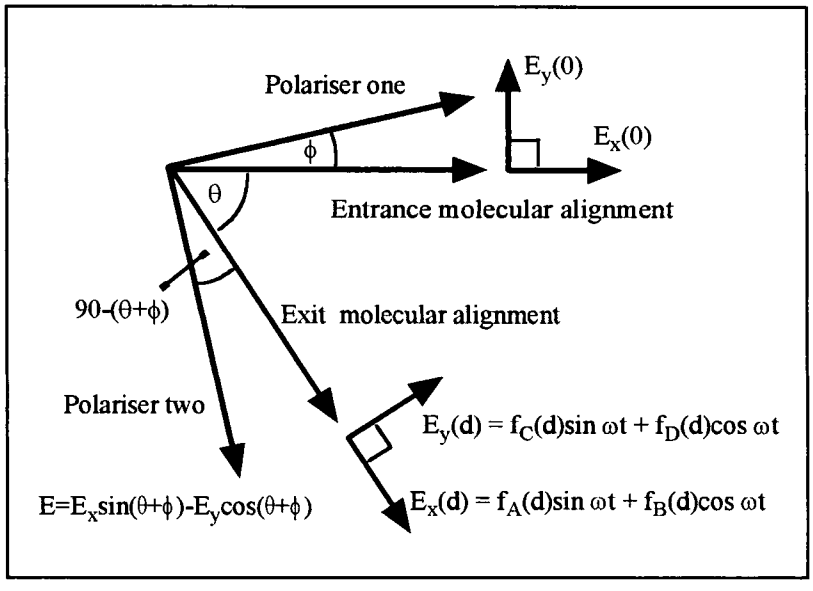


The total overall E-field exiting the liquid crystal helical layer in a direction lying parallel to the second polarising material is obtained from equation B52, with the amplitude functions $f_A(z)$, $f_B(z)$, $f_C(z)$ and $f_D(z)$ being defined above in equations B48-B51. It is this component that is transmitted through the analysing polariser and thus enables the overall transmission of the device to be calculated given the specific values of the parameters $d$, $\Delta n$, $\theta$, $\lambda$ and $\phi$ relevant for the system under consideration.

$$\underline{E}^{parallel}(\underline{r})_{out} = [\, f_A(d) \sin(\theta + \phi) - f_C(d) \cos(\theta + \phi) \,] \sin \omega t + \ldots\ldots$$

$$\ldots\ldots + [\, f_B(d) \sin(\theta + \phi) - f_D(d) \cos(\theta + \phi) \,] \cos \omega t \qquad \text{(B52)}$$

The total luminous transmittance of the unit is found by integrating over the visible spectrum. This is indicated in equation B53 where the function $y(\lambda)$ is defined as the standard relative sensitivity of the human eye.

$$T_{luminous} = \frac{\int_{380}^{760} T_{total}(d, \Delta n, \theta, \lambda, \phi) * y(\lambda).d\lambda}{\int_{380}^{760} y(\lambda).d\lambda} \qquad \text{(B53)}$$

As an approximation to $y(\lambda)$, we have taken equation B54. The motivation for this is displayed in figure B2 where values for the standard relative sensitivity of the human eye for daytime viewing[2] are plotted over a mathematical $sin^8(\lambda)$ function obtained via use of regression. This shows that there is good agreement between the two supporting the validity of the approximation.

$$y(\lambda) = \sin^8(0.008\,\lambda + 0.269) \qquad \text{(B54)}$$

**Figure B2: The relative sensitivity values of the human eye during daytime viewing plotted over the "$y(\lambda) = \sin^8(0.008\,\lambda + 0.269)$" mathematical function.**